USGS Research on Energy Resources—1990 Program and Abstracts

Sixth V.E. McKelvey Forum on Mineral and Energy Resources

U.S. GEOLOGICAL SURVEY CIRCULAR 1060

Cover.—Left Hand Collet Canyon, Kaiparowits Plateau, Utah. This canyon cuts through Coniacian and Santonian strata. Thick coal beds at the head of the canyon were deposited penecontemporaneously with shoreface deposits at the mouth of the canyon, only 2.5 km away. Original color slide by Peter J. McCabe.

Title page.—The John Henry Member of the Straight Cliffs Formation in Smoky Hollow, Kaiparowits Plateau, Utah. In this area the John Henry consists mostly of crevasse splay deposits that accumulated updip of extensive coal deposits, which accumulated in raised mires. Cliff is about 200 m high. Original color slide by Peter J. McCabe.

USGS Research on Energy Resources—1990 Program and Abstracts

Edited by L.M.H. Carter

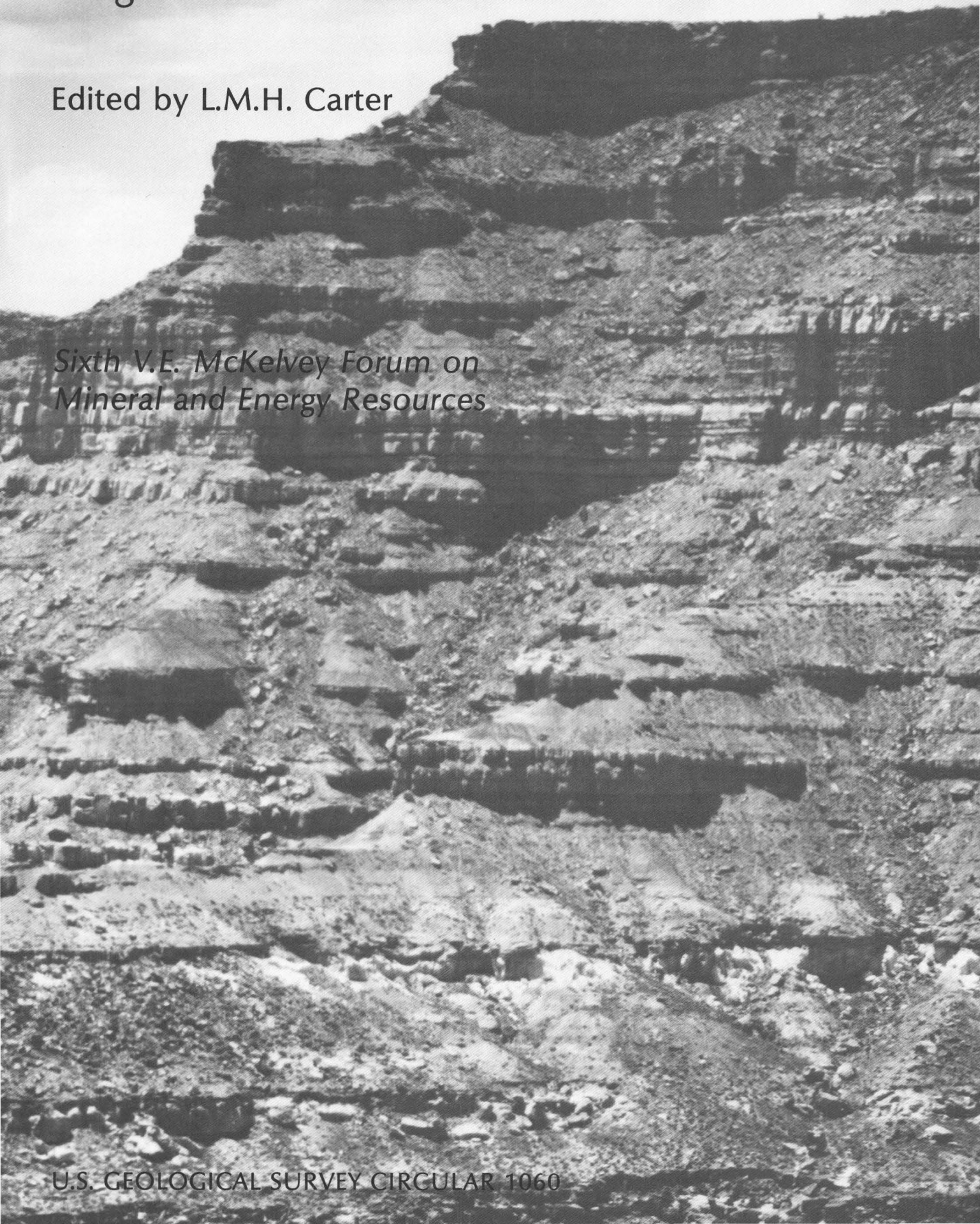

Sixth V.E. McKelvey Forum on Mineral and Energy Resources

U.S. GEOLOGICAL SURVEY CIRCULAR 1060

DEPARTMENT OF THE INTERIOR
MANUEL LUJAN, JR., Secretary

U.S. GEOLOGICAL SURVEY
Dallas L. Peck, Director

UNITED STATES GOVERNMENT PRINTING OFFICE: 1990

Organizing Committee for the 1990 McKelvey Forum:

Charles W. Holmes, Chairman
Michael E. Brownfield
Lorna Carter
Anny B. Coury
Edward Johnson
Peter J. McCabe
William H. Orem
James W. Schmoker
Christine E. Turner-Peterson
Brenda Williams

Library of Congress Cataloging in Publication Data

V.E. McKelvey Forum on Mineral and Energy Resources
(6th : 1990 : Houston, Tex.)
USGS research on energy resources—1990.

(U.S. Geological Survey circular ; 1060)
Supt. of Docs. no.: I 19.4/2:1060
1. Power resources—Congresses. I. Carter, Lorna M.
II. Geological Survey (U.S.) III. Title. IV. Series.
TJ163.15.V36 1990 553.2 89-600399

Free on application to the Books and Open-File Reports Section,
U.S. Geological Survey, Denver Federal Center,
Box 25425, Denver, CO 80225

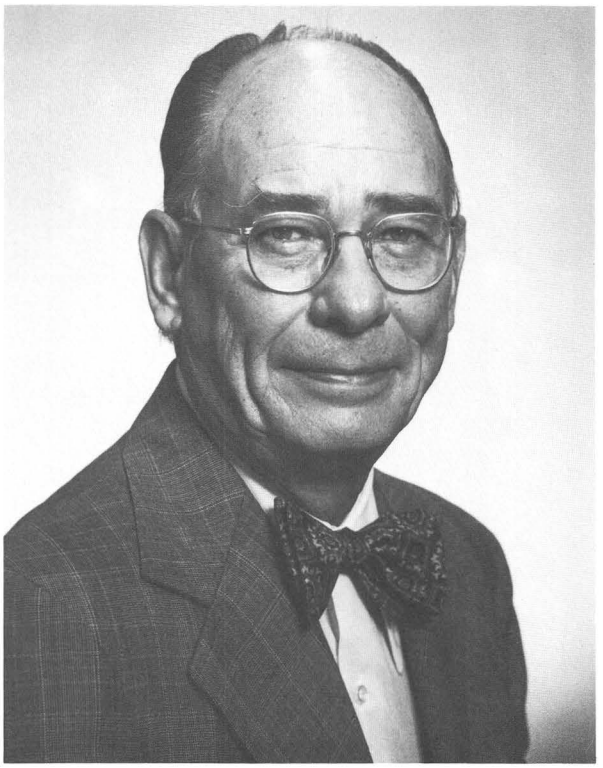

A society's wealth depends on the use it makes of raw materials, energy, and especially ingenuity.

—V.E. McKelvey

FOREWORD

Dallas L. Peck, Director, U.S. Geological Survey

The extended abstracts in this volume are summaries of papers presented orally and as posters at the sixth annual V.E. McKelvey Forum on Mineral and Energy Resources, entitled "Energy Research for the 1990's—Anticipating the Needs of the 21st Century." The McKelvey Forum serves as an opportunity for communication between the USGS and the earth-science and mineral and energy communities by presenting the results, recent progress, and pertinent data of current USGS research in formal lectures and posters. The poster sessions and the more informal meetings during the Forum provide many opportunities for concerned persons to meet individually with our scientists. I hope that the 1990 McKelvey Forum will help make our programs even more responsive to the needs of these communities, particularly to the fossil-energy industry, and that the interaction and cooperation begun here will continue to expand.

The Forum is named for former Director Vincent E. McKelvey in recognition of his lifelong dedication to the study of mineral and energy resources as research scientist, Chief Geologist, and Director of the U.S. Geological Survey. The Forum is an annual event that alternates in subject matter between mineral and energy resources; this year the emphasis is on energy. Although the format and topics addressed change somewhat from year to year, the primary purpose of the Forum remains the same: to encourage direct communication between USGS scientists, the representatives of other earth-science and mineral and energy organizations, and interested individuals.

Energy programs of the USGS include investigations related to oil and gas, coal, geothermal resources, uranium, thorium, and oil shale. Our studies encompass the entire National domain, including the offshore Exclusive Economic Zone. Presentations in this year's Forum summarize recent research in basin analysis, reservoir characterization, geochemistry applied to energy resources, and assessment of the Nation's energy resources. A growing number of citizens of this country are becoming increasingly aware of the importance of effective, efficient utilization of our Nation's energy endowment. Research results presented at this Forum will contribute directly to that goal, and we are excited by the opportunity to present them to you and to start discussions with our colleagues in industry and academia.

We welcome your suggestions concerning future energy research directions and projects and also for improving the McKelvey Forum.

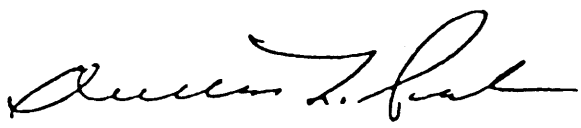

Sixth V.E. McKelvey Forum on Mineral and Energy Resources
Energy Research for the 1990's—
Anticipating the Needs of the 21st Century

HOUSTON, TEXAS, FEBRUARY 20–22, 1990

PROGRAM OF LECTURES AND DISCUSSIONS

TUESDAY, FEBRUARY 20, 1990

4:00–7:00 p.m.	Registration, Hyatt Regency Downtown
5:00–7:00 p.m.	Ice breaker - cash bar

WEDNESDAY, FEBRUARY 21, 1990

7:00 a.m.	Registration (registration desk will be open throughout the forum)

OPENING SESSION

Hal Gluskoter, presiding

8:15 a.m.	Welcome and opening remarks *Dallas L. Peck*
8:30	Energy research for the 1990's *Gary W. Hill*
9:00	Introduction of keynote speaker *Benjamin A. Morgan* KEYNOTE ADDRESS *Albert W. Bally*
9:40	Break for Coffee and Posters

TECHNICAL SESSION 1: GENERAL SESSION

Hal Gluskoter, presiding

10:05	Basin analysis as an exploration tool—Paradigms lost, insights gained *Christine E. Turner-Peterson and Neil S. Fishman*
10:30	Predictive and actual results from 2,500 wildcat wells, offshore Gulf of Mexico *L.J. Drew and J.H. Schuenemeyer*
10:55	Impact of drilling off Key West, Florida—Where's the beef? *Eugene A. Shinn*
11:20	Subsidence, eustasy, and climate—Controls on coal and clastic facies architecture, Cretaceous of Western United States *P.J. McCabe, R.D. Hettinger, M.A. Kirschbaum, J.D. Sanchez, and K.W. Shanley*
11:45	New insights from GLORIA sidescan-sonar images *T.R. Bruns and D.C. Twichell (combining work summarized in abstracts by Bruns and others and Twichell and others)*
12:00	Adjournment of Technical Session 1; lunch
1:00–1:40	POSTER SESSION

PROGRAM OF LECTURES AND DISCUSSIONS (CONTINUED)

TECHNICAL SESSION 2: APPLICATIONS OF GEOCHEMISTRY TO ENERGY RESOURCE STUDIES

T.S. Ahlbrandt, presiding

1:40 p.m.	Laser Raman and luminescence spectroscopy of carbonate minerals—Progress toward nondestructive microprobe techniques for stable isotopes, trace elements, and organic matter in zoned cements *R.C. Burruss, T.G. Ging, K.R. Cercone, V.A. Pedone, and T.S. Hayes*
2:05	Petroleum potential of Midcontinent Rift System, Iowa—Organic matter and porosity preserved in 1-billion-year-old rocks *James G. Palacas, James W. Schmoker, and Raymond R. Anderson*
2:30	The global methane hydrate reservoir—Impact on petroleum exploration *Keith A. Kvenvolden and Timothy S. Collett*
2:55	Domed, rainfall-dominated peat in Indonesia as a model for low-sulfur coal *Sandra G. Neuzil*
3:20	Enhanced upwelling and organic productivity during the late Quaternary in the northeastern Pacific Ocean *Walter E. Dean and James V. Gardner*
3:45	Once a menace, now a burgeoning source of energy—Coal-bed methane in the Warrior and San Juan Basins *James E. Fassett*
4:10	Controls, habitat, and resource potential of ancient bacterial gas *Dudley D. Rice*
4:35	Global changes in climate, carbon dioxide, and organic-carbon burial over the last 110 million years *Michael A. Arthur, Walter E. Dean, and David J. Allard*
5:00	Adjournment of Technical Session 2

WEDNESDAY EVENING, FEBRUARY 21, 1990

7:30	DIRECTOR'S LECTURE: Fractal geometry, chaos theory, and their application in the petroleum industry *Christopher C. Barton*
8:30–10:00 p.m.	POSTER SESSION

THURSDAY, FEBRUARY 22, 1990

TECHNICAL SESSION 3: RESERVOIR CHARACTERIZATION

Donald L. Gautier, presiding

8:15 a.m.	The search for subtle traps across onshore Alaska *David G. Howell*
8:40	Natural gas hydrates in the Prudhoe Bay-Kuparuk River area of northern Alaska *Timothy S. Collett*
9:05	Characterization of hydrocarbon reservoirs in eolian sandstones *C.J. Schenk*

PROGRAM OF LECTURES AND DISCUSSIONS (CONTINUED)

9:30	Architectural studies in eolian reservoir rocks—The Lower Jurassic Nugget Sandstone of northeastern Utah *Fred Peterson and C.J. Schenk*
9:55	Break for Coffee and Posters
10:20	Variation of modern siliciclastic turbidite systems and basin settings—Implications for reservoir development *C. Hans Nelson*
10:45	Application of ground-penetrating radar to development of reservoir models *Donald L. Gautier, C. J. Schenk, and Gary R. Olhoeft*
11:10	Prediction of sandstone porosity—An extension of the concept of thermal maturity *James W. Schmoker and Timothy C. Hester*
11:35	Adjournment of Technical Session 3
12:00	McKELVEY FORUM LUNCHEON Guest Speaker: John M. Sayre, Assistant Secretary—Water and Science, Department of the Interior

TECHNICAL SESSION 4: BASIN AND REGIONAL STUDIES

Walter E. Dean, presiding

2:00 p.m.	Comparative evolution of western North America and southern Kazakhstan, U.S.S.R.—Two early Paleozoic carbonate passive margins *Harry E. Cook and Michael E. Taylor*
2:25	Reassessment of tectonic history of the eastern Gulf of Mexico *Mahlon M. Ball, Ray Martin, and Richard Q. Foote*
2:50	Gulf of Mexico basin evolution—Geophysical and tectonic framework *Kim D. Kiltgord, D. R. Hutchinson, and Hans Schouten*
3:15	Deep-water fan deposits, Gulf of Mexico—Seeing through salt seismically *Robert E. Mattick and Frederick N. Zihlman*
3:40	Rifts and hot spots—A model for the Proterozoic Midcontinent Rift System of North America *D.R. Hutchinson and R.S. White*
4:05	Interplay of tectonism and sea-level change—Lessons from the U.S. Atlantic margin *C. Wylie Poag*
4:30	Conclusion of Forum

V. E. McKELVEY FORUM—POSTER SESSIONS

Coal Quality

Paleolatitude—A primary control on the sulfur content of United States coal
Ronald H. Affolter and Gary D. Stricker

Petrography of Permian "Gondwana" coals from boreholes in northwestern Bangladesh
Neely Bostick, Hal Gluskoter, M. Nazrul Islam, and Q.M. Arifur Rahman

Sulfur in coal—NCRDS applications
M.D. Carter, S.J. Tewalt, L.J. Bragg, and R.B. Finkelman

Origin and distribution of inorganic elements in the Wyodak-Anderson coal bed, Powder River basin, Wyoming
S.S. Crowley, R.W. Stanton, D.M. Triplehorn, and L.F. Ruppert

Carbon isotopic trends in peats and coals—Clues to carbon history and the environment of coal-forming mires
Charles W. Holmes

Quality parameters of Permian (Gondwana) coal, Khalaspir, Bangladesh
E.R. Landis, M.N. Islam, and Hal Gluskoter

Data analysis and display techniques of the National Coal Resources Data System, a geologic data system
William G. Miller, Kathleen K. Krohn, Carol L. Molnia, and Susan J. Tewalt

Early stage diagenesis of plant biomolecules in peats
William H. Orem and Harry E. Lerch

Pyritic sulfur and trace-element affinities in facies of the Upper Freeport coal bed, Allegheny Formation, west-central Pennsylvania
Brenda S. Pierce and Ronald W. Stanton

Microbially mediated fixation of uranium, sulfur, and iron in a peat-forming montane wetland, Larimer County, Colorado
E.I. Robbins, R.A. Zielinski, J.K. Otton, D.E. Owen, R.R. Schumann, and J.P. McKee

Diagenesis of organic matter and sulfur in sapropel and peat from Mud Lake, Florida
E.C. Spiker, P.G. Hatcher, V.J. Comer, A.L. Bates, and S.A. Stout

Liquefaction potential of facies of the Wyodak-Anderson coal bed, Powder River basin
R.W. Stanton, P.D. Warwick, and S.S. Crowley

Is there a future for 4.0 trillion tons of low-sulfur Alaskan coal?
Gary D. Stricker

Depositional and diagenetic controls on the residence and isotopic composition of sulfur in Middle Pennsylvanian coals, southeast Iowa and northwest Illinois
Michele L. Tuttle, Cynthia A. Rice, Joseph R. Hatch, and Richard D. Harvey

POSTER SESSIONS (CONTINUED)

Chemical and physical characteristics of coal beds from the Salt Range coal field, Punjab province, Pakistan
P.D. Warwick, T. Shakoor, S. Javed, S.T.A. Mashhadi, and M.I. Ghaznavi

Evolution of Sedimentary Basins

Thermal maturation in the Uinta basin, Utah
D.E. Anders

Subsurface studies, Santa Maria province, California
K.J. Bird, P.H. McClellan, and T.R. Bruns

The USGS Evolution of Sedimentary Basins program
Walter E. Dean, Samuel Y. Johnson, and Thomas D. Fouch

Sedimentology, diagenesis, and reservoir character of Paleogene fluvial and lacustrine rocks, Uinta intermontane basin, Utah—Evidence from the Altamont and Red Wash fields
T.D. Fouch, J.K. Pitman, Adam Szantay, and F. G. Ethridge

Basin development and resultant sedimentation patterns during the transition from Sevier- to Laramide-style tectonism, central Utah
Karen J. Franczyk, Timothy F. Lawton, and J.K. Pitman

Geologic evolution of the Uinta-Piceance basin province, northwestern Colorado and northeastern Utah
S.Y. Johnson, M.L. Tuttle, Bruce Bryant, R.F. Dubiel, T.D. Fouch, K.J. Franczyk, V.J.S. Grauch, M.A. Grout, R.C. Johnson, C.M. Molenaar, D.J. Nichols, K.M. Nichols, V.F. Nuccio, Fred Peterson, J.K. Pitman, W.J. Perry, Jr., D. Sawatzky, R.W. Scott, E.R. Verbeek, and R.B. Wanty

Applications of expert systems and geographic information systems to basin characterization—Case study for the San Juan Basin, New Mexico
Betty M. Miller

Stratigraphic cross sections of Upper Cretaceous rocks across the San Juan Basin, northwestern New Mexico and southwestern Colorado
Cornelius M. Molenaar and James K. Baird

Genetic lithofacies in the Dakota Sandstone, a major oil- and gas-producing formation, northern San Juan Basin, Colorado and New Mexico
J.L. Ridgley

Basin analysis study of the San Juan Basin, Colorado and New Mexico
J.L. Ridgley and A.C. Huffman, Jr.

Structural and basement-lithological implications of gravity and seismic-reflection data across the central Powder River basin from the Black Hills to the Bighorn Mountains
S.L. Robbins and J.A. Grow

Age, facies, and depositional environments of the lower Miocene Lospe Formation, Santa Maria basin, central California
Richard G. Stanley, Samuel Y. Johnson, John D. Obradovich, Michele L. Tuttle, Mary Lou Cotton Thornton, David R. Vork, Mark V. Filewicz, Mark A. Mason, and Carl C. Swisher III

POSTER SESSIONS (CONTINUED)

The Point Lookout Sandstone—Changing formation architecture from strandplain to delta
Robert S. Zech and Robyn Wright-Dunbar

Geochemistry

Uranium favorability in the Chadron Formation, southeastern Wyoming and northwestern Nebraska
K.A. Dickinson and P.L. Hansley

Sulfur isotope evidence for the origin of cap-rock-hosted sulfide deposits, Hockley salt dome, Texas
J. Richard Kyle, William N. Agee, Tim W. Johnson, and W.C. Shanks, III

Geochemical evaluation of gas-bearing coals with respect to maturity, Upper Cretaceous Fruitland Formation, San Juan Basin, New Mexico and Colorado
G.E. Michael, B.E. Law, and D.E. Anders

Manganese nodules and microbial fixation of oxidized manganese in the Huntley Meadows Wetland, Fairfax County, Virginia
E.I. Robbins, J.P. D'Agostino, Virginia Carter, D.S. Fanning, C.J. Gamble, J. Ostwald, R.L. Van Hoven, and G.K. Young

Genesis and distribution of uraninite in solution-collapse breccia pipes, northwestern Arizona
Karen J. Wenrich, Bradley S. Van Gosen, and Hoyt B. Sutphin

Marine Geology and the GLORIA Program

GLORIA images from the Gulf of Alaska and British Columbia—Subduction zones, transforms, and channels
T.R. Bruns, P.R. Carlson, A.J. Stevenson, M.A. Fisher, H.F. Ryan, D.M. Mann, Maxwell Dobson, Quentin Huggett, Lindsay Parson, and N.G.T. Fannin

Structural segmentation in an active submarine tectonic accretionary wedge, as disclosed by GLORIA sidescan sonar and multichannel seismic profiling, Caribbean plate boundary north of Haiti
William P. Dillon, James A. Austin, Kathryn M. Scanlon, N. Terence Edgar, Lindsay Parson, and Gordon E. Ness

Sedimentary patterns on the mid-Atlantic continental rise as discerned by a GLORIA sidescan survey
John S. Schlee and James M. Robb

A structural and stratigraphic transect across the Florida platform from the deep Gulf of Mexico to the deep Atlantic
B. Ann Swift, William P. Dillon, Myung W. Lee, and Mahlon M. Ball

Depositional processes revealed by GLORIA sidescan sonar images on the Mississippi fan
David C. Twichell, Neil H. Kenyon, and Bonnie A. McGregor

Reservoir Characterization and Petroleum Research

Evidence for a geologically rapid increase and stabilization of vitrinite reflectance in response to a short-term temperature increase, Cerro Prieto geothermal system, Mexico
Charles E. Barker

POSTER SESSIONS (CONTINUED)

Stabilization of kerogen thermal maturation—Evidence from geothermometry and burial history reconstruction, Niobrara Limestone, Berthoud oil field, western Denver basin, Colorado
Charles E. Barker and Bonnie L. Crysdale

A fluid-inclusion technique for determining peak temperature and its application to establish a refined calibration for the vitrinite reflectance geothermometer
Charles E. Barker and Robert H. Goldstein

Subsurface exploration with the aid of borehole gravimetry
Larry A. Beyer

Cretaceous and Tertiary Sagavanirktok Formation in the Prudhoe Bay–Kuparuk River area, northern Alaska
Timothy S. Collett and Kenneth J. Bird

New information on the Nuwok Member of Sagavanirktok Formation; implications for petroleum geology of the North Slope and Beaufort Sea—Evidence from Carter Creek, Arctic National Wildlife Refuge (ANWR), Alaska
T.D. Fouch, E.M. Brouwers, D.H. McNeil, Louie Marincovich, Jr., K.J. Bird, and H. Rieck

A seismic reflection study of Miocene listric faulting north of Lake Mead, Nevada
J.A. Grow, R.G. Bohannon, J.J. Miller, and R.E. Anderson

Effects of basin evolution on source-rock characteristics of the Woodford Shale, Anadarko basin, Oklahoma
Timothy C. Hester, James W. Schmoker, and Howard L. Sahl

Reservoir characteristics of the Lower Cretaceous J sandstone in the Kachina field, Denver basin, Colorado
Debra K. Higley

Computer display of petroleum exploration through time in the Denver basin of Colorado, Nebraska, and Wyoming
Debra K. Higley and Kenneth I. Takahashi

Petroleum geology studies in the Santa Maria province, California
Caroline M. Isaacs, J. David King, Richard M. Pollastro, and Colin F. Williams

Diagenesis of sandstones in the Norphlet Formation (Upper Jurassic), Escambia County, Alabama
C.W. Keighin and C.J. Schenk

Thermal evolution of the Upper Cretaceous Fruitland Formation, San Juan Basin, Colorado and New Mexico
Ben E. Law

Identified petroleum systems within the United States—A 1990 status report
Leslie B. Magoon

Preliminary reinterpretation of the Ouachita frontal zone near Hartshorne, Oklahoma, based chiefly on seismic reflection data
W.J. Perry, Jr., Warren Agena, and N.H. Suneson

POSTER SESSIONS (CONTINUED)

Algal mound carbonate reservoir, Aneth oil field, Paradox basin, Utah—Origin and related petroleum geology
James A. Peterson

Western tight gas reservoirs—Resource potential and development constraints
Charles W. Spencer, Ben E. Law, and Ronald C. Johnson

Resource Assessment

Play analysis methodologies for petroleum resource assessment
Robert A. Crovelli and Richard H. Balay

Deep oil and gas wells and reservoirs in the United States from the Well History Control System and Petroleum Data System
T.S. Dyman, D.T. Nielsen, R.C. Obuch, J.K. Baird, and R.A. Wise

New methodologies for assessment of U.S. oil-shale resources
John R. Dyni

New developments in uranium endowment assessment in the United States
Warren I. Finch, Charles T. Pierson, Richard B. McCammon, James K. Otton, Hoyt B. Sutphin, and Karen J. Wenrich

Coal Resources and Their Sedimentological Setting

Coal availability studies—A progress report
M. Devereux Carter, Nancy K. Gardner, Richard E. Sergeant, Elizabeth V.M. Campbell, and Nick Fedorko, III

Architecture of clastic facies and location of coals associated with a major marine transgression—The mid-Cretaceous of the Kaiparowits Plateau, Utah
Robert D. Hettinger and Peter J. McCabe

Alluvial sandstone geometries and their relationship to coal deposition in a transgressive systems tract, Dakota Formation, Utah
Mark A. Kirschbaum and Peter J. McCabe

Characteristics of coal-bearing strata in Tertiary basins, based on integrated sedimentary and structural field studies, southwestern Montana
J.W. M'Gonigle, M.H. Hait, Jr., and W.J. Perry, Jr.

New tonstein beds in the Middle Pennsylvanian of the central Appalachian basin—Time lines for basin analysis
W.F. Outerbridge, P.C. Lyons, and D.M. Triplehorn

Variations in facies architecture related to sequence stratigraphy of the Turonian-Campanian strata, Kaiparowits Plateau, south-central Utah
Keith W. Shanley and Peter J. McCabe

Coal resources in Sind province, Pakistan
Roger E. Thomas, Mohammed Riaz Khan, and Shafique Ahmed Khan

Sixth V. E. McKelvey Forum on Mineral and Energy Resources

USGS Research on Energy Resources—1990 Program and Abstracts

Edited by L. M. H. Carter

Paleolatitude—A Primary Control on the Sulfur Content of United States Coal

Ronald H. Affolter and Gary D. Stricker

Previous studies on sulfur in coal have stressed the importance of depositional environments in controlling sulfur content. For example, peats overlain by marine to brackish-water sediments often have high sulfur contents, whereas fresh-water peats are low in sulfur. Isotope studies have shown that microorganisms play a direct role in concentrating sulfur in humic substances and that most sulfur in coal is incorporated during the early development of the peat. Sulfur enters the peat environment as sulfate and is reduced by the action of sulfate-reducing bacteria. The rate of sulfate reduction by bacteria, however, is strongly dependent on temperature and seasonal variations. Rates of sulfate reduction are generally inhibited by lowering the temperature about 5–10 °C. Although other factors do influence the sulfur content of peats, we suggest that one primary control is the activity of the sulfate-reducing bacteria in peat, and that the latitude of formation of the peat swamp affects this activity.

Solar radiation striking the Earth at higher latitudes traverses greater distances and through a greater mass of atmosphere than at lower latitudes. This radiation at higher latitudes is also depleted by absorption, reflection, and scattering. Because of these factors, there is a surplus of solar energy between lat 0° and 38° (more incoming energy than outgoing)and a deficit between lat 38° and 90° (more outgoing energy than incoming). Assuming that the pattern of incident solar radiation has remained relatively constant through time, then the mean incident solar radiation averaged over a year can be calculated. Our calculations show that Interior and Appalachian Carboniferous peat swamps received approximately 845 cal cm^{-2} day^{-1}, Rocky Mountain province Cretaceous peat swamps 600 cal cm^{-2} day^{-1}, Northern Great Plains Tertiary peat swamps 550 cal cm^{-2} day^{-1} and Gulf Coast Tertiary peat swamps 660 cal cm^{-2} day^{-1}. Alaska Tertiary peat swamps received 380 cal cm^{-2} day^{-1} and Alaska Cretaceous peat swamps 365 cal cm^{-2} day^{-1}.

Our hypothesis that latitude and thereby solar radiation influence sulfur in peat is supported by an evaluation of more than 8,000 United States coals. Most Interior and Appalachian Carboniferous peats accumulated at latitudes between 0° and 15° S., Rocky Mountain province Cretaceous peats between 30° and 45° N., Northern Great Plains Tertiary peats between 40° and 55° N., and Gulf Coast Tertiary peats between 30° and 40° N. Alaskan Cretaceous and Tertiary peats accumulated at latitudes above 70° N. A comparison of paleolatitudes calculated from paleomagnetic poles and sulfur contents indicates that the higher the latitude in which a peat swamp developed, the lower the mean sulfur content of the subsequent coal (correlation coefficient –0.45; significant at the 99 percent confidence level). Mean sulfur contents are 2.34 percent ($n = 5{,}497$, range = 0.1 to 19.2 percent, std. dev. = 1.92) in low-latitude Carboniferous coal; 0.86 percent ($n = 2{,}754$, range = 0.02 to 18.9 percent, std. dev. = 0.97) for middle-latitude Cretaceous and Tertiary coals; and 0.32 percent ($n = 262$, range = 0.01 to 6.6 percent, std. dev. = 0.48) in high-latitude Alaskan Cretaceous and Tertiary coal.

The latitude of peat formation determines the amount of incident solar radiation (energy) available to the system. At high latitudes lower temperatures result in lower rates of sulfate reduction, whereas at low latitudes higher temperatures result in higher rates of sulfate reduction. Therefore, in general, lower sulfur coals formed at high latitudes and higher sulfur coals formed at lower latitudes.

Manuscript approved for publication December 15, 1989.

Thermal Maturation in the Uinta Basin, Utah

D.E. Anders

The Uinta basin (24,000 km^2) in northeastern Utah contains abundant energy resources including oil, natural gas, tar sands, coal, gilsonite, and oil shale. The principal source of the oil, tar sands, and gilsonite is the kerogenous/bitumen-rich sedimentary rocks of the Green River Formation deposited in late Paleocene to late Eocene age lacustrine systems. Based on classical chemical maturity parameters (n-alkane distribution and carbon preference indices, hydrocarbon/-non-hydrocarbon, API gravity, triaromatic/-(triaromatic+monoaromatic) steroid ratios, 22S/22R bishomohopane and 20S/20R–5α,14α,17α ethylcholestane), these energy resources were derived from source rocks covering a wide range of thermal maturities. In addition to hydrocarbons derived from thermally mature source rocks, numerous oil, tar sand, and gilsonite deposits have chemical properties characteristic of organic matter derived from immature source rocks. That these immature hydrocarbon deposits are widespread suggests that we have had a limited prior understanding of hydrocarbon generation within Green River source rocks.

In an effort to better understand the thermal histories of hydrocarbon generation in the Uinta basin, we investigated the level of thermal maturity at which Green River Type I kerogen produces liquid hydrocarbons, using vitrinite reflectance (percent), Rock Eval (T_{max}) and transformation ratio, atomic H/C ratio, hydrocarbon yield, time-temperature indices (TTI), subsurface temperature, and biological marker isomerization, degradation, and aromatization ratios.

Mean random vitrinite reflectance (R_m) values for surface rocks of the Uinta, Duchesne River, and Browns Park Formations in the north half of the basin range from 0.3 to 0.5 percent. R_m values for surface rocks of the Green River and Wasatch Formations in the south half of the basin range from 0.5 to 0.7 percent. Surface exposures of Cretaceous coals along the southern margin of the basin have R_m values in the range 0.6–0.7 percent. Reflectance values for subsurface rocks of approximately equal age and depth are variable throughout the basin. For example, at the 3,060 m depth, R_m values for Eocene rocks range from 0.4–0.5 percent at Starr Flats, to 0.7–0.8 percent at Red Wash, to 0.8–0.9 percent at Altamont, to 0.9–1.0 percent at South Ouray, to 1.0–1.1 percent at Natural Buttes. These variations reflect differences in geothermal gradient, maximum depth of burial, hydrologic cooling, and heat transfer across the basin. Generally, for a given stratigraphic unit, R_m values increase southward due to higher geothermal gradients, but also increase northward due to increased depth of burial.

Atomic H/C ratios for Type I kerogen are linearly related to R_m values in the stage of catagenesis (0.5 to 1.3 percent). Hydrogen/carbon ratios for Type I kerogens of the Uinta basin decline from a high of 1.4 at a R_m equivalence of 0.5 percent to a low of 0.65 at a R_m equivalence of 1.3 percent.

Rock-Eval temperature indices (T_{max}) show a greater increase (390 to 445 °C) in the early stages of thermal evolution (0.3 to 0.5 percent R_m) of Green River kerogen, but a lesser increase (445 to 455 °C) in the catagenesis stage (0.5 to 1.4 percent, R_o). Rock-Eval transformation ratios (T.R.) show little change until the main stage of catagenesis (oil window). Around 0.6 to 0.7 percent R_m, the T.R.'s begin to increase from average values of 0.1 to a maximum of 0.6 in the 1.1 to 1.3 percent R_m range.

Hydrocarbon yield as a function of R_m shows the main stage of liquid hydrocarbon generation is in the 0.7 to 1.2 percent R_m range with abundant liquid hydrocarbons preserved to at least 1.4 percent R_m.

The thermal gradients of the Uinta basin are locally variable, but systematically trend from higher values in the south (2.2 °F/100 ft; 39 °C/km) to lower values in the north (0.6 °F/100 ft; 11 °C/km). This systematic change parallels a thickening of less thermally conductive marls, shales, and conglomerate northward. Cooling in the north may result from downward movement of meteoric waters along faults and fractures associated with the Uinta Mountain front and (or) heat transfer from the less conductive sedimentary rocks to the more conductive quartzite-rich rocks of the Uinta Mountains.

Based on current thermal gradients and the level of thermal maturity necessary to bring about catagenesis of Green River kerogen, maximum depths of burial and temperatures at the beginning and end of oil generation were predicted for five basin wells using the Waples TTI model. The TTI model indicates oil production from Green River Type I kerogen begins at about 100 °C, maximizes at 115 °C and ends between 135 and 140 °C, with preservation of hydrocarbons continuing to at least 145–150 °C. R_m values corresponding to the beginning, peak, and end of oil generation are: 0.7, 0.9, and 1.2 percent R_m, respectively.

Extraction ratios (EOM/TOC) in thermally immature (< 0.6 percent R_m) Green River Formation shale were found to average 22.5 percent. Tuffs, microfractures, and sandstone contiguous to these immature shales were often filled with immature hydrocarbons. This indication of migration of immature hydrocarbons can be coupled with the presence of biomarker ratios indicative of hydrocarbons derived from rocks with reflectance values < 0.6 percent R_m (in the giant tar sand

deposits of Asphalt Ridge, P.R. Springs and Raven Ridge, the large gilsonite deposits of the East Central basin, and a significant number of shallow oils) to present convincing evidence of migration of large quantities of thermally immature hydrocarbons in the Uinta basin.

Global Changes in Climate, Carbon Dioxide, and Organic-Carbon Burial over the Last 110 Million Years

Michael A. Arthur, Walter E. Dean, and David J. Allard

Available paleoclimate data support the existence of a warm, equable global climate during the middle to Late Cretaceous, a climate which deteriorated in a series of steps toward the glacial late Neogene and Quaternary. Climate-model studies suggest that the concentration of CO_2 (carbon dioxide) in the atmosphere was 4 to 18 times higher during the Cretaceous than today, and this would have been an important climatic forcing factor. The most likely cause of variation in CO_2 was change in the balance between the rate of tectonic CO_2 outgassing and CO_2 consumption resulting from organic-carbon burial. We have no straightforward, independent evidence for the magnitude of possible CO_2 changes, but two indirect lines of evidence provide some indication of the amount of CO_2 variation. (1) Variations through time in CCD (carbonate compensation depth) in the ocean and in the carbon-isotope gradient between surface- and deep-water masses (as measured by the difference in isotopic composition of calcareous planktonic and benthic organisms) indicate that dissolved CO_2 in the ocean decreased by as much as a factor of 5 from the Late Cretaceous to the Holocene. (2) The carbon-isotopic composition of marine organic matter (amorphous kerogen) changed substantially over the same time interval and may be a CO_2 "paleobarometer." Experimental data and geologic evidence suggest that, in the past, a higher concentration of dissolved CO_2 may have led to greater carbon-isotope fractionation relative to the carbon source and to isotopically lighter fixed carbon in Cretaceous marine organic matter in comparison to that at present.

The photosynthetic fractionation of carbon isotopes in the ocean is taken as the difference between the $^{13}C/^{12}C$ ratio of bulk organic matter and that of carbonate carbon, the latter being a monitor of the carbon-isotopic composition of dissolved inorganic carbon. This fractionation has varied significantly over the last 110 million years. The $\delta\ ^{13}C$ of most Cretaceous marine organic matter is –27‰ or lighter, in contrast to that of Neogene and Quaternary organic matter, which averages about –22‰ or heavier. The $\delta^{13}C$ of terrestrial higher plant material has remained approximately constant at about –25‰ over the last 110 m.y. The $\delta\ ^{13}C$ of Cretaceous marine organic carbon was not always as low as -27‰ , however: at least one major positive excursion in organic carbon $\delta\ ^{13}C$ to values as high as –21‰ took place at the Cenomanian/Turonian boundary (C/T; ≈91 Ma). This isotopic excursion is coincident with a major inferred high-productivity episode that lasted less than 1 m.y. and resulted in significantly increased rates of organic-carbon burial. The C/T carbon-burial event apparently drew down atmospheric CO_2 and may have resulted in global climatic cooling, as suggested by the oxygen isotopic composition of inoceramid mollusks from England and northwest Germany. After the C/T event, the $\delta\ ^{13}C$ of marine organic matter decreased and the climate warmed again in the Late Cretaceous, followed by relatively minor variations of 1–2‰ through the Paleogene. One of the most significant changes in the isotopic composition of marine organic matter occurred in the early middle Miocene, coincident with major global cooling and Southern Hemisphere glaciation. It is likely that a sharp drop in CO_2 occurred in conjunction with a widespread increase in the rate of burial of organic matter in circum-Pacific upwelling zones (the so-called "Monterey hypothesis"), but it is not clear whether the CO_2 drop was the cause of global cooling.

Further information on changes with time of the isotopic composition of marine organic matter compared with that of pelagic carbonate will provide important constraints on compositional changes of the ocean-atmosphere system, evolution of the global climate system, and partitioning of carbon between crustal, sediment, and oceanic reservoirs.

Reassessment of Tectonic History of the Eastern Gulf of Mexico

Mahlon M. Ball, Ray Martin, and Richard Q. Foote

Our initial working hypothesis regarding the regional structural geology of the eastern Gulf of Mexico envisioned a set of northwest-trending fracture zones extending into the gulf across the Florida-Bahamas carbonate province. These faults were believed to have acted as transforms accommodating the opening of the Gulf of Mexico contemporaneously with initial spreading of the North Atlantic during the Late Jurassic. Working primarily with gravity and magnetic data, Kim Klitgord and others have proposed that blocks of pre-Mesozoic crust within the transform zones were separated by local zones of extension underlain by rifted thin transitional

crust or Jurassic oceanic crust. Reflection seismic data and subsurface control further constrain this interpretation. Paleozoic sedimentary rocks underlie the Western Florida Shelf north of lat 26° N. It follows that this region is not underlain by Jurassic oceanic crust. The crust north of lat 26° N. is essentially continental.

The deepest horizon that can be mapped seismically beneath the Western Florida Shelf is a major composite unconformity. The youngest known Paleozoic sedimentary rocks beneath this unconformity are Devonian. To the north in the Apalachicola basin and on the northern flank of the Middleground arch, rifting associated with the Mesozoic opening of the Atlantic and Gulf of Mexico formed half grabens that filled with Triassic red beds. These fills were deposited at least in part during rifting and erosion on adjacent highs. Erosion continued after cessation of graben formation with the result that Triassic block-faulted terrain was reduced to a peneplain. Subsequent onlap by Jurassic sediments and evaporites formed the angular unconformity revealed so clearly above infilled rifts in the reflection seismic lines crossing the Apalachicola basin. This relationship has resulted in identification of this erosion surface as the "post-rift unconformity" or "pre-Cretaceous" post-rift unconformity. To the south, on the Middleground arch, folding of Paleozoic rocks beneath the unconformity may be related to late Paleozoic compressional tectonism associated with the Carboniferous and Permian closing of the proto-Atlantic. Erosion on this regional unconformity may have begun in some places as early as the late Paleozoic and continued on the Peninsular arch of onshore Florida until the earliest Late Cretaceous. Most of the names applied to this unconformity have tended to obscure the extent of its composite nature.

The northwest-trending fault zones crossing South Florida and the Western Florida Shelf became active in the Late Jurassic and continued into the Early Cretaceous during the opening of the Gulf of Mexico. There are two schools of thought concerning these fault zones. Some believe them to be transforms with predominantly strike-slip offsets. Others question the sense of motion on these faults. The Bahamas fracture zone of Klitgord and others, more recently referred to as the Florida lineament of Christenson, is of particular interest. This feature appears to continue northwestward into the Gilbertown-Pickens-Pollard portion of the circum-Gulf fault system. This fault has normal displacement down to the south and west on the north and east flanks of Destin dome in the Apalachicola basin. The Middle and Upper Jurassic Louann Salt thins abruptly to the north and east across this fault. Toward the southeast, along the north margin of the South Florida basin, gravity data have been interpreted to indicate coincidence of this fault zone with a "hinge zone" and local relief on the Mohorovicic discontinuity. This interpretation reflects the use of erroneously low densities for the sedimentary fill of the South Florida basin.

Salt tectonism is inferred to have begun as early as Late Jurassic in the Apalachicola basin. The inferred salt swell forming the Destin dome began later in latest Early Cretaceous time and continued into the Cenozoic. Late faulting cutting to the sea floor on the crest of Destin dome may provide chimneys for escape of natural gas.

Evidence for a Geologically Rapid Increase and Stabilization of Vitrinite Reflectance in Response to a Short-Term Temperature Increase, Cerro Prieto Geothermal System, Mexico

Charles E. Barker

A short-term pulse of hot water affected rocks below 1,300 m in well M-94 (fig. 1, facing), Cerro Prieto geothermal system, and sharply increased the vitrinite reflectance (thermal maturity) of sedimentary organic-matter. A 1981 study of apatite fission-track annealing by S.J. Sanford indicates that this hot-water pulse passed through these rocks in about 10^1 yr. The paleotemperature rapidly changed from about 75–125 °C, the present measurement above 1,300 m depth, to a peak paleotemperature of 250–300 °C below 1,300 m in the hydrothermally-altered sedimentary rocks. Present (equilibrium log) temperature below 1,300 m has declined to 150–210 °C. The peak paleotemperature is estimated from the homogenization of reequilibrated fluid inclusions in calcite, and the calcite-water oxygen-isotope geothermometer, as discussed in 1981 papers by Barker and W.A. Elders, and S.J. Sanford, and a 1985 paper by S.M. Sterner. Clay mineralogy also changes sharply below 1,300 m, as indicated by the disappearance of smectite + kaolinite and the concomitant appearance of illite + chlorite; but these reactions indicate a paleotemperature of only 150–180 °C, as determined in a 1980 study by W.A. Elders and others. This discrepancy is possibly caused by slowness of metamorphic reactions in minerals.

Vitrinite reflectance of sedimentary organic-matter below 1,300 m increased to a level that is consistent with the other peak geothermometers. The correspondence of peak recording geothermometers with the vitrinite reflectance geothermometer suggests that sedimentary organic-matter reacts quickly to temperature increases of 50–100 °C above ambient even when that increase existed for only a short time—about 10^1 yr.

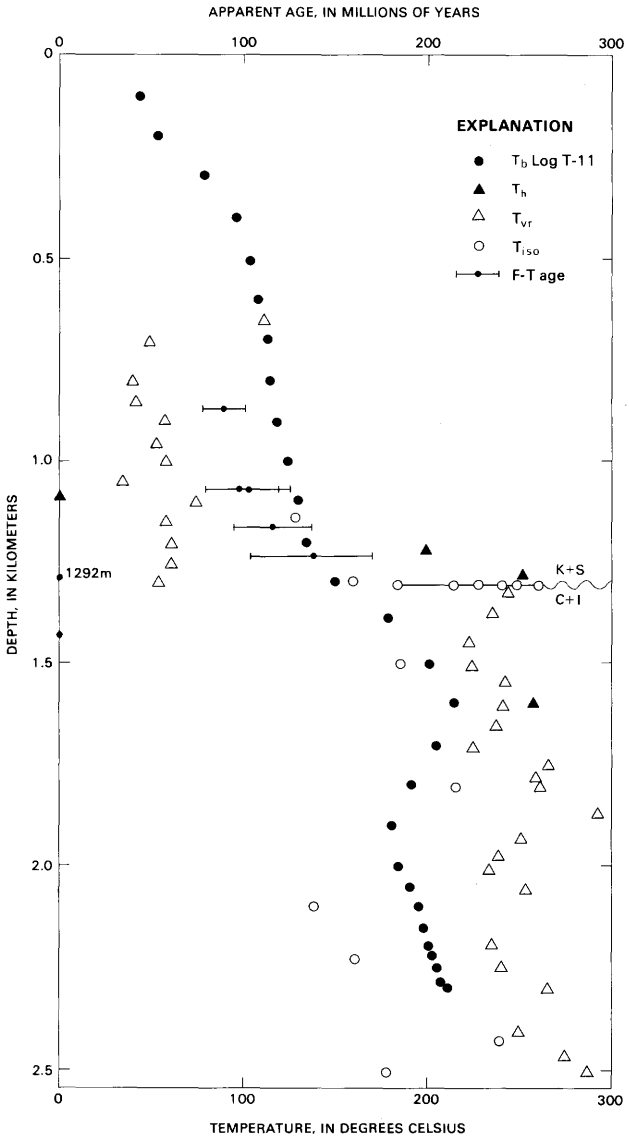

Figure 1 (Barker). Comparison of borehole temperature (T_b) data and other geothermometers in borehole M-94, Cerro Prieto system. Fission-track apatite age (F-T), fluid inclusion (T_h), and oxygen isotope (T_i) data are from 1981 study by S.J. Sanford. Mineral data are from 1978 report of W.A. Elders and others. Vitrinite reflectance data are from 1981 report by Barker and Elders. F-T dates are plotted with ± one standard deviation error bars.

Stabilization of Kerogen Thermal Maturation—Evidence from Geothermometry and Burial History Reconstruction, Niobrara Limestone, Berthoud Oil Field, Western Denver Basin, Colorado

Charles E. Barker and Bonnie L. Crysdale

The burial history of a fractured Niobrara Limestone reservoir and source rock (fig. 1, overleaf) offers a unique setting for studying the stabilization of thermal maturity, because soon after peak temperature of about 100 °C was reached, exhumation lowered temperature to about 60–70 °C. Vitrinite reflectance (Rm = 0.6–0.7 percent) and published clay mineralogy data from the Niobrara Limestone indicate that peak paleotemperature was approximately 100 °C. Fluid-inclusion data also indicate that oil migration occurred at 100 °C. Burial history reconstruction indicates that 100 °C was reached in the Niobrara Limestone only during maximum burial, which occurred at 70 Ma and 8,000 ft depth. However, erosion beginning at 70 Ma and continuing until 50 Ma removed more than 3,000 ft of rock. This depth of erosion agrees with an Rm of 0.4 percent measured in surface samples of the Pierre Shale above the field. The exhumation of the reservoir decreased temperature by about 30 °C to near the present-day bottom-hole temperature of 50–70 °C. Lopatin TTI analysis suggests that the Niobrara Limestone as a source rock matured to the oil-generation stage (TTI = 10) about 25 Ma, significantly later than maximum burial, and after exhumation caused cooling. The Lopatin TTI method in this case seems to overestimate the influence of heating time. If time is an important factor, thermal maturity should continue to increase after deepest burial and peak temperature, so that vitrinite reflectance will not be comparable to peak paleotemperatures estimated from geothermometers set at near-peak temperature and those estimated from burial history reconstruction. The good agreement between geothermometry and the burial history reconstruction in Berthoud State 4 suggests that the influence of heating time is negligible in kerogen thermal maturation. We infer from this conclusion that kerogen thermal maturation stabilizes after a geologically small reaction-time at peak burial temperature.

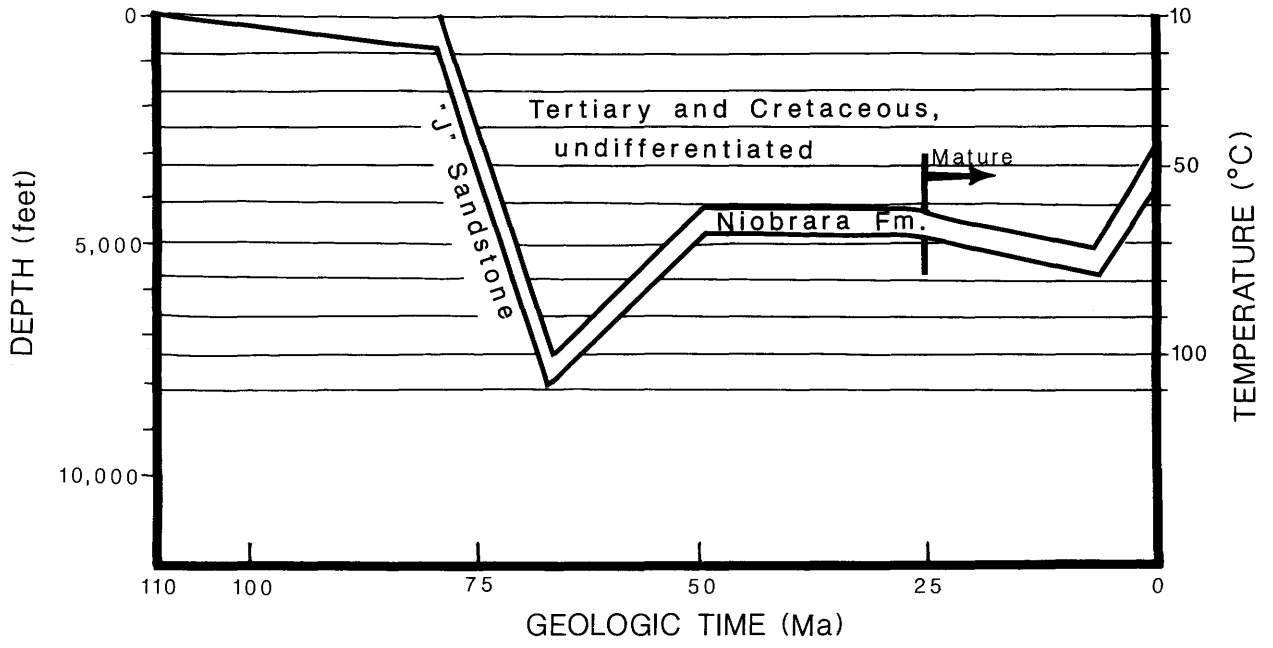

Figure 1 (Barker and Crysdale). Burial history of Niobrara Limestone reservoir through time. Modified from a 1982 thesis by P.A. Tainter.

A Fluid-Inclusion Technique for Determining Peak Temperature and its Application to Establish a Refined Calibration for the Vitrinite Reflectance Geothermometer

Charles E. Barker and Robert H. Goldstein

Theory, laboratory experiments, and empirical observation suggest that many low-temperature, aqueous fluid inclusions in calcite should reequilibrate and approach the peak temperature (Tpk) during natural overheating. Plots of homogenization temperature (Th) and Tpk for systems now at peak temperature (fig. 1, facing) demonstrate a direct relationship between the variables. Although caution should be applied, the relationships suggests that Th of fluid inclusions in calcite may be a useful measure of peak temperature.

Relationships between Tpk, heating duration, and thermal maturation of sedimentary organic-matter have been obscured by imprecise geologic data. This study uses the Th approximation of Tpk and compares it to mean random vitrinite reflectance (Rm) (fig. 2, p. 8) to develop a refined calibration for the vitrinite reflectance geothermometer. Fluid-inclusion and Rm data were measured or compiled from diverse geologic systems that have been at peak temperature from 10^4 to millions of years. Present Tpk ranged from 72 to 345 °C, Th from 55 to 347 °C, and Rm from 0.4 to 4.6 percent, spanning the temperature and thermal-maturity range associated with burial diagenesis, hydrothermal alteration, and low-grade metamorphism. The refined calibration is: $\ln(Rm) = 0.00776(Tpk) - 1.24$.

The strong correlation ($r = 0.90$) between Tpk and Rm in these systems suggests that peak temperature is the major control on thermal maturation.

Fractal Geometry, Chaos Theory, and Their Application in the Petroleum Industry

Christopher C. Barton

Fractal geometry and chaos theory provide a means of mathematically describing and modeling the complex repetitive patterns which earth scientists map, measure, and describe in ever-increasing detail. Fractal geometry is a branch of mathematics for quantifying how the geometry of self-similar systems changes from one scale to another. The self-similar repetition of many geologic patterns over a range of scales is demonstrated by the need to place an object of known size, such as a coin, hammer, or person, into photographs of geologic features in order to establish scale. A useful property of fractals is that small pieces are representative of the whole, and this permits prediction from the geometry of a small sample to the geometry of the larger system over a wide range of scales. The geometry of a fractal pattern is represented by a fractional number, termed the fractal

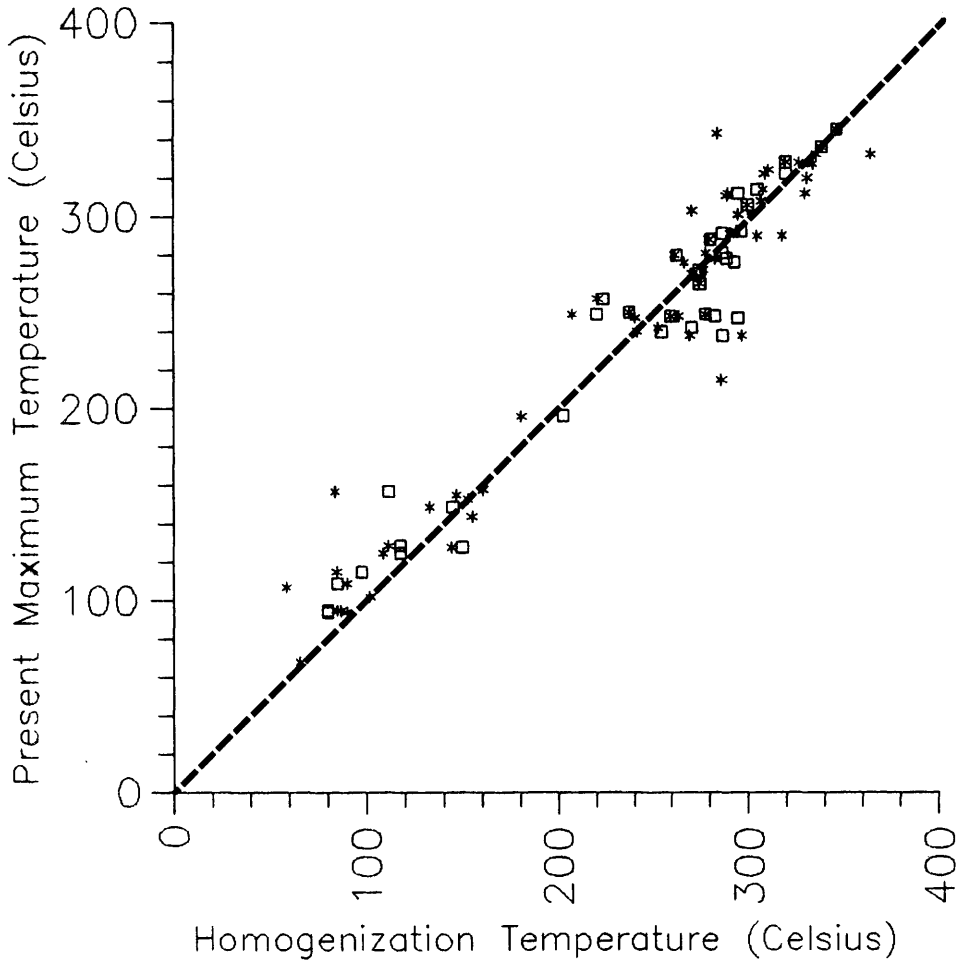

Figure 1 (Barker and Goldstein). Present maximum temperature (Tmax) versus the mean (stars) and modal (squares) homogenization temperature (Th) in calcite. Only data from systems now at maximum temperature and that have a measured value (bottom hole temperature) or a geothermal gradient reported are included. A 45 degree line is shown to illustrate perfect 1:1 correlation between Th and Tmax.

dimension. The scale over which a fractal dimension applies is bounded by the upper and lower fractal limit.

Many geologic patterns have been shown to be fractal, including reservoir heterogeneity, size and spatial distributions of pores, sequences of stratigraphic thickness, size and spatial distribution of petroleum reservoirs, fracture networks, porous-media flow, tributary river patterns, and topography. Fractal geometry provides a method for generating synthetic geometric analogs once the fractal dimension of the natural pattern has been determined. Fractal geometry also permits extrapolating geologic patterns from a one-dimensional sample (boreholes) to two or three dimensions.

Chaos theory studies the paths along which nonlinear differential equations converge upon multiple solutions termed strange attractors. The paths are generated by iterating nonlinear equations and plotting the pattern of the solutions. Initially, the solutions plot along a single path, but with continued iteration the solution path bifurcates into two, four, eight, etc. solutions in what is called period doubling. The cascading pattern of period doubling of solutions as one approaches the boundary of chaos is often a fractal pattern. The ratio of bifurcation for all iterated nonlinear differential equations that follow the period-doubling route to chaos has been found to be a universal constant, like pi, known as the Feigenbaum number, 4.6692.... Iteration of nonlinear equations provides a new basis for modeling the dynamic systems of nature.

Fractal geometry and chaos theory are major advances over previous methods for quantifying complex patterns encountered in nature. They provide methods for creating highly complex, detailed, and accurate synthetic analogs of natural systems. They redefine the way we think mathematically about the behavior of

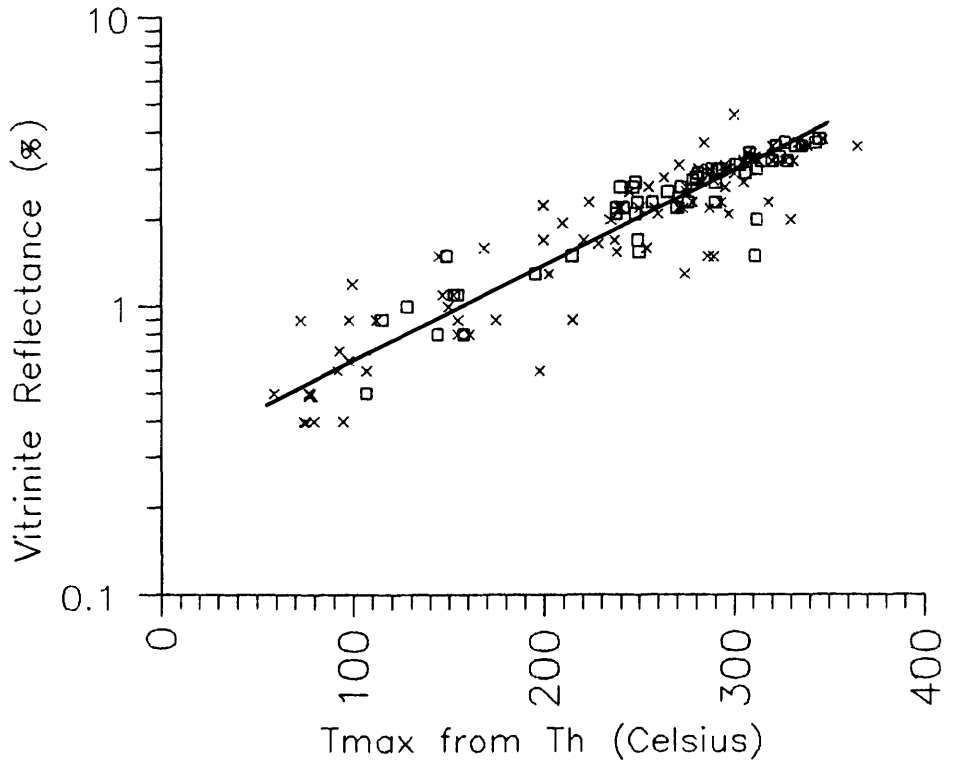

Figure 2 (Barker and Goldstein). Maximum temperature (Tmax) from homogenization temperature (Th) (squares) of aqueous inclusions in calcite versus vitrinite reflectance (Rm). The plotted line is computed from the reduced major axis regression equation given in the text. Present Tmax (crosses) versus Rm is also plotted in figure 2 for comparison but was not included in the regression analysis. We preferentially used Th mode to estimate Tmax for this plot, but in a few cases only Th mean was available (as noted in supplementary data).

natural systems, much as the theory of relativity brought a deeper level of understanding to physics. Like other branches of mathematics, they do not necessarily provide a physical or mechanistic understanding. However, in natural systems, fractal behavior often breaks down or changes to a different fractal dimension at scales where the physics changes. Systems that exhibit fractal scaling, such as earthquakes, have been shown to be self-organized critical phenomena, which means that they internally establish their own dynamically stable critical points. A challenge for the future will be to develop a method to go from a fractal pattern in nature to its governing nonlinear iterated equation.

The application of fractal geometry in the earth sciences has focused on demonstrating that geologic patterns are fractal, and on reporting the fractal dimension and the range of scales over which the dimension applies. Examples of published studies of interest to the petroleum industry are as follows. The topography of pore surfaces in sandstones, shales, and carbonates and the size distribution of pore volume in sandstones were shown to be fractal in the range 10^{-9}–10^{-4} m with fractal dimensions 2.27–2.90 and 2.55–2.75, respectively, in a series of seven papers by Krohn, Katz, Thompson, and others between 1985 and 1988. The initial potential for gas wells and the cumulative gas production in Upper Devonian shales of West Virginia were found to be fractal with dimension 1.46–2.0, as calculated by LaPointe from variograms published in 1988 by Hohn. A series of papers by Hewett, Arya, and others published between 1985 and 1988 has shown that in petroleum reservoirs, dispersivity in the range 5–10,000 m and porosity in the range 1–300 m are fractal with dimensions of 0.75 and 1.13–1.30 respectively. LaPointe, in a 1988 study, has shown that fracture densities in the range 0.2–25 m are also fractal with the dimension 2.37–2.69. In a 1987 paper, Maloy and others have shown that the viscous fingering patterns of low-viscosity fluid (air) penetrating a two-dimensional porous medium filled with a high-viscosity fluid (glycerin) are fractal, with a dimension of 1.64. The size frequency of fault offsets for faults in the range 0.1 to 1,000 m in length has been shown in Villemin's 1987 study to be fractal with a dimension of 1.2. Finally, in a series of papers published between 1985 and 1987, my coworkers and I have reported that the spatial and size distributions

of fractures in the range 0.02–3,000 m within fracture networks are fractal, with the dimension 0.5–0.7 in drill holes and 1.6–1.8 in planar sections. We have demonstrated that rock-fracture networks are fractal and that one can use data from a one-dimensional drill-hole sample of fracture spacing to predict the two- and three-dimensional spatial attributes of the fracture network.

The use of fractal geometry and chaos theory in the earth sciences has increased greatly in the past 5 years. Fractal geometry and chaos theory will redefine the way that we conceptualize many natural systems in the earth sciences. I expect that many geophysical records will prove to be fractal in both time and space. I expect that the size and spatial distributions of oil and gas fields and the compartmentalization of permeability within them will prove to be fractal, just as the porosity and dispersivity have proven to be, and that this will have significant impact on drilling strategy and resource assessment.

Subsurface Exploration with the Aid of Borehole Gravimetry

Larry A. Beyer

Borehole gravity (BHG) measurements are unique among well-logging measurements because they (1) respond directly to the bulk density of rock formations surrounding a well, (2) investigate surrounding volumes of rock greater by at least three orders of magnitude than those investigated by conventional well-logging methods, (3) provide profiles of vertical density that have high relative or absolute accuracy, and (4) are unaffected, for practical purposes, by well casing, cement, or borehole fluids. With sufficient independent information, BHG density profiles can be reliably converted to porosity profiles. In some cases, BHG density profiles may delineate zones whose relatively low density can be attributed to indicate the presence of hydrocarbons. Also, anomalous gravity effects due to lateral variations of density or porosity in the vicinity of the borehole may be detectable and interpretable in terms of geologic structure or facies changes.

Hundreds of mostly commercial BHG surveys have been made worldwide since the U.S. Geological Survey (USGS) pioneered development in 1966–1967 of the reliable, high-precision LaCoste and Romberg borehole gravity meter. Although results of most commercial surveys remain proprietary, work by the USGS and some published reports of industrial surveys show that BHG measurements can be applied to (1) pre-discovery exploration for porous reservoirs, (2) post-discovery evaluation and monitoring of porous (principally hydrocarbon-bearing) reservoirs, (3) evaluation of rock density and porosity or subsurface structure for engineering and other purposes, (4) evaluation of, or aid to other surface and downhole geophysical methods, and (5) fundamental studies of rock density and porosity in a variety of geologic settings.

Recent BHG studies by the USGS in the Kuparuk oil field (Alaska), Enewetak Atoll (Marshall Islands), Cajon Pass Scientific Drill-hole (California), and Ventura oil field (California) illustrate the latter four application areas. These BHG studies evaluated (1) an unproduced oil reservoir and a possible gas hydrate-bearing interval (Kuparuk field), (2) perturbing effects of a thermonuclear event on backreef deposits of Pliocene to Holocene age (Enewetak Atoll), (3) local geologic structure and performance of conventional well logs in crystalline basement rocks (Cajon Pass), and (4) effects of abnormally high pore-fluid pressure on the porosity of Pliocene turbidite sandstones (Ventura field).

Present-day BHG logging sondes have outer diameters that generally range from 10.8 to 12.7 cm (4.25 to 5.0 in.), and they contain heat-shielding dewar flasks. These flasks give the instrument package resident times of several tens of hours at well temperatures of about 200 °C (392 °F). A new USGS logging sonde with high temperature and pressure tolerance (and high corrosion resistance) is under development. This new sonde should permit BHG surveys to depths of about 6 to 9 km (19,700 to 29,500 ft), depending on drill-hole temperature and fluid pressure. If successful, use of this new sonde should provide unique data about the porosity of rocks at these depths.

Subsurface Studies, Santa Maria Province, California

K.J. Bird, P.H. McClellan, and T.R. Bruns

Seismic-reflection records and well data are being analyzed to provide a subsurface geologic framework for the U.S. Geological Survey's Santa Maria project. This project, jointly sponsored by the Evolution of Sedimentary Basins and Onshore Oil and Gas Investigations Programs, is a basin-evolution study focusing on the geologically complex and tectonically active south-central California margin. The area embraces several basins and basin fragments: the Santa Maria (onshore and offshore), Pismo, Huasna, Sur, Santa Lucia, and western Santa Barbara-Ventura. These basins have many similarities, including generally synchronous formation at about the end of the Oligocene, basin development on a complex assemblage of Mesozoic tectonostratigraphic terranes, and basin fill

consisting of Neogene clastic marine and nonmarine deposits, minor volcanic rocks, and organic-rich biogenous deposits (Monterey Formation). Despite these similarities, basin origins are controversial, and basin paleogeographies uncertain.

Large petroleum resources, collectively more than a billion barrels of oil, and a long exploration history are primarily responsible for an abundance of subsurface information in these basins; yet relatively few published studies since the early 1950's provide subsurface documentation. We are constructing a network of well-correlation sections, supplemented where possible with seismic-reflection data and synthetic seismograms, which integrate surface and subsurface geology, one basin with another, and the onshore with the offshore region. Offshore seismic records offer an opportunity for improved stratigraphic understanding, including the discrimination of tectonic from eustatic sea-level patterns, by calibrating the stratigraphy penetrated in wells with the seismic-reflection records. Subsurface information will contribute to facies studies and paleogeographic reconstructions necessary to test hypotheses of basin origins.

Petrography of Permian "Gondwana" Coals from Boreholes in Northwestern Bangladesh

Neely Bostick, Hal Gluskoter,
M. Nazrul Islam, and Q.M. Arifur Rahman

In northwestern Bangladesh, drilling through alluvium and Tertiary cover at sites of local low-gravity anomalies has confirmed the presence of Permian sedimentary rocks in depressions that may be as much as a thousand meters deep in the crystalline basement. These sedimentary rocks contain low-sulfur, high-volatile bituminous coals reported in seams as thick as 40 meters. We describe coals from corehole GDH–40 in the Barapukuria coal area and from GDH–45 in the Khalaspir area, 250 and 225 km northwest of Dhaka.

Judging by 16 spot samples from GDH–40 and 41 bench channel samples from GDH–45, many of these coals have features of "Gondwana coal" type. High-mineral (>30 percent) coals are mostly a nonlayered "plum pudding" of minerals and inertinite grains in an inertinite groundmass—with little vitrinite. True fusinite is rare in high-inert samples, but occurs in some vitrains.

A half-dozen samples contain more than 70 percent vitrinite and have microscopic aspects in common with non-Gondwana bright banded coals, though with more total inertinite (10–30 percent). But most of the samples would stand apart from the usual bright or gelititic coals of European and North American commerce and would be classed as semi-dull or inertogelitite types.

Well-layered grains observed all contain very dispersed, fine cuticle-spore chaff that may constitute as much as 5–10 percent of the organic volume; none of the samples would be classed as liptinitic or sapropelic. Neither separate resinite nor sclerotinite was seen. Visible pyrite is in veinlets or small nodules; framboids and dispersed pyrite are absent.

Only the channels sampled from GDH–45 are of quality to permit quantitative evaluation. These are 10 benches each (1/10 to 3 m thick) taken from core of the three major seams; the upper (14 m) and middle (16 m) seams are separated by only 2 m of non-coal rock, whereas the lower (13 m) is 33 m below the base of the middle seam. Ash in the coal ranges from 8 to 52 percent (dry basis) in individual benches, with composite seam averages of 15, 14, and 24 percent. Inertinite is 7 to 100 percent in benches, but averages 41, 54, and 67 percent composited in the upper, middle, and lower main seams.

In GDH–45 the free swelling index reaches 7.5 in several vitrinite-rich benches, which can indicate good coking coal, but the FSI value in mined coal may be as low as 3 depending on how the benches are combined during mining. Inertinite, and to some extent the ash, increases toward the top of each main seam so the bottom benches would yield the most valuable first mine slices—3 m, 7 m, and 1 m of coal with FSI about 6, ash 12 percent, inertinite 10–30 percent and 30 percent volatile matter (d.a.f.). Some benches with extremely high inert content, such as the top 7 m of the lower seam, might be mined especially for blending coke, and would have an advantage for handling that fusinite dust would be slight, unlike the case of many inertinite-rich coals.

In the Barapukuria borehole samples, from depths of 200 to 500 meters, the average vitrinite "A" random reflectance ranges from 0.60 to 0.80 percent Ro, and vitrinite "B" averages from 0.55 to 0.65 percent. In borehole GDH–45, from 287 to 442 m, the reflectance of grains of crushed vitrinite ranges from 0.79 to 0.94 percent. In individual cases the vitrinite is difficult to define because of semivitrinite at higher reflectance (in several samples a distinct peak on reflectance histograms) and because of surface bitumen films or resinous(?) inclusions at lower reflectance.

Samples from deeper in borehole GDH–40 contain more fluorescent vitrinite, visible mobile bitumen, and fluorescing minerals than do shallow samples; and the deeper levels, as well as all of GDH–45, can be considered to have entered the "main phase of bitumen generation" of organic thermal maturation.

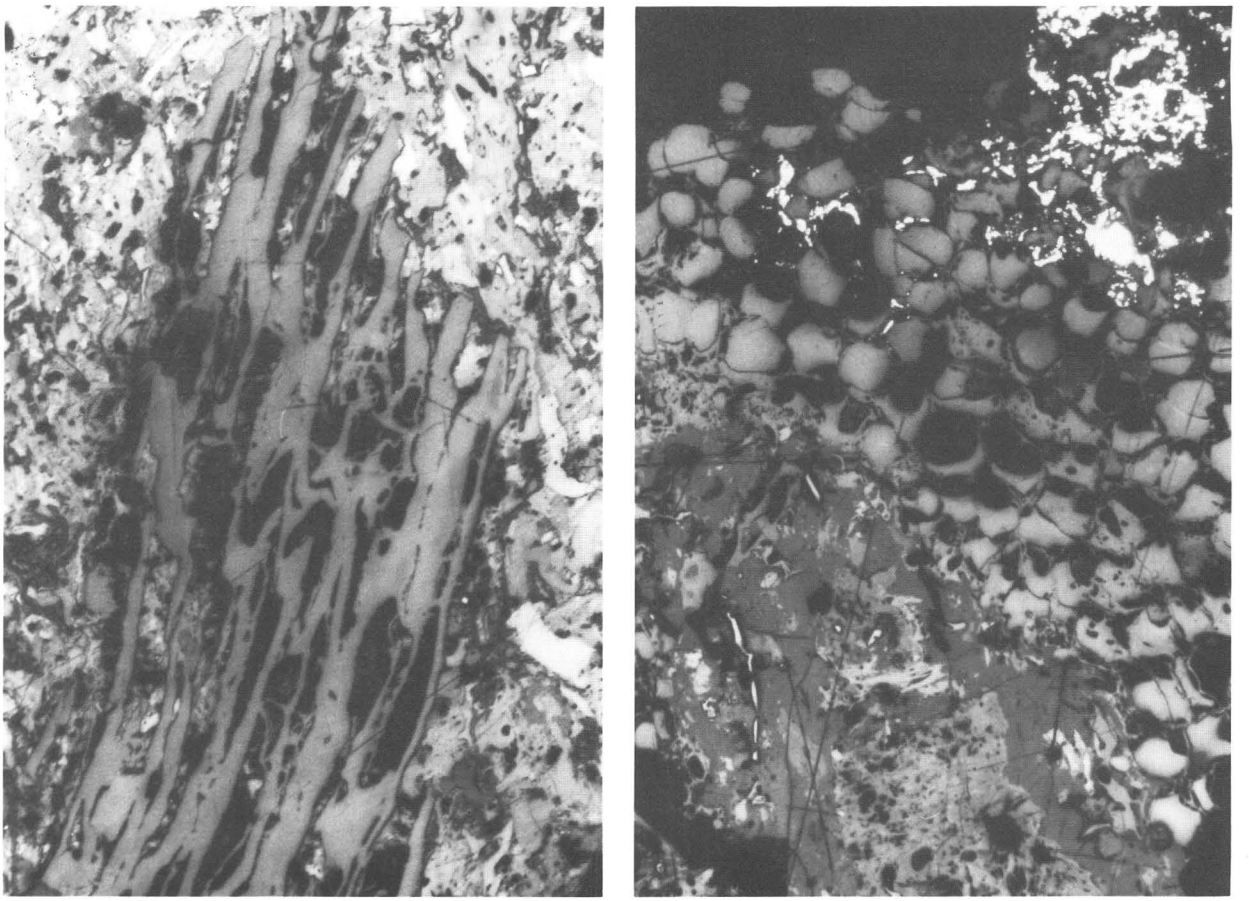

(Bostick) Many Permian coals from equatorial and southern lands are markedly different from northern commercial coals. These "Gondwana" coals generally have a high content of clastic mineral grains, and the concentrated fossil woody material which forms the coal is weathered and broken. The latter circumstance shows in maceral analyses in which vitrinite (the dominant component of other coals) is only 30–60 percent, while inertinite, originating from oxidatively altered wood, is dominant. Newly discovered coals in Bangladesh share these "Gondwana" features as shown here. In the left photomicrograph (0.37 mm actual width) the distinctive good preservation of woody tissues in a piece of semifusinite contrasts with the enclosing matrix of broken oxidized woody fragments. The lack of crushing in the large piece is a consequence of the inertness of the entire coal at the time of deposition and a relatively strong resistance to compression. This sample is the uppermost bench of the upper main seam; it contains 35 percent vitrinite and 58 percent inertinite, with 12 percent ash. The right photomicrograph (0.45 mm actual width) shows coal 3 m deeper in the same seam where vitrinite is 65 percent and inertinite 30 percent. Round phlobaphinite cell fillings in semifusinite make up much of the photo, but enclosing matrix in the lower part is vitrinite that was still a humic gel when deposited, though not fluid enough to penetrate the semifusinite. The bright filling at upper right is pyrite, which in these coals is vein and nodule precipitate, not bacteriogenic aggregates, and is associated with zinc sulfide. The photos show polished surfaces under immersion liquids. By Neely Bostick.

GLORIA Images from the Gulf of Alaska and British Columbia—Subduction Zones, Transforms, and Channels

T.R. Bruns, P.R. Carlson, A.J. Stevenson, M.A. Fisher, H.F. Ryan, D.M. Mann, Maxwell Dobson, Quentin Huggett, Lindsay Parson, and N.G.T. Fannin

GLORIA data obtained during 1986, 1988, and 1989 in the Gulf of Alaska show the sea-floor morphology from Unimak Pass to Dixon Entrance, from the shelf break seaward to about 400 km. An additional 70-km-wide swath was imaged along the British Columbia margin to follow the trace of the Queen Charlotte fault south of Dixon Entrance. Major features seen include the following continental-margin deformational structures and submarine-channel systems: (1) The Aleutian convergent margin is characterized by canyons and numerous slumps along the upper and middle slope. Unimak Ridge is a prominent midslope feature from Sanak Island to Unimak Pass. Along the

lower trench slope, the structure ranges from highly discontinuous folds to long continuous folds. (2) Southeast of the Aleutian Trench, ocean plate structural and bathymetric features are either parallel to magnetic anomalies, or are parallel to the trench and caused by normal faults as the plate bends into the Aleutian Trench subduction zone. (3) The margin between Middleton Island and Cross Sound is commonly either extensively cut by dendritic drainages or covered by glacially derived sediment. Large actively growing structures are present beneath the slope between Middleton Island and Pamplona Spur, but they are notably absent from Pamplona Spur to Cross Sound. (4) From Cross Sound to south of the Queen Charlotte Islands, the active trace of the Queen Charlotte fault is strikingly imaged as a narrow linear feature composed of ridges and troughs that have vertical offset. Horizontal offset is visible on a canyon wall and on offset channels. Numerous large anticlines are present seaward or, and trend parallel to, the fault. The active fault trace steps westward at the Tuzo Wilson Knolls, which structurally may be part of a small spreading ridge segment or pull-apart basin. (5) On the abyssal plain, turbidite channels form three separate drainage systems. The Surveyor channel system is comprised of tributary channels that arise along the margin between Pamplona Spur and Alsek Canyon, and that coalesce on the abyssal plain into a single channel (Surveyor channel) which ends at the Aleutian Trench southeast of Kodiak Island. The Chirikof channel system (new name) similarly arises from the margin between Fairweather Ground and Cross Sound, eventually forming a single channel that terminates in turbidite fans south of the Kodiak-Bowie Seamount chain. The Mukluk-Horizon channel system starts along southeast Alaska, with drainages from submarine fans joining to form Mukluk and Horizon channels. Both channels end more than 1,000 km away on the Tufts abyssal plain.

Laser Raman and Luminescence Spectroscopy of Carbonate Minerals—Progress Toward Nondestructive Microprobe Techniques for Stable Isotopes, Trace Elements, and Organic Matter in Zoned Cements

R.C. Burruss, T.G. Ging, K.R. Cercone, V.A. Pedone, and T.S. Hayes

Carbonate cements in reservoir rocks and migration pathways may record the chronology (paragenesis, radiogenic isotopes), temperature (stable isotopes, fluid inclusions), redox conditions (Fe/Mn), and composition (trace elements, fluid inclusions) of paleofluids. However, cements are commonly zoned at the micrometer scale and require microprobe techniques to resolve the cement stratigraphy and to allow petrologists to infer aspects of diagenetic history and paleo-fluid flow. Laser Raman and luminescence spectroscopy are new microprobe technologies for nondestructive trace analysis of geologic materials such as these cements.

Raman spectroscopy examines the vibrational energies of molecules, polyatomic ions, and crystal lattices, whereas luminescence (fluorescence and phosphorescence) spectroscopy examines the electronic energies of atoms and molecules. Laser spectroscopy through a microscope has high spatial resolution because objectives of 50× or higher magnification focus the laser beam to a diffraction limited spot of <2 μm. The USGS laser Raman microprobe laboratory has an ISA U-1000 spectrometer with an Olympus microscope, a Spectra-Physics argon ion laser source, a photon-counting photomultiplier detector, and an intensified, 700-channel diode array detector. The laser operates at 11 discrete wavelengths in the ultra violet (351 and 364 nm) and the blue-green (454 to 528 nm) for observation of Raman and luminescence spectra.

Vibrational energy levels of molecules are sensitive to isotopic substitution, such as ^{18}O for ^{16}O, and Raman spectroscopy can detect isotopically substituted molecules at natural abundance. Raman measurements of stable isotope ratios are difficult because the natural abundance of ^{13}C is 1.11 percent and ^{18}O is 0.204 percent. Geochemical variations in the isotope ratio of an unknown (R_{unk}) are measured in parts per thousand (ppt) relative to the ratio in a standard (R_{std}), calculated as:

$$((R_{unk}-R_{std})/R_{std})\times 1000 = \delta, \text{ ppt}$$

Therefore, variations in the δ value of 1 ppt in ^{13}C or ^{18}O are, in fact, variations in the absolute abundance of 1 part in 10^5 in $^{13}C/^{12}C$ and 2 parts in 10^6 in $^{18}O/^{16}O$. Counting statistics are the fundamental limitation, but a spectrometer with a single-channel photomultiplier is sensitive to noise in the laser intensity which limits the precision to ±10 to 50 ppt, regardless of the total signal. Therefore, geochemically useful isotope measurements with a standard single-channel Raman spectrometer are impossible. Multichannel, intensified, diode array detectors measure all isotope peaks simultaneously, eliminating laser noise from the spectra. Initial $^{18}O/^{16}O$ ratios in calcite from 3 of 5 localities (reported in a 1989 study by Burruss, Ging, and D. Carlson) using a multichannel detector have precisions (±7 ppt) limited by counting statistics. However, the accuracy of the Raman measurement compared to ratio mass spectrometry is limited by background fluorescence from the mineral.

Current research is aimed at improving the precision to ±2 ppt $\delta^{18}O$ and eliminating interference from fluorescence.

Fluorescence microscopy of carbonate rocks is an important tool for diagenetic and petroleum migration studies. Spatially resolved spectra can help identify the fluorescence activators and their concentrations in zoned minerals. Initial studies have distinguished organic and Mn^{2+} activation in red algae, Mn^{2+} activation and concentration in zoned calcite cement from the Canning basin, Northwestern Australia, and Mn^{2+} activation, Pb^{2+} coactivation, and Fe^{2+} quenching in zoned dolomite from the lower Paleozoic of northeastern Oklahoma, northern Arkansas, and southern Missouri. Identification of Pb^{2+} activation is tentative because Pb levels are below the detection limits of the electron probe. However, identifying Pb zoning may be critical evidence for constraining models of Pb transport in the regional fluid flow system that formed the world-class Pb-Zn deposits of the southern midcontinent. Research in progress is aimed at identifying organic activation of carbonate fluorescence in petroleum source rocks and migration pathways.

Coal Availability Studies—A Progress Report

M. Devereux Carter, Nancy K. Gardner, Richard E. Sergeant, Elizabeth V.M. Campbell, and Nick Fedorko, III

Many federal estimates of the Nation's coal resources do not account for numerous factors that could inhibit the availability of coal for development. As a result, these estimates may be mistakenly optimistic for long-term policy-planning purposes. In 1987, a cooperative program between the U.S. Geological Survey (USGS) and State geological agencies of Kentucky, Virginia, and West Virginia was initiated to identify the major current constraints to coal mining that could inhibit the availability of coal resources, and to estimate the amount of coal resources actually available for development within the Central Appalachian region. This program has been tested in nine 7.5-minute quadrangle areas (four in Kentucky, three in West Virginia, and two in Virginia) to determine if the identified constraints to mining in the region would significantly affect the availability of coal for development. It is estimated from these studies that only about 53 percent of the original resources of these quadrangles will be available for mining, before the application of recovery factors. The amount of coal that may actually be recoverable may only be about 30 to 40 percent of the original resource. The nine areas were selected to be representative of their general localities so that the results might be extrapolated to their surrounding regions. A pilot study was completed early in 1988 and the first eight studies to be formally funded under this program were completed by September 1989.

Restrictions were identified by consultation with local coal-industry engineers, geologists, mine operators, and State and federal regulatory personnel. Land-use restrictions applicable to the study areas resulted from the presence of power lines, pipelines, cemeteries, oil and gas wells, towns, major streams, public roads, railroads, airports, national and State parks, and one large forest preserve. Technologic constraints included coal beds considered too thin or too deep to mine, buffer zones around active or abandoned mines, mined and minable coal beds too close to one another, oil and gas wells penetrating underground-minable coal beds, and such geologic factors as washouts, faults, disturbed areas, and organic constituents that prevent rapid and complete burning. Computer programs of the USGS National Coal Resources Data System (NCRDS) were used to (1) combine and manipulate all data on coal-bed thickness and depth-of-burial with the constraints to mining, and (2) calculate original, remaining, and available resources.

There is a wide variation among the individual resource categories, but the overall results are fairly consistent for the study areas. Approximately 53 percent (ranging from 27 to 64 percent) of the original resource is estimated to be available for mining. Coal mined and lost-in-mining accounts for 12 percent of the reduction of the original resource, whereas land-use restrictions entail a 3 percent reduction, and technologic restrictions a 30 percent reduction. More than 2.5 billion tons of coal are estimated to be rendered unavailable for mining by land-use and technologic restrictions within the areas studied.

Chemical data are sparse in the areas studied. However, statistical analyses of those beds with available sulfur data indicate that approximately one-half of the available coal resources in these areas could be expected to meet current new-source performance standards of 1.2 pounds SO_2 per million Btu input.

Economic considerations (such as mining costs, available transportation, and proximity to markets) and the application of recovery factors were beyond the scope of this study, but if applied, they would further reduce the amount of coal estimated to be available. In any case, it seems evident that, under current conditions, less than one-half of the coal resources remaining in these study areas could ever be mined.

As expected, results of the first nine studies are inconclusive in terms of delineating regional trends. Studies in about 20 strategically placed 7.5-minute

quadrangles may be necessary to adequately represent the entire Central Appalachian region.

Sulfur in Coal—NCRDS Applications

M.D. Carter, S.J. Tewalt, L.J. Bragg, and R.B. Finkelman

The National Coal Resources Data System (NCRDS) is a geographic information system (GIS) that includes several data bases containing information on the sulfur content of coal. Each data base contains different types of sulfur data related to sample type, date of analysis, and source of data. Table 1 lists pertinent information for two of these data bases, BMALYT (U.S. *B*ureau of *M*ines *A*na*LYT*ical Data) and USCHEM (*U*nited *S*tates Geo*CHEM*ical Data).

NCRDS sulfur data can be used in a variety of applications. For example, data from BMALYT have been utilized to determine mean sulfur contents of sampled coal beds in major coal regions in the United States (fig. 1). Potential SO_2 emissions (lb SO_2 per million Btu) were derived for coal in the same regions. Differences in coal rank (and Btu) between regions were reflected in the varying amounts and percentages of sulfur that would have to be removed to meet Environmental Protection Agency SO_2 emission limits.

Data on the forms of sulfur in coal are available in the USCHEM data base. As an example of the utility of these data, the mean contents of sulfur as pyritic, sulfatic, and organic forms have been determined in Eocene coals of the Gulf Coast region (table 2).

In recent coal-resource assessment studies, data on sulfur and heating content of coal have been combined with information on thickness and mining restrictions. Using NCRDS software, the amount of compliant and noncompliant available resources has been calculated for coal in selected quadrangles. A pilot coal availability project examined 22 coal beds in the Matewan quadrangle, Kentucky. Although most coal beds are either completely above or below the limit, two beds contain both compliant and noncompliant resources based on an emissions limit of 1.2 lb SO_2 per million Btu for new-source coal-fired power plants (fig. 2, p. 16).

Natural Gas Hydrates in the Prudhoe Bay–Kuparuk River Area of Northern Alaska

Timothy S. Collett

Gas hydrates are crystalline substances composed of water and gas in which the solid-water lattice accommodates the gas molecules in a cage-like structure, or clathrate. Significant quantities of naturally occurring gas hydrates have been detected in many regions of the Arctic including Siberia, the Mackenzie River delta, and the North Slope of Alaska. Gas hydrates are generally regarded as a potential (unconventional) source of natural gas. Soviet researchers, however, have demonstrated that hydrates are an immediate, producible source of natural gas; their Messoyakh gas field in the West Siberian Basin has reportedly produced about 100 billion cubic feet of gas from hydrates over an eight-year period (1971–1978).

Table 1 (Carter, Tewalt, others). NCRDS data bases containing data on sulfur content of coal

Data base	Type of sulfur data	Data source	Analytical lab	Types of samples	Total Number of analyses (in thousands)
BMALYT	Total S	U.S. Bur. Mines	U.S. Bur. Mines	Tipple, delivered	53
USCHEM	Total S, forms of S	USGS, State geological agencies	U.S. Bur. Mines, Commercial	Channel, drill core	13

Table 2 (Carter, Tewalt, others). Arithmetic mean values of sulfur contents (weight percent, as-received basis) for Gulf Coast lignites

[N, number of samples]

Stratigraphic group	N	Total sulfur*	Pyritic sulfur	Organic sulfur	Sulfate sulfur
Claiborne	26	0.72	0.24	0.45	0.04
Jackson	13	1.64	0.31	1.36	0.04
Wilcox	149	1.01	0.36	0.62	0.09
Midway	10	2.05	0.78	0.97	0.30

*Calculated separately.

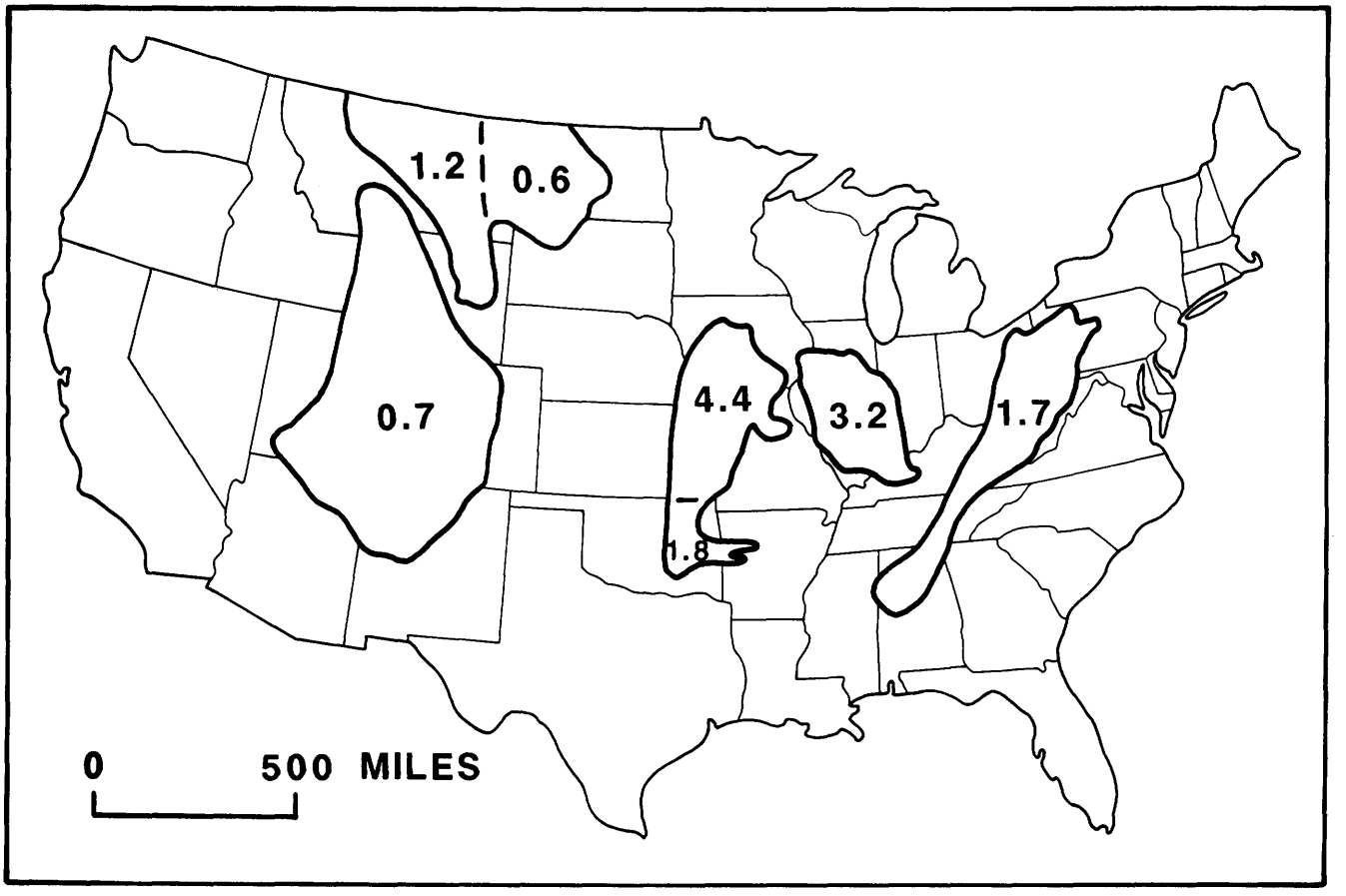

Figure 1 (Carter, Tewalt, others). Mean sulfur content (weight percent, as-received basis) of raw coal samples from major coal regions in the United States as determined from the BMALYT data base.

The primary purpose of the U.S. Geological Survey Gas Hydrate Project is to identify gas hydrates and to evaluate the geologic properties controlling their distribution on the North Slope of Alaska. Our North Slope studies suggest that the methane-hydrate stability zone is areally extensive beneath most of the coastal plain province and has thicknesses greater than 3,000 feet in the Prudhoe Bay area. Thermal conditions, however, preclude the occurrence of gas hydrates in the north-central part of the National Petroleum Reserve in Alaska and in the foothills east of Umiat.

Gas hydrates have been identified in 34 exploratory and production wells by using well-log responses calibrated to the response of an interval in one well where gas hydrates were recovered in a core by ARCO Alaska and Exxon. Most gas hydrates that we have identified occur in six laterally continuous Upper Cretaceous and lower Tertiary sandstone and conglomerate units; all these hydrates are geographically restricted to the area overlying the eastern part of the Kuparuk River oil field and the western part of the Prudhoe Bay oil field. Many wells have multiple gas-hydrate-bearing units, with individual occurrences ranging in thickness from 5 to 60 feet. Most of the gas hydrates occur below the base of ice-bearing permafrost; however, high gas readings on mud logs from some wells in the Kuparuk River oil field suggest that several of the gas-hydrate-bearing units extend up-dip into the ice-bearing permafrost sequence. Recent drilling and geologic/geochemical sampling have revealed the presence of a gas-hydrate/free-gas contact at the predicted base of the methane-hydrate stability zone in the west end of the Prudhoe Bay oil field. Our calculations suggest that the volume of gas within the delineated gas hydrates of northern Alaska is approximately 8 to 10 TCF (trillion cubic feet) (2.4×10^{11} to 2.9×10^{11} m^3), or about one-third the volume of conventional gas in the Prudhoe Bay field. Because of the low drilling density outside the Prudhoe Bay–Kuparuk River area, many more gas hydrate occurrences may exist.

Stable carbon isotope geochemical analysis of well cuttings in the Kuparuk River area indicates that rocks within and below the zone of hydrate stability contain a mixture of microbial and thermogenic gas. We suggest

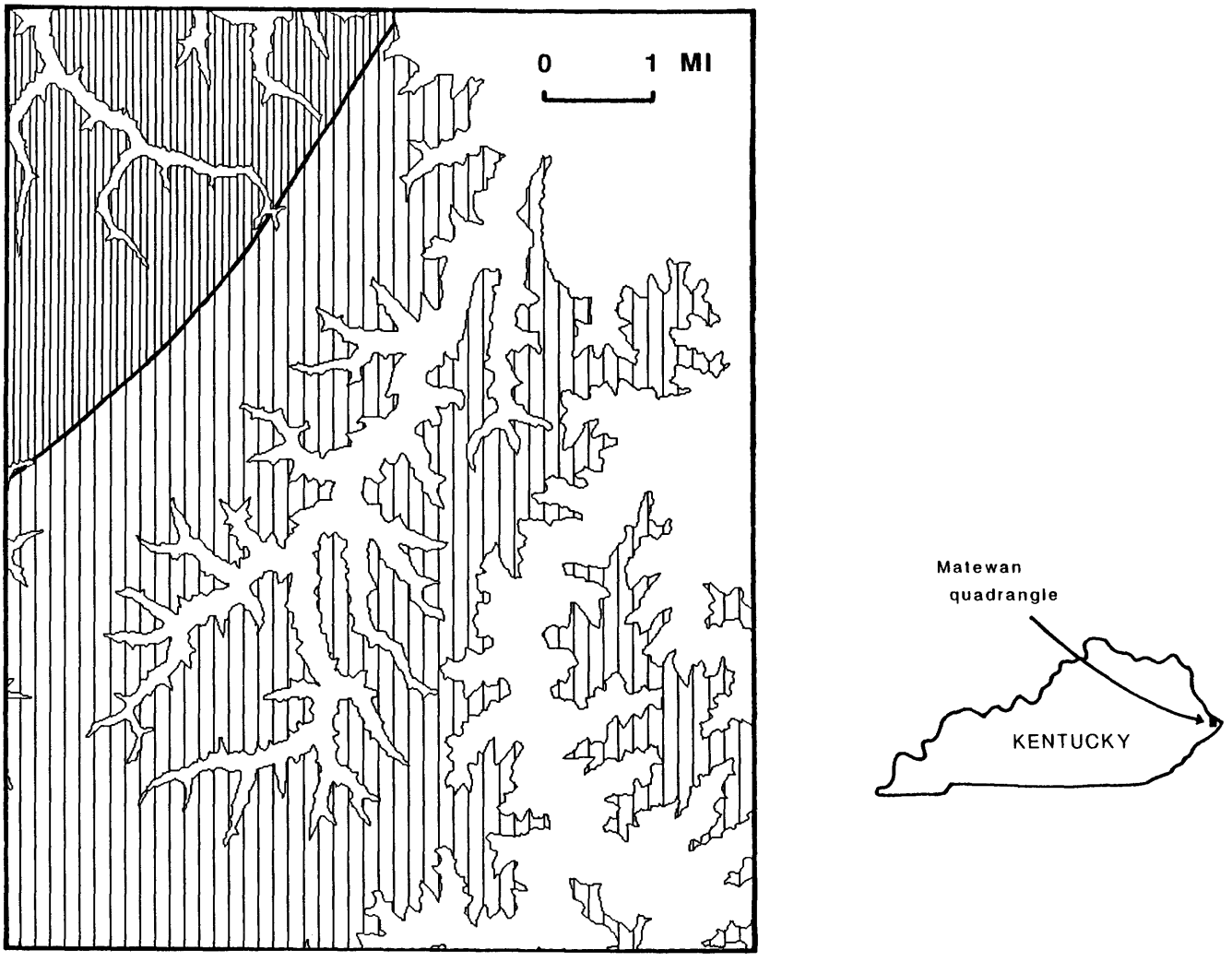

Figure 2 (Carter, Tewalt, others). Areas underlain by the Upper Elkhorn No. 1B coal bed in Matewan 7.5-minute quadrangle, Pike County, Kentucky, Appalachian basin. Heavy line separates areas of compliance (widely spaced pattern) and noncompliance (closely spaced pattern) coal. Blank, no coal.

that the identified hydrates originated from a mixture of deep-source thermogenic gas and shallow, microbial gas that was either directly converted to gas hydrate or first concentrated in existing traps and later converted to gas hydrate. We postulate that the thermogenic gas migrated from deeper reservoirs along the same faults thought to be migration pathways for the large volumes of shallow, heavy oil that occur in this area.

Cretaceous and Tertiary Sagavanirktok Formation in the Prudhoe Bay–Kuparuk River Area, Northern Alaska

Timothy S. Collett and Kenneth J. Bird

Detailed well correlation sections and ongoing USGS studies of gas hydrates and basin evolution have provided new insights on the stratigraphic framework of the Cretaceous and Tertiary Sagavanirktok Formation in the Prudhoe Bay–Kuparuk River area of the North Slope. The Sagavanirktok Formation is the youngest part of the Brookian sequence, a sequence composed of siliciclastic rocks whose provenance is the Brooks Range, to the south. The study area overlies the axis of the Barrow arch and marks the boundary between a foreland basin to the south (Colville basin) and a passive margin (Beaufort margin) to the north. The principal oil accumulations of the Brookian sequence in the Prudhoe Bay–Kuparuk River area are in the informally named West Sak and Ugnu sands of the Sagavanirktok Formation. ARCO Alaska estimates that the combined oil in-place in these two reservoirs could be as large as 40 billion barrels. Our studies of gas hydrates, crystalline substances composed of water and gas, within the Saga-

vanirktok Formation suggest that the volume of methane gas within the hydrates of this area is about 8 to 10 trillion cubic feet at standard temperature and pressure.

The Sagavanirktok Formation consists of Upper Cretaceous and Tertiary shallow-marine shelf and delta plain deposits composed of sandstone, shale, conglomerate, and coal. The areal distribution of the Sagavanirktok Formation is limited to the coastal plain of the eastern half of the North Slope and the adjacent continental shelf. The regional structure of the Sagavanirktok Formation in this area is a gentle (1°–2°) northeasterly-dipping monocline. The present regional northeast tilt is the combined result of sediment loading and continued thermal subsidence of the Beaufort margin. In the study area the Sagavanirktok Formation thickens from southwest (≈1,000 m) to northeast (≈2,000 m), and conformably overlies marine shale of the Canning Formation. Depositional strike migrated from a nearly north-south trend in Late Cretaceous time to its present west-northwest trend in about Eocene time.

Detailed well-correlation sections show the Sagavanirktok Formation in this area consists of complexly interbedded marine and nonmarine deposits that include at least one regional unconformity. The lowermost sandstone sequence within the Sagavanirktok Formation includes the West Sak and Ugnu sands. The Late Cretaceous West Sak interval represents transitional inner-shelf and delta-front deposits. The primary West Sak reservoirs are within the upper part of the sequence, which consists of two distinct and laterally extensive sandstone units. The West Sak interval is separated from the overlying Ugnu interval by a regionally extensive marine (30–45-m-thick) mudstone. The Late Cretaceous–early Tertiary Ugnu interval (80 to 100 m thick) consists of a series of interbedded sandstone and mudstone units. Overlying the Ugnu interval is a 250–300-m-thick nonmarine interval composed of numerous fining-upward channel and overbank siltstone and sandstone units. This nonmarine sequence is overlain by a 200–300-m-thick interbedded sandstone and mudstone marine sequence that was deposited during a basin-wide marine transgression in Eocene time. This sequence thins southwesterly and laterally coarsens to a sandstone in the eastern part of the Kuparuk River field. The upper boundary of this marine sequence is an erosional unconformity. East of Prudhoe Bay field, near the delta of the Sagavanirktok River, this unconformity has eroded part of the underlying marine sequence; however, to the southwest into the Kuparuk River area, the unconformity apparently disappears and the sequence becomes conformable. The rocks overlying the unconformity are generally of uniform composition both laterally and vertically in the section, and appear to have been deposited in a delta-plain environment. Individual sandstone units in this interval thicken to the northeast, which may represent the direction of the northeast-prograding deltaic depocenter. Other unconformities may occur within the Sagavanirktok Formation; however, with our present well-log data base we are unable to identify any additional hiatuses.

In the Kuparuk River area the Sagavanirktok Formation is cut by northwesterly-trending high-angle normal faults, generally downthrown to the east. A similar set of northwesterly-trending faults cut the older rocks in this area, suggesting a genetic linkage with the faults within the Sagavanirktok Formation. These faults are important in that they may serve as conduits for oil and gas migration from the underlying Prudhoe Bay field. Geochemical similarities suggest that oils, and presumably the associated gas, within the Sagavanirktok Formation were "spilled" from the underlying Prudhoe Bay Sadlerochit Group reservoir as a consequence of regional tilting during middle to late Tertiary time. We also note that the shallow heavy-oil and gas hydrates occur either up-dip from or near one of the major through-going faults, the Eileen fault zone.

Comparative Evolution of Western North America and Southern Kazakhstan, U.S.S.R.—Two Early Paleozoic Carbonate Passive Margins

Harry E. Cook and Michael E. Taylor

The ancient continental margin of western North America formed when a rift and spreading center developed within Laurentia and fragments drifted apart, forming a new ocean—the proto-Pacific. Stratigraphic backstripping and thermal subsidence curves show that the main breakup and onset of spreading probably occurred in the Late Proterozoic and earliest Cambrian. In Nevada, lower Paleozoic carbonate sediments were deposited on a distally steepened, nonrimmed carbonate ramp. Thus, deep-water carbonate environments characterized the platform margin and slope in central Nevada with shoal-water carbonate environments being restricted to eastern Nevada and western Utah. However, in some of the more northerly parts of western North America, such as in east-central Alaska, the carbonate-platform margin was characterized by ooid sand-shoal environments. With continued separation of continental fragments and postrift thermal subsidence, the western edge of North America became a site where 3–5 km of shoal-water and deep-water carbonate rocks accumulated during a 200-m.y. interval from Early Cambrian through Late Devonian time. This thick carbonate megaplatform reflects the tectonic stability of the Laurentian continental margin over a width of several hundred kilometers.

Southern Kazakhstan is composed of several amalgamated microcontinental blocks that exhibit a complex evolution, which began with Late Proterozoic (Riphean) rifting of continental crust. During rifting, a passive continental margin developed in the region of the Malyi Karatau–Tien Shan structural belt in southern Kazkhstan and western People's Republic of China. In contrast to western North America, which evolved as a relatively stable continental margin attached to the craton, this central Asian continental margin was broken into a series of large isolated blocks during rifting. With continued spreading and postrift thermal subsidence these isolated blocks became the loci for shallow-marine carbonate sedimentation during the Late Proterozoic (Vendian) and early Paleozoic. In the Malyi Karatau region, one of the isolated blocks became the site of a 40-km-wide carbonate seamount. Sedimentation on the seamount kept pace with postrift thermal subsidence, resulting in at least 1,000 m of carbonate sediments. This seamount was virtually devoid of any siliciclastic input. The oceanward margins of the seamount became the sites of robust *Epiphyton* cyanobacterial bioherms and mobile ooid-sand shoals. Seamount interior environments were characterized by shallow subtidal lagoons with scattered, small *Epiphyton* mounds, and supratidal islands. This feature, named the "Aisha-Bibi seamount" in honor of a twelfth-century Kazakh princess, is the oldest early Paleozoic seamount reported in the literature. It may be one of many carbonate seamounts that formed an early Paleozoic archipelago extending from southern Kazakhstan southeastward into the Tien Shan region of People's Republic of China.

During the Late Cambrian and Early Ordovician, sedimentation in both western North America and Kazakhstan was dramatically punctuated numerous times by carbonate-platform-margin collapse during sea-level lowstands. In western North America rapid seaward progradation of the continental margin, in combination with eustatic changes, resulted in mass failure of deep-water slope deposits. In Nevada, these failed slope deposits were transported seaward as submarine slides, channelized debris flows, and turbidity currents, resulting in the formation of slope-generated carbonate submarine fans. Some of the carbonate fan facies are admixed with siliciclastic sands, which were probably transported across the shelf during sea-level lowstands. Shallow-water carbonate sites to the east developed disconformities as represented by faunal hiatuses, as well as solution surfaces. In Alaska, where the continental shelf/slope break was dominated by ooid-sand shoals, 75-km-wide segments of this margin collapsed and were transported downslope by boulder-bearing mass flows. Here the redeposited debris formed linear carbonate aprons several hundred meters thick that are composed of ooid and slope-derived lime mudstone clasts.

During early Paleozoic eustatic events in Kazakhstan, 200–800-m-wide segments of the Aisha Bibi seamount margin collapsed. These collapsed margins were transported seaward as channelized boulder-bearing debris flows, turbidity flows, and submarine slides. Repeated large-scale, episodic mass-transport processes contributed to the development of 500-m-thick carbonate submarine fans that extend several kilometers onto the basin plain. Interior parts of the seamount exhibit tidal-flat facies and solution breccia that may correlate with sea-level lowstands.

Evidence for four coeval sea-level lowstands occurs in both North America and in the Malyi Karatau region of southern Kazakhstan. Timing of these four lowstands from oldest to youngest is as follows: (1) an Early/Middle Cambrian transition; (2) a transition between the Late Cambrian Sakian and Aksayan ages (*Ivshinagnostus ivshini* and *Pseudagnostus pseudangustulobus* trilobite zones) in southern Kazakhstan, which correlates with the *Elvinia/Taenicephalus* trilobite zone transition in North America; (3) a Late Cambrian *Eoconodontus* conodont zone (Batyrbayan/late Trempealeauan); and (4) a Lange Ranch eustatic event near the Cambrian/Ordovician boundary (*Cordylodus proavus* conodont zone).

Events recognized in western North America and southern Kazakhstan that we interpret to be related to eustasy are coeval with other sedimentologic and faunal evidence of Late Cambrian and Early Ordovician sea-level changes in Estonia, western Newfoundland, and the People's Republic of China. The corroborating evidence includes mass failure of carbonate platform margins, presence of solution surfaces in shallow-water carbonate settings, and disconformities in both low- and relatively high-paleolatitude sites.

Play Analysis Methodologies for Petroleum Resource Assessment

Robert A. Crovelli and Richard H. Balay

The petroleum resource assessment studies of the U.S. Geological Survey (USGS) have resulted in a wide variety of analyses, geologic models, quantitative methods, and computer programs. The type of analysis refers to the basic geologic assessment unit, for example, province, basin, or play. The geologic model consists of the geologic assumptions and mathematical description of the assessment approach, for example, reservoir engineering, volumetric yield, field size, or direct assessment. The quantitative method is the type of probabilistic methodology that is mathematically derived from the geologic model, for example, Monte Carlo

simulation or analytic probability theory. Computer programs are written on the basis of the probabilistic methodology.

During recent years, the USGS has made major strides in designing and developing play analysis and analytic probabilistic methodology with a variety of geologic models. Play analysis is a general approach using various geologic models and probabilistic methods for analyzing a geologic play. In applying play analysis, a petroleum assessment area is first partitioned into geologic plays, and then the individual plays are analyzed. The individual play estimates of oil and gas are aggregated, respectively, in order to estimate the petroleum potential of the entire assessment area.

A probabilistic system of petroleum resource assessment for play analysis has been designed to meet the following requirements: (1) includes a variety of geologic models, (2) uses an analytic methodology instead of Monte Carlo simulation, (3) can aggregate estimates from many areas that have been assessed by different geologic models, and (4) runs quickly on a microcomputer. The geologic models consist of four basic types: reservoir engineering, volumetric yield, field size, and direct assessment—listed in order of decreasing amount of geologic information required. The reservoir-engineering model, the most data-intensive, was used in the three recent studies by the USGS described herein. These three assessments are followed by a National assessment using a field-size model.

Arctic National Wildlife Refuge Assessment

The Arctic National Wildlife Refuge (ANWR) study completed in 1987 assessed in-place oil and gas resources of geologic plays in the North Slope of Alaska using a reservoir-engineering model. An analytic methodology using probability theory was developed, and a package consisting of six computer programs was created and called Fast Appraisal System for Petroleum, Reservoir Engineering (FASPRE).

Hungary Assessment

The Hungary assessment of the Békés basin generalized the reservoir-engineering model and the aggregation model that were used in the 1987 ANWR study, which was site-specific to the North Slope of Alaska. The modifications required that the system produce output in metric units and run on an IBM-PC-XT compatible computer.

The analytic probabilistic methodology was adapted from the 1987 ANWR study by replacing the site-specific reservoir-engineering equations with general equations and parameters. The *u*niversal *m*etric version of the play analysis software was called FASPUM.

Tight Gas Sands Assessment

The Tight Gas Sands study assessed low-permeability gas resources of the Upper Cretaceous Mesaverde Group in the Piceance basin of western Colorado. The system used in this study (FASPUE) was adapted from FASPUM by conversion to *E*nglish (inch-pound) units. An entire play area is treated as a single gas accumulation.

National Assessment

The USGS recently completed its first petroleum resource appraisal of the entire United States using the field-size model of play analysis. An analytic probabilistic methodology was developed based upon the field-size model and a new risk structure. A computer package called Fast Appraisal System for Petroleum, Field Size (FASPF) was written for play analysis, subplay analysis, economic analysis, and aggregation analysis. Subplay analysis includes estimation of resources on State offshore areas. Economic analysis truncates field-size distributions using a minimum economic cut-off value. Aggregations of individual play and subplay estimates of oil and gas are made at the provincial, regional, and national levels.

Origin and Distribution of Inorganic Elements in the Wyodak-Anderson Coal Bed, Powder River Basin, Wyoming

S.S. Crowley, R.W. Stanton,
D.M. Triplehorn, and L.F. Ruppert

The distribution of selected major, minor, and trace elements indicates detrital, volcanic, and peat-forming origins for inorganic elements in two cores of the Wyodak-Anderson coal bed of the Fort Union Formation (Paleocene) of the Powder River Basin, Wyoming. Of particular interest are altered volcanic-ash layers, which may be useful in correlating thick coal beds of the Powder River Basin. The ash layers in these cores are not partings that can be easily observed in outcrop sections or core, and although the layers can be observed as sharp peaks in geophysical logs, the peaks are easily confused with those for detrital partings and pyrite. For these reasons, we found in this study that the volcanic ash layers are best identified using geochemical and mineralogical methods.

The coal bed recovered from corehole A, located 80 km southeast of Gillette, is 22 m thick and was divided into 29 separate interval-samples selected on the basis of

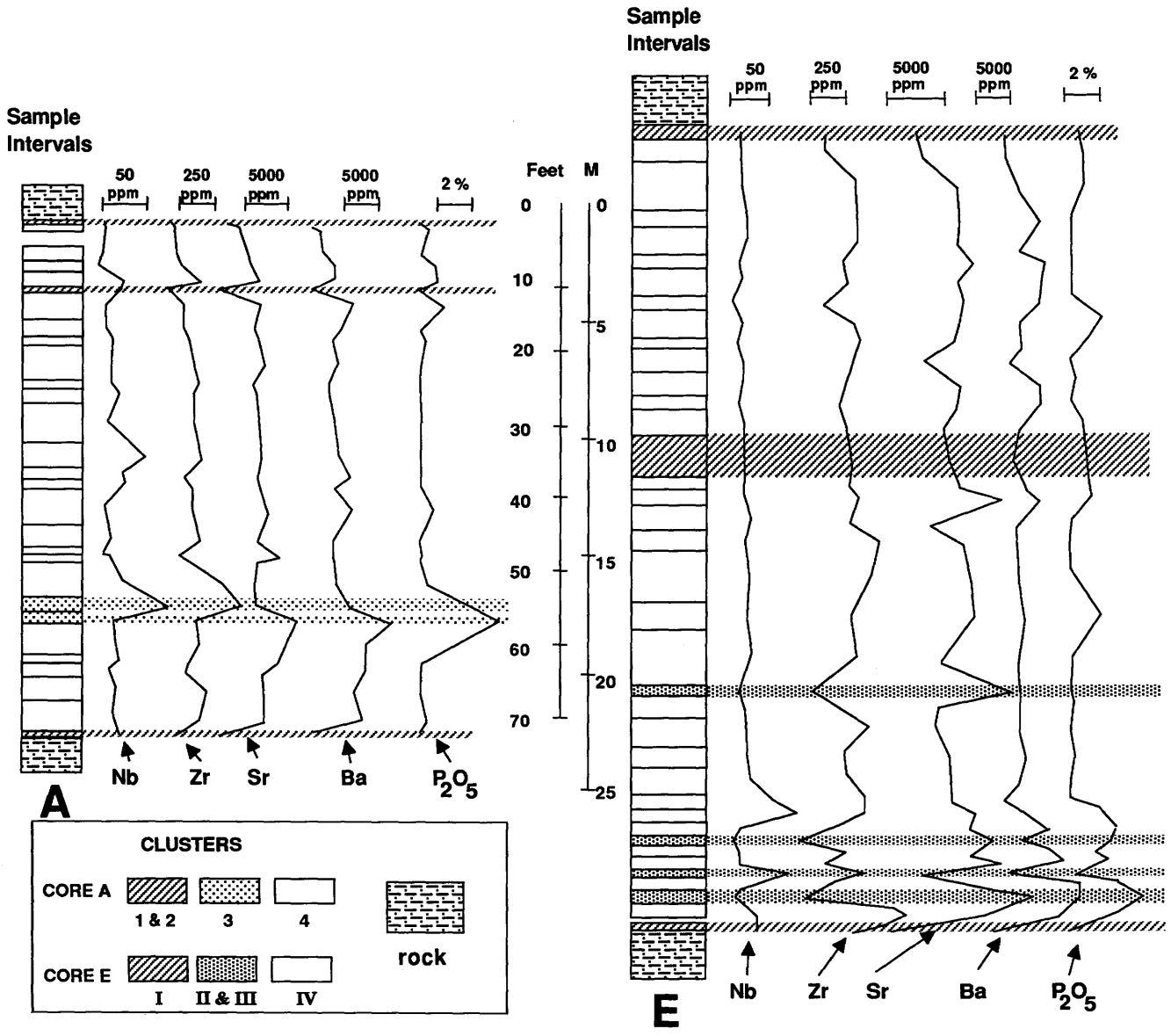

Figure 1 (Crowley). Chemical profiles of two series of samples of cores A and E from the Wyodak-Anderson coal bed.

megascopic lithologies and X-ray radiography (fig. 1). The coal bed recovered in corehole E, located 10 km north of Gillette, is 36 m thick and was divided into 38 separate interval-samples.

Samples in each core were grouped by their elemental compositions (30 elements) using cluster analysis. All data used in the analysis were reported on (or calculated to) an ash basis and standardized. In core A, based on the analysis, four major sample clusters were evident: (1) coal samples nearest the roof rock, (2) samples from partings and the coal samples nearest the floor rock, (3) coal samples about 5 m above the base of the coal bed, and (4) coal samples throughout the rest of the coal bed (fig. 1).

The following elements are concentrated in samples from cluster 3, compared to other samples: Nb, Zr, Sr, Ba, and P_2O_5. Previous studies, such as a 1988 study by D.A. Spears and others, reported that in volcanically derived tonsteins, Sr, P_2O_5, and Ba are found in aluminum phosphate minerals. From binocular microscope and SEM examination, the cluster 3 layers were found to contain two separate suites of minerals: (1) the beta form of quartz, euhedral zircons, and (2) several authigenic minerals: calcite, pyrite, kaolinite, quartz, anatase, barite, and an aluminum phosphate (crandallite?).

Based on the cluster analysis, four sample clusters were evident in core E: (I) samples from partings and

coaly samples nearest roof and floor rock, (II) coal samples from intervals 1.5 to 10.4 m above the base of the coal bed, (III) one sample about 2.4 m above the base of the coal bed, and (IV) samples throughout the rest of the coal bed (fig. 1).

We infer that the chemical compositions of samples in clusters 1 and 2 of core A and cluster I of core E were influenced by detrital processes, because of the proximity of the samples to detrital material. The chemical compositions of the samples in cluster 4 of core A and cluster IV of core E are inferred to be derived principally from the peat-forming plants.

On the basis of the distribution of elements and mineralogy of core A, we suggest that layers in the cluster 3 samples of core A originated as volcanic ash. The glass and less stable minerals probably altered relatively quickly, and the morphology of the resistate minerals (quartz and zircon) remained relatively unchanged. Although the analysis of inorganic elements in core E is preliminary, the distribution of elements suggests that certain layers in coal samples (clusters II and III) may also have originated as volcanic ash that underwent a large degree of alteration. Work is in progress to examine the mineralogy of the possible volcanic ash layers in this core.

Enhanced Upwelling and Organic Productivity During the Late Quaternary in the Northeastern Pacific Ocean

Walter E. Dean and James V. Gardner

The present upper water mass of the northeastern Pacific Ocean off California and Oregon has a well-developed oxygen-minimum zone (OMZ) between 600 and 1,000 m wherein concentrations of dissolved oxygen are less than 0.5 mL/L. The OMZ is caused by decomposition of large seasonal stocks of plankton supported by high concentrations of nutrients within the California-Current upwelling system. Even at such low concentrations of dissolved oxygen, benthic burrowing organisms are abundant enough to destroy millimeter-scale seasonal laminations (varves), and surface and near-surface sediments are thoroughly bioturbated. However, laminated and microbioturbated sediments are preserved in the upper Pleistocene and lower Holocene sections of cores collected on the continental slope at water depths within the present OMZ (fig. 1, p. 22).

Laminated sediments are most prominent in cores collected in water depths of about 700 m, and are present laterally from at least as far north as the Klamath River area, and as far south as Point Sur. Detailed analyses of the laminae, and correlation with seasonal components of pelagic "snow" collected in sediment traps demonstrate that the laminae are indeed varves. These varved sediments contain more abundant lipid-rich "sapropelic" (Type II) organic matter than the bioturbated and oxidized upper Holocene sediments deposited within the last 5,000 years. The decrease in Type II organic matter after about 5 ka might be due to a change in either source or degree of preservation of the organic matter. However, because the stable-carbon isotopic composition of the organic carbon does not change with time, we can eliminate a change of source as a possibility. The organic-carbon-rich, laminated sediments also contain higher concentrations of sulfide-sulfur, relative to the bioturbated sediments, indicating a higher rate of sulfate reduction due to the presence of more "reactive" organic matter. Concentrations of several trace elements, especially Cr, Cu, Ni, V, and Zn, also are enriched in the laminated sediments. The presence of carbon-, sulfur-, and metal-rich sediments, as well as the lack of bioturbation, all suggest that the OMZ in the northeastern Pacific Ocean was more intense prior to 5 ka.

The intensity of an OMZ may be partly related to the rate of advection of dissolved oxygen, but is mainly controlled by the biological oxygen demand imposed on the water column that is modulated by the rate of primary productivity. We infer, therefore, that prior to about 5 ka, productivity of the North Pacific Ocean off California and Oregon was greater than today. One possibility is that upwelled intermediate to deep water contained higher concentrations of dissolved nutrients (mainly N and P). Another possibility is that the California-Current upwelling system was more intense and persistent for a longer season (perhaps 6 months or longer) during the late Pleistocene. This second possibility further implies that the summer North Pacific high-pressure system that drives the California Current must have been more persistent in order to supply more nutrients to support increased productivity. This change in atmospheric circulation would have resulted in more intense upwelling along the west-coast margin, a longer period of supply of high nutrient concentrations, a longer period of sustained primary productivity, and a longer season of oxygen depletion in the water column, thereby preserving varves on the seafloor.

The USGS Evolution of Sedimentary Basins Program

Walter E. Dean, Samuel Y. Johnson, and Thomas D. Fouch

The USGS Evolution of Sedimentary Basins (ESB) Program was created to provide a mechanism for

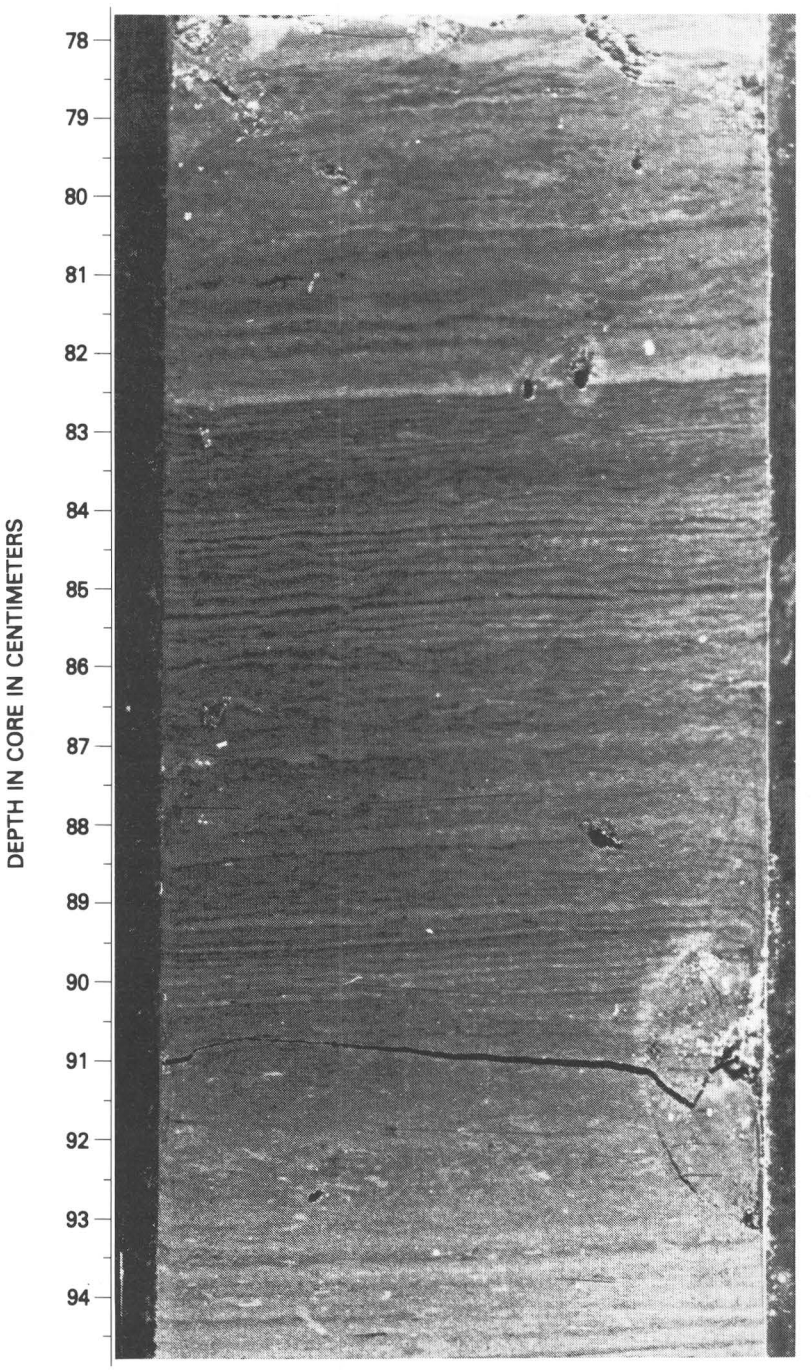

Figure 1 (Dean and Gardner). Typical laminated (varved) and microbioturbated Pleistocene-Holocene sediments from a core taken on the continental slope off northern California.

conducting multidisciplinary, integrated geologic research in energy-rich sedimentary basins. Coordinated research topics include geophysics, structural geology and tectonics, physical stratigraphy, biostratigraphy, sedimentology, paleogeography, paleoclimatology, petrology and diagenesis, geochemistry, heat flow and thermal maturity, paleohydrology, and basin modeling. Data are collected from outcrops, borehole logs and cores, and geophysical surveys (magnetics, gravity, seismic reflection and refraction, and remote sensing). Results of regional and topical basin research are being published as reports, maps, and charts that provide data summaries, interpretation, and synthesis.

The ESB studies concentrate on basic geologic research and thus are distinct from the commodity-focused USGS energy research programs (oil and gas, coal, uranium, and oil shale). In practice, however, ESB and commodity-program research are closely coordinated in order to maximize impact for resource exploration, development, and assessment. ESB studies generate and place in the public domain important information products and data bases used by Federal, State, and local governments to assess and predict energy and metal resources and potential, as well as geologic hazards. Private energy companies use ESB data and products to develop and test exploration strategies and to evaluate their own proprietary data bases. Similarly, academic researchers commonly utilize ESB framework studies in conducting their own basic or applied research. Reports of work in progress have been regularly provided to participants in ESB-sponsored basin workshops.

The ESB Program began in 1985 with studies by multidisciplinary research teams of six energy-rich basins: (1) the North Slope basin, Alaska; (2) the Anadarko basin, Oklahoma; (3) the Powder River basin, Wyoming and Montana; (4) the San Juan Basin, New Mexico and Colorado; (5) the Uinta-Piceance basin, Utah and Colorado; and (6) the Central Appalachian basin, West Virginia, Virginia, Tennessee, and Kentucky. These initial six basin efforts are in their completion phase. A study of the Santa Maria basin, California, began in 1987 and will be completed in 1991. Five-year USGS-ESB studies of (1) the eastern Great Basin, Utah and Nevada; (2) the Paradox basin, Utah and Colorado; and (3) the Illinois Basin (in cooperation with the Illinois, Indiana, and Kentucky State geological surveys) were started in October 1989. A study of Tertiary sedimentary basins in southwest Washington and northwest Oregon is slated to begin in 1991. Studies of one or more Laramide basins of western Wyoming will be initiated in 1991 or 1992. Pilot studies of the Washington-Oregon and Wyoming basins are being conducted in FY1990.

Uranium Favorability in the Chadron Formation, Southeastern Wyoming and Northwestern Nebraska

K.A. Dickinson and P.L. Hansley

The Chadron Formation of the Oligocene White River Group is the host rock of the Crow Butte uranium deposit (at least 30 million pounds of U_3O_8) located near Crawford in northwestern Nebraska. The uranium-mineralized rock is present in a basal medium- to coarse-grained arkosic sandstone member of the otherwise clayey Chadron. Locally this basal sandstone member is called the Chadron sandstone. It was deposited in fluvial channels that in most areas are incised into the underlying Cretaceous Pierre Shale.

The Chadron Formation contains abundant rhyolitic ash that is partially altered to smectite and silica minerals. Uranium was probably released during this alteration. The relatively permeable channel sands appear to have served as conduits for the flow of the uranium-bearing ground water. The impermeability of underlying shale aided in confining ground water flow to the Chadron sandstone. The predominant uranium mineral is cryptocrystalline coffinite, which is concentrated along the margins of the channels with closely associated pyrite and marcasite. Corrosion textures of the pyrite suggest that oxidation resulted in reduction and precipitation of the uranium. Oxidized rock is confined to the center of the channel where the flow of oxidizing ground water was greatest, whereas the reduced rock is confined to the channel margins. Organic material deposited in the channel sands probably aided in forming the reducing environments, but little of that material is now present. Sulfides introduced from the underlying black shale of the Pierre may also have provided a reductant.

The Chadron is favorable for uranium in areas other than the Crow Butte area, but it is favorable only where the basal sandstone member is present. The Chadron sandstone extends from areas northwest of the Hartville uplift near Douglas, Wyoming northeast, east, and south into northwestern Nebraska where the Crow Butte uranium deposit is located. Where the sandstone is thickest, the volume of uraniferous ground water flowing through the unit was potentially greater and favorability for uranium deposits is correspondingly increased. The maximum thickness of the Chadron sandstone is more than 280 feet in Nebraska in the vicinity of the Crow Butte deposit, but in Wyoming its thickness is much less, exceeding 100 feet in only a few areas.

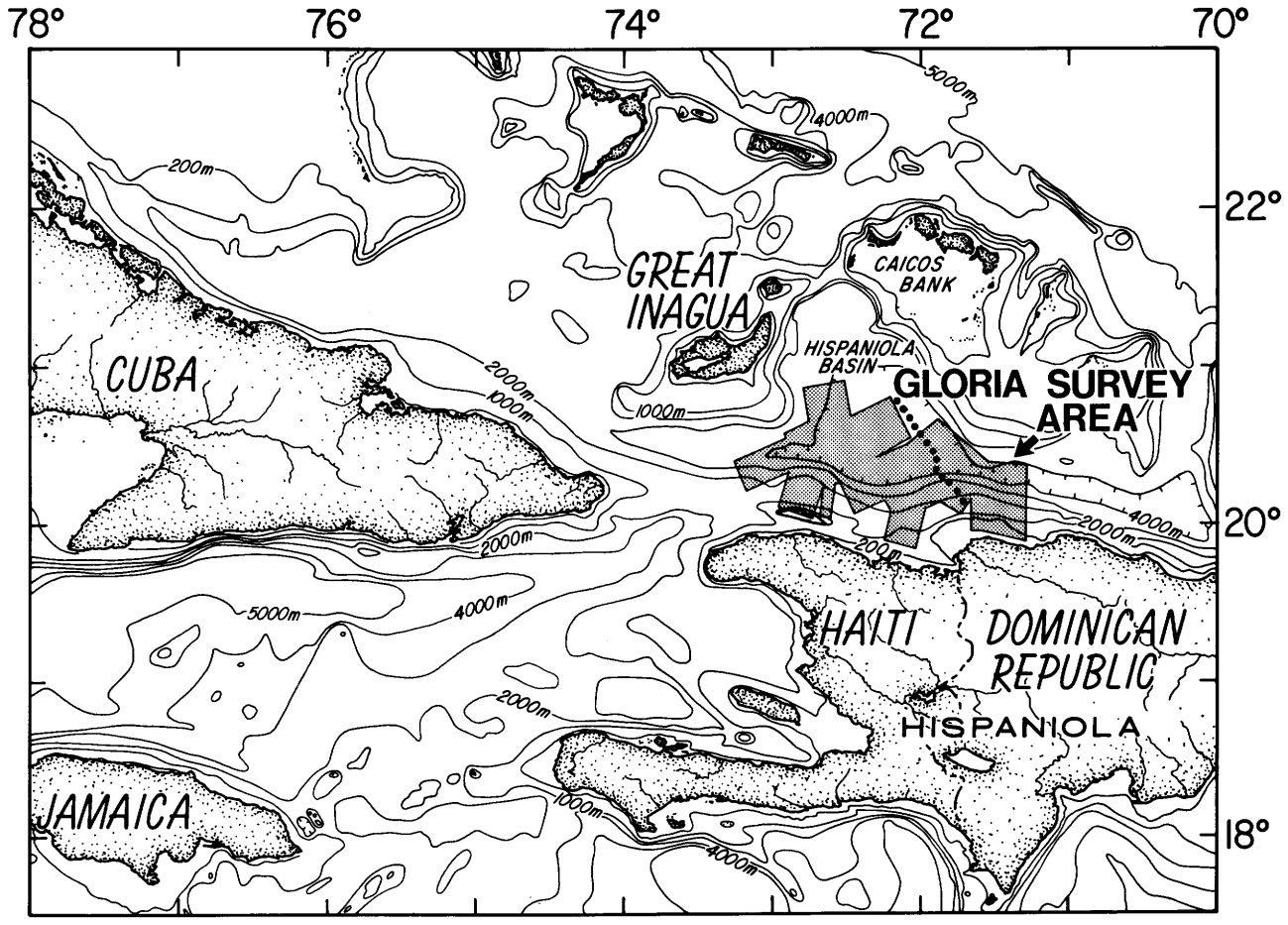

Figure 1 (Dillon). Study area, showing GLORIA sidescan survey location. Dotted line indicates location of profile shown in figure 2.

Structural Segmentation in an Active Submarine Tectonic Accretionary Wedge, as Disclosed by GLORIA Sidescan Sonar and Multichannel Seismic Profiling, Caribbean Plate Boundary North of Haiti

William P. Dillon, James A. Austin, Kathryn M. Scanlon, N. Terence Edgar, Lindsay Parson, and Gordon E. Ness

The insular margin off the northwestern coast of Hispaniola (Haiti and the western Dominican Republic) occupies a region of strongly oblique collision of the Caribbean and North American plates that results from the general trajectories of the plates and the presence of a restraining bend on the Caribbean plate boundary. The study area (fig. 1) is the insular slope, which is shown by profiles to be a tectonic accretionary wedge (fig. 2), created by folding and thrusting of Hispaniola Basin strata against the backstop formed by the island of Hispaniola. The structure of the slope indicates only the effects of collision, with no evidence of transcurrent motion. The regional seismicity pattern suggests that the plate boundary actually is situated south of the insular slope, near the present coastline, and therefore that the tectonic accretionary wedge is situated on North American plate basement.

Bathymetry, GLORIA sidescan-sonar images, and seismic-reflection profiles demonstrate that the insular slope and underlying wedge are characterized by two morphological/structural styles that occur in three distinct and rather abruptly bounded compartments along the insular slope. In the central compartment, (1) the insular slope dips gently (about 4°); (2) the average slope profile is planar to concave but marked by broad fold ridges; (3) internal structure consists of broad anticlines (wavelength about 4.5 km) separated by thrust faults; and (4) the structural contact of slope to basin strata is gradational. In contrast, in the compartments to the east and west, (1) the insular slope dips steeply (9°-16°); (2) the slope profile is convex; (3) internal

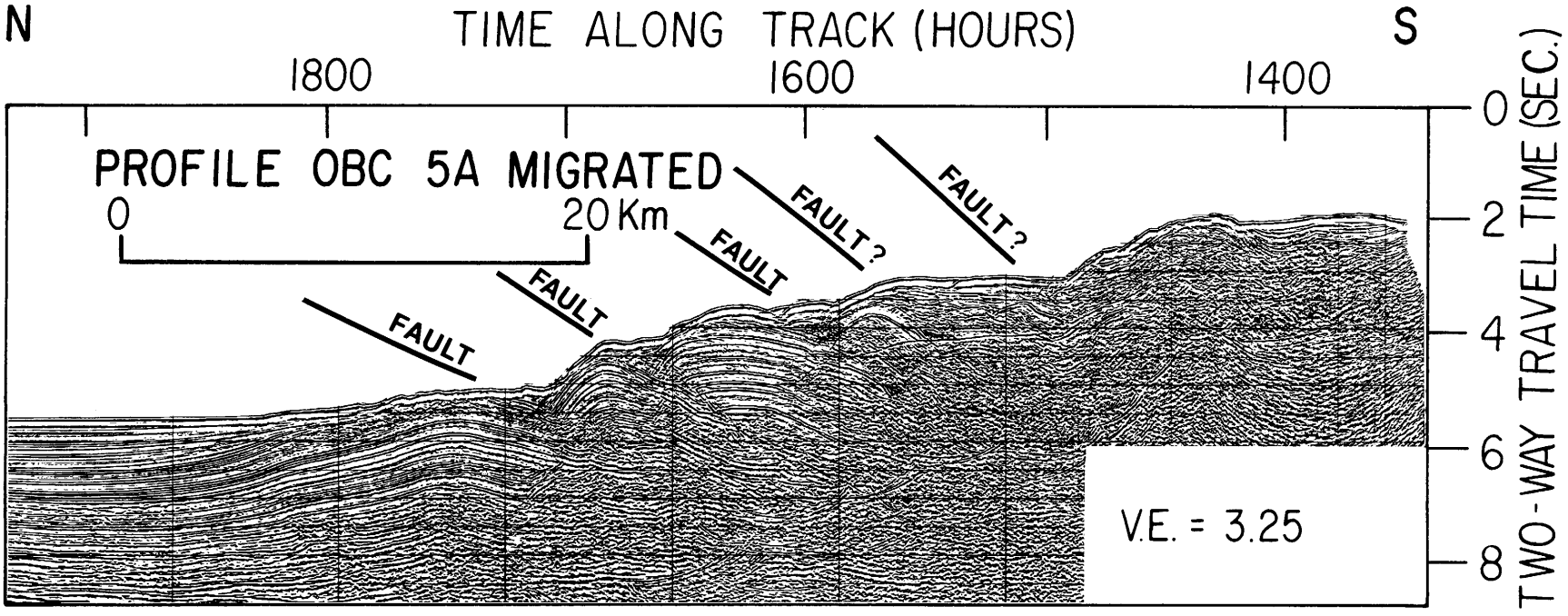

Figure 2 (Dillon). Seismic profile across the central compartment. V.E., vertical exaggeration.

structure appears chaotic in seismic reflection profiles; and (4) the toe of the slope forms an abrupt structural front against Hispaniola Basin strata.

The geologic settings of the two slope types seem quite similar. The interplate motions should be approximately the same along this rather straight section of the plate boundary, and the sedimentary strata entering the tectonic accretionary wedge should be identical, because they are derived from the same small turbidite basin. There is no obvious change in the backstop (Hispaniola). Inasmuch as these factors appear to remain the same, why are the slopes in the two morphological/structural styles so different? Why are the internal structural styles so different?

Tectonic accretionary wedges are comparable to the pile of snow in front of a moving snowplow; that is, as long as conditions remain constant, the snow will maintain a constant slope in front of the plow. In a tectonic accretionary wedge, the angle between the sediment surface and the decollement (known as the critical taper) is modeled as a balance between the internal strength of the wedge against the forces of the compressional push (from Hispaniola), the basal frictional resistance (at the decollement), gravitational body force (tendency of the slope to spread out flat under the influence of gravity), and water pressure (in this submarine wedge). Although some of these factors might change and thus affect the angle of critical taper, we would not expect such abrupt changes in such a small area, and see no evidence for them. We suggest that the critical taper is likely to remain the same across the area and that the changes in slope merely reflect changes in dip of the decollement. If critical taper in the wedge is comparable to that of other wedges reported, it is less than 10°. Such an angle would cause the decollement to rise toward Hispaniola in locations where sea-floor slope is steepest, and space requirements would dictate a complicating structure, such as a duplex. The difference in internal structure may result from the difference in dip of the sea floor between the two styles. Weaker sediments are more easily folded, and sediment strength is increased by overburden loading. Therefore, the steeper slopes might result in much narrower zones of relatively weak sediment that is appropriate for folding (thickening occurs 3.6 times faster on crossing a slope of 14° than at 4°).

This study shows that, in the setting of a tectonic accretionary wedge, structural styles can change very rapidly along the structural trend, so that zones that might present petroleum traps (broad folds of turbidite sediments) can terminate abruptly against regions of intense faulting and crumpling.

Predictive and Actual Results from 2,500 Wildcat Wells, Offshore Gulf of Mexico

L.J. Drew and J.H. Schuenemeyer

The accuracy of a forecast made in 1980, of the number and sizes of oil and gas fields expected to be discovered in the Miocene-Pliocene and Pleistocene trends in the offshore Gulf of Mexico, was determined by comparing the predicted and actual results from the drilling of 1,832 wildcat wells in the Miocene-Pliocene trend and 682 wildcat wells in the Pleistocene trend during the 1977–85 time period. This forecast was made using a two-stage procedure comprising both a discovery process model and the concept of economic truncation. A modified version of the Arps-Roberts discovery process model estimated the number of larger fields remaining to be discovered in each field size class (untruncated portion of the field size distribution). A geometric multiplier of the log geometric distribution allowed estimation of the number of fields remaining to be discovered in the truncated portion of the distribution (to the left of the mode) down to fields as small as 729,000 barrels of oil equivalent. This assessment of the undiscovered oil and gas resources was in turn used, in a 1982 report by Drew, Schuenemeyer, and W.J. Bawiec, as a basis to forecast the number and sizes of the fields that would be discovered in the future.

During the 1977–85 period, 280 oil and gas fields were discovered in the Miocene-Pliocene trend, each containing more than 729,000 barrels of oil equivalent. Collectively, these fields contain 17.0 trillion cubic feet of natural gas and 542 million barrels of crude oil and condensate (3.38 billion barrels of oil equivalent) as viewed from a 1988 reserve estimation basis. The 85 fields discovered during the same time period in the Pleistocene trend contained 4.8 trillion cubic feet of natural gas and 240.1 million barrels of crude oil and condensate (1.04 billion barrels of oil equivalent).

The forecast made in 1980 for the period 1977–85 for the Miocene-Pliocene trend estimated that 222 fields would be discovered, containing 1.79 billion barrels of oil equivalent. This is an underestimate of 1.59 billion barrels of oil equivalent in this trend (47 percent low). The forecast for the same period in the Pleistocene trend stated that 79 fields would be discovered containing 713.2 million barrels of oil equivalent. Actually, 4.8 trillion cubic feet of natural gas and 241 million barrels of crude oil and condensate were discovered, or 1.04 billion barrels of oil equivalent (30 percent low) as viewed from a 1988 reserve estimation basis.

This underestimation of the amounts of oil and gas discovered in both the Miocene-Pliocene and the Pleistocene trends during the 1977–85 period can for the most

part be attributed to the field growth phenomenon. The field size data used to calibrate the discovery process model for the 1980 forecast were taken from the FRRE file, maintained at that time by the U.S. Geological Survey, and now maintained by Minerals Management Service. These estimates were based on engineering calculations without complete data on reservoir area or numbers of reservoirs or quality of the pays; and statistical growth factors were not applied to estimate the contribution to field growth through the process of extensions and revisions. For example, as a group the reserves in the 293 fields upon which the 1980 forecast was based, that is, fields discovered in the Miocene-Pliocene trend between 1946 and 1976, grew 18.7 Tcf of natural gas and 1.57 billion barrels of crude oil and condensate through the extension and revision processes between 1980 and 1988. The parallel growth in the Pleistocene trend was 7.2 Tcf of natural gas and 698 million barrels of crude oil and condensate. The growth in reserves of the oil and gas fields discovered before 1976 in both geologic trends during the 1980–88 period is then of the same numerical order as the volume of oil and gas discovered during the same period as viewed from the end of the time period. This result makes it clear, as suggested in a 1985 report by K.C. Manger, E.H. Vidas, and T. Woods, that a correction for field growth must be calculated and added to those oil and gas fields used to assess the size and number of undiscovered fields and to forecast future discovery rates. This has been done for both the Miocene-Pliocene and the Pleistocene trends.

Deep Oil and Gas Wells and Reservoirs in the United States from the Well History Control System and Petroleum Data System

T.S. Dyman, D.T. Nielsen, R.C. Obuch, J.K. Baird, and R.A. Wise

Deep wells and hydrocarbon production are widely distributed in the U.S. in rocks of various ages and lithologies. Sixteen thousand six-hundred fifty wells have been drilled deeper than 15,000 ft in the U.S. since the first deep well was drilled in 1920, according to Petroleum Information Corporation's Well History Control System (WHCS) as of February 1988. Of these 16,650 deep wells, 8,705 were completed as producing wells that could be producing oil and (or) gas at any depth (above or below 15,000 ft). Nearly as many gas wells exist (6,347) as dry holes (7,090); gas wells are three times more abundant than oil wells (2,181). In the WHCS file, 1,442 wells have a total depth greater than 20,000 ft.

Of these 16,650 deep wells, 7,251 were drilled in the offshore region of Louisiana. Of the 2,860 deep wells in the Midcontinent region, 2,211 were drilled in the Anadarko basin and 354 in the Ardmore basin. Of the 841 deep wells in the Rocky Mountain region, 175 are in the Uinta basin, 136 in the Wyoming thrust belt, 113 in the Green River basin, and 100 in the Wind River basin. Of the 3,547 deep wells in Mississippi, Alabama, and Florida, 1,876 were drilled in the Cretaceous-Jurassic trend; and 1,157 wells were drilled in the Gulf basin. A total of 19 deep wells have been drilled in the Appalachian, Michigan, and Illinois basins.

In the WHCS file, 2,981 producing wells drilled deeper than 15,000 ft have a formation at total depth equal to the producing formation. These wells represent a minumum number of those wells that are actually classed as producing oil and gas deeper than 15,000 ft; they are referred to as deep-producing wells and form the basis for statements made in the following discussion. The ratio of gas-producing deep wells to total producing deep wells increases with increasing total depth of well. The gas-producing proportion of total deep-producing wells increases from a consistent 72 percent in the 15,000-ft range to 90 percent in the 19,000-ft range. In the Rocky Mountain region, deep gas-producing wells account for 34 percent of the total deep-producing wells (265 total wells, 91 gas wells). The Uinta and Powder River basins are oil-rich below 15,000 ft whereas the Green River, Wind River, Washakie, and Bighorn basins and Wyoming thrust belt are predominantly gas-rich.

Only eight wells classed as producing from reservoirs deeper than 15,000 ft were completed before 1960, all of which were reported as gas producers. The first three wells to produce gas deeper than 20,000 ft were completed in 1967. The two deepest hydrocarbon-producing wells (producing deeper than 26,000 ft) were completed in 1977 and 1979. Deep gas-producing wells account for 70 percent of the total deep-producing wells completed during 1970 through 1975 and more than 80 percent completed during the 1976–87 period. For all years together, more than 90 percent of the wells that are classed as producers below 20,000 ft are producing gas.

Seventy-five percent of the oil wells completed deeper than 15,000 ft produce from clastic rocks (467 wells, 7.6 million drilled ft). The greatest depths to clastic reservoirs occur in the New Mexico part of the Permian basin (average = 18,243 ft). In Utah, 136 deep-producing wells (more than 2 million drilled ft) were completed in clastic reservoirs. Three hundred sixty-six deep oil wells produce from Tertiary rocks; of these 168 produce from the Miocene in the Gulf Coast region and 134 from the Paleocene Wasatch Formation in the Rocky Mountain region. One hundred twenty-five deep-producing wells are Jurassic oil producers; 92 of these produce from the Smackover Formation.

More than 75 percent of the deep wells completed as gas wells have produced from clastic rocks (1,740 wells, >29 million drilled ft). The Anadarko basin and the Rocky Mountain region produce deep gas primarily from clastic reservoirs (352 wells, 5.6 million drilled ft). In Texas, 55 percent of the deep-producing wells (377), accounting more than 7 million drilled ft, were completed as producing from carbonate rocks; most of these are producing from the Ordovician Ellenburger Group in the Permian basin. Texas and Louisiana have more deep wells which produce from carbonate rocks than from clastic rocks. Ninety-nine deep-producing wells produce from carbonate rocks in the Jurassic Smackover Formation in Alabama, Mississippi, and Florida.

Approximately 7 billion barrels of oil and 50 trillion ft^3 (TCF) of nonassociated gas have been produced from 2,007 deep reservoirs through 1985 according to the Dwight's Energy Data Petroleum Data System (PDS). Deep gas accounts for about 8 percent of the U.S. cumulative gas production (698 TCF), and deep oil accounts for about 5 percent of the U.S. cumulative oil production (143 billion barrels). The Midcontinent, Texas, and Gulf Coast regions, with 1,900 deep reservoirs, account for 95 percent of the cumulative deep oil and gas production in the U.S.

Cumulative nonassociated gas production for deep reservoirs discovered prior to 1970 equals 9.2 TCF, which is 18 percent of the cumulative deep gas production in the U.S. Thirty-four of the 260 active deep reservoirs in the PDS file were discovered prior to 1970. The oldest reservoirs were discovered in the Permian basin and Gulf Coast region.

New Methodologies for Assessment of U.S. Oil-Shale Resources

John R. Dyni

During the past 20 years, the U.S. Geological Survey has developed a large database of Fischer assays as well as a collection of drill cores and crushed samples of oil shale for assessment of oil-shale resources of the United States. Assessment of these resources for future energy needs will require additional analyses to better characterize the deposits with respect to: types and maturity of organic matter, amounts of oil and gas obtainable by pyrolysis, amounts of residual carbon recoverable as thermal energy, potential mineral byproducts, and oil-shale components that may impact the environment. Such information will be vital in order to evaluate individual oil-shale deposits for recovery of oil and gas by conventional technologies as well as by newer processes such as hydroretorting and downhole gasification.

Among the important analytical methods available for resource assessment of oil shale are Rock-Eval, ultraviolet fluorescence microscopy, ^{13}C nuclear magnetic resonance, hydroretorting assay, pyrolysis fluorescence, and X-ray analysis. These methods, in combination with improving the Fischer assay procedure, can provide more complete information about (1) kind and degree of thermal maturity of organic matter, as well as (2) types of organic matter that respond best to different methods of extracting oil, gas, and thermal energy from oil shale. Application of some of these methods to evaluating oil-shale deposits should be of value not only to economic geologists, but also to mining and process engineers who will be developing these resources.

Once a Menace, Now a Burgeoning Source of Energy—Coal-Bed Methane in the Warrior and San Juan Basins

James E. Fassett

During the 1980's, coal-bed methane has come to be recognized as an enormous energy resource. As much as 850 Tcf (trillion cubic feet) of coal-bed methane is estimated to be trapped in coal-bearing basins of the United States. This estimate is more than four times larger than present estimates of natural gas reserves in conventional reservoirs. Natural gas produced from coal beds is essentially methane and can be added to natural-gas pipelines without any special treatment. The gas is generated first biogenically and later thermogenically during the coal-forming process and is stored in the micropore and macropore porosity of the coal beds. Coal-bed methane is adsorbed on and (or) absorbed in the coal microstructure. Typical recovery entails pumping water out of the macropore system (cleats), thereby lowering the hydrostatic pressure on the coal-bed reservoir and allowing the gas to desorb from the coal micropore system. Production problems include controlling coal-fines produced with the water and gas and disposing of produced water in areas where surface disposal is environmentally unacceptable. Coal-bed methane wells typically demonstrate an increase in gas production and a decrease in water production over time; they are thus characterized by incline production curves in contrast to the customary decline curves associated with gas production from conventional reservoirs.

The Warrior Basin of Alabama and the San Juan Basin of New Mexico and Colorado are the only large-scale, commercial producers of coal-bed methane in the United States. Warrior Basin coals are in the Pottsville Formation of Pennsylvanian age, are usually less than 5 ft

(1.5 m) thick, have ranks ranging from high-volatile to low-volatile bituminous, and are present under a large area at depths less than 3,000 ft (900 m). The Alabama part of the Warrior Basin contains 54 billion tons of coal that is estimated to contain 39 Tcf of gas (1.1 trillion m^3), of which 15 Tcf (0.4 trillion m^3) or more is considered recoverable. Through June 1988, the Warrior Basin has produced 60 Bcf (billion cubic feet) (1.7 billion m^3) of coal-bed methane.

Nearly 95 percent of San Juan Basin coal is in the Upper Cretaceous Fruitland Formation. Fruitland coal beds range from 1 or 2 ft (0.3–0.6 m) to 40–50 ft (12–15 m) thick; total Fruitland coal thickness exceeds 70 ft (21 m) in the northern part of the basin. Fruitland coals range in rank from subbituminous to medium-volatile bituminous. Fruitland coals are less than 4,000 ft (1,200 m) deep throughout most of the basin. The Fruitland contains more than 200 billion tons of coal that is estimated to hold 50 Tcf of gas (1.4 trillion m^3). It has been estimated that 25 Tcf (0.7 trillion m^3) of this gas is recoverable. Through 1987, the San Juan Basin has produced 85 Bcf (2.4 billion m^3) of coal-bed gas.

The immediate future of coal-bed methane is somewhat unclear, largely because of as-yet-unmade political decisions regarding energy use in the United States. For example, if laws were passed creating incentives to use natural gas instead of more polluting fuels to create electrical energy, the economics of gas production could literally change overnight. At the present time, coal-bed methane receives a gas-tax credit that is clearly helping to encourage the accelerating development of this exciting new resource. Will the scheduled expiration of this gas-tax credit at the end of 1990 put a damper on the coal-bed methane development activity? Certainly, some of the larger coal-bed methane gas wells of the San Juan Basin would be commercial, with or without the gas-tax credit.

Whatever is decided politically in the near future, however, will have little bearing on the ultimate future of coal-bed methane; it is an enormous resource that is waiting for its time to come and it will be used, as present supplies of generally-less-expensive energy resources are used up, making coal-bed methane more competitive in the market place.

New Developments in Uranium Endowment Assessment in the United States

Warren I. Finch, Charles T. Pierson, Richard B. McCammon, James K. Otton, Hoyt B. Sutphin, and Karen J. Wenrich

Responsibility for assessing the uranium endowment in the United States was returned to the U.S.

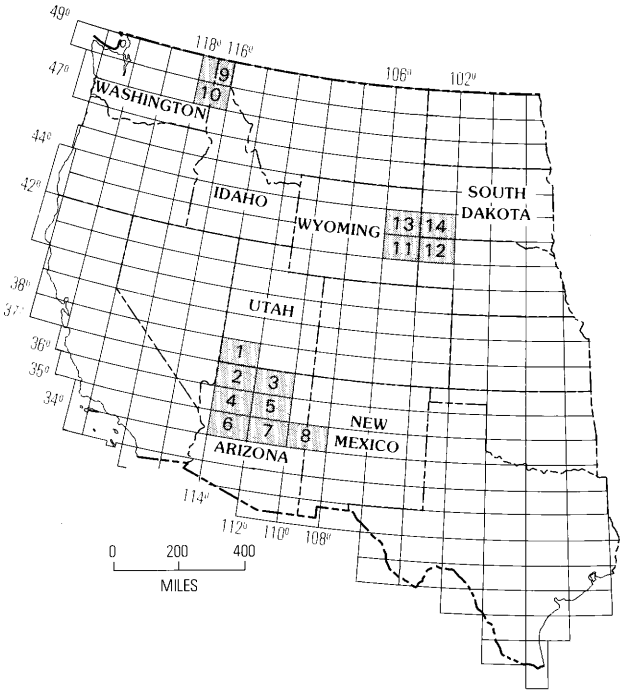

Figure 1 (Finch). Index map showing the location of the NTMS 1°×2° quadrangles mentioned in this report. 1, Cedar City; 2, Grand Canyon; 3, Marble Canyon; 4, Williams; 5, Flagstaff; 6, Prescott; 7, Holbrook; 8, St. John; 9, Sandpoint; 10, Spokane; 11, Alliance; 12, Torrington; 13, New Castle; 14, Hot Springs.

Geological Survey by the Memorandum of Understanding of 1984 between the U.S. Department of Energy and the Department of the Interior. (Uranium endowment is the uranium estimated to occur in rock with a grade of at least 0.01 percent U_3O_8. The economic portion of endowment is calculated using a higher grade cutoff, commonly 0.10 percent U_3O_8.) Since that time the USGS has developed a new assessment method (outlined in a 1987 report by Finch and McCammon), which is a modification of the NURE (National Uranium Resource Evaluation) method. Two regions have been assessed using the new method, and a third is currently being assessed.

The new method is called the "deposit-size-frequency" (DSF) method and consists of a modification of the NURE uranium endowment (U) estimation equation, $U = A \cdot F \cdot T \cdot G$, in which the factors F•T (F = fraction of area, A, that is favorable for endowment; T = tons of endowed rock per unit area) are replaced by a single factor. This factor is the summation of the estimates of the number of deposits of different deposit-size classes within the area being assessed, or, equivalently, the spatial density of deposits; hence, the name "deposit-size-frequency." The average grade (G) of the endowment is the same in both methods. The DSF

method requires (1) that a deposit-size-frequency (a matrix of the lower limit, most likely, and upper limit of number of deposits in each size class) be established in a well-known to fairly well known area, called the control area, and (2) that the geologic factors that produced this frequency be determined. Using these requirements for a control area, the assessor estimates the size frequency of undiscovered deposits for the favorable area based on similarity to the control area. The probabilistic estimates of undiscovered uranium endowment are calculated using the computer program TENDOWG, published in a 1988 study by McCammon and others.

In 1987, the undiscovered uranium endowment was estimated for "young organic-rich uranium deposits" in the Colville-Okanogan favorable area in the Sandpoint and Spokane NTMS 1°×2° quadrangles, Washington and Idaho (fig. 1). These uranium deposits occur in surficial organic-rich fluvial, alluvial, and lacustrine sediments laid down in the past 15,000 years. The deposits average from 0.03 to about 0.10 percent U_3O_8, and contained U_3O_8 ranges from a few hundred pounds to as much as a million pounds. The uranium endowment in the Colville-Okanogan favorable area is estimated to lie between about 6,750 and 122,000 short tons of contained U_3O_8, and the mean (unconditional) undiscovered uranium endowment is 35,300 short tons U_3O_8.

In 1988, the undiscovered uranium endowment was estimated for the solution-collapse breccia pipes in the Grand Canyon region in the Grand Canyon, Marble Canyon, Williams, Flagstaff, Holbrook, St. Johns, and Prescott NTMS 1°×2° quadrangles in Arizona and the Cedar City quadrangle in Utah (fig. 1). Solution-collapse breccia-pipe uranium deposits occur in pipes that formed as a result of solution collapse within the Mississippian Redwall Limestone and stoping of the overlying Pennsylvanian, Permian, and Triassic rocks (Wenrich and others, this volume). Most of the uranium deposits are high grade by U.S. standards, averaging between 0.43 and 0.65 percent U_3O_8. Typical deposits contain 125,000 to 500,000 tons of ore, yielding 1,000,000–6,000,000 lb of U_3O_8. The uranium endowment was estimated for 26 favorable areas that total 16,728 mi^2. The mean (unconditional) uranium endowment totals about 1,300,000 short tons U_3O_8. This value is about eight times the total endowment of 158,000 tons estimated for these breccia pipes in a 1980 study, part of the U.S. Department of Energy NURE program. The larger USGS endowment value is due to three factors: (1) the DSF method allows for greater partitioning of input data and results in less biased (generally larger) estimates, (2) current knowledge of grade and tonnage of post-1979 discovered deposits is significantly greater, and (3) understanding of the geology of the region has greatly improved.

During 1989, an assessment of undiscovered uranium endowment was initiated for the roll-type uranium deposits in the Oligocene Chadron Formation in the Alliance, Torrington, New Castle, and Hot Springs NTMS 1°×2° quadrangles, Nebraska, Wyoming, and South Dakota (fig. 1; Dickinson and Hansley, this volume). We expect to complete this assessment in 1990.

New Information on the Nuwok Member of Sagavanirktok Formation; Implications for Petroleum Geology of the North Slope and Beaufort Sea—Evidence from Carter Creek, Arctic National Wildlife Refuge (ANWR), Alaska

T.D. Fouch, E.M. Brouwers, D.H. McNeil, Louie Marincovich, Jr., K.J. Bird, and H. Rieck

Examination of the Nuwok Member of the Sagavanirktok Formation has identified at least 220 m of Nuwok-like strata, a significant addition to the previously described 80 m assigned to the member. The beds are exposed on the north limb of the Marsh Creek anticline along Carter Creek, which is located about 160 km east of Prudhoe Bay and 0.8 km south of the Beaufort Sea (lat 70° N.). Beds are deeply weathered and eroded, but where trenched, yield exposures sufficient for stratigraphic reconstruction, and for sedimentologic, paleomagnetic, and biostratigraphic sampling and analysis.

The Nuwok at Carter Creek represents marine shelf and prodeltaic sedimentation and consists primarily of lithified and unconsolidated pebbly fine sands and silts. Upper parts of the Nuwok contain concretions, and medium- and coarse-grained sandy units. Lower strata of the Nuwok contain laminated to thin flat beds of siltstone, argillaceous claystone, and fine-grained sandstone, associated with ostracode and benthic foraminifers that suggest middle-shelf water depths. Abundant suspended siliceous pebbles (dropstones?) and a high proportion of rafted plant material (fine organic debris, twigs, limbs, and mineralized and woody logs) express considerable terrestrial input. Some units contain pebbles, their long axes randomly aligned, suspended in a poorly sorted, very fine grained structureless matrix; these probably represent submarine debris flows.

The section displays an overall upward-shoaling trend indicated by progressive upward coarsening of the overall sequence and of individual units, increasing thickness of bed sets and scale of crossbeds, concentrations of large log fragments upsection, and the appearance of inner-shelf mollusk and ostracode assemblages. Coarsest strata are best developed between 95–105 m and 155–176 m above the base of the

measured exposures; they include units several meters thick composed of prograding unconsolidated medium- and coarse-grained sand units in multiple cycles of offlap-downlap crossbed sets (some greater than 10 cm thick) each mantled by clayey drapes (traction and suspension cycles). This association suggests periodic episodes of near-shore progradational sediment transport across a shallow (inner-shelf?) sea floor.

The precise age of the Nuwok Member at Carter Creek is uncertain. Benthic fossil groups yield widely disparate ages. A prolific calcareous benthic foraminifer assemblage ranges through the entire Nuwok sequence. The ubiquitous occurrence of *Turrilina alsatica*, known from the western North Atlantic, the North Sea, and northwestern Europe, indicates a late Oligocene age; this age is supported by Sr 87/86 ages of 23.8–27.0 Ma from Nuwok foraminifers and mollusks. The foraminifer assemblage is diverse and abundant for a high-latitude site; absolute diversity is greater than 70 species, and specimen abundance is as high as 100 per gram. The fauna is dominated by *Cibicidoides*, *Cribroelphidium*, *Elphidiella*, *Melonis*, *Nuttallides*, *Trifarina*, *Turrilina*, as well as miliodids, nodosarids, polymorphinids, and unilocular genera. A normal marine shelf environment is indicated.

The Nuwok contains two distinct mollusk assemblages with mutually exclusive species: a lower *Chesapecten nuwokensis* zone, ranging from the base of the sequence to a concretionary unit at 95 to 105 m, and an upper *Arctica carteriana* zone, extending from 105 to 300 m from the base. The mollusks are all Atlantic-derived, indicating a pre-Bering Strait age (>3 Ma). Generic level correlations and the evolutionary lineage of *Chesapecten* imply a maximum age of middle Miocene.

Age arguments based on ostracodes are weaker, being based on the presence of extant species, correlation with global climatic trends, and genus-level comparison with lower latitude faunas. Two ostracode assemblages are recognized: the lower assemblage ranges from 60 to 90 m above the base and includes warm-water genera (*Cytheretta*, *Echinocythereis*, *Cytherelloidea*); the upper assemblage, ranging from 90 to 245 m above the base, consists of temperate to warmer subfrigid genera (*Rabilimis*, *Robertsonites*, *Cytheropteron*, *Paracyprideis*). Several taxa range throughout the section, but most species show stepwise disappearance believed related to changes in climate and water depth. Warm-water genera do not occur above 110 m, most dropping out just below a concretionary zone at 95 to 105 m.

Paleomagnetic analysis indicates that the Nuwok strata have normal polarity from the base of the measured section to about 40 m, reversed polarity from the 40 to 180 m level m with several ≈10-m-thick sequences of normal polarity, one of which corresponds to the concretionary zone extending from 95 to 100 m; and normal polarity from 180 to 190 m. Lack of adequate exposures precludes collection of samples from 190 to 300 m. Laboratory analysis indicates some magnetization is carried by secondary minerals. However, the presence of clearly defined polarity zones suggests that the mineralogic changes occurred shortly after deposition.

Strata that are presumably partial age equivalents to the Nuwok (Oligocene and younger—based upon palynomorph interpretations) have been penetrated in drill holes west of Carter Creek near the Canning River, and in the Beaufort Sea north of Camden Bay. Excellent petroleum reservoir sandstone units were penetrated in these tests that may be represented by the thick inner-shelf progradational sand sequences exposed along Carter Creek.

Sedimentology, Diagenesis, and Reservoir Character of Paleogene Fluvial and Lacustrine Rocks, Uinta Intermontane Basin, Utah—Evidence from the Altamont and Red Wash Fields

T.D. Fouch, J.K. Pitman, J.B. Wesley, Adam Szantay, and F.G. Ethridge

Examination of the Paleogene part of the oil-bearing strata in the Uinta basin indicates that most reservoirs formed in an internally drained intermontane depositional system. Two major phases of lake development gave rise to deposition of sediments that became petroleum source and reservoir rocks, tar sandstone, thick sequences of evaporite units, oil shale, and local uraniferous beds.

Lake sediments of the first phase of development (Maastrichtian to earliest Eocene) are typical of deposition in shallow water within the photic zone. Fossil mollusk species, gypsum beds, and subsurface units containing anhydrite indicate that alkaline lake water was relatively low in chlorides. Although permanent lakes existed, many were intermittent, and large areas were subject to long periods of subaerial exposure and soil-forming processes. During the second phase of development in early Eocene to early Oligocene(?) time, a single large lake complex developed and reached its greatest areal and volumetric extent. The thickest fluvial and lacustrine sequence formed near Altamont field in front of the rising Uinta Mountains along the central segment of the axis of the subsiding Uinta basin. In this area, more than 3,000 m of Paleocene and Eocene lacustrine rock are preserved, and the strata contain more than 1,200 m of fine-grained kerogenous carbonate and mudstone units, including oil shale, that formed during the middle and late Eocene between 46 and 42 Ma.

The thickest and most widespread lake deposits of the second phase principally comprise chemical precipitates, including carbonate units and basin-centered halite and sodium bicarbonate evaporite units, that formed from sulfate-depleted, saline, alkaline lake water in the clastic sediment-starved center of the hydrologic basin. The northern and western fault-bounded margins of the basin are marked by synorogenic coarse conglomerate and conglomeratic sandstone units that extend from the mountain front into or near the lake.

Rocks of the first phase of sedimentation produce oil and gas from deeply buried, overpressured, fractured reservoirs in the Altamont-Bluebell and Cedar Rim fields. Though overpressured strata exist locally, second phase rocks yield oil and gas primarily from normally pressured rocks at Altamont, Bluebell, Red Wash, Pariette Bench, River Bend, and Duchesne fields.

Principal petroleum reservoir rocks are diagenetically altered fluvial channel, deltaic, and open lacustrine sandstones (including turbidites in Altamont) that formed near the lake margin, and nearshore lacustrine bars and beaches that apparently developed parallel with the northeastern margin of the lake in Utah. The channel-form bodies in petroliferous surface exposures of the basin's south flank can be separated into two distinct types with respect to geometry and W:D(width/:depth) ratio. "Type one" is characterized by a tabular geometry controlled by a planar lower bounding surface, an average channel depth of 7.6 m, and an average W:D ratio of 8.9. The planar channel bottom results from underlying resistant carbonate units whose early lithification restricted downcutting and caused more extensive lateral channel migration compared to that of streams forming "type two" bodies. Type two bodies are characterized by a lenticular geometry, by an average channel depth of 5.7 m, an average W:D ratio of 3.6, and a concave-upward lower bounding surface. The absence of resistant carbonate rocks underlying streams that deposited type two bodies resulted in stream channels that, although similar in size, did not migrate laterally as much as those of type one. The size of individual marginal-lacustrine channel sandstone bodies (and therefore reservoir units) is largely dependent upon induration of the substrate across which streams flowed.

Along the south shore of the lake, erosion associated with numerous shoreline fluctuations and relatively shallow nearshore water depths precluded the development and preservation of thick, areally extensive, lacustrine clastic beach and bar deposits. However, lacustrine siliciclastic bars up to several meters thick formed excellent reservoirs along the northeast margin of the lake near Red Wash field, where the depositional dip was apparently steeper and shoreline fluctuations more restricted than those of the lake's southern margin. Carbonate-grainstone-packstone reservoir units, which were generally deposited as carbonate shoals, commonly as thick as 1 m, yield minor oil in the northeastern area of the basin.

Deeply buried overpressured strata are characterized by reservoirs whose matrix permeability values are near, and are commonly below, 0.1 md and whose porosity values (most porosity being secondary) range from 5 to 10 percent. These same strata contain open fractures and transmissivity (T=permeability×height) values through producing intervals that are commonly high. Combined primary and secondary porosity values of 10 to 16 percent are common in normally pressured oil reservoirs, and matrix permeability values may be as high as 1 d. Transmissivity values for such sequences can be relatively high because of their high matrix permeabilty. Gas-bearing sandstone reservoirs in the basin that commonly contain porosity values ranging from 8 to 16 percent, but whose matrix permeability values are 0.1 md or less, are frequently termed "tight gas" sandstones. Transmissivity values for productive "tight gas" intervals are very low because of few natural open fractures.

Basin Development and Resultant Sedimentation Patterns During the Transition from Sevier- to Laramide-Style Tectonism, Central Utah

Karen J. Franczyk, Timothy F. Lawton, and J. K. Pitman

The final phase of Sevier-style tectonism and the initiation of Laramide-style tectonism in central and east-central Utah during latest Cretaceous time segmented the foreland basin and formed several intermontane basins, both on the thrust sheets and in the foreland basin area. An unsegmented foreland basin adjoined the eastern edge of the thrust front from late Early Cretaceous until late Campanian time. The Castlegate Sandstone and its inferred western equivalents were the last strata deposited prior to segmentation of the foreland basin. Within the study area, the Castlegate depositional system consisted of two major alluvial-fan complexes that fringed the thrust belt. The fans graded laterally into a sand-rich alluvial plain (Castlegate Sandstone) across which sediment was transported dominantly eastward toward the coastline. Thereafter, eastward-propagated thrusting along a blind thrust fault created, within the study area, a triangle zone near the thrust front that segmented the most proximal part of the Castlegate depositional area. Consequently, this foreland-basin sequence cannot be traced continuously from proximal alluvial-fan deposits into distal fluvial deposits.

East of the thrust front, isopachs of the Castlegate indicate thickening westward and northward from the southeastern Wasatch Plateau area; the thinner area might have resulted from postdepositional erosion caused by the initial uplift of the San Rafael structure. West of the thrust front, small intermontane basins formed on top of the thrust sheets. Sediment transported into these basins came from both eastern and western sources. In these intermontane basins, facies graded within a few kilometers from conglomeratic alluvial-fan deposits near the margins to floodplain and lacustrine deposits in the interior parts. These beds previously have been correlated with formations of the foreland basin depositional sequence. These intermontane basins existed from latest Campanian through late Paleocene time, and during their formation probably migrated a short distance eastward during their formation atop the thrust sheets.

East of the thrust front, latest Campanian deposition was associated with northward-flowing rivers that transported sediment from feldspar-rich source areas southwest of the study area. A thin unit of uppermost Campanian strata immediately east of the thrust front indicates either extensive postdepositional erosion or, more likely, slow subsidence combined with depositional onlap of the thrust front in this area.

Further segmentation of the foreland basin occurred when a major uplift of the San Rafael structure in very late Campanian or early Maastrichtian time gave rise to a new intermontane basin in the area between the thrust front and the west flank of the San Rafael uplift. Northwestward-flowing, pebble-bearing braided rivers deposited the first sediments in this new basin. Subsequently, a thick Maastrichtian clastic sequence formed in this basin. Like the uppermost Campanian strata, these Maastrichtian beds were derived from sources to the south, but they contain significantly less feldspar than the youngest rocks of the foreland basin system in this area.

East of the thrust front, during the Paleocene, deposition was intermittent and within restricted areas; centers of basin subsidence and locations of uplifts shifted rapidly. During this time, the last phase of Sevier-style thrusting occurred in north-central Utah, and Laramide-style structural elements, such as the Uncompahgre and Uinta uplifts, became active. By early Eocene time, the isolated basins both east and west of the thrust front had filled, and the depositional systems of the region were integrated into a single, large, lacustrine-dominated complex where the youngest part of the Flagstaff Member of the Green River Formation accumulated.

Application of Ground-Penetrating Radar to Development of Reservoir Models

Donald L. Gautier, C. J. Schenk, and Gary R. Olhoeft

Studies of recent sandy sediments can be used to predict reservoir heterogeneities if we are able to investigate sand bodies in three dimensions over appropriate distances. Many studies of recent sediments have relied upon examination of relatively small samples in cores or trenches. Ground-penetrating radar permits the examination of bedforms, bedsets, and individual strata or sets of strata over distances of several centimeters to a few tens of meters, which are the same distances over which significant variations in reservoir properties are commonly observed.

Ground-penetrating radar was used to analyze structures of eolian dunes at Great Sand Dunes National Monument, Colorado. Transceivers of five frequencies (900, 500, 300, 150, and 80 MHz) were used along perpendicular traverses, each approximately 300 m in length. A small area of the sand dunes was selected for investigation, consisting of a large (>30 m thick) dune complex with small (< 1 m thick) superimposed dunes on its eastern flank. The locations of the traverses were carefully surveyed with laser theodolite, and appropriate corrections were made for topography and electrical conductivity of the sand. The investigative power of ground-penetrating radar is inversely proportional to the depth of investigation: higher frequences yield greater resolution and lower frequencies provide greater penetration. Resolution of features a few centimeters thick was possible in the upper few meters of the dune complex by means of the 500 or 900 MHz transceivers. Lower frequency radar (80 to 150 MHz) was capable of penetrating to depths of several tens of meters.

The radar sections showed that the lee slope of the dune complex prograded eastward across fluvial sands and gravels. The internal structure of the dune complex consisted of a large set of cross strata that graded east-northeast into a complex of smaller, multiple sets and then back to a large set with multiple smaller sets along its present lee slope. Bounding surfaces of various sizes were evident within the larger dune sets. Of particular interest were the common low-angle, down-wind bounding surfaces within the large dune complex. These surfaces bounded sets of low-angle strata probably of wind-ripple origin. The cut-and-fill structures observed along the eastern flank of the dune complex probably reflect "vortex scour" and fill resulting from east winds blowing opposite the principal wind direction

for sand transport. The location of the water table was visible as subparallel reflections beneath the dune complex.

Our results indicate the potential of ground-based radar for the detailed interpretation of structures in recent sediments over distances ordinarily out of reach of the sedimentologist or reservoir engineer. Radar studies have potential for revealing complex structures within otherwise relatively homogeneous sand bodies—complex structures that can be expected to affect reservoir quality in ancient sediments.

A Seismic Reflection Study of Miocene Listric Faulting North of Lake Mead, Nevada

J.A. Grow, R.G. Bohannon, J.J. Miller, and R.E. Anderson

Six industry seismic reflection profiles in the Virgin River valley north of Lake Mead, Nevada, are tied to the Mobil Virgin River No. 1A exploration well (TD = 5,964 m, deepest well in Nevada; top of Precambrian crystalline rocks at 5,837 m; top of Paleozoic at 3,355 m; top of Mesozoic at 2,044 m; Miocene and younger above 2,044 m). This part of Virgin River valley is in the Basin and Range province near the western edge of the Colorado Plateau and lies between the Mormon and North Virgin Mountains. The well data and seismic lines show no evidence of the Mesozoic thrust faults or associated compressional structures described in the Mormon Mountains and Tule Springs Hills to the north. Because this area probably did not inherit a strong Paleozoic or Mesozoic structural fabric, it provides an excellent opportunity to study the structures formed during the late Cenozoic extensional deformation.

East-west lines show three subbasins beneath the Neogene valley fill. The subbasins are separated by two large east-tilted fault blocks with north-trending axes. In the western subbasin, well-imaged Miocene syn-extensional basin-fill sediments fan downward against a west-dipping listric fault that decreases in dip from 40° at 0.8 seconds depth (two-way travel time) to 0° at 3.0 seconds. North-south lines show gentle folding contemporaneous with the Miocene extensional deformation, confirming earlier geologic studies suggesting that north-south shortening occurred simultaneously with east-west extension, and that the overall direction of motion for the extensional blocks in this part of the Basin and Range province was to the southwest.

Both the sedimentary strata and listric fault are expressed by strong reflections (where the fault separates basement and cover), but the listric fault shows only weak intermittent reflectors where it penetrates the basement, at depths between 2.4 and 3.0 seconds (increasing to the southwest). Other weak intermittent, subhorizontal reflections can be seen to depths of 7 seconds on Vibroseis® lines which have been reprocessed using the extended correlation technique. We see no evidence in these reflection data for or against a postulated major regional detachment fault beneath the Virgin valley. If such a fault exists, it juxtaposes rocks of such low impedance contrast that lateral coherence of reflections is precluded.

Effects of Basin Evolution on Source-Rock Characteristics of the Woodford Shale, Anadarko Basin, Oklahoma

Timothy C. Hester, James W. Schmoker, and Howard L. Sahl

The Woodford Shale (Late Devonian–Early Mississippian) is an organic-rich, highly compacted, "black" shale that is a significant hydrocarbon source rock in the Anadarko basin of Oklahoma. The Woodford is divided here, on the basis of log character, into three informal stratigraphic units—the upper, middle, and lower members of the Woodford Shale. Higher kerogen content of the middle member is the physical basis for this subdivision.

Depositional patterns of the three Woodford members within the study area reveal a positive structural feature parallel to and about 120 km north of the Wichita Mountains front (along the trend of cross section *E-E′*, fig. 1) that divided the Woodford into northeast and southwest depocenters. This positive structural feature was a hinge line separating areas of regional basement flexure during Woodford deposition. From the hinge line, each member thickens to the southwest (cross sections *A-A′*, *B-B′*, *C-C′*, *G-G′*) in response to subsidence along the axis of the southern Oklahoma aulacogen. To the northeast, thickness of the lower and middle Woodford members remains nearly constant, reflecting a stable shelf environment, whereas the upper member thickens significantly (cross sections *A-A′*, *B-B′*, *C-C′*, *D-D′*) reflecting and dating initial development of the Sedgwick basin of south-central Kansas.

The Woodford Shale was deposited during the transition between two major stages of structural development that together formed the present-day Anadarko basin—the first-stage southern Oklahoma aulacogen (early Paleozoic) and the second-stage foreland-style

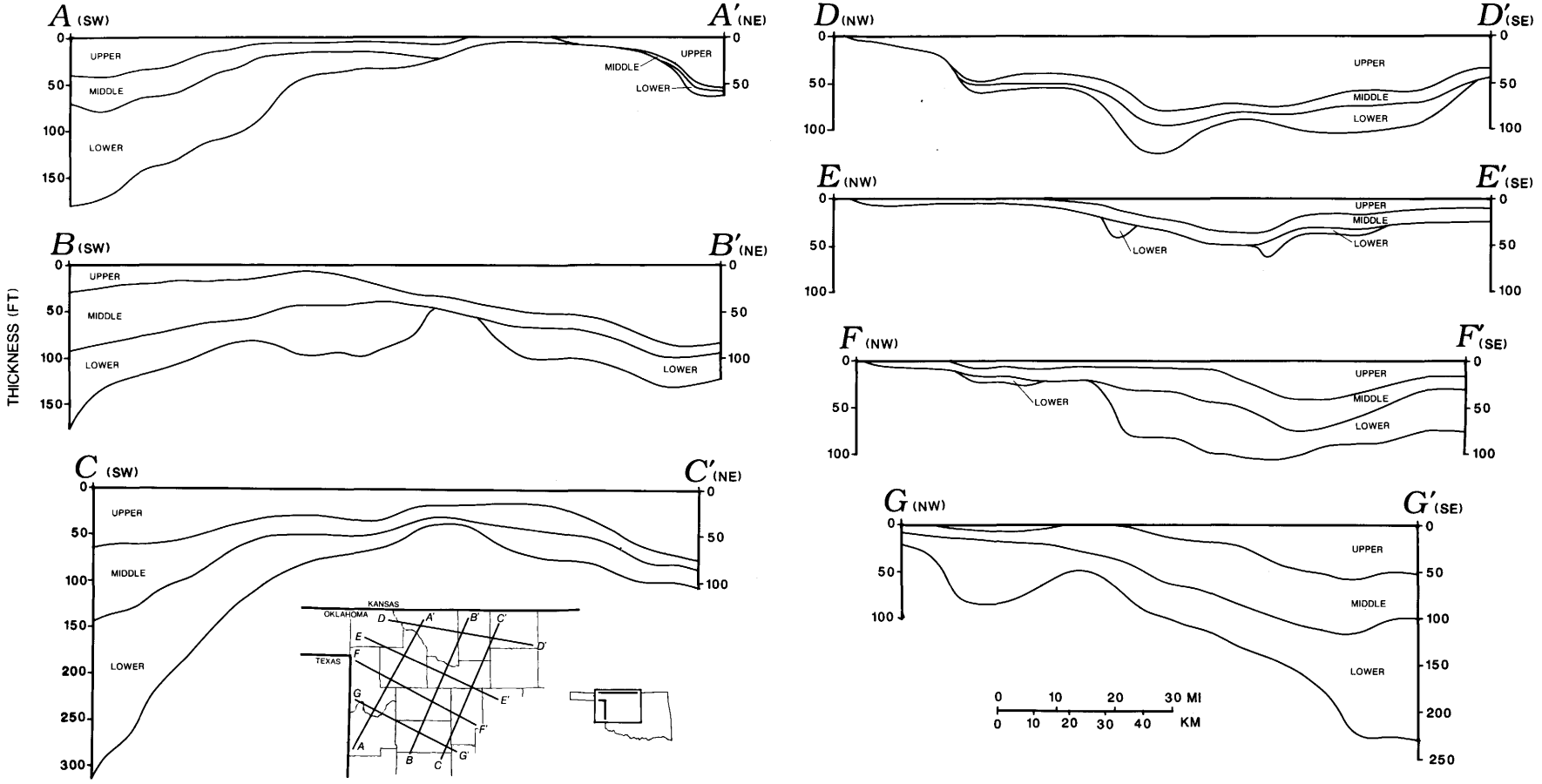

Figure 1 (Hester). Smoothed regional cross sections of the three informal members of the Woodford Shale (Late Devonian–Early Mississippian) depicting the influence of Anadarko basin evolution on the distribution of Woodford Shale sediments. Index maps show study area, lines of cross section, and State and county boundaries.

downwarping (late Paleozoic). Varying burial depths of the Woodford during the second stage of Anadarko basin development overprinted thermal maturity patterns onto Woodford depositional patterns. As a result, Woodford sediments in the northeast portion of the study area (cross section *D-D´*), which are dominated by the upper member (TOC (total organic carbon) averages 2.7 wt. percent), remain immature to marginally mature with respect to oil generation. More deeply buried Woodford sediments in the southwest portion of the study area (cross section *G-G´*), which are dominated by the middle and lower members (TOC averages 5.5 and 3.2 wt. percent, respectively), are mature to postmature with respect to oil generation. Thus, most hydrocarbons sourced by the Woodford Shale of the study area were generated from the lower and middle members, which contain about three-fourths of the thermally mature organic carbon.

Architecture of Clastic Facies and Location of Coals Associated with a Major Marine Transgression—The Mid-Cretaceous of the Kaiparowits Plateau, Utah

Robert D. Hettinger and Peter J. McCabe

The upper part of the Smoky Hollow Member and lower 100 m of the John Henry Member of the Straight Cliffs Formation are well exposed along depositional strike and dip in the region west of the town of Escalante in the northern part of the Kaiparowits Plateau, southern Utah. A series of sections tied into photo mosaics help explain the complex facies architecture of this interval. The strata are divided into two parasequence sets of intertonguing tidal channel, shoreface, and offshore marine deposits. The lower set appears to backstep toward the southwest, whereas the upper set clearly forward steps toward the northeast. These deposits are correlated over 19 km to the northwestern part of the plateau, where the strata contain significant coal deposits.

The lower parasequence set is underlain by about 30 m of trough crossbedded pebbly sandstones that are laterally amalgamated. This distinct and laterally extensive pebbly unit, informally called the Calico bed, is thought to have been deposited by braided rivers. The Calico grades upward into interbedded sandstones and mudstones which form the base of the lower parasequence set. The sandstones have erosional bases and contain basal lags of mud clasts and logs with *Teredolites*. Bidirectional trough and planar tabular crossbeds and ripple laminae suggest accumulation under tidal influence. These sediments are truncated by an erosion surface which gently dips toward the northeast. It is covered by a thin conglomerate of extraformational pebbles and cobbles, interpreted to be a lag deposit on a ravinement surface. The conglomerate lag is overlain by about 2 m of swaley cross-stratified sandstone which is capped by a shark-tooth lag that marks the condensed interval between the two parasequence sets.

The upper parasequence set, which forms the lower part of the John Henry Member, contains about 10 parasequences that are arranged in a forward-stepping stack. A typical parasequence consists of interbedded mudstones and hummocky cross-stratified sandstones that pass upward into pebbly sandstones with swaley cross-stratification. In the western end of Upper Valley, only 2 m of strata separates the shark-tooth lag from the lowest swaley cross-stratified sandstone. In less than 8 km eastwards, this 2-m interval thickens to about 55 m because of the forward-stepping geometry. Tidal channel deposits intertongue with and replace shoreface sediments in a landward direction. These channels are infilled with pebbly sandstones containing abundant broken oyster and *Inoceramus* shells.

Major deepening events have tentatively been correlated into the strata of the northwestern part of the plateau. In this region tidal channel sandstones interfinger with terrestrial mudstones and coals. The coals, which are up to 4 m thick, accumulated lateral to the forward-stepping shoreface deposits of the Escalante area and appear to have formed in mires several kilometers landward of the shoreline.

Reservoir Characteristics of the Lower Cretaceous J Sandstone in the Kachina Field, Denver Basin, Colorado

Debra K. Higley

Thin-section petrography, well logs, and core porosity-permeability studies show that porosity loss in the Lower Cretaceous J sandstone in the Kachina field was primarily the result of early precipitation of quartz cement. Porosity and permeability were further reduced by authigenic kaolinite and other pore-filling clays. Reservoir facies are primarily fine- to medium-grained quartzarenite and sublitharenite. Producing facies are thin-bedded, trough- and planar-crossbedded distributary channel sandstone. More than 1.3 million barrels of oil have been produced from the Kachina field. Overlying mudstone is the seal for structurally/stratigraphically trapped hydrocarbons.

J sandstone core from 4,269 to 4,328 ft depth in the B-1 Sheetz (SW¼SW¼ sec. 14, T. 3 S., R. 52 W.), Sheetz

no. 6 (SW¼SW¼ sec. 23, T. 3 S., R. 52 W.), and Raymond Thomas no. 1 (NE¼NE¼ sec. 23, T. 3 S., R. 52 W.) drill holes was sampled and analyzed petrographically. Core median permeability is 87, 72, and 281 millidarcies, and core median porosity is 21, 23, and 24 percent, respectively, for the three drill holes. Intergranular porosity in the thin sections studied ranges from 14 to 22 volume percent; minus-cement porosity ranges from 26 to 43 percent. Porosity is mainly primary and secondary intergranular in origin; minor amounts of intragranular and microporosity may be present. Volumetrically, the most important authigenic mineral is syntaxial quartz cement, which ranges in amount from about 4 to 21 percent. Kaolinite plus other clays vary from 4 to 14 volume percent. These clays are generally incorporated with fine-grained detrital material and occur within pores and pore throats.

Paragenesis of reservoir facies comprises the following sequence of events: (1) minor sediment compaction prior to (2) formation of quartz and feldspar overgrowths, (3) calcite cementation and replacement of lithic grains, (4) dissolution of calcite, which results in restoration of primary porosity and creation of secondary porosity, (5) collapse of detrital material into resulting pore spaces and growth of illite-smectite, chlorite, and other pore-filling clays, and (6) formation of authigenic pore-filling kaolinite.

Computer Display of Petroleum Exploration Through Time in the Denver Basin of Colorado, Nebraska, and Wyoming

Debra K. Higley and Kenneth I. Takahashi

Denver basin petroleum exploration through time is animated and displayed on a Macintosh computer. Trends in basin-wide and individual county exploration are shown with drill-hole data for 5-year increments from 1900 through 1983.

The source of drill-hole data is the Petroleum Information Corp. Well History Control System database. Drill-hole location, completion date, and production data were analyzed using a series of U.S. Geological Survey computer programs which divided the Denver basin into approximately ¼ mi^2 grid cells and calculated the type and highest level of petroleum production within each cell. Mapped data show the earliest time interval of exploration and the oil and gas, oil, gas, or nonproducing category of each grid cell. A grid cell with an oil and gas symbol, for example, might contain an oil and gas, a gas, and a nonproducing drill hole, whereas a dry-hole cell has only one or more nonproducing drill holes within it.

The exploration maps were generated with Dynamic Graphics Interactive Surface Modeling software on a VAX 11/780 minicomputer. The maps were then scanned and processed with Super Paint software on a Macintosh Plus computer. Denver basin political boundaries were created with Macintosh Mapmaker software. Hypercard software is used to select and present basin, county, and field map images.

In this animated display, petroleum exploration begins with scattered shallow drilling concentrated around basin margins, and with development in the late 1800's and early 1900's of the Florence oil field (which produces from the Cretaceous Pierre Shale). Exploration proceeds to a Cretaceous J and D sandstones surge in drilling in the 1950's, and continues with discovery in 1970–83 of Wattenberg gas field and other Cretaceous Dakota Group fields, and Paleozoic fields in the southeast part of the basin.

Carbon Isotopic Trends in Peats and Coals—Clues to Carbon History and the Environment of Coal-Forming Mires

Charles W. Holmes

The global biogeochemistry of carbon is extremely complex. Carbon dioxide released into the atmosphere as a result of the combustion of fossil fuel is added to that naturally respired by the biosphere and released from the hydrosphere. The carbon cycle has been and continues to be a subject of much concern as it is CO_2 that is held responsible for much of the so-called "greenhouse" effect. Recent modeling studies have revealed significant gaps in information that limit our ability to define the paths and interactions of the gases within the biosphere and oceans. The measurement of carbon and carbon isotopes in coal and in modern peat-forming environments has been undertaken as a means of better defining the balances within the carbon cycle and determining the usefulness of $\delta\,^{13}C$ trends as clues to the environmental development of coal-forming mires.

The $\delta\,^{13}C$ of plants, the original materials that form coal, is a function of plant physiology and the isotopic composition of the atmosphere in which plants grow. The physiological effect is created by the photosynthetic path (C_3 plants are significantly depleted in ^{13}C with respect to C_4 plants) and (or) habitat (mesic plants are depleted in ^{13}C with respect to hydric plants). In the Okefenokee Swamp, Georgia, for example, the hydric C_3 water lily (*Nymphaea ororata*) has a $\delta^{13}C$ of –22.5‰ , whereas the C_3 mesic fern (*Woodwardia virginica*) has a $\delta^{13}C$ of –30.0‰. Measurements on the same plants, subjected to atmospheric CO_2 with varying $\delta^{13}C$, have demonstrated

that carbon fixed in plants does reflect these systematic variances between hydric and mesic plants.

Peats forming in environments that are progressively inundated as a result of a relative rise in base level would be expected to show a succession of plants from mesic to hydric. The carbon signature of these peats is initially negative (relatively light) but becomes heavier as the peats are formed from plants with an increasing hydric component. The $\delta^{13}C$ trends in the Anderson, Smith, and Lake De Smet coals of the Powder River basin are of this lighter-to-heavier type. This information, coupled with the palynological data from these beds, suggests that the plant physiological environment resulting in the formation of these coals was similar to the modern environment within the Okefenokee Swamp of southern Georgia.

In raised mires, the isotopic composition of the atmosphere is the dominant factor in influencing the isotopic variability of the plants. Measurements have shown that, due to recycling, the CO_2 in the local air is depleted in ^{13}C with respect to atmospheric averages. Continued recycling and deposition of plant material on the forest floor would lead to progressive lighter carbon being available to the plants, which would be reflected in the more negative $\delta^{13}C$ in the resultant peat. This process accounts for the trend observed in the modern peats and Tertiary coals of Borneo.

The data therefore suggest that the trends of $\delta^{13}C$ in peats and the resultant coal are a measure of the environment of formation, and the $\delta^{13}C$ of coals may also provide data on the variation in isotopic composition of atmospheric carbon through geologic time.

The Search for Subtle Traps Across Onshore Alaska

David G. Howell

For most of this century the U.S. Geological Survey has collaborated with industry and academic scientists exploring and characterizing the petroleum potential of Alaska. Discoveries in Cook Inlet, Point Barrow, and Prudhoe Bay are the obvious successes. These three oil and gas fields lie along north and south margins of continental Alaska; between these two areas Alaska is viewed as a collage of tectonostratigraphic terranes that have agglomerated since approximately Middle Jurassic time. The stratigraphy of these terranes indicates a tectonic mixing of oceanic magmatic arcs and continental slivers. The latter presumably represent truncated portions of the North American margin. Mapping and geophysical experiments indicate that these terranes are either enveloped or underlain by a vast volume of graywacke. Although these rocks initially posed as an intriguing potential hydrocarbon source, numerous Rock-Eval and associated thermal studies now suggest that the sedimentary strata are over-mature, rendering a deep-gas scenario only improbable.

The greater part of the accretion tectonism of interior Alaska had ended by the close of the Mesozoic. Latest Cretaceous to Neogene sedimentary overlap sequences reflect three general phases of basin accumulation, all of which are nonmarine. Locally these basin strata are as thick as 5 km, but nowhere is there thought to be anything other than small quantities of dry-gas resources.

In spite of this pessimistic forecast, two areas remain of interest owing to recent preliminary studies that suggest the potential for oil accumulations. The first is the Yukon Flats–Kandik basin area of east-central Alaska. Here, thermally over-mature Mesozoic strata lie structurally(?) above a thick Precambrian to lower Mesozoic sequence that remains thermally within the oil window; furthermore, several horizons within this lower sequence are excellent potential hydrocarbon source rocks. Understanding the tectonic history, the regional structural patterns, and the subsurface extent of thermally cool strata will better enable us to evaluate this region.

The second area is the region along the northern margin of the Brooks Range. Here, tectonic duplexing likely thickened and shortened sequences of organically rich lower and middle Mesozoic strata along with early foreland basin deposits (Upper Jurassic and Lower Cretaceous). These same beds are the source of the oil trapped in the giant Prudhoe Bay field, and migration of the oil probably followed pathways up the south flank of the northerly migrating lithospheric bulge, which formed as a consequence of tectonic loading in the interior zone of the Brooks Range thrust belt. Because this bulge once existed farther south, tracking its movement history may predict other occurrence of trapped oil.

Rifts and Hot Spots—A Model for the Proterozoic Midcontinent Rift System of North America

D.R. Hutchinson and R.S. White

Hot spots beneath young, rifted continental margins have been identified by their association with massive short-lived eruptions of basalts that contain distinctive geologic, geophysical, and geochemical signatures. This volcanism can be explained by decompression melting and rapid extrusion of igneous

material during lithospheric extension above a broad, asthenospheric, thermal anomaly—a hot spot. Perhaps the best studied modern hot-spot/rift system is in the North Atlantic, where the continental margins of Norway, Greenland, and Rockall formed in association with the Iceland hot spot.

The Middle Proterozoic (1.1 Ga) Midcontinent Rift System (MRS) of North America shares many characteristics with modern rifted continental margins and flood basalt provinces. The volume of synrift extrusive basalts in the MRS (1.3×10^6 km^3) rivals that of some of the Earth's largest and much younger flood basalt provinces, such as the Deccan traps. The areal limit of MRS basalts can be roughly contained within a circle 1,600 km in diameter, well within the size range of oceanic hot-spot swells. Basalts in the MRS were extruded over a period as short as 10 to 13 m.y., with the bulk of the eruption possibly concentrated in as little as 2 to 3 m.y., a time frame consistent with the rapid extrusion estimated in younger flood basalt provinces such as the Columbia River, Parana, Deccan, or North Atlantic Tertiary provinces. Stratigraphic and structural studies indicate that much of the MRS volcanism occurred at or above sea level, which is predicted by the dynamic and isostatic uplift associated with a mantle thermal anomaly. Geochemical signatures of the basalts, such as the presence of basal picrites, are consistent with higher melt percentages associated with higher mantle temperatures.

Deep seismic-reflection profiles collected as part of the Great Lakes International Multidisciplinary Program on Crustal Evolution (GLIMPCE) can be used to constrain end-member models of melt thickness and stretching factors, and therefore yield an estimate of the potential temperature of the mantle at the time of rifting. (The potential temperature is the temperature that the mantle would have if brought to the surface adiabatically without melting.) We determine that the mantle potential temperature was about 1,500 to 1,570 °C during rifting, which is about 350 °C hotter than the modern mantle potential temperature (1,280 °C) but may have only been 100 to 200 °C hotter than 1.1-Ga mantle. A thermal anomaly of 100–200 °C is consistent with that estimated for modern hot-spot swells, such as the Cape Verdes or Hawaii, and for modern hot-spot/rift systems, such as the North Atlantic province. We call this thermal anomaly in the MRS the Keweenaw hot spot.

Gravity modeling requires that much of the lower crust beneath the basalts of the MRS is more dense than the adjacent rift flanks or unrifted crust; this density anomaly is interpreted as evidence for massive igneous (probably gabbroic) underplating. The thickness of the upper Keweenawan postrift clastic deposits can be used in conjunction with the gravity model to examine subsidence and stretching factors. Our combined analysis yields stretching factors of 3 to 4 within the MRS, and suggests that the thermal anomaly associated with the Keweenaw hot spot either dissipated or migrated away during the accumulation of the postrift units. Why this huge continental rift ceased extending when it was so close to complete break-up is unknown, but tectonic forces operating in the nearby coeval Grenville orogen probably played a critical role.

Petroleum Geology Studies in the Santa Maria Province, California

Caroline M. Isaacs, J. David King, Richard M. Pollastro, and Colin F. Williams

The Santa Maria Province Project is a basin evolution study undertaken in the coastal California margin by the U.S. Geological Survey's Evolution of Sedimentary Basins Program and the Onshore Oil and Gas Investigations Program. The basins included within the Santa Maria province are the onshore Santa Maria, offshore Santa Maria, Huasna-Pismo, Santa Barbara-Ventura, Sur, and Santa Lucia basins (fig. 1). The province has significant petroleum reservoirs and is especially important as the major location of fractured siliceous reservoirs within the Miocene Monterey Formation (fig. 2). The province is ideally located for study of the hydrocarbon-source characteristics of the prolific Monterey Formation, as this formation is the only petroleum source rock in the onshore and offshore Santa Maria basins, as well as a principal source rock throughout the province. Studies of the fractured reservoirs and hydrocarbon-source rocks within the Santa Maria province are also important to ongoing assessment of undiscovered hydrocarbon reserves in the little-explored basins offshore central and northern California, where the Monterey Formation is regarded

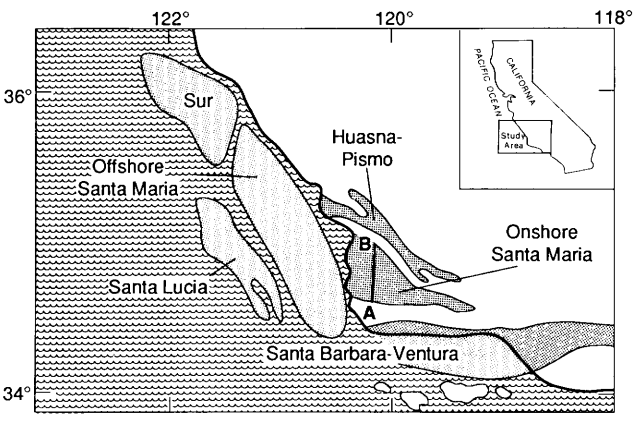

Figure 1 (Isaacs). Neogene marine basins in Santa Maria province area.

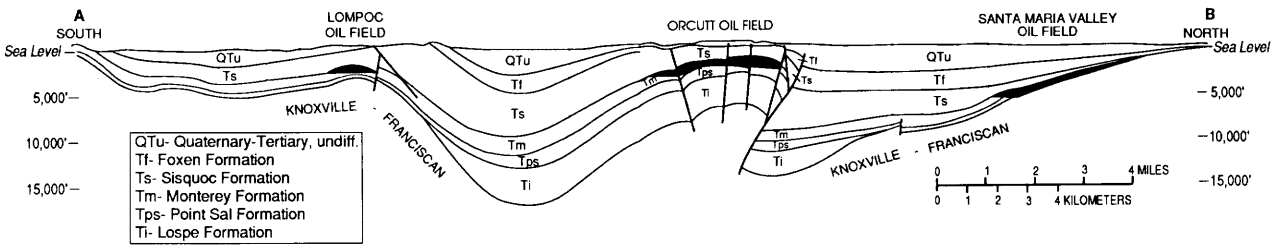

Figure 2 (Isaacs). South-to-north cross section on line *A-B* of figure 1. Knoxville-Franciscan, Knoxville Formation and Franciscan Complex.

both as a major potential petroleum source and as an important potential petroleum reservoir.

Despite its importance to petroleum geology in California, the Santa Maria province has been little studied in the public domain as a petroleum province, and many questions remain about its thermal evolution, its petroleum reservoir-rocks, and the source, maturation, and migration of its hydrocarbons. For example, the viscosity and density of the oils within the province are highly variable; is the variation due to characteristics of source, maturation, or migration? Do various facies of the Monterey Formation mature differently? Are particular facies or lithotypes better petroleum source rocks, and why? What organic maturity parameters are useful, and how are they related to other measures of diagenesis and thermal exposure? Reported present-day thermal gradients vary considerably over the region (range, 24–67 °C/km); does this variation reflect variations in heat flow or in thermal conductivity of the sedimentary cover? How has the thermal history of the province been affected by tectonism?

To examine these questions, the USGS Santa Maria Province Project has initiated a wide-ranging study of diagenesis, thermal history, and organic geochemistry of the province. Specific regional efforts underway include: (1) a coordinated study of thermal history involving clay diagenesis, silica diagenesis, biomarker maturation characteristics, and fission-track thermal analysis of subsurface sections throughout the province; (2) a major survey of present-day thermal gradients and heat-flow distribution; and (3) an international cooperative effort with colleagues from industry and academia focused on the organic geochemical characteristics of Monterey kerogens and oils from the province. In addition, topical efforts underway include: (1) isotopic study of fluid inclusions in fractured reservoir rocks; and (2) characterization by scanning electron microscopy of lithotypes within the fractured reservoirs.

Geologic Evolution of the Uinta-Piceance Basin Province, Northwestern Colorado and Northeastern Utah

S.Y. Johnson, M.L. Tuttle, Bruce Bryant, R.F. Dubiel, T.D. Fouch, K.J. Franczyk, V.J.S. Grauch, M.A. Grout, R.C. Johnson, C.M. Molenaar, D.J. Nichols, K.M. Nichols, V.F. Nuccio, Fred Peterson, J.K. Pitman, W.J. Perry, Jr., D. Sawatzky, R.W. Scott, E.R. Verbeek, and R.B. Wanty

The Uinta-Piceance Basin province (UPBP) of northwestern Colorado and northeastern Utah has undergone a complex Phanerozoic history characterized by at least five distinct phases (Cambrian through Mississippian, Pennsylvanian-Permian, Triassic-Jurassic, Cretaceous, Paleogene) of regional tectonism, basin development, and sedimentation. Basinal strata were deposited on a Precambrian basement of crystalline and metasedimentary rocks cut by Proterozoic faults of variable orientation. The UPBP formed part of the continental platform-shelf on the northwestern flank of North America during the early and middle Paleozoic.

Cambrian through Mississippian strata consist mainly of shallow-marine limestone, dolomite, shale, and quartzite; contain major unconformities; and thicken westward. Pennsylvanian-Permian block uplifts associated with the transpressional(?) ancestral Rocky Mountain orogeny segmented this early to middle Paleozoic platform-shelf into the Eagle, Paradox, and Oquirrh basins. Both basin-margin tectonics and cyclic eustatic/climatic fluctuations strongly controlled deposition of the nonmarine/marine, mixed clastic, carbonate, and evaporitic fill of these basins.

During the early Mesozoic, the UPBP formed part of a slowly subsiding continental platform. Triassic-Jurassic rocks include considerable eolian, alluvial, and

lacustrine deposits that become significantly thicker and grade into more marine facies from east to west. Paleozoic and early Mesozoic strata in the westernmost part of the UPBP were uplifted and thrust eastward during the late Mesozoic Sevier orogeny, which resulted in subsidence in the bordering foreland basin. The sedimentary history of the UPBP portion of this foreland basin is recorded by thick nonmarine deposits within and adjacent to the thrust belt that grade eastward into thinner accumulations of marginal-marine and marine rocks. The geometry and style of regional compressional deformation changed dramatically in the latest Cretaceous with onset of the Laramide orogeny. Laramide uplifts segmented the UPBP Cretaceous foreland basin into the Uinta and Piceance intermontane lacustrine basins. The geometry of these lacustrine basins is notably different from that of the Pennsylvanian-Permian segmented UPBP basins.

Major scientific problems addressed in the UBPB study include the following: (1) documenting and (or) refining basin stratigraphy and chronostratigraphy; (2) clarifying relations between sedimentation and the diverse Phanerozoic tectonic styles; (3) describing and modeling the geochemical and diagenetic evolution of basin constituents; and (4) relating the tectonic-sedimentary and geochemical-diagenetic histories to development of energy and mineral resources. The UPBP has important hydrocarbon resources, including oil, gas and tar sands. Paleogene lacustrine rocks host 90 percent of the Nation's oil shales. The UPBP also contains significant coal, evaporite, phosphate, uranium, and metal deposits.

Publications that are planned for the UPBP study include the following: (1) gravity and magnetics maps; (2) a remote-sensing-lineament map; (3) basement structure contour and Phanerozoic sedimentary rock thickness maps; (4) a series of regional stratigraphic and chronostratigraphic cross sections of Phanerozoic rocks; (5) balanced structural cross sections across the Sevier orogenic belt; (6) detailed stratigraphic-sedimentologic charts of selected units; (7) surface vitrinite reflectance map; (8) paleogeographic maps; (9) a volume of papers describing and (or) modeling and synthesizing aspects of the geophysics, structural geology and tectonics, physical stratigraphy, biostratigraphy, sedimentology, paleogeography, paleoclimatology, petrology and diagenesis, geochemistry, heat flow and thermal maturity, and paleohydrology of the UPBP; and (10) a volume of papers on the geochemistry of Green River Formation oil shales.

Diagenesis of Sandstones in the Norphlet Formation (Upper Jurassic), Escambia County, Alabama

C.W. Keighin and C.J. Schenk

The Upper Jurassic Norphlet Formation is an important hydrocarbon reservoir in Baldwin and Mobile Counties, and offshore in Mobile Bay, Alabama. It produces gas condensate in the Flomaton field in Escambia County, and underlies the oil-bearing Smackover Formation in the Little Escambia Creek field (southeast of Flomaton field), at a depth of approximately 15,500 ft (4,725 m). Sandstones of the Norphlet examined in cores from two drill holes in the Little Escambia Creek field are largely fluvial in origin, are moderately well to well sorted, very fine to coarse grained, and feldspathic, and are extensively altered by a complex sequence of diagenetic reactions.

Evidence of chemical and mechanical compaction of these Norphlet sandstone units is slight, although small stylolites containing asphaltic oil are present in the Smackover Formation. The limited degree of compaction suggests that extensive early cementation by anhydrite and (or) calcite reduced compaction, and subsequently these cements were removed by migrating fluids (a theory shared by a 1989 study by B.E. Lock and S.W. Broussard). In a 1989 study, S.A. Dixon and others also suggested that high pore pressure, in conjunction with a lack of early calcite or anhydrite cement, may have reduced effects of compression due to deep burial. X-ray diffraction indicates the presence of halite, but none was preserved in thin section. Migrating fluids, in addition to removing cements, contributed to albitization of detrital feldspars, subsequent leaching of feldspars and rock fragments, and precipitation of chlorite cement. Chlorite, when present, occurs as well-crystallized grain coatings on most framework grains. Chlorite content is quite variable, however, not only within the samples examined, but also laterally; R.L. Kugler, and S.A. Dixon and others, both in 1989 studies, have noted that it ranges from zero to several volume percent.

Porosity is typically well developed. Intergranular pores are due primarily to partial-to-complete dissolution of cements and mineral grains, especially feldspar. Intragranular pores are largely the result of partial leaching of rock fragments, as well as due to

microporosity formed by precipitation of clay minerals in earlier dissolution pores. Our evidence indicates that most of the porosity present in the samples examined from the Little Escambia Creek field is secondary and due to leaching of cements and framework grains. S.A. Dixon and others' 1989 study reached an alternative conclusion, that primary porosity is most significant in the Norphlet Formation in Lower Mobile Bay.

Alluvial Sandstone Geometries and their Relationship to Coal Deposition in a Transgressive Systems Tract, Dakota Formation, Utah

Mark A. Kirschbaum and Peter J. McCabe

The terrestrial strata of the Dakota Formation were deposited during a eustatic rise in sea level. They are overlain by marine shales of Cenomanian age. Clastic strata in two areas (the western margin of the Kaiparowits Plateau in southern Utah and the southwest part of the San Rafael Swell in central Utah) present slightly different architectural relationships to associated coal deposits. In both areas, alluvial sandstones overlie a major unconformity. In the Kaiparowits region the basal Dakota fills paleovalleys incised into gently dipping Jurassic strata. In the San Rafael Swell the Dakota overlies the mid-Cretaceous Cedar Mountain Formation.

In the Kaiparowits region, the alluvial sequence in the Dakota is from 5 to 300 m thick. Differential subsidence in the foreland basin resulted in an increased thickness of section towards the western thrust belt. Four widespread coal zones separate clastic units that are up to 20 m thick. The coal zones contain carbonaceous mudrock, rooted and fossiliferous mudrock, thin rippled sandstone and coal. Coal beds are as thick as 1.5 m in the study area but reach 5.5 m farther to the west. Sediments of these zones are thought to have accumulated in mires containing minor lakes and low-energy fluvial channels. Intervening clastic units are composed of laminated mudrock, rippled sandstone, and ribbonlike bodies of crossbedded sandstone. Rippled sandstone and mudrock are interpreted as crevasse splay and overbank deposits. Ribbon sandstones are 5–10 m thick and 50–150 m wide and have pronounced basal scours and lateral accretion surfaces. They are interpreted as deposits of slightly sinuous streams. Within the clastic units, numerous coeval channels, of various sizes, suggest an anastomosed system of channels which may have resulted from avulsion of major river systems into the mire environment.

In the San Rafael Swell, the Dakota Formation is between 0 and 40 m thick. The alluvial sequence contains a lower unit of interconnected crossbedded sandstones that is traceable along depositional dip for about 80 km. These amalgamated channels are interpreted as valley-fill deposits. Few overbank deposits are preserved because channels were restricted to valleys and continually reworked finer sediment. Amalgamated channels are overlain by 2–3 m thick rippled sandstones, mudrock and a few discontinuous coal beds less than 1 m thick. The rippled sandstones are present as ribbon bodies which are highly sinuous. These facies are interpreted as the deposits of small meandering rivers and associated mires on a low-gradient coastal plain. They grade upward into crossbedded, burrowed and oyster-bearing sandstones and shales indicating an evolution into tidal and lagoonal environments.

The difference between the two regions in the relation of sandstone geometry to amount of coal may be related to relative rates of base level rise. The sediments of both areas are thought to have accumulated during the same eustatic rise in sea level but subsidence rates were different. In the San Rafael Swell, the highly interconnected channels of the lower unit of sandstones preclude any coal preservation, whereas the lenticular coals and enclosed channels of the upper unit reflect a gradual rise in base level. In the Kaiparowits Plateau, the greater thickness of the sequence and the significantly greater amount of coal are thought to be due to the increased rate of base level rise resulting from subsidence in this area; also there may have been a tectonic control on river avulsion into the area.

Gulf of Mexico Basin Evolution—Geophysical and Tectonic Framework

Kim D. Klitgord, D. R. Hutchinson, and Hans Schouten

Sedimentary basins seaward of the Gulf Rim fault zone in the Gulf of Mexico region (fig. 1*A*) form the Gulf basin, which developed along extensional and rift-shear zones that linked the Atlantic rift and spreading-center systems with plate boundaries in the Pacific during the early Mesozoic (fig. 2). Crustal zones in the Gulf basin are delimited by seismic structure, magnetic-anomaly character, sediment-distribution patterns, and density structures derived from gravity modeling within the framework of the plate-tectonic model in a 1986 report by Klitgord and Schouten and a 1988 report by Klitgord, Hutchinson, and Schouten. We can identify continental, rifted-continental, rift-stage (thick-continental), marginal-oceanic (thin-continental), and oceanic crustal zones (fig. 1*B*) that are modified from the crustal zones of a 1985 study by R.T. Buffler and D.S. Sawyer. This

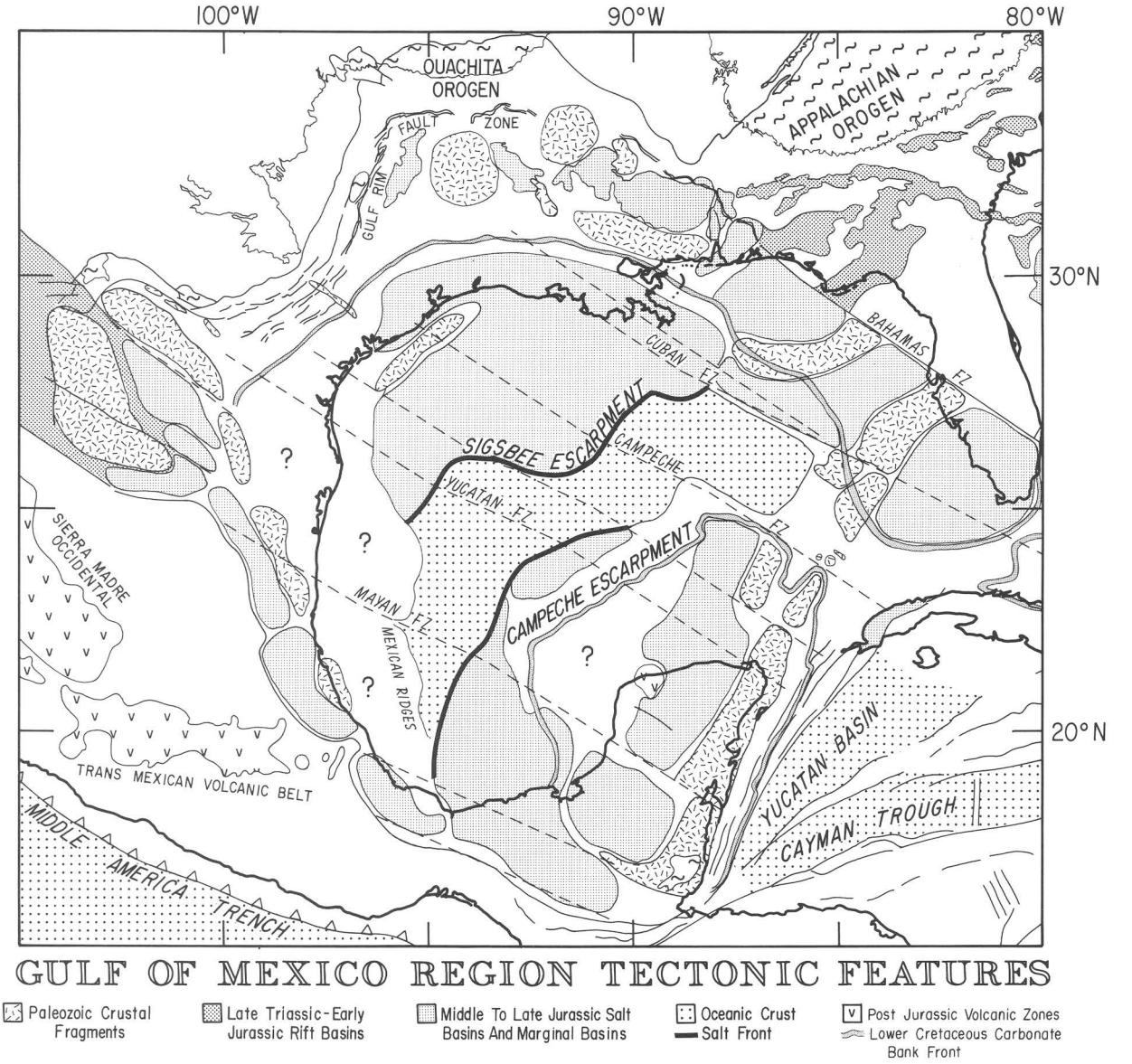

Figure 1 (above and following page) (Klitgord). Gulf of Mexico region. *A*, Tectonic features.

crustal-zone distribution and paleogeographic reconstructions for the region are used to assess the paleoenvironment and shifts in centers of basin evolution during the Mesozoic.

The northern Gulf basin (fig. 1*A*), including the onshore salt basins of Texas, Louisiana, and Mississippi and the offshore basins beneath the West Florida Shelf, evolved during the Late Triassic and Early Jurassic within a rift-shear zone bounded by the Bahamas and Cuban fracture zones. The shear-zone boundary then shifted southward between the Cuban and Campeche fracture zones, where it remained during the Middle to Late Jurassic (fig. 2). Geophysical data from the Gulf basin are consistent with a simple plate-tectonic model in which the Yucatan microplate remains attached to the South American plate until the end of the Jurassic. As the Gulf basin evolved between the separating North American and South American–African continents, the Yucatan microplate formed its southeastern margin and moved southeastward from the Texas-Mexico border region. Regional geophysical data and limited well data suggest the existence of marginal rift basins beneath much of Yucatan, where a carbonate platform formed atop rift-stage crust, as in the west Florida province.

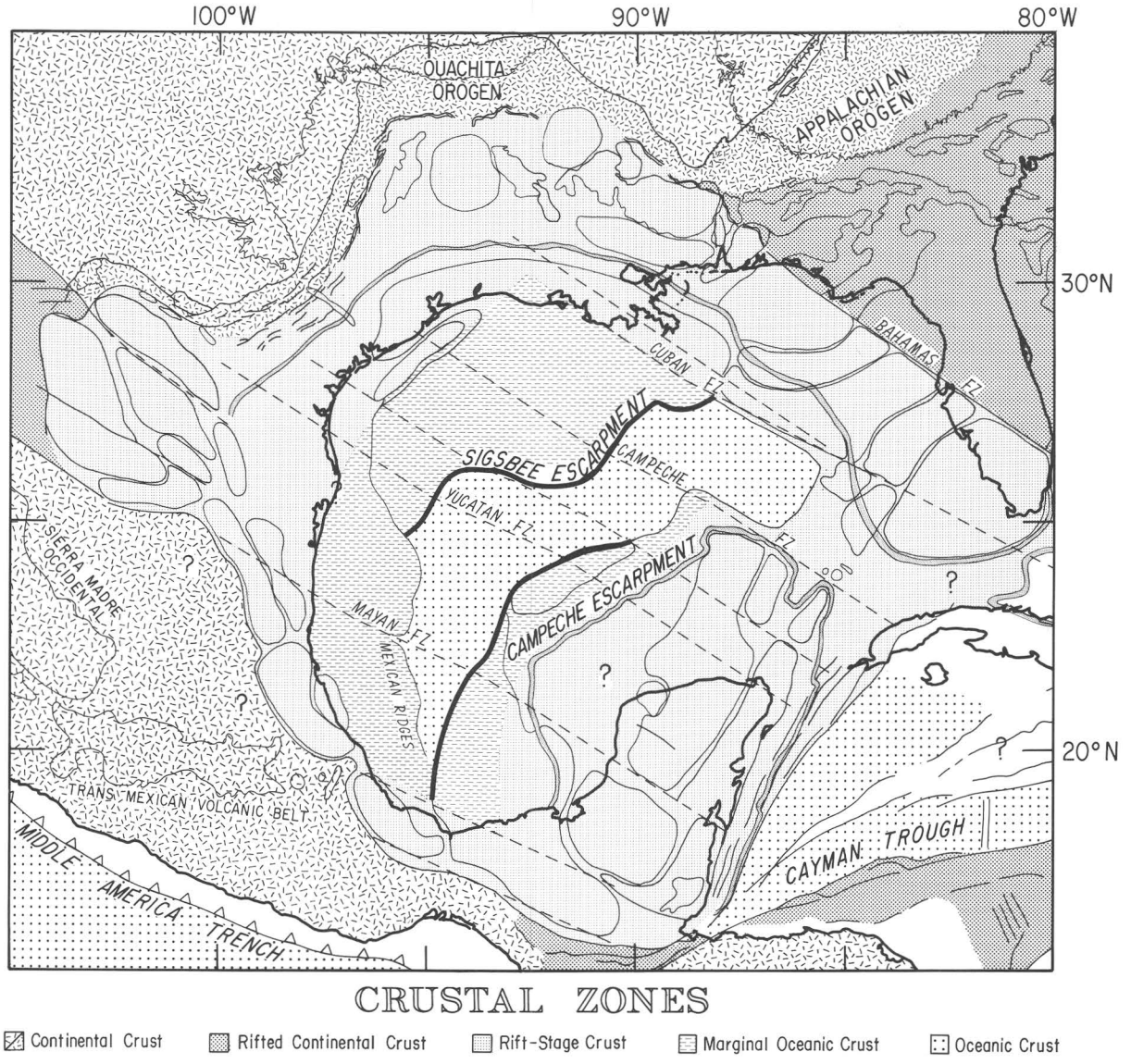

Figure 1 (Klitgord)—Continued. Gulf of Mexico region. *B*, Crustal zones.

The Global Methane Hydrate Reservoir—Impact on Petroleum Exploration

Keith A. Kvenvolden and Timothy S. Collett

Gas hydrate is a naturally occurring solid composed of rigid cages of water molecules that entrap mainly methane. Gas hydrate deposits are globally widespread in two distinct settings: (1) offshore, in sediments of outer continental margins where water depths exceed 300 m, and (2) nearshore and onshore, in polar areas where gas hydrate is associated with the occurrence of permafrost. The stability of naturally occurring gas hydrate is controlled by specific requirements of pressure, temperature, and concentration of methane in water. The amount of methane in gas hydrate in the shallow geosphere (subsurface depths of less than about 2,000 m) is very large; however, estimates of the amount are speculative and range over three orders of magnitude, from 3×10^{15} to 8×10^{18} m^3 (1×10^5 to 3×10^8 Tcf). We favor a value of about 2×10^{16} m^3 (7×10^5 Tcf), an estimate that is

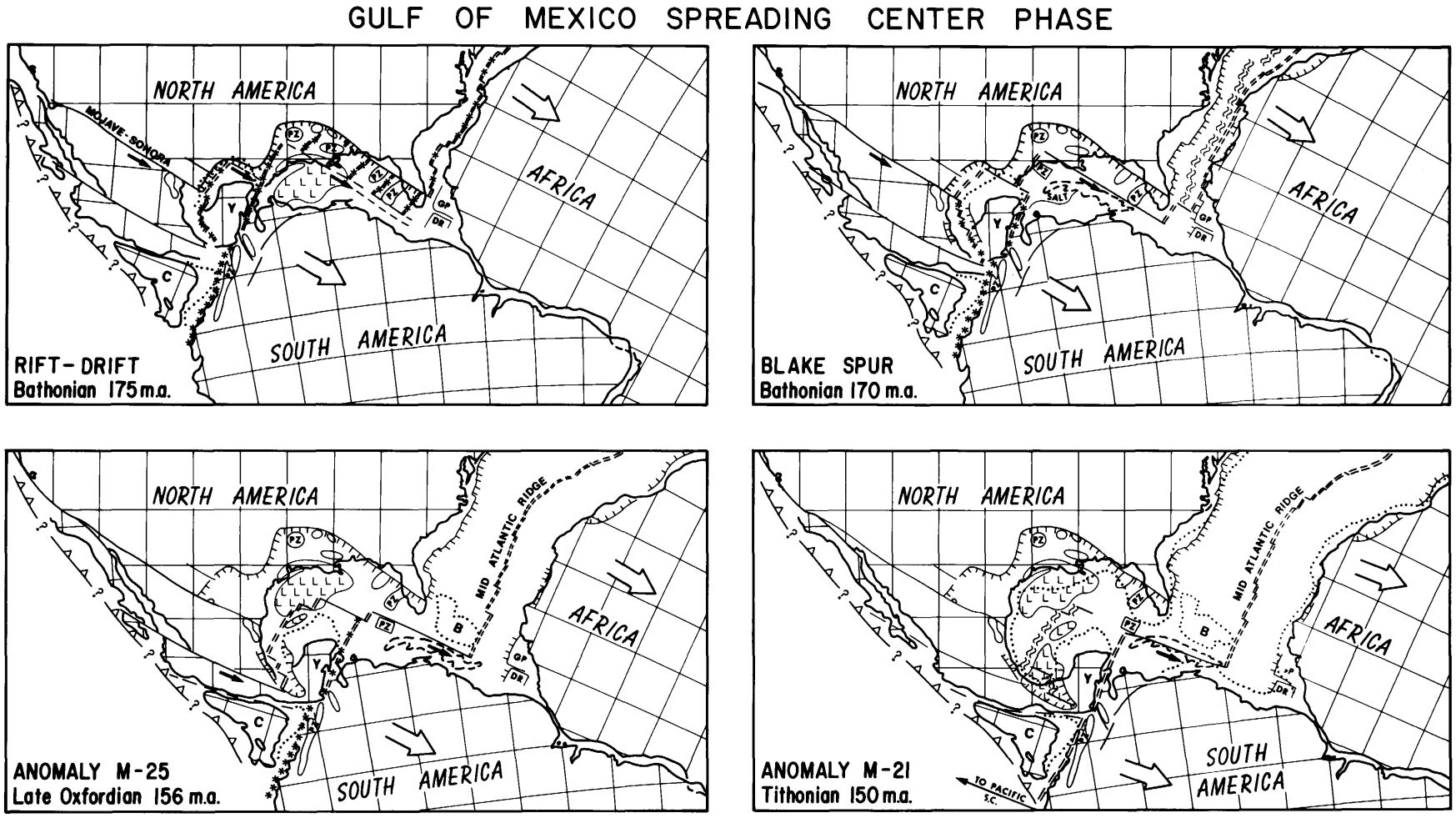

Figure 2 (Klitgord). Paleogeographic reconstructions of the continental configurations around the Gulf of Mexico region during the Jurassic. Active plate boundaries and plate motions relative to North America are shown. Modified from figure 10 of a 1986 report by Klitgord and Schouten.

exclusive of methane possibly trapped in reservoirs immediately beneath gas hydrate. This estimated volume of methane in gas hydrate greatly exceeds the estimated volume of methane remaining as a conventionally recoverable resource [3×10^{14} m^3 (1×10^4 Tcf)].

The presence of such large quantities of methane at such shallow depths should have an impact on petroleum exploration and production. Consideration has been given to gas hydrate as an unconventional energy resource. But at least four factors have deterred serious efforts to explore for gas hydrate: (1) insufficient information concerning the extent of gas hydrate and its reservoir parameters, (2) locations in hostile environments of polar regions and the deep sea, (3) no agreement on adequate production schemes, and (4) no economic incentive while conventional gas reserves meet global energy needs. Only in the U.S.S.R. at the western Siberian Messoyaka gas field has methane been recovered from gas hydrate deposits, and this production has now been shut-in due to limited pipeline facilities.

Because gas hydrate occurs at shallow subsurface depths, exploration drilling in polar regions and on continental margins beyond the shelf will undoubtedly encounter these solid gas deposits. The explorationist should be aware that certain drilling and production problems have already been attributed to the presence of gas hydrate in Alaska, Canada, and the U.S.S.R. These problems include uncontrolled gas release during drilling as well as casing collapse during production. As exploration and production activities continue to move farther offshore into deeper water and to higher latitudes in the Arctic, the frequency of gas-hydrate-related incidents is likely to increase.

Because the global methane hydrate reservoir is located so near the surface, portions of this reservoir are vulnerable to global climate change. A question of current interest concerns possible consequences of adding methane, a significant "greenhouse" gas, to the atmosphere from destabilized methane hydrate as a result of global warming. Models of greenhouse warming predict that climatic change will be greatest in the Arctic. Permafrost warming and release of methane from gas hydrate may already be in progress, but the amount of methane that has been or will be released is unknown. Any methane that comes from destabilized gas hydrate will add to methane that is currently lost to the atmosphere as a result of industrial activities involved in methane production. Methane from these sources augments methane from current biological processes resulting in an increase in atmospheric methane concentrations during recent time.

As the search for future energy resources continues, gas hydrate will either be eagerly sought or assiduously avoided. Either way, the petroleum explorationist will need to be cognizant of this substance.

Sulfur Isotope Evidence for the Origin of Cap-Rock-Hosted Sulfide Deposits, Hockley Salt Dome, Texas

J. Richard Kyle, William N. Agee, Tim W. Johnson, and W.C. Shanks, III

The Gulf Coast basin is a dynamic hydrologic environment in which mixing of multi-source fluids is a plausible mechanism to account for sulfur isotope variations of metal sulfide concentrations in salt dome cap rocks. Stratiform sulfide laminae have been documented within the anhydrite cap rocks of several Gulf Coast salt domes (fig. 1). Textural evidence indicates that these sulfide laminae represent episodic mineralization at the salt/cap rock contact as the cap rock formed by sequential underplating. Thus, their metal contents and isotopic characteristics can be evaluated in terms of a progressive paragenesis from top to base representing a relatively long history of rock-fluid interactions in the cap rock environment. Reservoirs of reduced sulfur and metals evolved during the several million year accumulation history of the typical anhydrite cap rock.

The best documented sulfide-bearing cap rock mantles the Hockley salt dome in south-central Texas where subeconomic Fe-Zn-Pb-Ag sulfide concentrations have been defined on the basis of 60 drill holes. Hockley is a relatively young diapir with the cap rock believed to have developed within the last 45 m.y. Sulfides occur throughout the 285-m-thick cap rock and show progressive trends with regard to metal ratios and sulfur isotope composition. If the Hockley cap rock formed at accretion rates of the same magnitude as the Winnfield, Louisiana, anhydrite cap rock where paleomagnetic studies indicate formation rates of 3–6 m/m.y., then the mineralization history at Hockley dome likely lasted several million years. Major metal concentrations at Hockley occur in a 20-m zone within the central cap rock "stratigraphy." The general metal trend is an overall increase of Zn relative to Pb downward in the cap rock; Ag concentrations are also higher in the lower cap rock. These data suggest that the sulfide-precipitating fluid became more Zn- and possibly Ag-rich during anhydrite cap rock accumulation.

$\delta^{34}S$ values of sulfide minerals within the Hockley cap rock range from +4 to –35‰ ($n=100$). $\delta^{34}S$ values of pyrite within a single drill hole are progressively heavier with depth to the approximate middle of the cap rock, where the isotopic trend is reversed (fig. 2, p. 48).

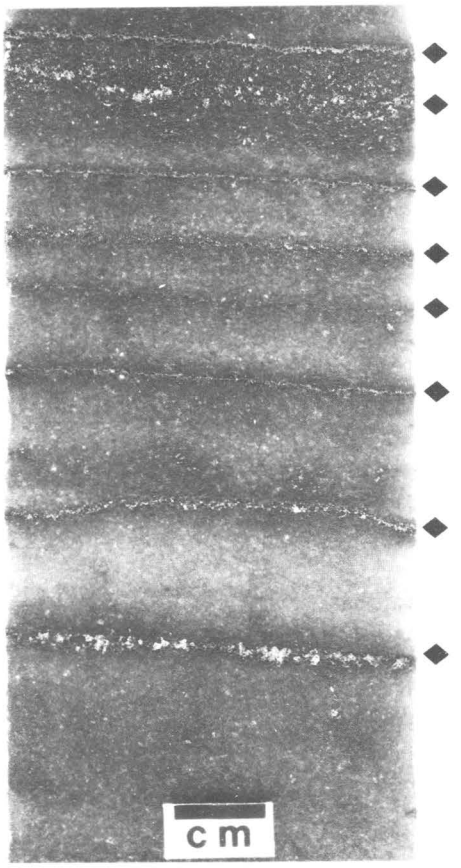

Figure 1 (Kyle). Stratiform sulfide laminae (diamonds) in a banded anhydrite cap rock core from the Hockley salt dome, Harris County, Texas. These pyrite laminae are relatively enriched in ^{32}S downward, that is, in the paragenetically younger direction, with $\delta^{34}S$ values changing from –0.3 to –5.0‰, CDT.

The inflection point corresponds with a local highly mineralized bioepigenetic calcite zone. Relatively heavy $\delta^{34}S$ values generally correlate with more intensely mineralized intervals throughout the cap rock. Analyses of closely spaced sulfide laminae (fig. 1) in a 1.5-m anhydrite intercept indicate a range of $\delta^{34}S$ values from –0.3 to –7.9‰ ($n = 23$). Vertical trends and clustering of values for adjacent lamine suggest that local/temporal variations affected the sulfur reservoir at this scale.

The complementary metal and $\delta^{34}S$ data indicate that two isotopically distinct sulfur components were involved in cap rock sulfide mineralization. An isotopically light H_2S is attributed to bacterial reduction of aqueous sulfate derived from dissolution of anhydrite cap rock ($\delta^{34}S = +16 \pm 1$‰). The correlation between intensity of sulfide mineralization and sulfide $\delta^{34}S$ indicates a genetic relationship between the generation of heavy H_2S and the supply of metals by relatively hot, deep-source formation waters. Heavy H_2S could have been supplied along with metals in these formation waters. Conversely, if petroleum was present in the formation waters, then thermochemical reduction of cap rock sulfate could produce isotopically heavy H_2S.

The highly mineralized intervals with heavy $\delta^{34}S$ values are interpreted to represent a sustained supply of relatively hot, deep-source fluids to the cap rock environment. These events resulted in a greater contribution of heavy H_2S to the mixed sulfur reservoir, either through extrinsic supply or by local thermochemical production of H_2S. Large volumes of heated metalliferous formation waters also could indirectly affect the supply of isotopically light H_2S. Episodic introduction of ≥ 100 °C fluids would periodically decimate the bacterial population. Heavy H_2S would dominate the sulfur reservoir until the salt dome environment returned to lower temperatures for bacteria regeneration.

The preferred mineralization model for Hockley dome proposes that warm metal-bearing formation waters migrated up the salt dome flanks and mixed with ambient cool meteoric waters containing isotopically light H_2S produced by bacterial activity. Introduction of metalliferous fluids, perhaps episodically released during basin dewatering, overwhelmed the light H_2S component by the combined effects of supplying heavy H_2S and suppressing local bacterial H_2S production. The trend of progressively heavier $\delta^{34}S$ values of sulfide laminae toward the middle of the cap rock along with high metal concentrations suggests that basin-derived fluids reached a maximum during the middle history of anhydrite cap rock accumulation. Biogenic H_2S then began to dominate the mixed sulfur reservoir resulting in the trend toward relatively light $\delta^{34}S$ values of the scattered mineralized zones to the present cap rock/salt contact.

Acknowledgments: This research was partly conducted during a University Research Institute Faculty Research Assignment to RK; additional support was provided by NSF grant EAR-8709319.

Quality Parameters of Permian (Gondwana) Coal, Khalaspir, Bangladesh

E.R. Landis, M.N. Islam, and Hal Gluskoter

A recently completed exploratory drill hole in the northwestern part of Bangladesh penetrated more than 500 feet of coal-bearing strata in the Gondwana sequence of Permian age. The hole was drilled by the Geological Survey of Bangladesh at a site selected on the basis of geophysical interpretation of gravity measurements. Coal of Permian age is now known to be

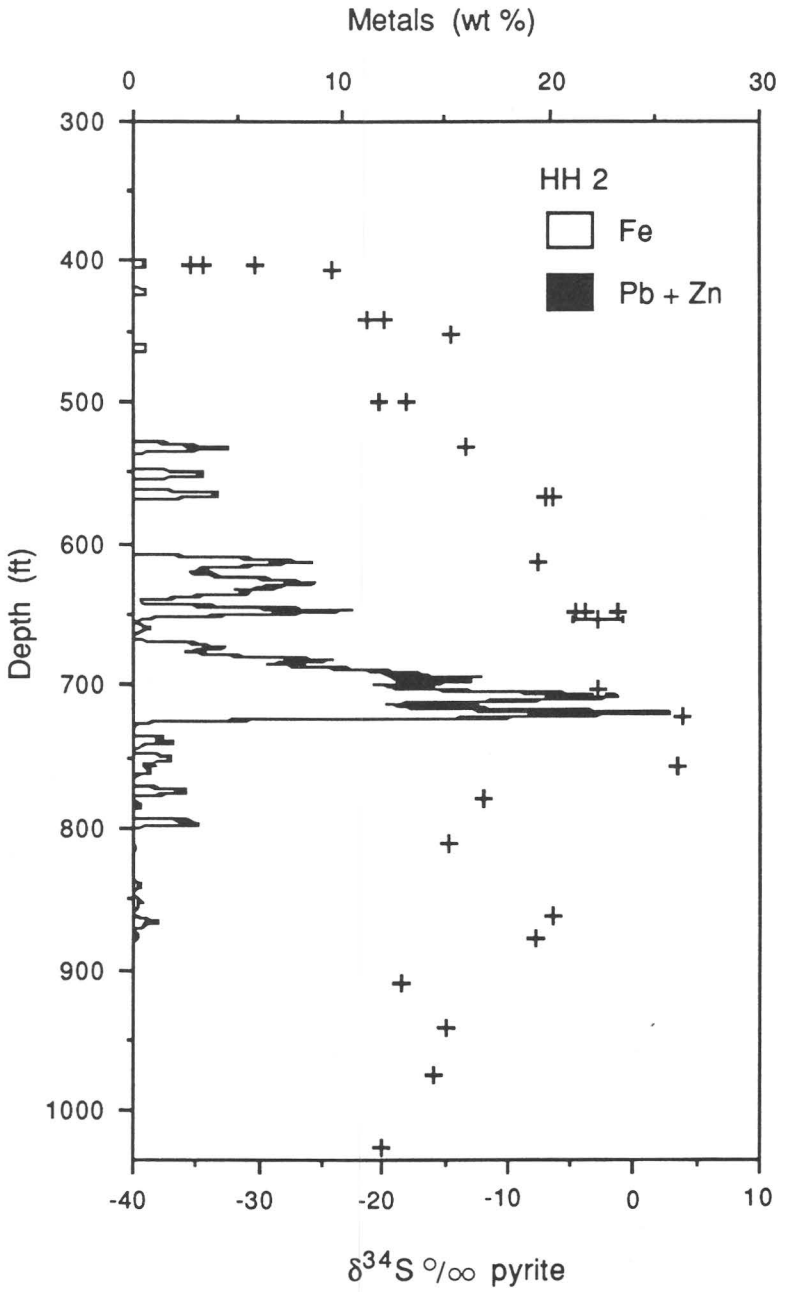

Figure 2 (Kyle). Histogram showing metal content of cap rock drill hole HH2 at Hockley dome compared with $\delta^{34}S$ composition (+) of selected stratiform sulfide laminae. Note general correlation of relatively heavy $\delta^{34}S$ values with greater metal abundances.

present in three different areas of northwestern Bangladesh, and other potential coal areas await exploration. Coal is not presently mined in Bangladesh but might in the future constitute a valuable energy resource for the country.

A total of 41 core samples of coal and associated coaly rocks from 12 different coal beds were selected megascopically to represent grade and type differences in the coal. The samples were collected, packed, and shipped to an analytical laboratory in a standard manner.

The coal beds that were sampled range in thickness from less than 2 feet to almost 50 feet. The uppermost coal bed occurs at a depth of about 935 feet. Further exploration is needed to determine the lateral extent of the coal beds.

Preliminary results from the standard coal analytical procedures indicate that according to ASTM Standards, 31 of the individual samples have an apparent rank of medium-volatile bituminous coal, and the other samples have apparent ranks ranging from high-volatile A bituminous to anthracite. The individual coal samples range in ash content from 7.6 percent to almost 50 percent: two-thirds of the samples contain less than 25 percent ash and almost half contain 15 percent or less ash. Sulfur content ranges from 0.26 percent to 1.7 percent: three-quarters of the samples contain less than 1 percent sulfur. The Free Swelling Index of individual samples ranges from 0 to 7.5: the index of 26 samples is 2.5 or less, and 14 of those samples had an index of 1.0. The Hardgrove Grindability Index of the samples ranges from 43 to 59.

Weighted (by thickness) average analyses for coal beds, or benches of thick coal beds, were calculated. Almost all fall in the apparent rank category of medium-volatile bituminous coal, have medium (less than 15 percent) to high ash contents, and have low (1 percent or less) to medium (less than 3 percent) sulfur contents. The coal beds are thicker and contain less ash in the upper part of the coal-bearing sequence. For example, two thick beds (about 45 and 50 feet thick, respectively) in the upper 116 feet of the Gondwana sequence have a weighted average analysis, on the equilibrium moisture basis, of 2.6 percent moisture, 13.9 percent ash, 1.0 percent sulfur, 24.3 percent volatile matter, and 59.2 percent fixed carbon, and a heat value of 12,519 Btu/lb.

The available information indicates that the coals of the Khalaspir area are suitable for most or all forms of thermal conversion, such as generation of electricity. An undefined but probably smaller part of the resource might also be suitable for use in the manufacture of metallurgical coke.

Thermal Evolution of the Upper Cretaceous Fruitland Formation, San Juan Basin, Colorado and New Mexico

Ben E. Law

The source of heat during the thermal evolution of the coal-bearing Upper Cretaceous Fruitland Formation in the northern part of the San Juan Basin of Colorado and New Mexico has been the subject of controversy for many years. In recent years, the successful exploitation of gas from coal beds in the San Juan Basin has revived the controversy and provided additional impetus to learn more about the thermal history of these coal beds. Nearly all previous work dealing with the thermal history of the Fruitland has alluded to volcanic activity in the nearby San Juan Mountains to the north as a probable source of heat. However, based on the interpretations of time-temperature modeling and thermal maturity patterns derived from a recently completed project of thermal maturity mapping in the San Juan Basin, the high levels of thermal maturity in the northern part of the San Juan Basin are postulated to be due to a deep, localized source of high heat flow in conjunction with convective heat transfer associated with vertically directed fluid flow. There does not appear to be any evidence supporting the notion that the observed levels of thermal maturity are due to a heat source located in the San Juan Mountains.

Mean random vitrinite reflectance (Rm) values of coal beds in the Upper Cretaceous Fruitland Formation in the San Juan Basin of Colorado and New Mexico range from 0.42 percent in the southern part of the basin to 1.54 percent in the northern part of the basin, where a northwest-trending irregular-shaped area of high thermal maturity occurs. North of the area of high thermal maturity, in the subsurface and in outcrops, Rm values in the Fruitland decrease to less than 1.0 percent. Isoreflectance lines drawn on structural cross sections intersect dipping bedding planes at large angles at either end of the cross sections where they cross the basin's steeply dipping monoclinal rims. In the central part of the basin, isoreflectance lines are far above the same bedding planes on these cross sections. This relationship between structure and thermal maturity indicates that the levels of thermal maturity were achieved after structural deformation of the basin.

Rm profiles of wells drilled through Cretaceous and Tertiary rocks in the basin are commonly nonlinear with two to four segments. In the southern, less mature part of the basin, nonlinear Rm well profiles have two segments, an upper steep-sloping segment and a lower moderate-sloping segment. The intersection of these segments occurs at Rm values ranging from 0.55 to 0.60 percent. In the northern, more mature part of the basin, where Rm values of the coal-bearing Fruitland Formation are greater than 0.8 percent, nonlinear Rm well profiles have as many as four segments, in descending order: a moderate-sloping segment, a nearly vertical steep-sloping segment, a low-sloping segment through the coal-bearing Fruitland Formation, and a moderate-sloping segment. In the area of high thermal maturity, Rm gradients through the coal-bearing Fruitland are high, ranging from 1.0 to 1.5 percent/1,000 ft, compared to gradients in overlying and underlying rocks that range from 0.01 to 0.30 percent/1,000 ft, respectively. These gradients most likely represent the combined effects of contrasting thermal conductivities

associated with lithologic variations and differences in heat transfer processes (conductive vs. convective). In the area of low thermal maturity there is no distinct Rm gradient coincident with the coal-bearing Fruitland, perhaps due to the facilitation of heat transfer through the coal beds by the relatively large amounts of moisture contained in low-rank coals.

Time-temperature modeling of a few wells in the San Juan Basin indicates that present-day heat flow is insufficient to account for the measured levels of thermal maturity. The modeling shows that heat flow reached a maximum of about 200 mW/m^2 during Eocene and Oligocene time. Furthermore, in order to match the nonlinear Rm well profiles, artificially high thermal conductivity values must be assigned to nearly all the stratigraphic units. The unreasonably high thermal conductivity values could be interpreted as evidence of heat transfer by vertically directed fluid flow.

Identified Petroleum Systems Within the United States—A 1990 Status Report

Leslie B. Magoon

Exploration and resource assessment can be made more efficient if the processes responsible for petroleum occurrence can be studied in the context of a genetic unit—the petroleum system. Such a study is intermediate between basin analysis and play or prospect evaluation. Basin analysis emphasizes structural depressions and the included sedimentary rocks, regardless of the relation to any petroleum deposit; study of the petroleum system emphasizes the genetic relation between a particular source rock and the resulting petroleum accumulations; play evaluation emphasizes structural and stratigraphic reservoir trends; and prospect evaluation emphasizes individual traps. Economics are less important in a basin analysis or in a petroleum system study than in a play or prospect evaluation.

A petroleum system encompasses a hydrocarbon source rock and all generated oil and gas accumulations, and includes all those elements that are essential for an oil and gas deposit to exist. *Petroleum* includes concentrated occurrences of any of the following: thermal and microbial natural gas found in conventional reservoirs as well as in gas hydrate, tight sandstone, fractured shale, and coal; condensates; crude oils; heavy oils; and solid bitumen found in siliciclastic and carbonate reservoir rocks. *System* describes the interdependent geologic elements that create oil and gas accumulations. These elements include a petroleum source rock, migration path, reservoir rock, seal, trap, and the geologic processes that create each element. All these elements must be correctly placed in time and space for a petroleum deposit to occur.

The stratigraphic, areal, and temporal extent of a petroleum system is specific. The system includes the following stratigraphic units: a petroleum source rock, rocks through which migration has occurred, a sealed reservoir rock (trap), and the rock overburden (representing time and temperature) required for maturity. The areal extent of the petroleum system is defined by a line that circumscribes the mature source rock and all oil and gas deposits, conventional and unconventional, originating from that source. The events of a petroleum system are defined by two timespans, the duration time and the preservation time. The duration of a petroleum system is the time it took to deposit the basic elements and generate the hydrocarbons, or to form the system. The preservation time is the length of time that some hydrocarbons within the system have been preserved in the geologic record.

The system nomenclature combines the geologic names of the source and reservoir rock units, and also expresses a level of certainty. For example, the Tuxedni-Hemlock(.) is a petroleum system in the Cook Inlet, Alaska. The level of certainty is the likelihood that a particular hydrocarbon accumulation originated from a particular source rock. Petroleum systems are classified by using criteria such as source- and reservoir-rock type and the complexity of their geologic history.

The list of petroleum systems within the United States has been revised and expanded to include new information published since the last tabulation in 1988, in which 119 systems were identified. Presently 130 petroleum systems have been identified, of which 89 are purebred (structurally simple) and 41 are hybrid (structurally complex). Of 12 possible categories, the 2 most common systems are in the purebred siliciclastic category and have either type II (32) or type III (19) source rocks (rocks containing type II or III organic matter). Presently, all hybrid carbonate systems contain type II source rocks. Siliciclastic reservoirs (90) occur more than twice as often as carbonate reservoirs (40). The most common source rock is type II (73), followed by type III (41); the least common source rock is type I (16).

By characterizing petroleum systems using these and other geologic criteria, various elements of each system can be more clearly identified and compared to determine their efficiency in the generation, migration, and trapping of hydrocarbons. Characterizing the efficiency of each petroleum system and of each element within it will help focus research, resource assessment, and exploration programs.

Deep-Water Fan Deposits, Gulf of Mexico—Seeing Through Salt Seismically

Robert E. Mattick and Frederick N. Zihlman

The hypothesis that the Sigsbee Escarpment in the northwestern Gulf of Mexico is not associated with deep-rooted structural uplift, but is an expression of horizontally intruded and (or) extruded tongue-shaped salt lobes covered by a veneer of upper Pleistocene sediments less than 1,000 m thick, is supported by at least four lines of evidence from seismic data: (1) the top and bottom of the inferred salt mass are marked by strong reflections; (2) a distinct velocity inversion can be measured at the base of the inferred salt mass; (3) seismic horizons recorded on the rise continue, without change in character, into the interior of the slope beneath the inferred salt mass; and (4) the thickness of the inferred salt tongue is about equal to the height of the escarpment above the sea floor.

Formation of the Sigsbee Escarpment apparently influenced construction of a 2,000-m-thick deep-water fan complex that is mapped on the rise at the base of the escarpment. The fan complex is of Pleistocene age. The oldest fan units may have been derived from sediments shed from an early escarpment located landward of the Sigsbee Escarpment. The short-lived, early depocenters of turbidite deposition appear to have migrated back and forth (in an east-west direction) for distances in excess of 200 km. During and following formation of the Sigsbee Escarpment, which may have involved two phases of salt intrusion or extrusion during late Pleistocene time, the principal depocenter of turbidite deposition has migrated about 250 km westward.

Some of these fan deposits, at water depths of 2.5 km and buried beneath 2–3 km of salt and Pleistocene sedimentary rocks, may be potential reservoirs for oil and gas.

Subsidence, Eustasy, and Climate—Controls on Coal and Clastic Facies Architecture, Cretaceous of Western United States

Peter J. McCabe, Robert D. Hettinger, Mark A. Kirschbaum, J. David Sanchez, and Keith W. Shanley

In order to develop more predictive models of the geometry and quality of coal deposits, it is important to better understand the roles of subsidence, eustasy, and climate in controlling coal accumulation. These same parameters also control clastic facies architecture. As part of a major study of the controls on Cretaceous coal accumulation, high-resolution facies studies are being carried out on outcrops of coal-bearing strata in various locations in the western United States. Lessons learned from these studies can be applied not only in coal exploration but also in oil and gas exploration for sandstone reservoirs.

Outcrop studies in the Kaiparowits Plateau area of southern Utah allow examination of fluvial deposits, shoreface sequences, and coals within a variety of systems tracts. Major coal deposits are present in both the Dakota Formation and the John Henry Member of the Straight Cliffs Formation. The Dakota Formation, of Albian to Cenomanian age, is part of a transgressive systems tract which separates the underlying Jurassic strata from the overlying marine Tropic Shale. Coal zones in the Dakota can be traced over several tens of kilometers, and individual seams are locally as thick as 5.5 m. Ribbon-shaped channel sandstones, interpreted as anastomosed river deposits, are present between the coal zones. Other facies include thin rippled sandstones, rooted mudstones, and fossiliferous mudstones which are interpreted respectively as crevasse splay, overbank, and lacustrine deposits. These clastic deposits are thought to have been introduced during periods of major river avulsion into the mire environments. By contrast, the John Henry Member was deposited as an early highstand systems tract during the Coniacian to early Campanian. Coals of this member lie within a 25-km-wide band that parallels the paleoshoreline trend; coal seams are locally as thick as 5 m. To the northeast in this systems tract are vertically stacked shoreface sandstones; to the southeast are vertically aggraded fluvial deposits. The latter consist of tabular meanderbelt sandstone bodies lying within thick overbank mudstones.

In contrast to the Dakota and John Henry, the late highstand systems tracts of the Turonian Tibbet Canyon Member and lower part of the Smoky Hollow Member of the Straight Cliffs Formation contain coals that are thin and laterally discontinuous. Shoreface deposits show a marked forward-stepping pattern and are overlain by tidal channel and meandering river deposits. Coals are not associated with the braided river deposits of the upper part of the Smoky Hollow Member or the Campanian Drip Tank Member of the Straight Cliffs Formation, which are interpreted to have formed in broad incised valleys above sequence boundaries.

The nature of the mires in which the coals accumulated appears to be important in controlling the facies architecture of some of the associated clastics. The ribbon-like nature of the sandstones in the Dakota may be due to the style of avulsion into the vegetated mires. During the Coniacian and Santonian, however, the

climate appears to have favored the formation of raised mires. The elevated nature of these mires would have restricted the landward inundation of marine waters during transgressions. The mires may, therefore, have been a critical element in determining the unusual vertical stack of more than 250 m of shoreface deposits within the John Henry Member.

Characteristics of Coal-Bearing Strata in Tertiary Basins, Based on Integrated Sedimentary and Structural Field Studies, Southwestern Montana

J.W. M'Gonigle, M.H. Hait, Jr., and W.J. Perry, Jr.

The Medicine Lodge (ML) and Horse Prairie (HP) topographic basins, which are partly separated by the north-trending Maiden Peak spur, are bounded by the Tendoy and Beaverhead Mountains in the eastern part of the Cordilleran thrust belt. The similarity of deposits in both basins, depicted in restored structural-stratigraphic sections, indicates that the original depositional basin extended far beyond the present ML and HP basins. Eocene(?) to mid-Miocene strata deposited in the original basin are coal bearing, whereas younger strata are not.

Tertiary deposition began with the accumulation of as much as 900 m of Eocene volcanic rocks, which were then locally eroded before the start of Eocene(?) and Oligocene fluvial and lacustrine sedimentation. Limestone and shale deposits in the southern part of the ML basin represent a >300-m-thick lacustrine facies that interfingers northward with a marginal-lacustrine facies of shale, some conglomeratic sandstone, and carbonaceous shale and coal. After local uplift and erosion of some of these sediments, fan-delta and delta plain deposits (700–900 m thick) advanced during the Oligocene(?) and Miocene into the southern margins of the lake. Source area for the deltas was a highland to the south, as evidenced by the types of clasts in the conglomerates. Coal-forming environments developed on inactive fan-delta platforms and in inter-distributary depressions. Thick (1,300 m) mud-rich lacustrine deposits subsequently dominated basin sedimentation. A second influx of coarse clastics, of probable late early Miocene age, from Tertiary, Archean, and Mesozoic sources, formed fans hundreds of meters thick. Ephemeral coal-forming environments developed lateral to the fans.

The eastward tilt of Eocene to mid-Miocene units suggests that considerable low-angle westward extension occurred after the original basin was largely filled. These tilted beds dip into low-angle, westward-dipping detachment surfaces exposed in the western Tendoy Mountains. In the southern HP basin, tilted lower Miocene beds are overlain by thick, massive, middle Miocene mudstone deposits which dip slightly to the west. We suggest that extension of the HP and ML basins took place after early Miocene and prior to middle Miocene time. In addition, exposure and erosion of the Maiden Peak spur and the Tendoy Mountains were probably enhanced if not caused by isostatic uplift accompanying tectonic denudation.

Coal-bearing parts of the Tertiary basins in this area: (1) appear to have been formed in relatively large, mud- and carbonate-rich Eocene(?) to mid-Miocene lacustrine basins that were subject to incursions of coarser clastic debris, and (2) occur in association with thick facies sequences, suggesting that deposition took place in relatively stable, long-lived basins. Most of the coal-bearing strata of this age would probably have been tilted by regional westward extension. Post-early Miocene basins were smaller, and therefore probably more susceptible to minor structural and sedimentary disturbances that, irrespective of climatic conditions, tended to inhibit the development of widespread coal deposits.

Geochemical Evaluation of Gas-Bearing Coals with Respect to Maturity, Upper Cretaceous Fruitland Formation, San Juan Basin, New Mexico and Colorado

G.E. Michael, B.E. Law, and D.E. Anders

Coal units from the Fruitland Formation of the San Juan Basin were analyzed for bulk compositional and biomarker changes relative to maturity. Coal in the Fruitland ranges in maturity from volatile B bituminous to medium-volatile bituminous. (Rm values range from 0.42 to 1.54 percent.) Forty-six samples were analyzed by Rock-Eval pyrolysis and vitrinite reflectance (Rm). Fifteen samples were chosen for further analysis of sterane and terpane biomarkers and saturated and aromatic hydrocarbon fractions.

Fruitland coal is relatively hydrogen rich and oxygen poor. The hydrogen indexes (HI) (S2/TOC) are primarily between 100 and 350 and oxygen indexes (S3/TOC) range between 10 and 45. When plotted against Rm both S1/TOC and S1/(S1+S2)

(transformation ratio) show the onset of hydrocarbon generation at Rm 0.70 percent (Tmax 442) with maximum generation in the Rm 0.80 to 0.85 percent range (Tmax 447 to 451). The hydrogen index decreases linearly with increasing Rm.

At low maturities up to 0.75 percent Rm, n-alkanes range from C25 to C31 with strong odd/even predominance, typical for immature type III organic matter. Above 0.75 percent Rm, odd/even predominance is lost and distributions become increasingly unimodal toward lower molecular weight n-alkanes. The pristane (Pr):phytane (Ph) ratio decreases linearly with increasing Rm. The Pr:n-C17 ratio also decreases, however, in a logarithmic relationship with increasing Rm. Four mature samples were nearly devoid of n-alkanes and therefore did not fit into the n-alkane maturity trend. These differences could be due to heterogeneous organic matter type in the coals, to variation in expulsion as a result of fracturing, or to biodegradation. The samples which do not fit the n-alkane maturity trend are from areas of anomalously high gas production.

Aromatic hydrocarbon distributions show the loss of triaromatic pentacyclic compounds at maturity greater than 0.60 percent Rm, whereas lower molecular weight bicyclics and tricyclics continue to remain at higher maturity. Triaromatic pentacyclics in the C25 to C27 range constitute a large portion of aromatics in the low maturity samples from the Fruitland coal. Methylphenanthrene ratios were used to determine the maturity in Rm equivalent values.

Pentacyclic terpanes are present in higher concentration relative to steranes at all levels of maturity in the sample suite. The relative amount of rearranged steranes to regular steranes was low in all the samples, even at high maturity. The sterane maturity reactions reach completion between 0.75 and 0.80 percent Rm. Complete conversion of monoaromatic steroids to triaromatic steroids is achieved by 0.75 percent Rm, a process which often does not occur until 1.00 percent Rm. High molecular weight triaromatic steroids disappear by 0.93 percent Rm, leaving only low molecular weight triaromatics.

Hopane maturity parameters reach equilibrium around 0.90 percent Rm in the sample suite. The source and (or) maturity parameter Tm:Ts ratio varied unsystematically with respect to maturity. The ratio of tricyclic to pentacyclic terpanes varies inconsistently with maturity.

The extractable hydrocarbon yields range from 5,600 ppm to 40,000 ppm, which indicates good potential for oil generation. Minor amounts of condensate have been found associated with the Fruitland Formation and are likely generated from adjacent coal beds.

Applications of Expert Systems and Geographic Information Systems to Basin Characterization—Case Study for the San Juan Basin, New Mexico

Betty M. Miller

The U.S. Geological Survey (USGS) is currently applying geographic information systems (GIS) technology to develop a geologic knowledge base that will provide the framework for an integrated basin analysis for the San Juan Basin. GIS technology involves the integration of mapping and data-base functions that enable the user not only to integrate and manipulate spatial (coordinate) data with attribute (thematic) data in order to combine complex geographic, geologic, and geophysical data sets into resultant overlay and composite maps, but also to conduct multivariate exploratory data analysis and to access a variety of options for analyzing these data bases.

The analysis of a sedimentary basin requires a multidisciplinary approach drawing on many areas of geologic expertise supported by the integration and analysis of large volumes of multivariate spatial data. One such method being investigated for analyzing sedimentary basins in conjunction with GIS is the application of expert systems techniques that simulate the logic of basin experts to model geologic concepts, to document and analyze geologic attributes, and to interpret the history of a sedimentary basin. This knowledge of the geologic settings, histories, and processes characterizing these basins is important for predicting the occurrence of oil and gas, uranium, oil shale, coal, phosphate, and many other essential energy and mineral resources.

The San Juan Basin, a 13,500-mi^2 Laramide structural basin in northwestern New Mexico, was chosen for the initial pilot project. The basin encompasses a maximum of >15,000 feet of Paleozoic to Eocene sedimentary rock and contains economic deposits of natural gas, oil, coal, and uranium. Successful exploration in this basin requires an understanding of the complex stratigraphy and structure controlling the distribution of these resources.

Initially the basin analysis project focuses on the integration of the multivariate data bases for merging large volumes of surface and subsurface data. GIS technology applied to the San Juan Basin is used to establish a three-dimensional perspective of the basin's fundamental stratigraphic and structural framework and to aid in the identification of its temporal and tectonic relationships relative to origin and occurrence of its resources. Digital data bases being used for surface mapping include: the Digital Elevation Models (DEMs)

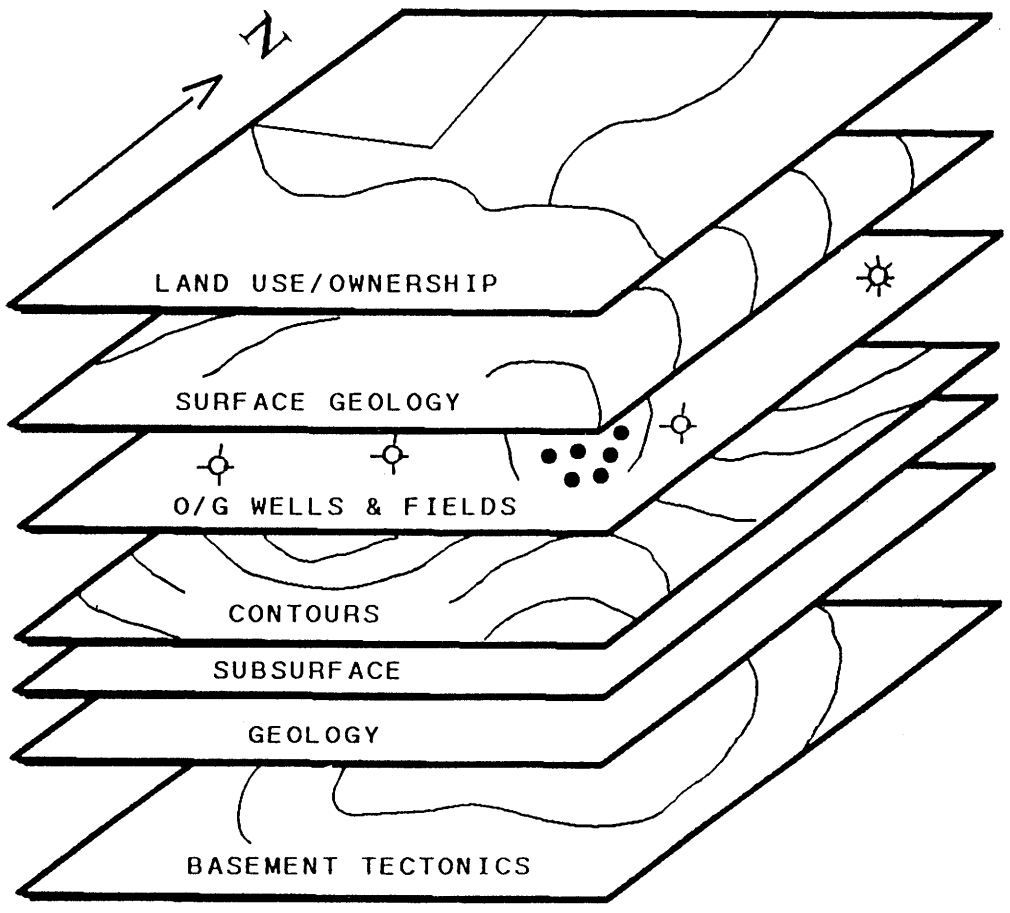

Figure 1 (B. Miller). Three-dimensional sedimentary basin analysis.

for terrain elevations; Digital Line Graphics (DLGs) for planimetric information on boundaries, transportation, and hydrography; the U.S. Public Land Survey System; and Land Use and Land Cover (LULC) data. Additional data bases used for surface mapping include surficial geology, locations of oil and gas wells, well status, and oil and gas fields.

Information data bases providing the attributes for subsurface mapping include those for geologic maps such as structure-contour, isopach, and facies maps for the major oil- and gas-producing formations within the basin; cross sections; paleogeographic reconstructions; geophysical maps; and geochemical maps showing organic richness and maturity relative to source bed distribution.

The GIS manipulates data such that an overlay of data layers can produce a new layer of information, or data can be merged from multiple maps into single new maps. (See figure 1.) Current GIS technology and mapping software being used for the three-dimensional analysis of the San Juan Basin includes the ARC/INFO system (Environmental Systems Research Institute) using the PRIME computer and the Interactive Surface Modeling (ISM) software package (Dynamic Graphics, Incorporated). The Petroleum Information-Well History Control System (PI-WHCS) well data base provides one of the major sources for well information (Petroleum Information Corporation).

Expert systems techniques included in the basin study are used to develop knowledge-based expert systems documenting the basic geology and geologic concepts that characterize a basin; provide a diagnostic tool to understand and predict the occurrence of energy and mineral resources on the basis of a basin's geologic history, including the interaction between tectonics and sedimentation; and provide an "intelligent" data management system, an "intelligent" system for processing and understanding spatial data relationships, an efficient system for exploring and viewing spatial data bases, and methods and algorithms for exploratory data analysis and data-base queries.

GIS technology, when integrated with an expert advisor system, provides new tools for innovative research in geologic interpretation, for updating information data bases, for developing new concepts in

basin analysis, and for new resource appraisal methodology. GIS and expert systems technologies can document and preserve invaluable, complex, and very large knowledge bases that are essential to the evaluation of energy and mineral resources.

This project will demonstrate the feasibility of applying GIS and expert systems techniques to building data bases and making these data bases available to the USGS and other resource management agencies.

Data Analysis and Display Techniques of the National Coal Resources Data System, a Geologic Data System

William G. Miller, Kathleen K. Krohn, Carol L. Molnia, and Susan J. Tewalt

The National Coal Resources Data System (NCRDS) of the U.S. Geological Survey is an integrated GIS digital system that accesses a master data base and a suite of 2- and 3-dimensional mapping, display, and statistical capabilities for data analysis and visualization.

Currently the system operates on a network with main nodes in Reston, Va., and Denver, Colo., and is accessed by scientists and other coal experts within and outside the USGS. Twenty-two State geological agencies have cooperative agreements with NCRDS and access the system from remote sites via commercial and USGS telecommunications networks. Software modules operate on a range of equipment platforms: three Sun 4 servers, minicomputers (Prime), desktop Unix-Xwindow-based workstations, microcomputers (IBM-PC compatibles), and mainframes. Development of software and the acquisition and integration of hardware are ongoing to provide coal geologists with the means to analyze multiple coal-data elements and to create a variety of map products with enhanced flexibility and interactivity.

The data-base information includes: stratigraphic descriptions and coal quality data (trace element, Btu, ash, and sulfur analyses) located by latitude and longitude, as well as summary files (coal tonnage and coal quality information) located by geographical area. The basic geologic data are used primarily to model coal deposits and analyze resource estimates in 2- and 3-dimensional maps and diagrams.

Necessary and desirable procedures for NCRDS include using a combination of both in-house developed software and commercial software; not all requirements for USGS coal resource assessment techniques are fully addressed by commercial vendors. At present NCRDS has the following programs available for use for resource assessment and mapping: USGS's GARNET; Dynamic Graphic's Interactive Surface Modeling (ISM); a USGS version of Krieging geostatistics; and aspects of ARC-INFO, a geographic information system (GIS). Image analysis techniques are being investigated for their applicability to coal geology analysis.

Coal resource tonnage calculation provides an example of how multiple digital mapping software capabilities are used. First, the data specified are gridded and contoured. Then the areas of interest are defined by (1) digitized boundaries (outcrop, geologic, geopolitical); (2) boundaries constructed from contoured data at a chosen interval (such as thickness, sulfur, overburden from digital elevation models (DEMs), structure); and (3) the intersection of the boundaries of interest (such as the area where a coal bed has a thickness of 14–28 in., a sulfur content less than 1 percent, and an overburden thickness less than 200 ft). Finally, the tonnage of coal meeting specified criteria is calculated. These techniques have been used successfully in a variety of projects of various scales, including lease tract studies, quadrangle-based studies, and various county studies, as well as coal basins and regions.

The main advantages of digital graphical analysis of geologic data, in contrast to manual methods, are that (1) many data elements can be examined efficiently by digital techniques, and (2) with these digital techniques available, multiple questions can be asked in new combinations of data that otherwise would be impossible or impractical to address.

Stratigraphic Cross Sections of Upper Cretaceous Rocks Across the San Juan Basin, Northwestern New Mexico and Southwestern Colorado

Cornelius M. Molenaar and James K. Baird

Detailed stratigraphic cross sections are excellent for visually portraying facies relations and to help interpret the depositional history of sedimentary basins. The time-transgressive Upper Cretaceous rock units of the San Juan Basin of northwestern New Mexico and southwestern Colorado, which have large-scale facies changes, are especially well suited to this type of analysis.

The San Juan Basin, once part of the larger Western Interior basin, is an early Tertiary structural depression in which a thick section of Cretaceous rocks is preserved. In and flanking the basin, these rocks contain large reserves of gas, oil, and coal; the coals contain large reserves of coal-bed methane, which are currently being developed and produced. The extensive exposures of Cretaceous rocks rimming the basin, the large number of drill holes (20,000 ±), and the relatively simple structure

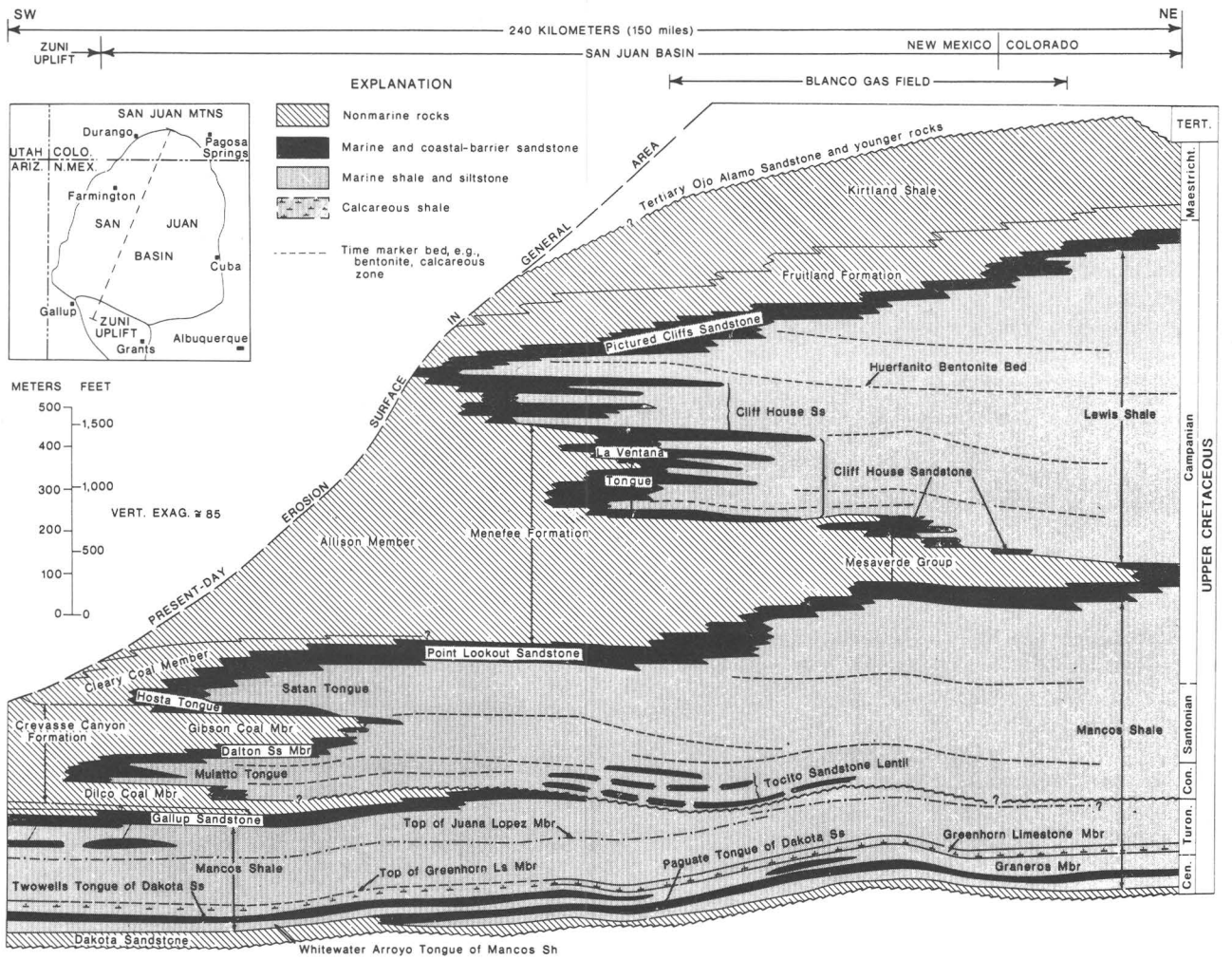

Figure 1 (Molenaar). Northeast-trending stratigraphic cross section showing Upper Cretaceous rocks of the San Juan Basin of New Mexico and Colorado. Location of line of section is shown on inset map in upper left corner. Control for section is based on detailed measured outcrop sections and well-log interpretation. Cen. = Cenomanian, Turon. = Turonian, Con. = Coniacian, Maestricht. = Maestrichtian (now spelled Maastrichtian).

of the basin make this area ideal for stratigraphic analyses through the use of stratigraphic cross sections.

Upper Cretaceous rocks of the basin, which are as much as 6,500 ft (1,980 m) thick, comprise a classic sequence of intertonguing marine and nonmarine facies. Geophysical logs from closely spaced drill holes throughout most of the basin provide data for detailed rock-unit correlations which can be made by using numerous time marker beds within the marine shale sections. These marker beds provide a time framework for construction of cross sections that show (1) diachronism and stratigraphic rise of shoreface-sandstone bodies associated with the four major transgressions and regressions of the Western Interior seaway within the basin, (2) shelf to very low angle slope (< 0.25°) to basinal topography, (3) the Coniacian (basal Niobrara) unconformity, (4) low-amplitude paleostructural features, and (5) low-relief differential compaction features associated with lateral heterogeneities in sand-shale sections.

Variation of Modern Siliciclastic Turbidite Systems and Basin Settings—Implications for Reservoir Development

C. Hans Nelson

Studies of a number of turbidite system elements (*conduits* of canyons and deep-sea channels, *depositional*

bodies of fans and aprons, *connecting channels* of channel-levee complexes and axial channels) show that no single submarine fan model suffices to describe reservoir characteristics (table 1, p. 58). Slope canyons and deep-sea channels provide point-source conduits for channelized fans. Fans can vary from smaller ($\approx <100$ km) sand-rich fans with good vertical-continuity reservoirs in short channels and mid-fan lobes to larger ($\approx >100$ km) mud-rich fans with reservoir beds in extensive channel floors, but unknown reservoir potential in thin sheetlike distal sand lobes. Multiple slope failures and numerous local debris chutes can feed base-of-slope aprons that lack significant development of channels and depositional lobes, but consist of sediment gravity flow and turbidite sheet-flow deposits. Aprons also can vary from smaller (few kilometers) sand-rich wedges with apparent good reservoir continuity throughout to larger (tens of kilometers) mud-rich lobes with poor continuity. Channel-levee complexes, axial channels, canyons and deep-sea channels may be associated with aprons and fans. Channel-floor facies in any of these connecting or conduit turbidite systems may provide good sand-rich reservoir beds (table 1).

Turbidite-system reservoirs in basin settings may vary from a simple case such as the mud-rich Astoria Fan filling the trench off Oregon to the complex example of the western Mediterranean Valencia Trough, which contains prograding slope canyons, channel-levee complexes, aprons, a deep-sea channel, and a submarine fan that form a connected series of coeval turbidite-system elements (table 1). Present-day trench floors and rift basins also contain combinations of canyon, apron, fan, and axial-channel turbidite-system elements. Ancient analogs such as the North China and North Sea rift basins appear to contain similar complex patterns of aprons, fans, and channels; these basins also show that the turbidite systems may change from one type to another at the same location as the basin setting evolves through geologic time. Development of excellent turbidite reservoir beds in these ancient basins indicates the value of defining modern turbidite systems as a guide for exploration and secondary recovery of petroleum in complex ancient turbidite systems.

Domed, Rainfall-Dominated Peat Deposits in Indonesia as a Model for Low-Sulfur Coal

Sandra G. Neuzil

Aproximately 270,000 km^2 of peat are present on the coastal lowlands of Indonesia and Malaysia. Most of the peat is domed (raised), rainfall dominated (ombrogenous), and thick (1–15 m), and most also overlies marine sediments. Preliminary data from the analysis of peat samples collected at 16 sites distributed over three of these peat deposits in Riau and West Kalimantan Provinces, Indonesia, suggest that these peats are excellent analogs for some low-sulfur coal deposits in the Appalachian basin as well as others worldwide.

Overall, the peat has a low ash content (93 samples average 2.5 percent ash) and a low sulfur content (71 samples average 0.16 percent sulfur). Ash and sulfur contents are lower in peat that is more than 1 km from the deposit margin, more than 1 m below the peat surface (below the living root mat and fluctuating water table), and more than 1 m above the base of the peat (37 samples, average 0.80 percent ash; 30 samples, average 0.12 percent sulfur). Ash and sulfur contents are higher in the basal 1 m of the peat deposit (17 samples, average 8.5 percent ash; 13 samples, average 0.28 percent sulfur). At each sample site the pH is higher near the base of the peat, increasing from an average of 3.9 (pH range 3.0–6.0) in the main peat body to an average of 4.9 (pH range 3.2–6.4) <1 m above the base of the peat. Microbial activity and sulfur reduction and fixation may be more intense in these more neutral conditions at the base of the peat.

The base of the peat deposits is generally less than a few meters above mean sea level and rarely below sea level. The peat appears to be hydrologically isolated from marine water based on the concentrations of total dissolved cations in peat pore water(1–260 ppm). The maximum of these values is less than 2 percent of their total concentration in sea water. Also, incursion of high-sulfate sea water (2,700 mg/L) into the peat would be expected to result in high-sulfur peat. Comparing peat samples from locations in close proximity to sea water to peat samples from other locations farther inland, sulfur contents are similar (16 samples <10 km from sea water, average 0.12 percent sulfur; 18 inland samples >10 km from sea water, average 0.13 percent sulfur), surface and basal peats are not included.

Organic sulfur is the dominant form in a suite of 34 samples from the three peat deposits (table 1, p. 59). As total sulfur increases, the organic sulfur fraction increases slightly. Note that all samples are low in total sulfur (<1 percent) and only two basal peat samples (<1 m above the peat substrate contact) are represented in this sample set for forms of sulfur.

During coalification, the content and form of sulfur may change, for example, by introduction of sulfur in ground water or by continued microbial reduction of sulfate. However, the major portion of each coal bed formed from tropical domed ombrogenous peat deposits such as these would be expected to have a low sulfur content, even where the coal is overlying marine sediments. Exploration for low-sulfur coal deposits should take into consideration an interpretation of the

Table 1 (Nelson). Elements of modern siliciclastic multi-event turbidite systems in base-of-slope and basin floor settings

[Modified from Nelson and Maldonado, 1988; Nelson and others, in press]

End-member	Source type	Morphologic characteristics	Facies development proximal - distal	Examples
		Channelized depositional bodies		
"Sand-rich" fan	Small point-source of a local river or littoral drift cell.	Typically small (<100 km) radial fan with leveed channels and mid-fan sand lobes or suprafans.	Upper fan: channel-levee deposits. Mid fan: sand lobes or suprafans. Lower fan: fringe turbidites. Basin plain: thin-bedded turbidite sheets.	California continental borderland basin fans (Dume, Hueneme, Magu, Navy, Redondo).
"Mud-rich" fan	Large point-source of a single major mud-rich river or deep-sea channel.	Typically large (>100 km) elongate fan with extensive leveed channels and lower fan sand lobes or sheets.	Upper fan: channel-levee deposits. Mid fan: bifurcated channel-levee deposits. Lower fan: sand lobes. Abyssal plain: sand lobes to thin-bedded turbidite sheets.	Amazon, Astoria, Indus, Mississippi fans.
		Non-channelized depositional bodies		
"Sand-rich" apron	Line source of multiple debris chutes, typically in tectonically active basins (trench floor, pull apart, rift, caldera).	Typically small (few km) unchannelized slope base radial cone or coalesced cones that taper to a flat basin plain.	Slope: chaotic sand and gravel in valley floors. Apron: wedges of sand and gravel sheets. Basin plain: thin-bedded turbidites.	Chile trench floor; Crater Lake caldera floor, African rift lake basins.
"Mud-rich" apron	Line source of multiple failures, typically on gullied slopes of muddy delta fronts and mature passive margins.	Typically large (tens of km) unchannelized, elongate, slope base sediment tongue or tongues of irregular thickness, shape, hummocky surface and abrupt termination.	Slope: mounds of organized slide blocks and slumps of mud. Apron: slide debris lobes of chaotic mud and sand.	Amazon, Ebro and Mississippi turbidite systems.
		Connecting channels		
Channel levee complex	Lobate delta?	Linear depositional channel without significant distal sand lobes.	Channel floor: coarse-grained sediment-gravity-flow deposits. Levees: sand-rich thin-bedded overbank turbidites.	Ebro channels;
----------	----------			----------
Axial channel	Drain canyons fans and aprons on trench or rift basin floor.			Chile trench floor and African rift lake floor axial channels.
		Conduits		
Slope canyon	Slope mass-wasting or river.	Erosional and (or) depositional slope valleys that connect downstream to fans, aprons, or deep-sea channels.	Walls: with outcropping beds, mass movement or overbank deposits. Floors: erosional or with aprons and channel-levee deposits.	Astoria, Oropesa, Peñiscola Redondo.
Deep-sea channel	Multiple canyons and (or) connecting channels.	Tectonically controlled basin floor erosional channels that connect downstream to fans or abyssal plains.	Walls: with outcropping beds, mass-movement or overbank deposits. Floors: erosional or with channel-levee deposits.	Bounty Channel, Cascadia Channel, Valencia Valley.

Table 1 (Neuzil). Forms of sulfur in a 34-sample suite from three Indonesian peat deposits

	Complete sample set	Low sulfur <0.2 percent	High sulfur ≥0.2 percent
Number of samples ----------	34	26	8
Average total sulfur (percent dry peat)	0.19	0.13	0.36
Organic sulfur (percent of total sulfur)	82.7	80.9	88.7
Pyritic sulfur (percent of total sulfur)	8.9	10.1	5.0
Sulfate sulfur (percent of total sulfur)	8.4	9.1	6.4

type of precursor peat deposit based on paleoclimate and paleotopographic reconstructions.

Early Stage Diagenesis of Plant Biomolecules in Peats

William H. Orem and Harry E. Lerch

In the transformation of plant biomolecules to fossil fuels, many of the most pronounced chemical structural changes occur during the early stages of diagenesis. In the case of coal, early-stage diagenetic alteration of plant biomolecules occurs in peatlands where organic matter may accumulate due to the high productivity of algae and vascular plants and the stagnant, water-logged conditions, which inhibit bio-oxidation of the deposited plant remains. Few detailed studies on early diagenesis of the organic matter in peats have been conducted. We present herein the results of organic geochemical studies of peat cores that represent a number of different wetland environments. Several different analytical approaches (such as ^{13}C nuclear magnetic resonance spectroscopy, analytical pyrolysis, and gas chromatography/mass spectroscopy) were utilized to examine changes occurring in the solid-phase organic matter in the peat and to study the chemical structures of extractable organic compounds in the peat and dissolved organic matter (DOM) in the associated pore water.

In figure 1 (p. 60), solid-state ^{13}C nuclear magnetic resonance (NMR) spectra of peats from two very different wetlands (the Everglades, Florida, and Okefenokee Swamp, Georgia) are shown. In the core from a sawgrass area in the Everglades, the major change in the organic matter with depth is the loss of labile carbohydrates (primarily cellulose) by biodegradation. This change is shown in the ^{13}C NMR spectra of the whole peat as a gradual decrease in the intensity of the peak at 72 ppm. Aliphatic organic matter (broad peak in 0–50 ppm region of NMR) and lignin from vascular plant remains (peaks at 56 ppm, 110–150 ppm, and 150–160 ppm) are selectively preserved in this peat core. Analytical pyrolysis and gas chromatography/mass spectroscopy have shown that these aliphatic residues may originate from vascular plant waxes.

In contrast, the ^{13}C NMR spectra of whole peats from a core taken in Okefenokee Swamp show that the organic matter is much more biodegraded than that from the Everglades. The Okefenokee peats show a rapid loss of carbohydrates and vascular plant lignin with increasing depth, leaving only refractory aliphatic substances preserved. Note the near total absence of peaks for lignin at 56 ppm, 110–150 ppm, and 150–160 ppm in the ^{13}C NMR spectra at the bottom of this core (fig. 1). The biodegradation of lignin and carbohydrates distinctly differentiates the Okefenokee peats from those in the sawgrass area of the Everglades.

Geochemical studies of the dissolved organic matter (DOM) in peat pore waters may also provide information on the biodegradation of plant biomolecules in peats. The DOM is an intermediate in the degradation of organic matter from macromolecular biopolymers in the peat to mineralized organic matter in the form of CO_2 and (or) CH_4. ^{13}C NMR analysis of DOM from neutral pH peatlands such as the sawgrass area of the Everglades shows that the chemical structure of the DOM is dominated by carbohydrates. The dominance of carbohydrates in the DOM is consistent with the dominant degradative process occurring in the solid peat: the loss of carbohydrates, as mentioned previously. In contrast to the situation in neutral-pH peatlands, the chemical structure of DOM from acidic "blackwater" peatlands such as the Okefenokee Swamp is dominated by aliphatic and aromatic moities, with little or no carbohydrate content (^{13}C NMR analysis). Analytical pyrolysis and gas chomatography indicate that the aromatic structures in the DOM may be derived from the biodegradation of lignin, which is consistent with the nature of organic matter diagenesis observed in the whole peat (fig. 1). Other acidic, "blackwater" peatlands such as Dismal Swamp, Virginia, and several Indonesian

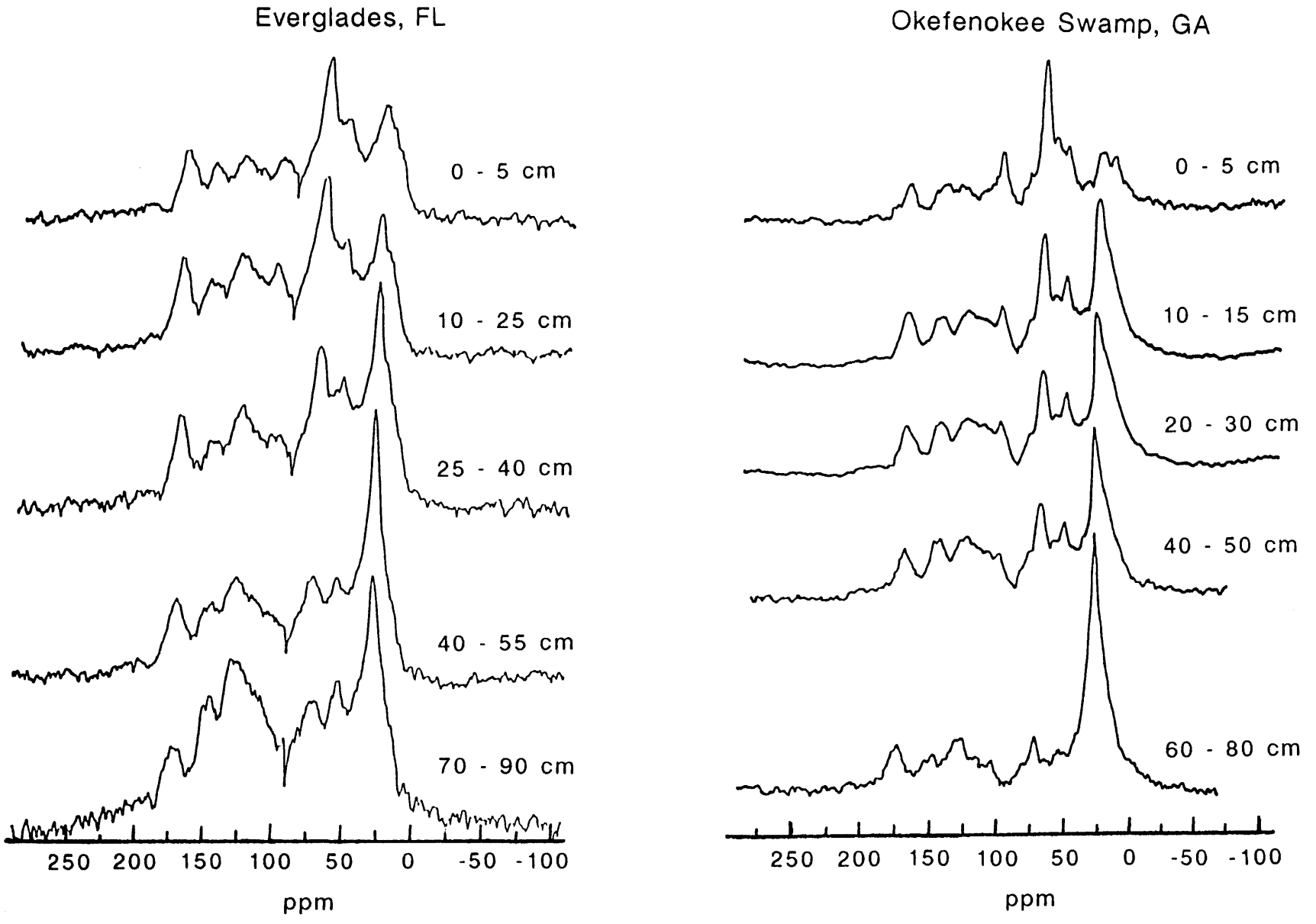

Figure 1 (Orem). ^{13}C NMR spectra of whole peats from two cores representing different peat-forming wetlands: the sawgrass peat area of the Everglades, Florida, and water-lily prairie area of the Okefenokee Swamp, Georgia. The NMR scale is in units of ppm relative to tetramethylsilane.

swamps also exhibit high degrees of lignin biodegradation in the peat and highly aromatic DOM in the pore water. This aromatic-rich DOM may play a significant role in imparting a low pH and dark, tea-color to the "blackwater" which is characteristic of these wetlands. Only aliphatic residues are preserved in these acidic peats, which may represent modern analogs of ancient coal-forming peatlands that produced aliphatic-rich coals, for example, the brown coals of southeastern Australia. The deposits of acidic peatlands may also represent environments responsible for oil-forming coals.

New Tonstein Beds in the Middle Pennsylvanian of the Central Appalachian Basin—Time Lines for Basin Analysis

W.F. Outerbridge, P.C. Lyons, and D.M. Triplehorn

Tonsteins, which are altered volcanic ash, mark instantaneous events over large areas and thus are excellent time markers for basin analysis. In the Middle Pennsylvanian of the central Appalachian basin, they are gray claystones, usually from 1 to 5 in. thick, and probably of an original rhyodacitic composition.

We can demonstrate six new tonstein beds—a flint clay bed from the Olive Hill Clay Bed of the Breathitt Formation, flint clay beds in the Upper Banner, Williamson, and Little Fire Clay coal beds, a flint clay from the Hitchens clay, and the flint clay beds associated with the Princess No. 6 coal bed—in stratigraphic order from oldest to youngest. They span most of the Middle Pennsylvanian (Westphalian A-D) in the central Appalachian basin.

These tonsteins are identified by the ubiquitous presence of quartz as clear monocrystalline flakes, thin blades, and euhedral α-quartz crystals pseudomorphic after β-quartz; high-temperature potassium feldspar (sanidine?); and euhedral, commonly acicular zircons. Aluminum phosphate minerals of the crandallite group, euhedral platy crystals of rutile(?), and grains of anatase perhaps derived from titaniferous magnetite are also common. The matrix is a mixture of microcrystalline kaolinite, quartz, and, commonly, some illite.

Some of the tonstein beds have been traced from West Virginia into Kentucky and Ohio, but more detailed thickness, mineralogical, trace-element, and geochronological data are needed to identify source areas, synchroneity with acidic plutons, and absolute age dates. However, that a source area lies in the eastern Piedmont is a reasonable hypothesis, based on isopachous data for the Fire Clay coal-bed tonstein and the published age ($\approx$311 Ma) that is coeval with some Piedmont granites. $^{40}Ar/^{39}Ar$ dating of potassium feldspar, now in progress, will allow estimation of Middle Pennsylvanian sedimentation rates, correlations with acidic plutons, and intercontinental correlations.

Petroleum Potential of Midcontinent Rift System, Iowa—Organic Matter and Porosity Preserved in 1-Billion-Year-Old Rocks

James G. Palacas, James W. Schmoker, and Raymond R. Anderson

Preliminary hydrocarbon source rock and reservoir evaluations have been made of the thickest section (14,100 ft; 4,298 m) of Middle Proterozoic sedimentary rocks sampled anywhere along the trend of the Midcontinent Rift System. Source rock and porosity assessments are based on analyses of core and drill cutting samples, and electric logs from the 17,851-ft (5,441-m) deep AMOCO M.G. Eischeid #1 well, which was drilled in 1987 in the Defiance basin northwest of the medial Iowa horst near the town of Halbur, Carroll County, west-central Iowa. A 7,200-ft (2,195-m) thick basal sequence of Precambrian clastic rocks encountered in the Eischeid well has lithologies similar to those of the Oronto Group of Wisconsin, and an overlying 6,900-ft (2,103-m) thick Precambrian clastic sequence resembles the rocks of the Bayfield Group in Wisconsin. The Oronto and Bayfield Groups are part of the Keweenawan Supergroup.

In the Eischeid #1 well, the fine-grained predominantly red rocks in the interval equivalent to the Bayfield Group contain minimal organic matter: total organic carbon (TOC) content is less than 0.10 percent, indicating no petroleum source-rock potential. The very low TOC content is attributed largely to oxidizing depositional environments.

The petroleum source potential of a large portion of the underlying rocks, equivalent to the Oronto Group, is also generally quite poor: TOC is commonly less than 0.10 percent and Rock-Eval genetic potential ($S_1 + S_2$) less than 0.10 mg HC/g rock. However, between depths of about 15,000 and 16,425 ft (4,570–5,005 m), medium- to dark-gray, pyrite-bearing, laminated shales (mudstones) are common. In these shales (mudstones), which are possibly equivalent to the Nonesuch Shale of Wisconsin and Michigan, TOC contents reach 0.1–1.4 percent, and average about 0.6 percent; genetic potentials range from 0.1 to 0.4 mg HC/g rock, hydrogen indices from 20 to 80 mg HC/g TOC, and chloroform-extractable bitumen contents from 10 to 60 ppm.

Based on Rock-Eval T_{max}, vitrinite-like reflectance, thermal alteration index (TAI), ratios of extractable hydrocarbons to TOC, and Lopatin modeling, the shales deeper than 15,000 ft (4,570 m) are

ranked as overmature with respect to oil generation. More precisely, the maturity of the shales is at least in the wet-gas zone of hydrocarbon generation and possibly extends into the dry-gas zone. Accordingly, although at present these shales have little remaining capacity to generate additional hydrocarbons, in the geologic past they could have generated significant amounts of hydrocarbons. We speculate that equivalent shale facies might have better source rock potential if present at shallower depths, under lower levels of thermal maturity, along the basin flanks away from the frontal fault zone of the medial horst.

Sandstone constitutes 1,721 net ft (525 m), or 29 percent of the interval between 11,450 and 17,340 ft (3,490 to 5,285 m) of the rocks equivalent to the Oronto Group in the Eischeid well. Sandstone is distinguished from the siltstone and shale that make up the remainder of the interval by differences in the photoelectric-absorption, density-porosity, and neutron-porosity log traces and (secondarily) by the lithologic descriptions prepared from drill cuttings.

Sandstone porosity below 11,450 ft (3,490 m), as determined from compensated density and neutron logs, ranges between 1 and 6 percent and averages only 2.3 percent. "Better" porosities of 3.5 percent or more are distributed throughout the interval studied and do not correlate with either (1) depth, (2) the zone of more reducing environment (the zone of dark-gray, pyritic, laminated shales), or (3) the reported presence of bitumen- or pyrobitumen-like "intergranular black residue." However, Th:K ratios derived from the spectral gamma-ray log suggest that intervals of better sandstone porosity may have a higher percentage of plagioclase feldspar. It is thus possible, but certainly not proven, that enhanced sandstone porosity in the Eischeid well may be diagenetically linked to plagioclase feldspar. We speculate that the porosity of equivalent sandstones may be higher on the basin flanks because of shallower burial and resulting lower levels of time-temperature exposure.

Preliminary Reinterpretation of the Ouachita Frontal Zone Near Hartshorne, Oklahoma, Based Chiefly on Seismic Reflection Data

W.J. Perry, Jr., Warren Agena, and N.H. Suneson

A north-south seismic reflection profile across the frontal zone of the Ouachita thrust belt in the Hartshorne, Oklahoma, region illustrates the triangle-zone style of deformation: a wedge-shaped structure, floored by a foreland-directed decollement, at the foreland tip of which a complementary hinterland-directed thrust of equal and opposing slip occurs shallower in the section, dipping toward the foreland. These opposing thrusts form the front of the triangle zone. In our interpretation, the Choctaw thrust is simply the frontal imbricate along the southern margin of this complex, partially eroded triangle zone. This triangle zone and associated imbricates appear to represent about 6 miles (10 km) of shortening. The Middle Pennsylvanian Hartshorne Sandstone appears to be merely peeled upward along the northern margin of this triangle zone and not significantly displaced with respect to the Arkoma basin to the north.

The Middle Pennsylvanian Atoka Formation, which underlies the Hartshorne Sandstone, is interpreted to form the roof of a deeper imbricate zone near the northern end of the profile. This zone is interpreted to be a duplex fault zone, that is, an imbricate zone bounded by floor and roof thrusts which structurally isolate the zone from the overlying roof and underlying floor sequences. The duplex interpreted on the seismic profile near Hartshorne is unusual because it contains two foreland-dipping backthrusts between the floor and roof thrusts. The floor thrust of this deeper zone appears to be a decollement for a distance of more than 7 miles (11 km) north-south within the Upper Devonian and Lower Mississippian Woodford Shale and Upper Mississippian Caney Shale. Beneath the floor thrust of this deeper imbricate zone, the Arbuckle through Hunton Groups (Cambrian to Devonian) are cut by steeply dipping extension faults, in which the sense of displacement appears generally down to the south. The floor thrust appears to rise more steeply to the north where it crosses each of the extension faults, suggesting that minor ramps in the floor thrust were sited by underlying structures. The extension-fault-bounded blocks beneath the floor thrust may illustrate the style of structural traps involved in the subthrust Arbuckle gas play near Wilburton.

In summary, typical triangle zone features, suspected by earlier workers, including J.K. Arbenz, are imaged by a high-quality seismic reflection profile across the frontal zone of the Ouachita thrust belt near Hartshorne, Oklahoma. Down-to-south extension preceded thrusting. Frontal thrusting is younger than the McAlester Formation of late Middle Pennsylvanian (Desmoinesian) age, the youngest Paleozoic stratigraphic unit preserved along the seismic profile.

Architectural Studies in Eolian Reservoir Rocks—The Lower Jurassic Nugget Sandstone of Northeastern Utah

Fred Peterson and C.J. Schenk

Lower Jurassic eolianites in the Western Interior of the United States include deposits of the largest erg (eolian sand sea) that ever existed in North America and perhaps in the world. Previous workers in northeastern Utah have applied several names to these rocks, including Glen Canyon, Navajo, and Nugget Sandstone. However, we prefer the term Nugget (a) because the beds closely resemble the type Nugget nearby in Wyoming, (b) because the strata correlate with the entire Glen Canyon Group farther south rather than just the Navajo Sandstone part of it, and (c) because Glen Canyon Sandstone is a junior synonym for the Nugget in this area. The Nugget is an excellent but anisotropic reservoir rock that produces hydrocarbons from about a dozen medium-sized oil fields in the southern part of the overthrust belt of southwestern Wyoming and northern Utah. There, it has been faulted against or near good source beds that were buried to sufficient depths to generate hydrocarbons.

Our study has concentrated on lateral and vertical variations in eolian dune, sand-sheet, and sabkha deposits that may influence fluid movement and sweep in reservoir sandstone beds of the Nugget. Because exposures tend to be poor and of limited areal extent in the Wyoming-Utah overthrust belt, most of the research was done near Vernal, northeastern Utah, where fairly continuous exposures are amenable to architectural studies. The Nugget in that area consists of a stacked sequence of eolian dune, sand-sheet, and clastic sabkha deposits with rare thin and areally limited lacustrine limestone beds.

Eolian dune sandstone beds range from simple to complex, the complex being more abundant. A simple dune deposit consists almost entirely of high-angle avalanche cross-strata that grade downward into wind-ripple and grain-fall apron strata. Of such deposits, most occur in a single tabular-planar or wedge-planar set that can be traced for hundreds of meters on outcrops oriented parallel to wind flow, which was roughly from north to south. Over this distance, set thicknesses range from several to 10 or more meters. Simple trough-shaped sets are also present, but not as abundant as the planar sets.

Complex dune deposits range from a coset of eolian dune cross-strata that resembles a simple set but has multiple downwind- or southward-dipping internal bounding surfaces, to compound cosets with nested large-scale trough-shaped sets, to thick sets (15 m or greater) that commonly grade downwind into several thinner sets. Some of the complex eolian dune deposits exhibit significant internal variation, including several orders of bounding surfaces, and a complex intercalation of avalanche and wind-ripple strata.

The best original porosity and permeability in these beds would be in the avalanche cross-strata, but at least moderate porosity and permeability can be expected in the wind-ripple and grain-fall apron laminae. Fluid flow should be more complicated in the complex eolian dune deposits than in the simple dune deposits, not only because of the multiple bounding surfaces, but also because of the complex distribution and orientation of the cross-strata and apron deposits. For both the simple and complex types of dune deposits, the individual eolian sets or cosets cannot be expected to extend across the areal extent of typical Nugget oil fields (roughly 3–10 km in width).

Some of the major bounding surfaces are marked by slight erosional irregularities 2–6 cm high that are mostly in the finer grained (very fine to fine-grained) cross laminae of the underlying set. In vertical exposures, these surfaces tend to be parallel to sabkha units higher or lower in the formation, or else thin sabkha units locally wedge in along some of these surfaces. These major bounding surfaces with slight erosional irregularities may be Stokes' surfaces that formed where eolian erosion in front of an advancing dune occurred down to the water table or at least down to the zone of capillary action just above the water table. Early cementation then took place by evaporative concentration of solutes in the ground water, especially in the finer grained laminae where capillary action is greatest. Thus, some of the major bounding surfaces, especially those associated with shallow water tables, may lie on slightly better cemented zones in the upper parts of underlying sets or cosets. Recent studies of major bounding surfaces ("super surfaces") in other eolian formations suggest that these zones may have considerable lateral extent, could easily extend across an entire oil field, and therefore could be slight but important barriers to vertical fluid movement.

Eolian sand-sheet deposits consist largely of laminae produced by the migration of wind ripples, but they also include intercalated structureless laminae that may be grain-fall or poorly defined wind-ripple deposits. Porosity and permeability are excellent although not as high as in the crossbedded dune facies. Nugget sand-sheet deposits are most abundant in Idaho and western-most Wyoming; they are much less common farther south and southeast, including the Vernal study area.

Clastic sabkha sandstone beds generally contain irregular or wavy-bedded laminae with a moderate

amount of lateral variation produced by thin remnants of eolian foreset cross-strata 1–20 cm thick, contorted strata, and wind-ripple laminae. Individual sabkha units characteristically range in thickness from less than a meter to several meters across a distance of several hundred meters. Sabkha deposits are especially abundant in the basal approximately 30 m of the Nugget where they form a continuous zone that can be traced throughout northern Utah, westernmost Wyoming, and central Utah. Higher in the Nugget, sabkha units form discontinuous lensoid bodies on the order of 1 to several kilometers in areal extent. Sabkha units typically are better cemented and more poorly sorted than dune and sand-sheet deposits, properties that make them significant barriers to fluid migration. However, fracture porosity in areas of intense structural deformation, such as in the overthrust belt, may improve their transmissivity. Similarly, the rare lacustrine limestone beds should impede fluid flow but also may be expected to be fractured in structurally complex areas. Because of their generally limited areal extent, sabkha units in the upper part of the formation would not be expected to extend completely across a typical Nugget oil field; however, their presence could well make field development difficult.

In summary, although the Nugget Sandstone can be an excellent reservoir medium, it contains numerous sedimentologic heterogeneities that make optimum field development a challenge. Vertical fluid migration may be expected to be hindered in various degrees by apron and persistent sand-sheet deposits, by slightly greater cementation beneath some of the major bounding surfaces (especially Stokes' surfaces), by sabkha deposits, and by lacustrine limestones. Lateral fluid migration should be optimal in the crossbedded dune facies, especially perpendicular to paleowind flow along cross-bed laminae. However, lateral discontinuities produced by inclined or curved bounding surfaces overlain by apron deposits may impede lateral fluid movement.

Algal Mound Carbonate Reservoir, Aneth Oil Field, Paradox Basin, Utah—Origin and Related Petroleum Geology

James A. Peterson

The Aneth oil field (approximately 400 million barrels ultimate recovery) contains three-fourths of the oil reserves discovered in Pennsylvanian reservoirs of the Paradox basin. The field occurs within an isolated northwest-trending Desmoinesian (Pennsylvanian) algal carbonate bank buildup located about 25 mi (40 km) basinward of the main carbonate shelf of the basin in Utah. Desmoinesian deposition was strongly cyclic, with as many as 30 main evaporite-carbonate cycles recognized. The Aneth algal bank is part of the Desert Creek cycle, which is the first cycle above that of the most widespread salt-bearing cycle. The Desert Creek carbonate facies grades basinward to increasingly prevalent evaporite facies, dominated by thick salt beds in the basin center. Within the isolated algal-mound facies, the Desert Creek cycle is characterized by a vertical succession that includes: (1) basal black, organic-rich, dolomitic, silty shale, and (2) overlying dark chalky, finely crystalline dolomite, which grades upward into (3) the main carbonate mound facies, dominated by accumulations of calcareous, leafy green algae with associated brachiopods, fusulinids, small foraminifera, ostracodes, and rarely, corals. Mound buildups are overlain by a relatively thin, black, organic-rich shale unit, the basal bed of the succeeding mound-bearing Ismay cycle. This upper shale unit thickens markedly on the flanks of the Desert Creek and other mounds.

The basal black shale unit is thickest beneath the Aneth mound facies and also is commonly thicker beneath many other Desert Creek and Ismay algal-mound buildups. Detailed regional studies suggest that the Aneth algal facies was deposited on a broad southeast-trending organic-rich mud and silt bank. This bank provided submarine topographic relief which localized the Aneth algal-mound complex. These interrelated carbonate and clastic depositional processes resulted in the close association between source rock, large reservoir, and seal at Aneth and contributed significantly toward the large size of the Aneth accumulation. Broader scale factors involved in development of the Aneth and other Paradox basin carbonate mounds include: (1) global paleolatitudinal position of the Paradox basin; (2) paleogeographic-paleotectonic framework of the basin region; (3) climatic, prevailing-wind, and ocean-current patterns, strongly influenced by the above factors; (4) eustatic changes in sea level; and (5) position of the Aneth mudbank-mound area with respect to the Paradox basin marine accessway.

Pyritic Sulfur and Trace-Element Affinities in Facies of the Upper Freeport Coal Bed, Allegheny Formation, West-Central Pennsylvania

Brenda S. Pierce and Ronald W. Stanton

The distribution of pyritic sulfur and associated trace elements indicates two sources of trace-element

enrichment in facies of the Upper Freeport coal bed. Samples were collected from 62 localities in a 120 mi^2 area of west-central Pennsylvania. A generalized stratigraphic section of the Upper Freeport coal bed (fig. 1, p. 66) shows the coal-bed facies (A to E), upper parting (UP), and lower parting (LP). The coal-bed facies, which represent developmental stages during peat formation, differ compositionally and are continuous and mappable over the study area.

The Upper Freeport coal bed began forming as a low-lying, topogenous peat (facies E and D) that was susceptible to sediment influx. The peat body became slightly raised (facies C and C'), which restricted clastic input to the margins of the swamp. In the western part of the study area, peat accumulation ended when freshwater lakes formed and the dark laminated shales that now overlie the coal bed were deposited. These shales are represented by the upper parting (UP) in the eastern part of the study area, where peat accumulation resumed (B) as peat islands on the emergent, slightly raised areas underlain by facies C. Facies A' (nonbanded coal) was formed by mixing at the edges of the peat island, and facies A (also nonbanded) was formed by the gradual inundation of the peat by shallow lakes.

The distribution and stratigraphic concentrations of total sulfur content, sulfur forms, and trace elements related to sulfur—As, Se, Hg, Pb, Zn, and Cd—were examined and correlated by facies. Mean values of these elements, plotted by facies, show that the highest concentrations are at the top and bottom of the coal bed. The lowest concentrations of these elements are most commonly in facies that constitute the middle of the coal bed. Elemental compositional means for the middle and the top facies, respectively, are as follows: As, 10.6 and 59.8 ppm; Se, 1.7 and 10 ppm; Pb, 4.76 and 25.8 ppm; and Zn, 8.8 and >61 ppm. The mean pyritic sulfur content varies from 0.8 to 2.6 percent in the various facies. The amount of organic sulfur in the Upper Freeport coal bed is relatively lower (0.5–1.3 percent) and much less variable than pyritic sulfur. Pyritic sulfur is responsible for variations in total sulfur and trace-element characteristics.

Correlation coefficients indicate that pyritic sulfur and As have a strong positive correlation in most facies data sets. Detailed geochemical cross sections show that As commonly follows the same trends as pyritic sulfur throughout the coal bed, both laterally and vertically (fig. 1). The pyritic sulfur and As values in the middle facies are very low throughout most of the coal bed. In the interior and eastern parts of the study area (represented by locations 3 and 4, fig. 1), pyritic sulfur and As values are highest at the top and bottom of the coal bed, perhaps indicating a relationship to associated strata. In the western part of the study area (locations 1 and 2, fig. 1), the highest pyritic sulfur and As values are found in the top and bottom of the coal bed in only half of the locations studied; in the other half, highest values were found in facies C.

In the top and bottom facies, the following statistically significant correlations exist: As-Se, As-Hg, Pb-Se, Pb-Cd, and As-Pb. These correlations may indicate diagenetic influence from associated strata. However, these elemental correlations are not significant in facies C', which is the uppermost facies in the western part of the study area. Therefore, either the epigenetic processes operative in the central and eastern part of the study area were not significant in the western part, or these correlations may indicate some degree of syngenetic relationship with the original peat facies.

Alternatively, certain elements correlate only within the middle facies of the bed: Zn-Cd, Cd-pyritic sulfur, Hg-pyritic sulfur, and Zn-Se. These correlations appear to have been related to conditions present during peat formation. The mode of occurrence of these elements is not yet known; however, sphalerite has not been detected from microscopic analyses or LTA mineralogy.

Although pyrite is inferred to contain As, Zn, Cd, Pb, and Se, there appear to be at least two suites of associations within the Upper Freeport coal bed: Hg-Cd-Zn-As, possibly a syngenetic phase found in the middle facies, and Se-Pb-As-Hg, possibly an epigenetic phase, associated with the top and bottom of the coal bed. These two suites imply a paragenesis of pyrite formation that first concentrated Hg, Cd, Zn, and As, and later Se, Pb, As, and Hg.

Interplay of Tectonism and Sea-Level Change—Lessons from the U.S. Atlantic Margin

C. Wylie Poag

Isopach maps (scale 1:1,000,000) of 23 successive stratigraphic sequences demonstrate that marine depocenters on the United States middle Atlantic margin have migrated significant distances during their 190-million-year postrift history (Early Jurassic to present). These depocenters migrated in two principal ways: (1) latitudinal shifts from north to south (and vice versa) and (2) bathymetric shifts from continental shelf to continental slope or rise (and vice versa). The major latitudinal migrations were caused by changing rates of differential uplift among the three principal highland source terrains (central Appalachians, Adirondacks, and New England Appalachians) that supplied the offshore basins with terrigenous detritus. The historical pattern of

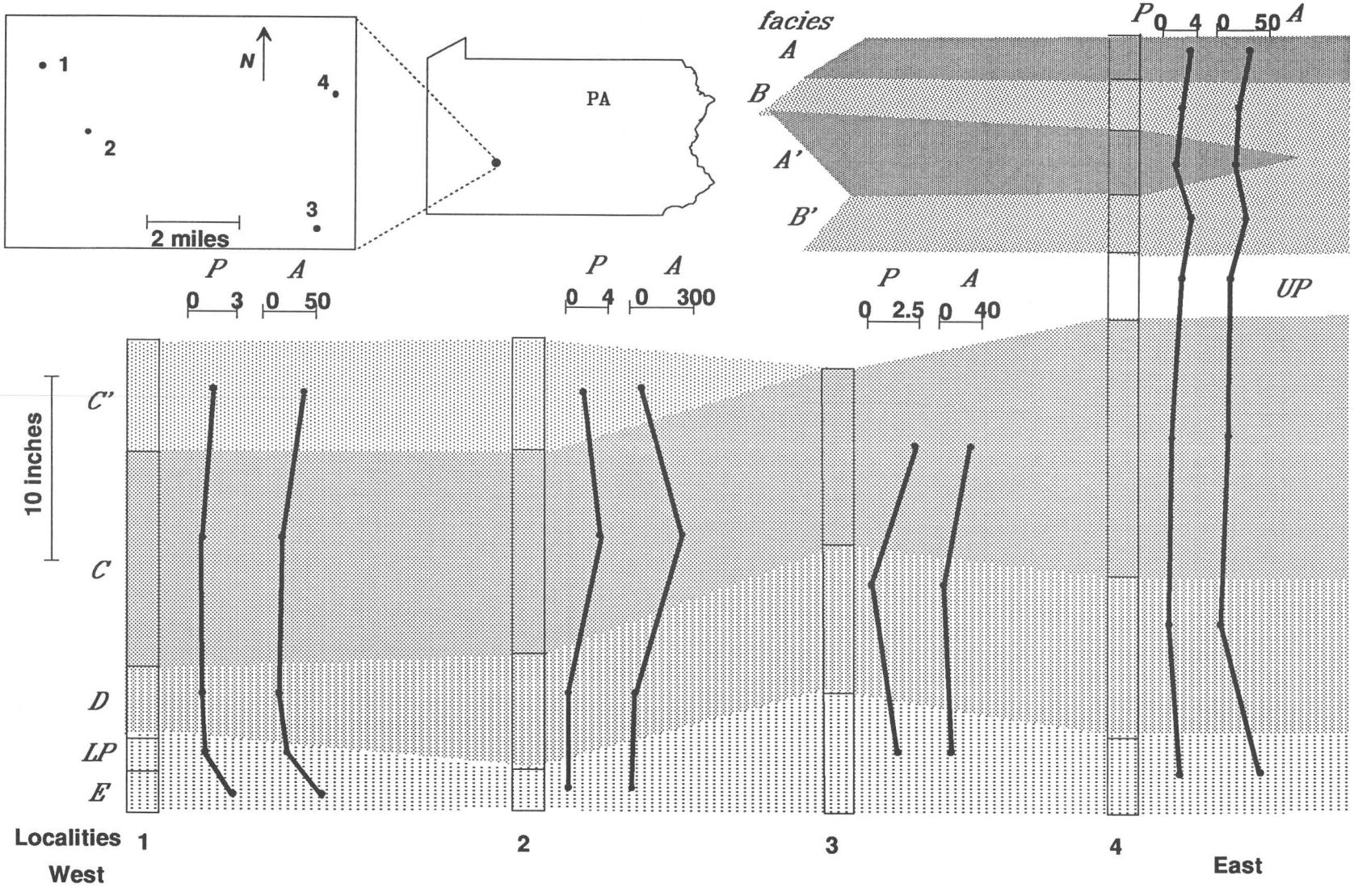

Figure 1 (Pierce). Element distributions in facies of the Upper Freeport coal bed. Four locations selected from 62 vertical sections examined throughout study area. *P*, pyritic sulfur values in percent; *A*, arsenic values in ppm.

latitudinal depocenter migration shows that the main source for terrigenous detritus during most of the postrift history of the offshore basins was the central Appalachian terrain. During the Late Cretaceous, however, the main terrigenous source was the New England Appalachians. The Adirondack terrain contributed less sediment than the other two principal terrains, but was an important source during the Jurassic and Early Cretaceous and throughout much of the Cenozoic.

Some bathymetric migrations of depocenters appear to have been unrelated to differential uplift of the source terrains; these migrations were caused by eustatic changes. For example, a eustatic fall at the end of the Cretaceous restricted principal depocenters to the continental slope and rise, while exposing the shelf to extensive erosion. In contrast, high global sea levels during the Hauterivian, Cenomanian-Turonian, and much of the Paleogene allowed mid-shelf depocenters to develop at the expense of deep-water depocenters. Abrupt surges in sediment supply could overcome the effects of relatively high sea levels, however, to produce thick depocenters on the continental slope and rise. Examples of such sediment-supply overprints are particularly conspicuous on the Neogene and Quaternary isopach maps.

Thick siliciclastic depocenters are attractive targets for petroleum exploration, but their migration through geologic time complicates the search for commercial reserves. A comparison of depocenter locations with the positions of exploratory wells in the middle Atlantic offshore region shows that few of the major depocenters have been adequately tested for hydrocarbons.

Controls, Habitat, and Resource Potential of Ancient Bacterial Gas

Dudley D. Rice

More than 20 percent of the world's natural gas reserves are estimated to have been generated by the decomposition of organic matter by anaerobic bacteria at low temperatures. Such gas is referred to as bacterial gas. This estimate does not include the enormous resources of bacterial gas contained in gas hydrates in both permafrost and deep-sea settings. Further large resources of bacterial gases probably remain to be discovered in frontier areas or are already known to be present in subcommercial accumulations and in accumulations bypassed in past exploration efforts.

The factors that favor significant generation and thus possible accumulation of bacterial methane are anoxic environment, low sulfate content, low temperatures, abundant organic matter, and sufficient space for the bacteria to thrive. Rapid deposition is also critical for the preservation of organic matter prior to and during methane generation and the preservation of methane after its generation. The interrelation of these key factors indicates that most bacterial gas is probably generated at burial depths less than 1 km.

Ancient bacterial gas can be distinguished by its chemical and isotopic composition. The hydrocarbon fraction of bacterial gases consists mainly of methane (C_{2+} values are generally less than 1 percent). The minor amounts of heavier hydrocarbon gases result from early thermogenic or diagenetic processes. The most diagnostic feature of ancient bacterial gases is the isotopic composition of their methane component: $\delta^{13}C$ values are generally lighter than –60 ppt and δD values are usually in the range of –150 to –250 ppt. This isotopic composition indicates that the methane resulted from CO_2 reduction, even though methane generation by fermentation is observed in recent sediments: methane derived by fermentation is depleted in deuterium in contrast to that generated by CO_2 reduction. Bacterial methane generation by fermentation is probably restricted to very young, recently deposited sediments, and the methane is largely lost to the atmosphere. In contrast, methane production by CO_2 reduction can take place in relatively older, more deeply buried sediments deposited in both marine and nonmarine environments and thus is more likely to be trapped.

Bacterial gas can be buried to much greater depths after generation ceases, where it is commonly mixed with varying amounts of thermogenic gas. Gases of mixed bacterial and thermogenic origin are characterized by $\delta^{13}C_1$ values of –60 to –50 ppt and C_{2+} values of as much as 5 percent.

Significant accumulations of ancient bacterial gas have been discovered on five continents: Africa, Asia, Europe, North America, and South America. These accumulations are in Mississippian and younger rocks, occur at burial depths as much as 4,500 m, are commonly mixed with some thermogenic gas, and are associated with a variety of rock types (carbonate, clastic, and coal) and marine and nonmarine depositional settings.

Genetic Lithofacies in the Dakota Sandstone, a Major Oil- and Gas-Producing Formation, Northern San Juan Basin, Colorado and New Mexico

J.L. Ridgley

The Cretaceous Dakota Sandstone in the northern San Juan Basin and vicinity, Colorado and New Mexico,

consists of three major transgressive sequences overlying an entirely fluvial sequence. Each transgression coincided with a westward shift of the shoreline. The Dakota consists of, in ascending order, the Encinal Canyon Member, Oak Canyon Member, Cubero Tongue, Paguate Sandstone Tongue, and Twowells Sandstone Tongue. The Cubero and Paguate Tongues are separated by the Clay Mesa Tongue of the Mancos Shale, and the Paguate and Twowells Tongues are separated by the Whitewater Arroyo Shale Tongue of the Mancos Shale. An erosional unconformity of regional extent marks the base of the Dakota. The Encinal Canyon Member consists of fluvial sandstone and conglomerate that filled incised valleys cut during a sea-level fall; the deepest valleys occur in a more seaward direction.

The Oak Canyon–Cubero, Clay Mesa–Paguate, and Whitewater Arroyo–Twowells intervals each comprise a single genetic package that coincides with a major depositional cycle; each cycle began with a marine transgression and ended with a regressive pulse. The Oak Canyon, Clay Mesa, and Whitewater Arroyo are marginal-marine and marine shale sequences. Deltaic and offshore marine sandstones, possibly remnants of barrier bars, characterize the Cubero and Paguate, which separate the marine shale members. The Twowells is entirely marine in this area.

Westward from the area of entirely marine deposits, each genetic package changes facies to entirely fluvial deposits. These fluvial sequences are commonly lumped with the Encinal Canyon Member as part of the main body of the Dakota. The sandstone and shale distribution and geometry of the entirely fluvial sequence permit separation of individual genetic packages. For each genetic package, lower delta plain rocks characterized by distributary channel fill, coals, or bay fill are laterally adjacent to thick coastal or nearshore marine sandstones. Upstream, lower delta plain rocks are replaced by meander-channel sandstone and overbank mudstone of the lower alluvial plain. Also upstream, the meander-channel sandstone units are thicker and more extensive laterally. During each subsequent transgression and resulting shoreline shift, the fluvial depositional environments also shift. For example, as a result of the shoreline shift between Paguate and Cubero time, lower delta plain rocks overlie lower alluvial plain rocks. Coals of the lower delta plain are especially useful in identifying major shoreline shifts that are due to transgression.

Oil and gas are produced from all sandstone facies in the Dakota, although marine sandstones are the primary exploration targets. Gas is the principal hydrocarbon produced in the deeper part of the northern San Juan Basin. Oil production or shows are confined to the Hogback monocline and Archuleta arch, which bound the northern San Juan Basin on the west and east, respectively. Syndepositional uplift of the Hogback monocline and Four Corners platform to the west of the San Juan Basin resulted in both a thinner sequence of Dakota in these areas and reduced reservoir continuity. Laramide folding and faulting have segmented sandstones into semi-confined reservoirs, but, except locally, do not appear to have destroyed their capacity to contain gas.

Basin Analysis Study of the San Juan Basin, Colorado and New Mexico

J.L. Ridgley and A.C. Huffman, Jr.

During 1985–1989, the U.S. Geological Survey conducted a basin analysis study of the San Juan Basin and vicinity under the Evolution of Sedimentary Basins Program. Major scientific problems addressed in the study were: (1) refining basin lithostratigraphy and biostratigraphy, (2) documenting periods of tectonism and relations of depositional sequences to tectonics, and (3) relating tectonic-sedimentary histories to development of energy and mineral resources. Final published results will include isopach and structure maps, regional cross sections, and numerous topical and synthesis reports documenting results of stratigraphic, sedimentologic, structural, and geochemical studies.

The San Juan Basin is located in northwest New Mexico and southwest Colorado in the southeastern part of the Colorado Plateaus physiographic province. More than 14,000 ft of Paleozoic, Mesozoic, and Cenozoic continental and marine rocks fill the basin. Regional structural, stratigraphic, and sedimentologic studies have revealed a complex history of deposition, nondeposition, uplift, and erosion from Cambrian to the present.

Preserved Mesozoic and older sedimentary rocks in the basin formed as part of widespread regional depositional systems. Paleozoic rocks consist of a thick sequence of marine clastics, carbonate rocks, and evaporites overlain by eolian and fluvial sandstones and mudstones. Mesozoic strata, accounting for more than 60 percent of the sedimentary basin fill, were deposited in a variety of fluvial, lacustrine, and marine depositional environments. Tertiary continental fluvial and lacustrine rocks were deposited within the San Juan Basin but are preserved only in its northern part.

The San Juan Basin assumed its present structurally asymmetric form during the Laramide orogeny in Late Cretaceous to Eocene time. The structural basin is bounded on the northwest and north by the Hogback monocline, on the northeast by the Archuleta anticlinorium, on the east by the Nacimiento uplift, on the south by the Zuni uplift, and on the west by the

Defiance Laramide-age uplift. Basinward-directed thrust faults underlie the Hogback monocline and parts of the Nacimiento uplift. The configuration of the subsurface faults, together with numerous folds and normal faults around the southern, western, and northern margins of the basin, suggests that the basin was formed by north-eastward compression during northeast rotation of the Colorado Plateau. Major faults and folds along the eastern side of the basin are part of a wrench-fault system along which a small amount of right-lateral movement may have occurred. Interpretation of more than 1,000 mi of reflection seismic lines from the basin suggests the presence of numerous northwest- and northeast-oriented faults bounding basement blocks of various sizes. Movement on these faults and on basin-bounding uplifts, recurrent during the geologic history of the basin, influenced the rates of sedimentation, the distribution of facies, and the preservation or erosion of rock.

The San Juan Basin contains significant resources of coal, uranium, and oil and gas. Coal occurs only in Upper Cretaceous sequences deposited during major shoreline regressions and stillstands. Uranium deposits in the basin account for more than 50 percent of the Nation's uranium reserves; these uranium deposits are principally in Jurassic sandstone and limestone. Major oil- and gas-bearing strata include Cretaceous marine sandstone, Jurassic eolian sandstone, and Pennsylvanian carbonate rocks. Significant nonconventional hydrocarbon resources occur in low-permeability sandstone and in coal beds.

Manganese Nodules and Microbial Fixation of Oxidized Manganese in the Huntley Meadows Wetland, Fairfax County, Virginia

E.I. Robbins, J.P. D'Agostino, Virginia Carter, D.S. Fanning, C.J. Gamble, J. Ostwald, R.L. Van Hoven, and G.K. Young

Observations of active processes in modern peat-forming wetlands can be used to explain the origin of metals in coal deposits. One metal that is easy to track in the modern environment is manganese, because its oxide precipitates are black. The iron bacteria that oxidize manganese are morphologically distinct, and oxidized manganese can be readily identified with the redox dye leucoberbelin blue (LBB).

The Huntley Meadows wetland in Fairfax County, Va., hosts an active Mn deposit. Manganese-rich ground water and streams enter the wetland; Mn accumulates in peat, coats rocks in stream riffles, and forms nodules in soils that accumulate in streams. Manganese-binding activity can be shown for all the iron bacteria in the wetland.

The >800-acre wetland is one of many floodplain wetlands along the course of Dogue Creek, which flows into the Potomac River. The wetland is located in a meander cut into Cretaceous sedimentary rocks by the ancestral Potomac River. In the Pleistocene, the meander channel was filled with a basal gravel, overlain by impermeable clay and silt that serve as a confining layer for the modern wetland, and locally by peat as thick as 23 feet.

In terms of vegetation, open ponds are colonized by pond weed and water starwort; marshes are dominated by soft rush and wool grass; shrub wetlands contain button bush, swamp rose, and lizard's tail; and forested wetlands are a mosaic of oak, maple, and sweet gum trees. Peat composed of the bog moss, *Sphagnum*, and plant litter are being actively deposited but not accumulating because of a fluctuating water table.

No water budget has been measured yet for the wetland, but annual inputs include surface water, ground water, and an average 39 inches of rainfall. Surface pH measurements in an open pond and inflowing streams range from 5.8 to 7.4. The Mn content of ground and surface water was measured at two localities in April 1989. At Mittendorff spring along Dogue Creek, the Mn content of an underlying sandy aquifer was 0.51 mg/L, and Mn content from surface water was 0.44 mg/L, as measured by direct current plasma atomic emission spectrometry. In Dogue Creek at our Telegraph Road bridge locality, the Mn content of an underlying sandy aquifer was 0.49 mg/L, and Mn from surface water measured 0.02 mg/L.

Manganese oxide is precipitating and accumulating in the wetland. A fibric peaty muck at the surface contained 680 ppm Mn (dry weight, dw); at a depth of nearly 100 feet, a 3-inch sapric muck in a core contained 870 ppm Mn (dw). Manganese oxide precipitates on the rocks of riffles of streams entering the wetland. Glass slides left in the riffles become coated with doughnut-shaped polygonal precipitates on the holdfasts of the Mn-binding iron bacterium *Leptothrix discophora*.

Manganese nodules accumulate in Deer Run, a tributary to Dogue Creek, and form in the surrounding soil. Initial estimates suggest that several hundred pounds of Mn oxide nodules are present in the soil and streams. Soil taxonomy classifies the Mn-rich hydric soil of the wetland as an Ochraquult; the nodules form in the transitional EB-BE horizon between a very dark grayish-brown (10*YR* 3/2) silt loam A horizon and the gray (10*YR* 6/1) silty clay of the Btg horizon. Knobby manganese oxide nodules as large as 3 cm in diameter have been collected from the transition zone. Glass slides left in this transition zone were colonized by cocci and bacilli and

became coated with soil particles, some of which tested positive for manganese oxide. Creek nodules, which probably formed as a lag concentrate from the surrounding soils, are rounded, pisolitic, and no larger than 1 cm in diameter. They can be characterized chemically as ferromanganese and have buff, iron-rich rims surrounding black, manganese oxide cores. The creek nodules are amorphous to poorly crystalline, as shown by X-ray diffraction, and are composed of the barium-rich psilomelane, romanechite - $(Ba, Mn^{+2})_3(O,OH)_6Mn_8O_{16}$. Glass slides left in the creek become competely coated with the black Mn oxide precipitates of *Leptothrix discophora*. Manganese-oxidizing activity, as shown by the bright-blue color of LBB, is present in the other iron bacteria as well, including *Leptothrix ochracea*, *Leptothrix/Sphaerotilus* sp., *Siderocapsa* sp., and *Gallionella ferruginea*.

The manganese cycle is complex, and many details remain to be determined. From this study of microbial populations and hydrological inputs, we conclude that a metal such as manganese can be incorporated into peat during deposition and therefore be inherited by the ensuing coal.

Microbially Mediated Fixation of Uranium, Sulfur, and Iron in a Peat-Forming Montane Wetland, Larimer County, Colorado

E.I. Robbins, R.A. Zielinski, J.K. Otton, D.E. Owen, R.R. Schumann, and J.P. McKee

Uranium and sulfur create major environmental concerns as problem elements in coal. To study processes that contribute to the initial fixation of these elements in peat, we selected a modern, minerotrophic, peat-forming environment. Microbiological, palynological, and geochemical techniques were used to characterize the biogeochemical conditions that affect the mobility and immobility of uranium, sulfur, and iron in the wetland.

The Boston Peak wetland is a fen/carr complex located at 8,800 feet elevation in the Colorado Rockies. The 8-acre wetland lies along the floor of the glaciated upper Laramie River valley and is surrounded by faulted, uraniferous, granitic and metamorphic rocks of Early Proterozoic age, mineralized fault zones, and Tertiary volcaniclastic rocks. The wetland is fed by metal-bearing ground water, and uranium has accumulated in Pleistocene and Holocene peat and lacustrine sediments in the subsurface.

Vegetation of the central fen is dominated by sedges (*Carex* spp.) and the spike rush (*Eleocharis rostellata*). Vegetation of the marginal carr is dominated by willow (*Salix planifolia*), but birch (*Betula glandulosa*) is also common. Coring in the wetland has revealed a sedimentary section as much as 35 feet thick, composed of a basal glacio-lacustrine clay as a confining layer and an overlying permeable peat, as much as 13 feet thick, composed predominantly of sedge and rush remains. Ash content of the peat ranges from 10 to 25 weight percent; the mean value is 15 percent. Pine and spruce pollen is abundant in the peat. Diatoms are particularly abundant through the basal section of the peat and most of the clay. Although the maximum uranium content of the clay is about 150 ppm, the uranium content of the peat varies from a few ppm to 3,300 ppm near spring sources.

Ground water dominates the water budget of the Boston Peak wetland. Seeps feed the wetland along the east and south edges, and ground water upwells in five spring pools. Spring pools provide the best samples of input ground water (SO_4 4.0–6.5 ppm, U 20–83 ppb, total Fe 0.02–0.20 ppm, pH 6.95–7.65, DO (dissolved oxygen) 2–3 ppm). Well waters sampled from the base of the peat represent ground water modified by residence in the reducing environment of the subsurface (SO_4 0.4–4.7 ppm, U $<$0.1–1.5 ppb, Fe 0.07–5.8 ppm, pH 6.15–7.0, DO $<$0.1 ppm).

The identified microbial populations were those having distinct morphologies or distinct mineral precipitates. Many of the bacteria use iron and sulfur as important energy sources. Iron-oxidizing bacteria include: *Leptothrix discophora* that forms floating surface films of iron oxide; *L. ochracea* that forms red flocculates of ferrihydrite; and *Siderocapsa* sp. that precipitates iron oxide in organic-matter-rich standing water. Sulfur-oxidizing bacteria include: *Thiothrix* sp., microaerophilic, white, filamentous bacteria in the suboxic zone at 10 cm water depth in one spring pool; and *Lamprocystis* sp., purple anoxyphotosynthetic sulfur bacteria in another spring pool. We did not determine the physiological characteristics of the microbial populations that reduce uranium, sulfur, and iron; but from anoxic ground water in piezometers, bacilli, cocci, and rare filamentous bacteria were filtered and counted; counts ranged from 2.7×10^5 to 1.65×10^6 cells/mL. One spring pool had sulfur-oxidizers in the near-surface waters. Below that surface, short, curved, black-rimmed rods (*Desulfovibrio*?) were collected from the anoxic, H_2S- and organic-matter-rich muds.

The cycles involving uranium, sulfur, and iron are entwined through microbial oxidation, reduction, and degradation. Data from four cores of peat and clay show that iron oxide occurs with pyrite at almost all depths, which suggests that the oxide precipitates of iron bacteria may serve as iron sources for pyrite production by microbial reducers. Near the spring pool that records the highest uranium concentration in peat, framboidal pyrite, resulting from the action of sulfur-reducing bacteria, is

present in samples collected at depths greater than 36 inches. Fission track radiographs of sliced peat indicate that uranium (1) is most abundant at depths where pyrite is abundant, (2) is primarily located on organic matter, and (3) is *not* concentrated immediately adjacent to authigenic pyrite.

Because the plant parts in the peat of these intervals are particularly degraded, we postulate that uranium reduction is microbially mediated but in a complex manner. Because anaerobes were not studied, direct reduction cannot be ruled out. Indirect reduction is interpreted from observations on the state of preservation of plant parts and from the presence of pyrite. Partial decomposition of organic matter by microbial degraders can act to produce organic compounds serving as carbon sources for heterotrophic sulfur-reducing bacteria and providing sites for uranium adsorption. The local microbial production of H_2S from upwelling SO_4-bearing ground water can reduce previously sorbed U(VI) and continually added dissolved U(VI) to relatively insoluble U(IV), further immobilizing and concentrating uranium in the peat.

Structural and Basement-Lithological Implications of Gravity and Seismic-Reflection Data Across the Central Powder River Basin from the Black Hills to the Bighorn Mountains

S.L. Robbins and J.A. Grow

The most conspicuous features on a colored complete Bouguer anomaly (CBA) gravity map of the central Powder River basin (lat 44°–45° N., long 104°–108° W.) are: (1) a northwest-trending gravity high (–106 mgal) over the Bighorn Mountains, (2) a north-trending gravity low (–186 mgal) over the deepest part of the basin (western edge), (3) a small, arcuate gravity high (–108 mgal) over the central part of the basin, (4) a small gravity low (–136 mgal) east of (3), and (5) a gravity high (–84 mgal) over the Black Hills near the northeast corner of Wyoming. These features and the following interpretations are based on several map compilations at the scale of 1:500,000: (a) complete Bouguer gravity anomalies in color, (b) isostatic residual gravity anomalies in color, (c) horizontal gravity-gradient anomalies in color, (d) residual-intensity aeromagnetic anomalies in color, (e) structure contours of the basin area. The maps are augmented by several profiles: (a) gravity and magnetic modeling of the thrust fault on the eastern side of the Bighorn Mountains, (b) an east-west gravity and magnetic model across the Powder River basin, and (c) two seismic-reflection profiles from Chevron USA, Inc.

The highest part of the gravity high over the Bighorn Mountains is situated west of the topographically highest part of the mountain range. Modeling of this offset relationship along with modeling of aeromagnetic profiles and the high-quality seismic-reflection profiles along the east flank of the Bighorn Mountains provide strong evidence that the Precambrian rocks of the mountain range have been thrust eastward, along a low-angle fault (dipping 20°–30°), several to 10 or more kilometers over sedimentary rocks within the Powder River basin. Modeling of the gravity data does not require density influences outside of the crust and can easily accommodate a westward flattening of the thrust fault into the middle or lower crust. When isostatic corrections are applied to the CBA data, this large gravity high over the Bighorns becomes even larger (by 25–30 mgals), suggesting that these mountains are rootless and not in local isostatic compensation.

Borehole and seismic data indicate only gentle westward dips for the strata within the central part of the basin. The gravity high in area (3), therefore, is probably caused by significant lateral differences in the densities of the Precambrian basement rocks that are related to basement lithologic variations. Aeromagnetic patterns within the basin also support this interpretation.

On a regional scale, the CBA values decrease from east to west probably as a result of: (a) westward thickening of the sedimentary basin-fill, and (b) westward increase in depth to base of the crust. When isostatic corrections are applied to the gravity highs over the Bighorn Mountains and the Black Hills, the corrections of the highs over the Bighorns are much greater; therefore, the residual values of these two highs become more equal than the CBA values, suggesting that, on a more regional scale, the area is in isostatic equilibrium.

Characterization of Hydrocarbon Reservoirs in Eolian Sandstones

C.J. Schenk

Eolian sandstones can be composed of eolian-dune, clastic sabkha/interdune, and sand-sheet facies, and can be intercalated with extra-dune (fluvial, tidal, evaporite) facies. Successful reservoir development and improved hydrocarbon recovery require an understanding of the vertical and lateral distribution of the different facies and their fluid-flow properties. Generally, eolian-dune sandstones are the best hydrocarbon reservoirs, whereas interdune/sabkha, sand-sheet, and extra-dune facies can be barriers to fluid flow largely because of depositional textures and diagenetic alterations, some of which are early.

Eolian-dune sandstone is generally well sorted, and comprises a coset of sandflow cross-strata and eolian ripple strata. The sandstones can range from a simple stacking of sets of cross-strata, to those in which the internal geometry is complicated by several scales of bounding surfaces. Eolian-dune sandstones generally exhibit little or no early diagenesis.

Clastic sabkha/interdune sandstones are not as well sorted as dune sandstones, and are more irregularly bedded. Structures common to sabkha/interdune sandstones include thin sets of eolian ripple strata, adhesion structures, irregular bedding, contorted strata, and thin, remnant foresets. Early diagenesis is common because of the association of these deposits with the local water table. Early diagenesis includes cementation by halite, gypsum, calcite, dolomite, aragonite, and silica. Early cements such as halite and gypsum can be pervasive, leading to a juxtaposition of cemented sabkha/interdune sands and uncemented eolian dune sands. Sand-sheet sandstones typically exhibit the same forms of early diagenesis as the clastic sabkha/interdune sandstones. These differences in early diagenesis persist and influence the pathways of later diagenesis.

Sedimentary Patterns on the Mid-Atlantic Continental Rise as Discerned by a GLORIA Sidescan Survey

John S. Schlee and James M. Robb

A detailed GLORIA sidescan survey (125,000 km^2) of the continental slope and rise off the mid-Atlantic coast has revealed a complex association of depositional features and transport channels on the upper continental rise. The relatively flat upper rise deepens from 2,000 to 4,000 m over a distance of 150 km. No submarine fans mark the base of the slope; instead, the upper rise has three large triangular zones where sediment conduits converge seaward in what we term "gather areas" (Norfolk, Baltimore-Toms, and Accomac). These are mainly sediment transport pass-through areas where many submarine canyons converge, or die out, or lose their identity at the base of the slope, in a broadly triangular region. The apices of the "gather areas" lead into major channelways that cross to the lower rise. High-resolution profiles of the gather areas show multilayered drape and zones of hyperbolic returns where minor channels are cut. The Accomac and Norfolk gather areas are associated with smaller submarine slides, now largely buried.

Irregular areas of hemipelagic drape that lie between the gather areas are uniform regions of low back-scatter (dark gray) on the GLORIA mosaic (fig. 1); in a few areas, the sediment drape is finely gullied and occurs adjacent to major channelways. High-resolution seismic profiles are marked by gently rolling multilayered signature.

Channelway systems traverse the rise in broadly curving bands, within which are narrow, active channels. Some of the channelways, like the Hudson, are fairly direct pathways to the lower rise and contain only a few meanders. Other channelways at the apex of gather areas are as much as 9 km wide and extend toward the lower rise in broad conduits that are well defined topographically.

The Albemarle-Currituck slump-debris flow is a complex tongue-shaped mass off North Carolina as much as 40 km wide that extends 120 km seaward of the base of the slope. The flow appears as light-gray discontinuous streaks on the mosaic. The varied acoustic texture on the mosaic is interpreted to represent a complex of slides, slumps, and debris flows. Seismic-reflection profiles in the shallower part of the complex show closely spaced diffuse hyperbolae that indicate bottom relief of about 300 m.

The GLORIA images show the upper rise topography to be dominated primarily by offshore-directed processes that are probably of Pleistocene and early Holocene age, when sea level was near the shelf edge. Evidence of contour-parallel processes is visible only in the seaward parts of the study area. For example, the Lower Rise Hills are an area of contour current scour covering at least 22,000 km^2 on the lower rise off Virginia-North Carolina. The mosaic of this area shows a distinctly rippled surface marked by alternating bands of high and low reflectivity whose crests are 8–10 km apart.

Prediction of Sandstone Porosity—An Extension of the Concept of Thermal Maturity

James W. Schmoker and Timothy C. Hester

The porosity of sandstones, which is roughly 40 percent at the depositional surface, commonly decreases during burial. The decrease is frequently treated as a function of burial depth. However, depth is a position coordinate that may not reflect the effects upon porosity of variations in thermal and burial histories. An alternate approach is to consider porosity decrease during burial as a function of thermal maturity. Advantages of this approach are: (1) it takes into account variations in time-temperature histories and (2) the thermal-maturity measurements used to define porosity trends can also be used to characterize petroleum generation and destruction. The timing of porosity change and of kerogen and petroleum maturation can thus be linked.

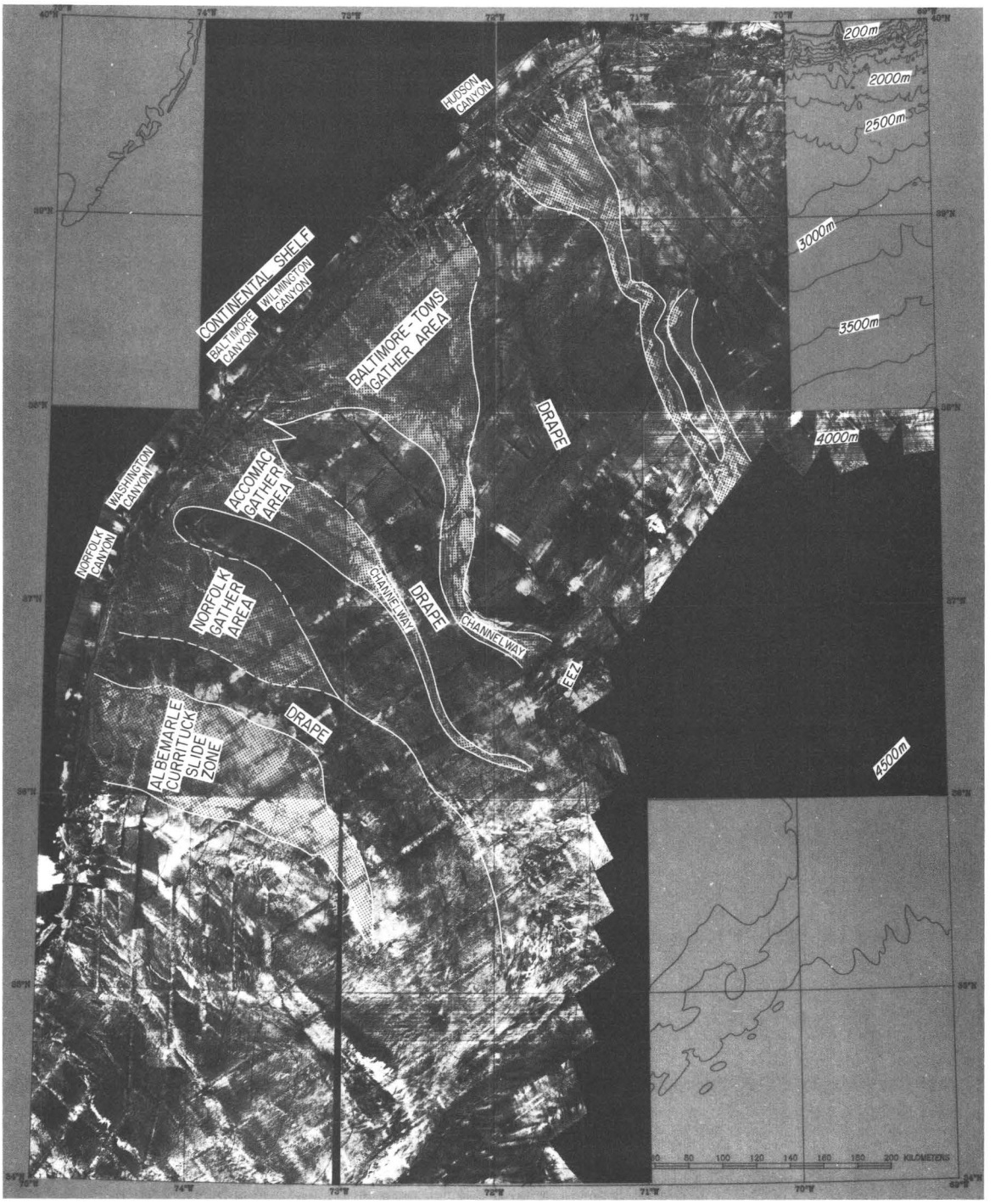

Figure 1 (Schlee). The GLORIA mosaic of the U.S. mid-Atlantic continental rise from the shelf edge (dark area to northwest) to the middle continental rise (in excess of 4,000 m water depth).

Low, average, and high sandstone porosities can each be represented by an equation of the form $\phi = AR_o^B$, where ϕ is porosity and R_o is vitrinite reflectance. B is a negative number. This result is derived from 131 measurement suites incorporating 4,353 individual porosity measurements. Diverse sandstone facies and geologic settings are represented. The data span a maturity range of $R_o = 0.25$–1.7 percent.

Plots of porosity versus R_o for the 10th, 25th, 50th, 75th, and 90th porosity percentiles of each measurement

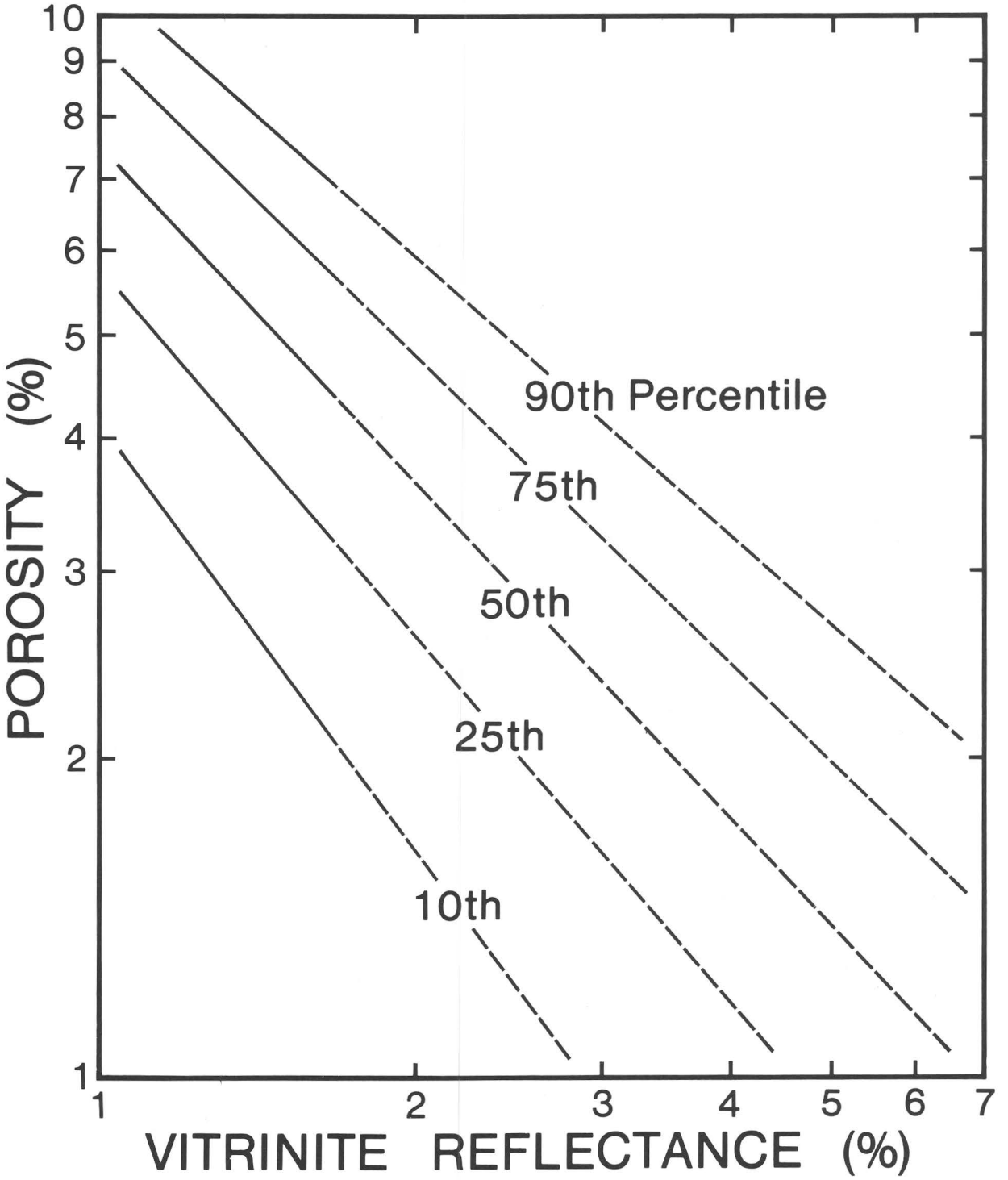

Figure 1 (Schmoker). Extrapolation of regression lines, fit to 10th, 25th, 50th, 75th, and 90th percentiles of sandstone porosity distributions, to thermal maturities characteristic of deep portions of sedimentary basins. Note that remarkably high porosities, which may be of great exploration importance but which represent a very small fraction of sandstones overall, are not represented by this figure.

suite form subparallel trends, with correlation coefficients of roughly r=–.7, from which regional porosity predictions may be extrapolated. Regression lines for the 10th through 90th porosity percentiles are projected in figure 1 (p. 74) to thermal maturities as high as $R_o = 7$ percent. These projections, taken together, predict the typical porosity distribution of deeply buried sandstones. As such, they are useful for basin modeling and as a framework against which to compare local porosity measurements.

Variations in Facies Architecture Related to Sequence Stratigraphy of the Turonian-Campanian Strata, Kaiparowits Plateau, South-Central Utah

Keith W. Shanley and Peter J. McCabe

The various facies developed within the Straight Cliffs Formation of the Kaiparowits Plateau have been studied in outcrop and placed within a sequence-stratigraphic framework. The strata are arranged in geometric patterns that can be related to lowstand, transgressive, and highstand systems tracts. This interpretation provides a new perspective to regional chronostratigraphic and lithostratigraphic relationships of Turonian through lower Campanian strata for southern Utah.

Shoreface deposits of the Tropic Shale and the overlying Tibbet Canyon Member of the Straight Cliffs Formation record progradation of highstand and late highstand systems tracts. Extensive reworking of the upper shoreface deposits by tidal processes may be explained by the relatively slow rates of base level rise, which provided ample time for lateral migration of tidal channels. Coarse, laterally amalgamated fluvial clastics of the Smoky Hollow Member of the Straight Cliffs Formation are interpreted as braided river deposits. This transition from shoreface to braided river deposits represents an abrupt seaward shift in facies tracts due to an increased rate of base level fall. The lower portion of the Ferron Sandstone Member of the Mancos Shale to the east may be part of the resulting lowstand systems tract.

Renewed base level rise is recorded within the Smoky Hollow by a vertical change from fluvial and floodplain deposits to tidally influenced sandstones capped by a ravinement surface characterized by a thin pebble lag. These strata and the upper portion of the Ferron Sandstone Member to the east compose the transgressive systems tract. A thin shark-tooth lag, a few meters above the ravinement surface, is thought to mark a condensed section recording maximum rate of water deepening.

Subsequent reduced rates of base level rise resulted in vertical aggradation of the overlying John Henry Member of the Straight Cliffs Formation which forms an early highstand facies tract. Aggradation of fluvial sediments is recorded in the western part of the plateau whereas vertical stacking of shoreface sandstones is characteristic of the eastern margin. The central part of the plateau was the site of major coal accumulation. Most of the fluvial strata show a high ratio of overbank to channel deposits. In the lower part, however, there is a low ratio of overbank to channel deposits which corresponds to a small forward step in the shoreface sandstones to the east, indicating a period of somewhat slower base level rise. In contrast to the Tibbet Canyon Member, most shoreface deposits of the John Henry Member show little evidence of reworking by tidal channels, presumably because of the more rapid rates of base level rise.

The John Henry Member is unconformably overlain by the laterally amalgamated, coarse fluvial sandstones of the Drip Tank Member of the Straight Cliffs Formation. The unconformity represents removal of increasing amounts of strata to the west. The braided river deposits of the Drip Tank resulted from a major lowering of base level during the Campanian.

Impact of Drilling off Key West, Florida—Where's the Beef?

Eugene A. Shinn

Geological and biological assessment of eight nonproductive offshore drill sites off South Florida revealed both positive and negative environmental impacts. Measurable impacts at all sites were of mechanical origin and limited to small areas adjacent to the borehole.

Environments near Key West, where six wells were drilled between 1959 and 1961, include coral reefs, sea grass, live bottom and rippled carbonate sands. Two modern wells off Fort Myers (1981 and 1986) were drilled in deep water (53 and 70 m). The deeper site was on a surficial algal/sponge community, whereas the other was on a relatively barren sand with scattered sponge-encrusted rocky outcrops. (Table 1 provides additional site data.)

Positive impact is limited to the "artificial-reef effect." Abundant debris discarded at sites on rippled sand was encrusted with corals and algae not present before drilling. Numerous species of fish and crustaceans reside among casing, cables, discarded core, and other materials that were routinely dumped overboard before enactment of OCS dumping regulations.

Table 1 (Shinn). Well site data, offshore Florida drill sites

Well name	Loran C TDs	Lat./Long.	Lease block	Date drilled	Rig type	Water depth (m)	Well depth (m)	Lessee
SL 1011 No. 2	13887.9 43748.5	24.32.07 82.06.25	State 1011	1961	Barge	5	2,354	California Co.
SL 1011 No. 3	13887.9 43748.5	24.32.07 82.06.25	State 1011	1962	Pontoon	5	3,917	California Co.
SL 826Y No. 1	13905.4 43729.1	24.37.05 82.02.14	State 826Y	1959	Unknown	5	4,481	Gulf Oil Corp.
OCS 0665 No.1	13845.7 43826.8	24.27.06 82.21.40	OCS Block 28	1960	Jackup	11	4,662	Gulf Oil Co.
OCS 0674 No. 1	13826.4 43867.9	24.26.01 82.29.18	OCS Block 46	1961	Jackup	23	2,399	Gulf & Calif. Co.
OCS 0672 No. 1	13809.8 43903	24.25.13 82.36.02	OCS Block 44	1961	Barge	20	1,429	California Co.
OCS G4950 No. 1	13854.67 30348.52	26.18.37.98 83.42.10.99	OCS Block 622	1986	Jackup	70	3,216	Shell Oil Co.
OCS G3906 No. 1	13978.88 30587.78	26.49.27.19 83.24.33.20	OCS Block 144	1981	Jackup	53	3,464	Gulf Oil Corp.

Negative impact resulted where drill rig legs and anchors impacted coral bottom, and at one site the bottom was altered when a barge load of pea gravel was dumped to level the bottom. Approximately 1 acre of gorgonian and sponge hardbottom was destroyed by the pea gravel. A new community of fleshy algae now grows on the pea gravel. At the same site several dozen bags of cement were piled over the well head. The cement bags support 8 species of corals and provide a habitat for 25 species of fish.

The most severe and long-lasting impact occurred where a 14-legged jackup rig (site OCS 0665 No. 1) drilled on coral reef bottom in 1960. In addition to the sand-filled 4.5-m-diameter "footprints," two >30-m-long anchor scars remain. The total amount of impacted bottom is 406 m^2 or approximately 1/10 acre. Sand in the impacted areas has prevented coral and gorgonian recruitment for the past 30 years. However, diversity and numbers of corals and gorgonians in a 10-m^2 quadrant bordering the borehole are the same as in a control site 1 km from the borehole. No positive or negative impacts could be detected where a floating rig was used to drill on a coral reef. Although all sites may have been initially impacted by drill mud and cuttings, no evidence of their effects could be detected in 1988.

Drill mud and cuttings were not apparent at either of the deep-water sites drilled in the 1980's. Neither cuttings nor drill mud was apparent at OCS G4950 No. 1 drilled in 70 m of water in 1986, 2.5 years before our observations. The most obvious impact consisted of a 1-m-high, 10-m-diameter mound of grout surrounding a 1-m-diameter borehole. Large fish lived in the borehole and the site was enveloped by a cloud of small sardinelike fish. Some debris was present, the most obvious of which were dozens of used welding rods.

The other deep-water site (53 m), drilled in 1981, consisted of a 1-m-diameter borehole centered on a patch of sponge-encrusted hardbottom. Two very large groupers occupied the hole and again the area was enveloped in clouds of small fish and schools of 1-m-long amberjacks. Debris was less obvious and no grout mound or cuttings pile was present. At both deep sites, the borehole and debris had created an artificial reef.

The purpose of our study was to determine what effects can be predicted during future drilling in tropical environments. We conclude that noticeable damage from offshore exploratory wells drilled on or around coral reefs will be of mechanical origin. Anchors and platform legs do impact on the environment; proper selection of drill sites can greatly reduce such damage. Because the only visual evidence of drilling at sites drilled on sandy

bottom was caused by discarded debris, I conclude that if no debris is thrown overboard there will be no lasting effect of drilling, assuming no blowouts or drilling accidents. In fact, it would have been impossible to verify six of the eight sites had debris been absent. Because impacts are largely mechanical, it seems likely that offshore wells can be drilled within a few meters of reefs without causing lasting harm.

Western Tight Gas Reservoirs—Resource Potential and Development Constraints

Charles W. Spencer, Ben E. Law, and Ronald C. Johnson

In 1985 the U.S. Congressional Office of Technology Assessment analyzed the availability of natural gas to the year 2000 and beyond. They concluded that tight gas reservoirs, located mostly in the western United States, had the greatest potential to replace declining conventional gas reserves. Tight reservoirs in the U.S. are currently producing about 1 TCF (trillion cubic feet) of gas per year. This volume is about 1/16 of total U.S. production.

The USGS, in cooperation with the U.S. Department of Energy (DOE), is conducting research on selected western tight gas basins and areas. Estimates of gas in place and recoverable gas have been made for three basins and areas: the northern Great Plains, the Piceance basin in northwest Colorado, and the Greater Green River basin in southwest Wyoming and northwest Colorado. The Greater Green River basin tight gas assessment, made in 1989, is the most recently completed evaluation. An assessment of tight gas resources in the Uinta basin in northeast Utah is currently in progress.

The Greater Green River basin tight gas-bearing interval is mostly overpressured and is as thick as 14,000 ft. The prospective rocks consist of sandstone, mostly Cretaceous in age but including some of early Tertiary age. The gas-bearing intervals were subdivided into five plays, and only gas-bearing sandstones more than 10 ft thick were included in the assessment. Several economic and technologic scenarios were used to estimate recoverable tight gas volumes in the Greater Green River basin. The most conservative estimate was made assuming state-of-the-art current technology and a gas price of $5/MCF (thousand cubic feet) in 1987 dollars. Using these criteria, the aggregated recoverable gas estimates for the five Greater Green River plays range from 27 to 148 TCF. The arithmetic mean estimate is 73 TCF.

The Piceance basin tight gas resource assessment, made in 1987, estimated a recoverable gas volume, using current technology, ranging from 8.46 to 20.65 TCF with an arithmetic mean of 13.42 TCF.

Recovery of much of the gas from tight reservoirs is heavily constrained. The two most significant constraints are gas price and recovery technology. Special incentive gas prices in the early 1980's exceeded $5/MCF in some areas of the U.S. These incentive prices encouraged a high level of exploration and development activity for gas in these low-quality reservoirs. Conversely, the current low gas prices have strongly discouraged tight gas research and development.

Major advances are needed in recovery technology in order to improve the productivity of these low-permeability reservoirs. Hydraulic fracturing is presently the most common method of reservoir stimulation, but this technique was developed approximately 40 years ago. More innovative drilling and completion methods need to be developed and tested, such as horizontal and inclined well drilling. New methods to reduce or prevent formation damage need to be tried.

Based on these assessments, tight reservoirs appear to be one of the best future sources of gas and should be a key factor in the Nation's energy and economic future.

Diagenesis of Organic Matter and Sulfur in Sapropel and Peat from Mud Lake, Florida

E.C. Spiker, P.G. Hatcher, V.J. Comer, A.L. Bates, and S.A. Stout

A study of Mud Lake, a small, shallow freshwater lake located in north-central Florida, was undertaken to further our understanding of the chemical changes occurring in peat during early diagenesis. The lake sediments are particularly interesting because they record a significant change in lake vegetation. The sediment grades from a gelatinous algal sapropel into a highly degraded aquatic *Nymphaea* peat at approximately 2.5 m depth, and to a fibrous *Mariscus* peat at approximately 3 m depth. The sapropel was studied in the 1960's by Wilmot Bradley, who considered the sapropelic deposit to be analogous to the organic matter in oil shale.

Our recent study mainly utilized solid-state ^{13}C NMR (nuclear magnetic resonance) to determine the bulk organic chemistry, and stable isotopes were used as natural tracers. The total organic carbon content ranges from about 30 to 45 percent. The carbohydrate carbon content decreases and lignin and paraffinic carbon contents increase with depth in the sapropel and *Nymphaea* peat. This major change in the bulk chemistry of the organic matter reflects the degradation of labile

material and the selective preservation of the more resistant aromatic and aliphatic (paraffinic) components. The carbohydrate content increases in the *Mariscus* peat, which is more fibrous and apparently better preserved than the overlying *Nymphaea* peat.

The stable carbon isotope content shows a strong correlation with the carbohydrate carbon content, decreasing nearly 8 per mil with decreasing carbohydrates in the sapropel and *Nymphaea* peat. This correlation may be due, in part, to the loss of ^{13}C-enriched carbohydrates, as studied in 1984 by Spiker and Hatcher. However, more than half this decrease in the carbon isotope composition is due to the change from algae to herbaceous plants, which also produced a large relative increase in lignin content in the *Nymphaea* peat.

The total sulfur in the sediment is moderately high, especially considering that this is a freshwater lake. The source of the sulfur is presumably sulfate from local streams and ground water. The sapropel smells of H_2S. Total sulfur content increases systematically from 2 percent in the near-surface sapropel to about 6 percent at 1.5 m depth and decreases to about 4 percent at 3 m depth in the *Mariscus* peat. The sulfur appears to be concentrated in the sediment as a result of the loss of labile organic matter. Forthcoming analyses of the forms and isotopic composition of the sulfur should help determine the origin and mode of sulfur formation.

Age, Facies, and Depositional Environments of the Lower Miocene Lospe Formation, Santa Maria Basin, Central California

Richard G. Stanley, Samuel Y. Johnson, John D. Obradovich, Michele L. Tuttle, Mary Lou Cotton Thornton, David R. Vork, Mark V. Filewicz, Mark A. Mason, and Carl C. Swisher III

The Lospe Formation is an 800-m-thick sequence of sedimentary and minor volcanic rocks that occurs at the base of the petroliferous Neogene section of the Santa Maria basin of central California. We are conducting a multidisciplinary study of the stratigraphy and sedimentology of the Lospe in its type area in the Casmalia Hills. Our preliminary results shed new light on long-standing problems concerning the age and depositional setting of the Lospe and provide additional insights into the early Neogene history and paleogeography of the Santa Maria area.

Until now, the age of the Lospe Formation has been constrained by the age of the underlying Jurassic ophiolite and the overlying lower Miocene Point Sal Formation. We have discovered palynomorphs of early Miocene age in the upper 200 m of the Lospe and calcareous benthic foraminifers of earliest Miocene (Saucesian) age in the uppermost 15 m of the Lospe and lowest 2 m of the Point Sal Formation. The lower part of the Lospe apparently lacks fossils but contains several horizons of pyroclastic crystal-vitric tuff that we are attempting to date isotopically.

The Lospe has long been considered to be entirely nonmarine in origin. However, new fossil discoveries and detailed analysis of sedimentary facies indicate that the Lospe accumulated in an orderly succession of paleoenvironments including alluvial fan and fan-delta, lake or restricted coastal embayment, and shallow marine shelf.

Alluvial fan and fan-delta facies within the basal part of the Lospe are up to 200 m thick and consist of reddish-brown and greenish-gray conglomerate and sandstone with minor mudstone and tuff. Many of the conglomerate clasts are angular, suggesting rapid first-cycle erosion from nearby fault-bounded uplifts of Mesozoic and Paleogene sedimentary and igneous rocks. Conglomerate clast compositions and paleocurrent directions suggest that this part of the Lospe Formation was deposited in at least two sub-basins separated by an east-west-trending paleohigh of Jurassic ophiolite located approximately in the same position as the present-day Point Sal Ridge.

The alluvial fan and fan-delta deposits grade upward into a 600-m-thick sequence of interbedded greenish-gray sandstone and mudstone that accumulated in a subaqueous environment, most likely a lake or coastal embayment with restricted connections to the ocean. Many of the sandstone beds are sheetlike and normally graded, and appear to have been deposited by turbidity currents. The associated mudstones contain sparse marine microfossils including dinocysts, foraminifers, radiolarians, and diatoms. Lenticular beds of pyroclastic tuff, as thick as 20 m, occur sporadically throughout this sequence; in places, the tuffs incorporate blocks of Jurassic ophiolite up to 50 m long and 20 m across.

Near the top of the Lospe Formation is a 5-m-thick bed of amalgamated, plane-laminated to bioturbated, fine-grained sandstone that can be traced laterally at least 6 km. This sandstone is underlain and overlain by mudstones bearing outer shelf to upper bathyal benthic foraminifers and is interpreted as a storm-generated shelf deposit. About 3 to 5 m above this sandstone, the characteristic gray-green mudstones of the Lospe are sharply overlain by black fissile shale of the Point Sal Formation, recording an abrupt change from a well-oxygenated marine shelf to an oxygen-poor, deeper-water slope environment.

Overall, the Lospe Formation provides a clear record of progressive deepening, active faulting, and regional volcanism during the earliest stages of formation

of the Santa Maria basin. This history is consistent with several competing tectonic models that variously explain the origin of the basin as the result of regional extension, regional transtension, local pull-apart rifting, or local tectonic rotation of small crustal blocks.

Liquefaction Potential of Facies of the Wyodak-Anderson Coal Bed, Powder River Basin

R.W. Stanton, P.D. Warwick, and S.S. Crowley

Low-temperature carbonization yields, from a modified Fischer Assay, of selected samples from petrographically distinct facies have a positive correlation with the amount of humic matrix material (crypto-eugelinite) in the Wyodak-Anderson coal bed of the Fort Union Formation (Paleocene, subbituminous). In contrast, the amount of total huminite, which varies little, does not correlate with carbonization yields.

Facies within the Wyodak-Anderson coal bed were delimited on the basis of maceral compositions of 100 samples from three localities in the Gillette Field, Wyoming. Four major classes of samples were indicated by cluster analysis. Facies were then defined on the basis of one or more of these sample classes. To evaluate the liquefaction potential of these facies, we selected 17 samples to represent the six type of coal facies.

Petrographic analyses were used to differentiate the samples by composition. Macerals on etched polished pellet surfaces were point-counted under white-reflected light and blue-light fluorescence. Relative response of the varieties to etching by acidified potassium permanganate solution facilitated identification of huminite-maceral varieties. In particular, structured huminite macerals (crypto-humotelinite, crypto-detrogelinite, and crypto-corpohuminite) are more resistant to etching than the humic matrix material (crypto-eugelinite).

Oil yields from Fischer Assays range from 0.7 to 9.9 wt. percent on an as-received basis and from 0.8 to 11 wt. percent on a dry basis. Crypto-eugelinite amounts vary from 17 to 58 percent on a dry, whole coal basis (dwc). The plot of oil yield (dwc) versus crypto-eugelinite (dwc) has a correlation coefficient of 0.72, a relation which is best shown by an exponential fit (fig. 1, p. 80). From these preliminary data, we infer that the more reactive and oil-yielding maceral is eugelinite, which resulted from chemical and physical degradation of plant cells and other, possibly hydrogen-rich plant parts.

In the Gillette area, the Wyodak-Anderson coal bed consists of 12–15 km^2 bodies that commonly exceed 30 m in thickness. Samples from the margins and the base of the bed contain generally greater amounts of structured huminitic materials than do samples from the upper and more interior parts of the deposit. Initial formation of the Wyodak-Anderson swamp deposits began with an accumulation of peat containing structured huminite premacerals. During later stages of accumulation, the margins of the swamp contained peat facies rich in structured premacerals. In the interior parts of the swamp, more degraded peat facies formed under wetter conditions, which probably were more suitable for the growth of peat-forming plants that were easily degraded. Swamp cessation was caused by lake flooding that deposited fine-grained sediments.

Based on this model for peat development, the highest pyrolysis yields should be found in the more interior parts of the coal bodies. The optimal liquefaction yield would depend on the process used, but from this preliminary study, samples characterized by large amounts of degraded humic material (eugelinite) should prove to be the most successful for liquefaction. Eugelinite can be also easily measured in higher rank coal by analysis of etched polished surfaces of coal. The eugelinite content of coal, therefore, may be an important parameter to determine if a coal bed were a source for petroleum.

Is There a Future for 4.0 Trillion Tons of Low-Sulfur Alaskan Coal?

Gary D. Stricker

With an ever-increasing interest in acid rain, the demand for and utilization of low-sulfur coal will increase. Alaska's coal resources have a unique position in the United States' overall coal resource picture and can only be described as enormous: 4.0 trillion tons of hypothetical onshore coal. Alaska's coal is also low in sulfur: mean total sulfur content of 0.34 percent (range is 0.06 to 6.6 percent, $n = 262$). Mean ash content is 10.9 percent and mean apparent rank is subbituminous B. By contrast, Carboniferous coal of the Appalachian region and Interior Province has a mean total sulfur content of 2.34 percent (range of 0.1 to 19.2 percent, $n = 5{,}497$); mean ash content of 11.16 percent; and a mean apparent rank of high-volatile A bituminous. Lower 48 Cretaceous and Tertiary coals have a mean total sulfur content of 0.86 percent (range of 0.02 to 18.9 percent, $n = 2{,}754$); mean ash content of 11.97; and a mean apparent rank of subbituminous B. Thus, Alaskan coal's mean sulfur content is 2.5 times less than the mean for western U.S. coal and 6 times less than the mean for Carboniferous U.S. coal.

A 1987 report by Wood and Bour lists 50 major and minor coal fields and occurrences of coal in Alaska.

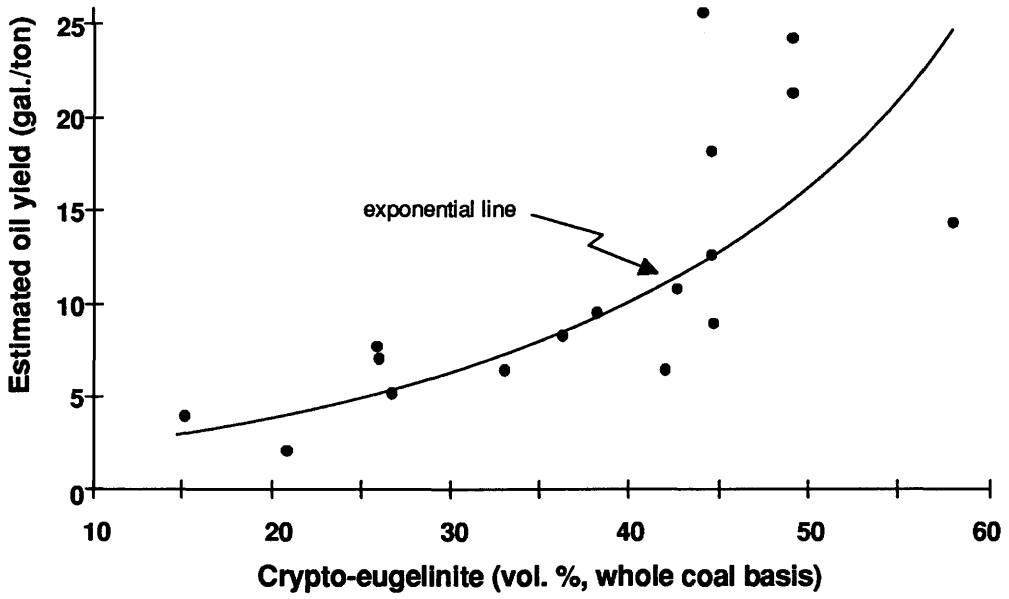

Figure 1 (Stanton). Low-temperature carbonization yields of Wyodak-Anderson coal samples.

The bulk of Alaska's coal resources are in six major coal fields, which are (in order of decreasing economic potential) Nenana, Cook Inlet, Matanuska, Chignik–Herendeen Bay, North Slope, and Bering River. The Tertiary Nenana coal basin, containing the only active coal mine in Alaska, has the most economic potential. Mean total sulfur content in that coal is 0.24 percent (range of 0.1 to 1.5 percent), mean ash content is 9.9 percent, and mean apparent rank is subbituminous C. Resources are estimated to be 1 billion tons of identified coal and 2 billion tons of hypothetical coal.

In the Cook Inlet region, two coal fields are of interest: Beluga and Kenai, in both of which coal is of Tertiary age. In the Kenai field, mean total sulfur content is 0.33 percent (range of 0.06 to 1.1 percent), mean ash percent is 14.3, and apparent rank is subbituminous C. Resources are estimated to be 320 million tons identified and 35 billion tons hypothetical. In the Beluga field, mean total sulfur is 0.18 percent (range of 0.08 to 0.33 percent). Mean ash content is 16.4 percent and apparent rank is subbituminous C. This field contains 10 billion tons identified and 30 billion tons of hypothetical coal.

The Tertiary Matanuska coal field has a mean total sulfur content of 0.45 percent (range of 0.2 to 1.5 percent). Mean ash content is 12.3 percent and mean apparent rank is high-volatile A bituminous. Coal resources are estimated as 150 million tons identified and 500 million tons hypothetical.

Coal in the Chignik–Herendeen Bay fields is Cretaceous in age. Total mean sulfur content for these coal units is 0.82 percent (range 0.3 to 1.3 percent), mean ash content is 13.6 percent, and mean apparent rank is high-volatile B bituminous. Resources are estimated to be 360 million tons identified and 3 billion tons hypothetical.

The Alaskan North Slope has the largest estimated coal resources in Alaska. Coal ranges in age from Cretaceous to Tertiary. For the Cretaceous coal the total mean sulfur is 0.32 percent (range of 0.01 to 2.02 percent), mean ash content is 10.4 percent, and mean apparent rank is subbituminous B. Resource estimates for the Cretaceous coal are 3.2 trillion tons of hypothetical coal. For the Tertiary coal, the total mean sulfur is 0.37 percent (range of 0.08 to 2.02 percent), mean ash content is 10.6 percent, and mean apparent rank is subbituminous C. No resource estimates are available for Tertiary coal.

The Tertiary Bering River coal field has a mean sulfur content of 1.2 percent (range 0.4 to 5.22 percent). Mean ash content is 13.6 percent and apparent rank is semianthracite. Resources for this tectonically deformed coal field are 110 million tons of identified and 3.5 billion tons of hypothetical coal.

Even though Alaska has 4.0 trillion tons of hypothetical low-sulfur coal, this resource has not been developed. Factors limiting coal development are: (1) increased shipping cost because of large distances to potential markets; (2) inhospitable climate during long and cold winters, which adds to the cost of mining; and (3) little infrastructure in areas where many coal fields are located. Unless the United States and world energy picture changes, this abundant resource will not be utilized in the near future.

A Structural and Stratigraphic Transect Across the Florida Platform from the Deep Gulf of Mexico to the Deep Atlantic

B. Ann Swift, William P. Dillon, Myung W. Lee, and Mahlon M. Ball

The U.S. Geological Survey has synthesized data from multichannel seismic profiles, boreholes, submersible dives, and two seismic-refraction lines to develop a structural/stratigraphic transect across the Tampa Basin, the Florida peninsula, and the Blake Plateau basin. This transect spans a carbonate depositional province, from deep ocean crust on either side of the Florida peninsula, across steep erosional escarpments and broad, flat continental borderlands. The Cenozoic platform strata continue across the central Florida peninsula. Seismic profile TD-3 begins in the deep Atlantic basin, crosses the Blake Plateau basin, the Blake Escarpment, and the Blake Plateau. Lower Cretaceous rocks, exposed by erosion on the escarpment and sampled by DSRV *ALVIN*, provide fossil age-control that complements ages derived from well samples (DSDP 391 and 536 and COST GE-1).

The offshore stratigraphy (Cenozoic and part of the Cretaceous) is carried across Florida by correlating biochronologic horizons with synthetic seismograms generated at six sites, using well-log data and extrapolating along multichannel lines. On the Gulf of Mexico side, seismic-reflection profile Mafla 15-16-17 crosses the West Florida Shelf (near the St. Petersburg area) and extends beyond the Florida Escarpment to the deep Gulf of Mexico basin.

Post-stack processing improved the seismic image of the platform features. A post-stack deconvolution filter was applied to the Mafla data and followed by migration. Line TD-3 (Blake Plateau basin) was treated similarly, except that a section near the Blake Escarpment was completely reprocessed to reduce multiple energy that obscured reflections immediately landward of the escarpment. Reprocessing also helped to better resolve a deep mantle(?) reflector seaward of the escarpment. The interpreted time sections were then depth-converted, using velocities from two oblique refraction lines and smoothed velocity functions.

Early structure and stratigraphy of the Blake Plateau basin were controlled by the extensive Jurassic rifting and extension of continental crust associated with the opening of the North Atlantic. On Line TD-3, synrift and early postrift deposits (inferred red beds and other clastics) are overlain by predominantly carbonate platform deposits that filled the main basin during the thermal subsidence phase. The postrift stratigraphy is essentially flat, with pre-Upper Cretaceous horizons terminating against a basement high on the landward edge. Erosion, concentrated on the seaward platform edge, created much of the present physiography.

On the West Florida Shelf part of the transect, rifting associated with opening of the North Atlantic and the Gulf of Mexico is reflected in basement faulting. On the landward end of Line 17, the Paleozoic to Jurassic basement forms a fault-related monocline structure, which is draped by overlying Mesozoic and Cenozoic deposits. Farther seaward on Line 16, intrabasement reflections indicate a synclinal structure. Another basement monocline is evident seaward on Line 15, upon which Jurassic deposits onlap and thin toward the escarpment edge.

Coal Resources in Sind Province, Pakistan

Roger E. Thomas, Mohammed Riaz Khan, and Shafique Ahmed Khan

Approximately 4.7 billion metric tons of coal, ranging from subbituminous C to lignite A in rank, has been estimated for the Sonda coal field and Indus East area in Sind Province, 80 km north of Karachi, Pakistan. This estimate was based on 34 exploratory drill holes completed between April 1986 and February 1988 in an area of 1,583 km^2. The drilling was part of the Coal Resource Exploration and Assessment Program (COALREAP) of the Geological Survey of Pakistan, the U.S. Geological Survey, and the U.S. Agency for International Development. Ten coal zones within the Paleocene Bara Formation were identified. Most of the coal resources are in the Middle Sonda (2,200 million metric tons) and Inayatabad (780 million metric tons) coal zones. Together, these two coal zones contain 63 percent of the total resources.

Isopach maps of the thickest coal bed in each zone were constructed for the 10 identifiable coal zones in the Indus East area. Resource estimates, based on the thickest coal bed in each zone, reflect a conservative amount of coal in this area. In the Indus East area, for example, the thickest coal bed (2.40 m) in the Middle Sonda zone was found in drill hole UAK-15, 5 km west of Mulla Katiar; the thinnest coal bed (0.25 m) was found in drill hole UAK-12, 1 km west of UAK-15. Isopachs constructed for both coal bed thicknesses indicated a great variation in coal thickness over a relatively small area. The Inayatabad coal zone (approximately 60 m above the Middle Sonda coal zone) contains coal beds that range from 0.35 to 1.50 m thick and average 0.75 m thick. Isopachs drawn for the thickest Inayatabad coal bed revealed a nearly symmetrical thick coal deposit in a

horseshoe-shaped area near the village of Tando Muhammed Khan and Chhari Dhand [lake]. The absence of coal in an area 9 km east-to-west and 24 km north-to-south suggests channels where the coal was eroded.

Resources for the Indus East area were calculated for three reliability categories—measured, indicated, and inferred. The most reliable estimates are those for the measured category. Total coal resources are approximately 31,000,000 metric tons or about 2 percent of the total resources; indicated resources are 241,000,000 metric tons or 14 percent of the total resources; and inferred resources are 1,414,000,000 metric tons or 84 percent of the total resources, the least reliable resource category. This percentage distribution is due to the spacing of data points and the construction radii around the inferred category data point that are larger than the radii constructed for indicated or measured coal.

Coal beds in the Sonda coal field and the Indus East area are difficult to correlate due to abrupt pinching out and swelling. They grade laterally to carbonaceous shale and rooted siltstone within 2 to 5 km. Seat rock can be sandstone, shale, or siltstone, and is commonly rooted. Most coal zones are separated by 5–10 m of interburden that can attain a maximum thickness of >100 m. Loose, unconsolidated sandstone and poor core recovery make interpretations difficult and coal bed correlations speculative. Closer spaced drill holes will clarify and significantly improve coal zone correlations in the Bara Formation.

Analysis of 90 coal samples indicates a rank of subbituminous C to lignite A and average contents of 13.7 percent ash and 3.6 percent sulfur. These coal analyses also indicate calorific values ranging from 6,000 to 8,000 Btu on an as-received basis.

Basin Analysis as an Exploration Tool—Paradigms Lost, Insights Gained

Christine E. Turner-Peterson and
Neil S. Fishman

Advances in geology, as in all sciences, result from the testing and overturning of paradigms and the replacement of old theories with new. Paradigms are useful in seeking solutions to complex geologic problems because "we have to start somewhere" in our analysis, and existing theory provides a convenient point of departure. Moreover, paradigms provide a framework within which to place what might otherwise be random observations. For example, a relatively new paradigm in geology is sequence stratigraphy, which provides a more systematic way to organize stratigraphic observations.

A problem with paradigms is that we become increasingly dependent upon the ready explanations they offer and find ourselves searching for data in support of the paradigm rather than treating the paradigm as one of many working hypotheses. The more a paradigm is cited in the literature, the more "correct" it becomes, and in the process the more difficult it is to overturn. So, although science advances by the overturning of paradigms, in practice our reliance on paradigms leads us to become increasingly reluctant to relinquish them even when faced with contradictory data. As a consequence, paradigms are more commonly applied than tested: what begins as hypothesis evolves into unalterable truth. This is in spite of the fact that the creators of new paradigms commonly are the most cautious in the extrapolation of their models and warn readers against indiscriminate application. The proponents of sequence stratigraphy, for example, urge us to use the concept as a "tool rather than a template" (H. Posementier, oral commun., 1989).

With these caveats, why do we still have the tendency to apply paradigms without questioning them? In large measure, this tendency stems from the need to interpret an increasingly bewildering amount of data from diverse specialties in which we have limited or no expertise and must rely on prevailing thought to narrow the number of possible interpretations. Also, the propensity of scientists to hold tenaciously to conventional wisdom is understandable in light of new knowledge of the partitioning of brain functions. The analytical and organizational left hemisphere of the brain seeks explanations for random information already in storage. Although this ordering is an important and necessary function, the left hemisphere becomes reluctant to give up a model that it sees as a satisfactory explanation for otherwise random information. With time, a paradigm can become deeply rooted and virtually ineradicable, even in the face of new data that may be contradictory to the paradigm. Moreover, paradigms stored in the left hemisphere filter new observations that enter the visual right hemisphere of the brain, a process that also hinders formulation of new concepts. In light of this inclination to override the implications of new observations, our objectivity as scientists is questionable. This coloring of our thought processes comes through in the humorous admission, "I would never have seen it if I hadn't believed it myself."

In the study of sedimentary basins, the basin analysis approach forces rigorous testing of scientific paradigms because the multidisciplinary nature of the approach necessitates the integration of data from diverse specialties. Feedback from diverse specialties provides numerous constraints so that no conclusion can be drawn about one aspect of a basin's history without affecting the interpretation of other aspects. Thus, when a conclusion from one line of evidence is at variance with

a conclusion drawn from several other lines of evidence, we must challenge the assumptions that led to the different conclusions—which usually involves examining cherished theories or paradigms. The reluctance to relinquish paradigms is more easily overcome when several lines of evidence point toward new concepts that have exciting implications of their own. Basin analysis, by its integrative nature, pushes us toward new perspectives and thus serves to promote new discoveries in geoscience.

A case study in the San Juan Basin of New Mexico serves as an example of the basin analysis approach to a geologic problem. It also points out that answers to questions not initially posed can sometimes be the most significant (and surprising) outcome of a basin study. The original goal of the San Juan Basin study was to develop a genetic model for sandstone-type uranium deposits in the Jurassic Morrison Formation. Tectonic, geophysical, sedimentologic, petrographic, hydrologic, and geochemical studies were drawn together so that mineralization could be evaluated in the context of the entire depositional, structural, and diagenetic framework. The result was not only a model for uranium mineralization, but also, somewhat unexpectedly, the overturning of several paradigms and their replacement with new concepts. Many of these new developments were unrelated to the solution of the original problem.

One new result of the San Juan Basin study is that it was possible to document that authigenic illitic mixed-layer clays in the Upper Jurassic Morrison Formation formed at near-surface conditions in the absence of elevated temperatures. This finding contrasts with the "Gulf Coast model" for illite formation, in which temperatures of at least 90 °C are thought to be required. The "Gulf Coast model," in which composition of illite/smectite mixed-layer clays is attributed to increasing temperatures attendant with increasing burial, had become a paradigm throughout the petroleum industry. In the San Juan Basin study, because the basin analysis approach was used, formation of authigenic illite was not viewed as an isolated event. The process instead was constrained by other lines of evidence, including inferences from associations with other authigenic minerals; vitrinite reflectance data; petrographic constraints; paragenetic relationships; reconstructions of burial and thermal history; and hydrogeochemistry. Thus, the "Gulf Coast" paradigm, requiring elevated temperatures, did not provide a valid model for illite formation in this study. It became apparent that, in certain instances, pore-water chemistry alone can facilitate formation of authigenic illite, and thus that illite is not always a reliable geothermometer. Therefore, the "Gulf Coast model" offers one, but not the only, mechanism by which authigenic illite can form. This example serves to illustrate that a paradigm cannot be generalized to include all cases. The paradigm was correct, yet did not provide a unique solution to the problem. In other cases, a paradigm is invalid because the underlying assumptions are incorrect. In either case, basin analysis provides internal checks on the validity of paradigms and highlights inconsistencies that would not be evident if only the constraints within individual subdisciplines were considered.

R.K. Matthews stated in a letter to the editor of *Geology* in 1985, "A paradigm is the framework within which we attempt to solve problems," not necessarily the solution to the problem itself. The integrative nature of the basin analysis approach allows a synoptic rather than a myopic view of specific geologic problems, and the multidisciplinary nature of the approach forces us to scrutinize each paradigm because each paradigm has consequences for the whole, beyond the solution of an isolated problem. The approach can be applied to any geologic problem and will serve to advance science by continuing to lead us away from current paradigms, as multiple lines of evidence force us to question our most cherished beliefs.

Depositional and Diagenetic Controls on the Residence and Isotopic Composition of Sulfur in Middle Pennsylvanian Coals, Southeast Iowa and Northwest Illinois

Michele L. Tuttle, Cynthia A. Rice,
Joseph R. Hatch, and Richard D. Harvey

In the Midcontinent region from Kansas and Oklahoma eastward, Pennsylvanian high-sulfur coal is found in cyclothems. These alternating sedimentation cycles record the contest waged in the Pennsylvanian between the sea and the rivers: when sediment deposited by rivers exceeded basin subsidence, deltaic clay-rich sediment was deposited in channels and organic matter (precursor to the coal) accumulated in vast swampy lowlands. When subsidence exceeded infilling, the sea crept eastward, drowning the swamps and depositing marine shales and limestones. The rapidly alternating environment profoundly affected the sulfur geochemistry of the Pennsylvanian coal. The depositional and diagenetic conditions associated with these changes were investigated by studying various forms of sulfur and their isotopic composition in the Colchester No. 2 coal in the Carbondale Formation and associated deltaic and marine shale from three different locations. We also analyzed acid-soluble metals and organic carbon and calculated the degree of iron and organic-matter sulfidization.

A 0.35-m coal seam in the Star Mine 12, Monroe County, Iowa, is overlain by two organic-rich, marine

black shales (1.2 and 3.6 wt. percent S; $\delta^{34}S_{FeS2} = -24.3$ and $-32.9‰$, respectively). The coal contains abundant sulfur (5.4 wt. percent), half of which occurs as sulfide minerals. Sulfide minerals are FeS_2 ($\delta^{34}S = -14.6‰$) in the upper coal bench, and FeS_2 ($\delta^{34}S = -8.7‰$) and ZnS ($\delta^{34}S = -16.9‰$) in the basal coal bench. Organic S ($\delta^{34}S = -14.1‰$) makes up 40 percent of the total S and 3.3 wt. percent of the organic matter. The ^{34}S-depleted isotopic composition and high sulfur content of the organic matter indicate that the organic matter has been sulfidized by bacteriogenic H_2S of similar isotopic composition to sulfur in sulfide minerals. The negative $\delta^{34}S$ values indicate that an unlimited sulfate reservoir was available to the sulfate-reducing bacteria. All the iron in the basal coal is sulfidized; excess bacteriogenic sulfide (possibly associated with organic matter) was available in the basal unit to react with Zn in possible hydrothermal fluids moving through the coal, as noted in a 1988 study by J.F. Whelan and others.

A 0.71-m coal seam in the Cedar Creek Pit 5, Schuyler County, Ill., is overlain by 2 m of gray deltaic shale (6.0 wt. percent S; $\delta^{34}S_{FeS2} = +10.9‰$), 1.7 m of black marine shale, and 1 m of marine limestone. FeS_2 ($\delta^{34}S = +7.6‰$) in the coal generally constitutes half of the total S (3.7 wt. percent); the other half is organic S ($\delta^{34}S = +11.2‰$) which constitutes 3.1 wt. percent of the organic matter. Similar $\delta^{34}S$ values for the FeS_2 and organic S and a high sulfur content of the organic matter indicate that the organic matter in the coal was sulfidized by bacteriogenic H_2S. The positive $\delta^{34}S$ values and sulfur content indicate that a large, but not unlimited sulfate reservoir was completely reduced by sulfate-reducing bacteria to H_2S that sulfidized nearly all the iron in the coal; excess H_2S sulfidized organic matter.

A 0.49-m coal seam in the Cedar Creek Pit 3 is overlain by at least 7.6 m of gray deltaic shale (0.14 wt. percent S; $\delta^{34}S_{FeS2} = +1.5‰$). FeS_2 ($\delta^{34}S = +14.6‰$) in the coal makes up 20 percent of the total S (1.5 wt. percent), whereas organic S ($\delta^{34}S = +13.9‰$) constitutes 58 percent of the total S and only 0.6 percent of the organic matter. Less than half the iron in the coal is sulfidized. The low degree of iron sulfidization, low FeS_2 content, and positive $\delta^{34}S_{FeS2}$ values indicate that a small sulfate reservoir was completely reduced by bacteria. The bacteriogenic H_2S was consumed by reaction with iron, leaving little, if any, to sulfidize the organic matter, hence the low sulfur content in the organic matter.

From these examples, the sulfur geochemistry in the Colchester No. 2 coal appears to have been controlled by the environment in which the overlying unit was deposited. Marine black shale overlying coal indicates that subsidence exceeded infilling and the swamp was flooded by seawater. Abundant seawater sulfate diffused into the swamp deposits, producing an unlimited sulfate reservoir for the sulfate-reducing bacteria. Where the coal is overlain by a relatively thin unit of deltaic shale, which in turn is overlain by marine black shale, seawater sulfate diffused into the swamp deposits, producing a large, but not unlimited sulfate reservoir for the bacteria to reduce. Where the coal is overlain by a thick sequence of deltaic shale, the swamp deposits were isolated from seawater sulfate. FeS_2 was formed when bacteria reduced the small freshwater sulfate reservoir in the swamp and the organic S was inherited from the sulfur assimilated in the growing vegetation.

Depositional Processes Revealed by GLORIA Sidescan Sonar Images on the Mississippi Fan

David C. Twichell, Neil H. Kenyon, and Bonnie A. McGregor

GLORIA (Geologic LOng Range Inclined Asdic) sidescan sonar images have been used in combination with 3.5-kHz high-resolution subbottom profiles to infer the depositional processes that formed the surface of the Mississippi Fan. These images show that three distinct depositional stages occurred in the formation of the surface of the fan. The stages are represented in the images by regions of distinctive acoustic backscatter. A region of low backscatter rims the margin of the fan. The overlapping relationships seen on the 3.5-kHz profiles indicate that this region is the oldest of the three stages. The 3.5-kHz profiles and available core data suggest that this peripheral region consists of hemipelagic and turbidite deposits.

The next oldest region of the fan is marked by linear high-backscatter stripes separated by areas of lower backscatter. These stripes are as much as 150 km long and as much as 10 km wide; they radiate southwestward from a large channel that originates in the Mississippi Canyon area and trends southeastward across the apex of the fan. The linear stripes apparently represent overbank flows that breached the levees of the main channel. The absence of channels coincident with the stripes suggests that these flows were largely non-channelized. Their presence downslope from sections of the main channel that have been buried by younger sediments indicates an intermediate age between the deposits having the low-backscatter surface and those having a high-backscatter surface.

The third, and youngest, backscatter region consists of a series of elongate, overlapping, lobe-shaped features. These lobes often exceed 200 km in length and 75 km in width and can reach 40 m in thickness. They have high-backscatter surfaces and coincide with

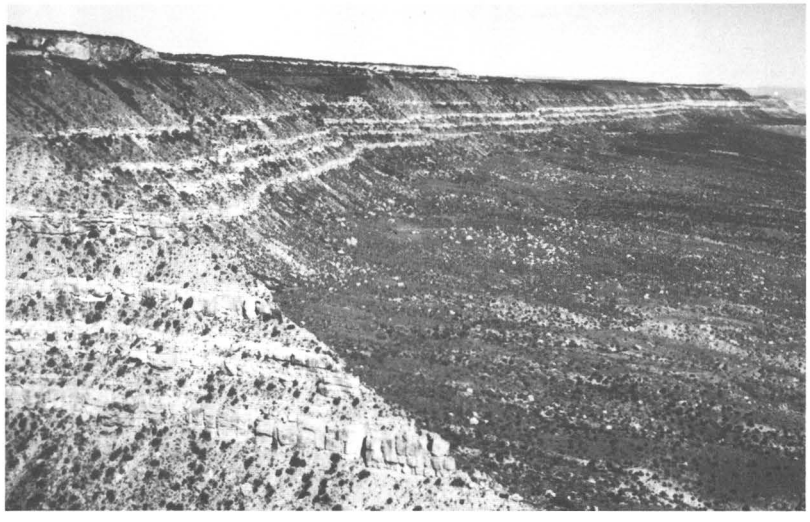

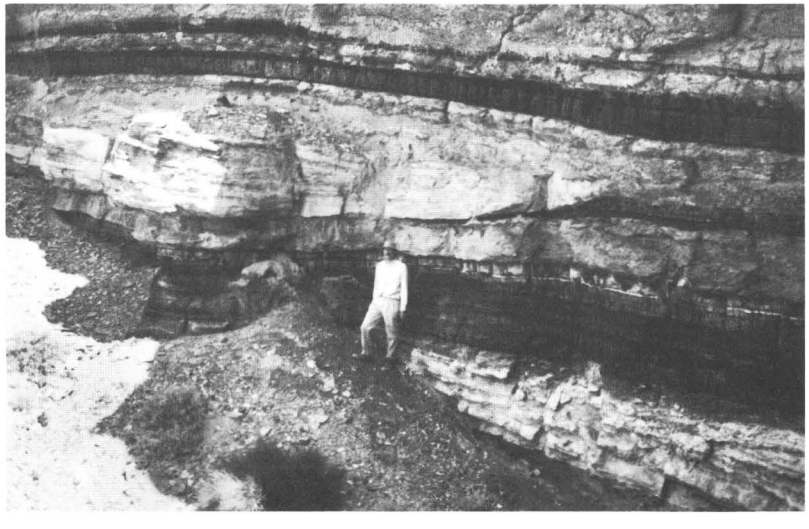

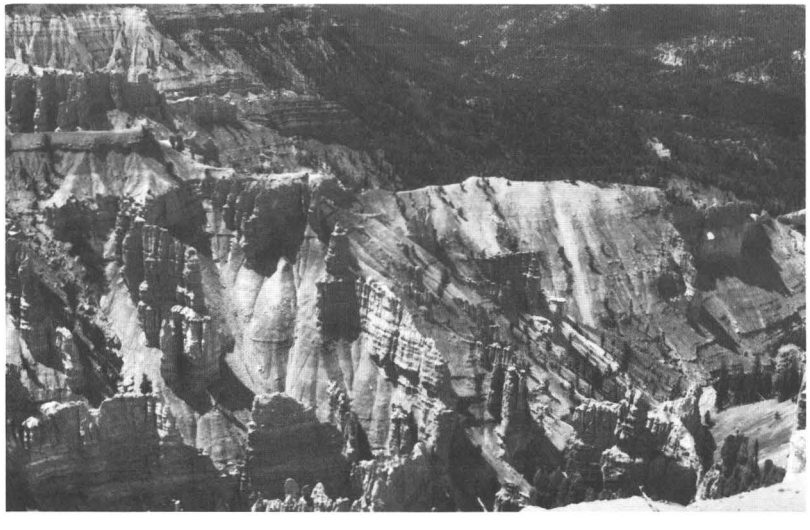

Upper left—Navajo Point from Lake Powell, southeastern corner of Kaiparowits Plateau, southern Utah. Cliffs in foreground are eolian Navajo Sandstone. Top of plateau (approx. 3,800 ft above lake level) consists of stacked shoreface deposits of the John Henry Member of the Straight Cliffs Formation (Coniacian to early Campanian). Original color slide by Peter J. McCabe. *Upper right*—Straight Cliffs of Fiftymile Mountain, Kaiparowits Plateau, Utah, composed of coarsening-upward parasequences of the John Henry Member of the Straight Cliffs Formation. Major coal deposts in central part of plateau lie lateral to the vertically stacked shoreface deposits. Original color slide by Peter J. McCabe. *Lower left*—Cross section of a swilley in a coal of the Straight Cliffs Formation. Swilleys are interpreted to be the deposits of crevasse splays into mires. Note erosion of middle coal bed and thinning of upper coal bed over sandstone due to differential compaction. Original color slide by Keith W. Shanley. *Lower right*—Cedar Breaks National Monument, a scenic feature of the Cedar City 1° × 2° area, southwestern Utah. Original color slide by L.M.H. Carter.

acoustically transparent lenses on the 3.5-kHz subbottom profiles. The lobes either radiate from the end of the main channel or eastward from a sharp bend in the channel. A study of one lobe shows that it consists of a series of smaller elongate high-backscatter areas (5–40 km in length) located at the ends of previously unrecognized small channels (< 5 m deep). These small channels extend as much as 120 km from the main channel, and the high-backscatter areas at their ends are interpreted to be sites of deposition. Channelized turbidites or debris flows are the inferred process of deposition.

The different backscatter patterns of the three regions and their relative age relationships suggest that different depositional processes were active at different times during the development of the present Mississippi Fan surface. The acoustic variability that is expressed in the GLORIA images on the surface of the fan suggests that laterally discontinuous and variable facies are present. This variability needs to be reconciled with the apparent uniformity of the facies inferred from low-frequency seismic-reflection profiles across these areas of the fan.

Chemical and Physical Characteristics of Coal Beds from the Salt Range Coal Field, Punjab Province, Pakistan

P.D. Warwick, T. Shakoor, S. Javed, S.T.A. Mashhadi, and M.I. Ghaznavi

From 1985 to 1988 forty-four coal samples were collected from the Patala Formation, Paleocene age, in the Salt Range coal field, a westerly-trending, 15×100 km area, in Punjab Province, Pakistan. Five of these samples were collected from drill core, and the remaining 39 were collected from channels cut in fresh coal faces in 35 underground mines. Coal bed thicknesses from 37 sample localities averaged 0.49 m, with std. dev. (standard deviation) 0.25. Results of proximate and ultimate analyses, reported here on an as-received basis, indicate that the coal beds have an average ash yield of 24.23 percent with std. dev. 9.76, average sulfur content of 5.32 percent with std. dev. 2.52, average pyritic sulfur content of 4.07 percent with std. dev. 2.5, and average calorific value of 8,943 Btu with std. dev. 1,467. Eleven samples, analyzed on a whole-coal, dry basis for selected trace elements and oxides, have anomalously high average concentrations of Ti, at 0.36 percent; Zr, at 382 ppm; and Se, at 11.4 ppm, compared to worldwide averages for these elements in coal.

Correlation coefficients were calculated among trace-element, oxide, proximate, ultimate, location, and coal-bed-thickness data. Sample localities were assigned to the eastern, central, and western parts of the coal field, which roughly correspond to areas of previously defined depositional facies of the coal-bearing strata: the coal beds in the western area are interbedded with deposits of a northerly-trending barrier-bar complex; the coal beds in the central part of the coal field are associated with lagoonal and tidal flat deposits; and coal beds in the eastern part of the coal field are associated with upper shore face and tidal channel deposits.

Some positive correlations, significant at the 0.01 level, are those between total sulfur and As, pyritic sulfur and As, total sulfur and location, organic sulfur and Se, calorific value (Btu) and location, and coal bed thickness and Se. In general, the thickest coal beds with the lowest total sulfur content are in the central part of the coal field. Organic sulfur and selenium contents are greatest in the eastern part of the coal field; pyritic sulfur content is greatest in the western part of the coal field. Total ash yields increase toward the east. Calorific values for the samples, calculated on a moist, mineral-matter-free basis, indicate that the rank of the coal is high-volatile C bituminous.

Some of the variations observed in the chemical and physical characteristics of the Salt Range coal beds may be related to the different depositional environments of the coal-bearing strata. The increase of ash and selenium concentrations in a landward direction probably indicates less stable, more fluvially influenced environments of peat deposition than elsewhere. Increased pyritic sulfur concentrations near the barrier-bar complex may be related to post-peat, pyrite-filled burrows commonly observed in the upper part of the coal bed. The thickest coal beds that have the lowest ash and sulfur contents and highest calorific values formed from peats deposited in back-barrier, tidal flat environments of the middle part of the coal field.

Genesis and Distribution of Uraninite in Solution-Collapse Breccia Pipes, Northwestern Arizona

Karen J. Wenrich, Bradley S. Van Gosen, and Hoyt B. Sutphin

Thick sequences of karst-forming Mississippian limestone extend across the Colorado Plateau and into adjacent areas of the Basin and Range and Rocky Mountain region. As much as 800 ft of the Redwall Limestone, which underlies or caps the various high plateaus of the southwestern Colorado Plateau in Arizona (fig. 1), is responsible for one of the finest karst terranes in the United States. By the close of the

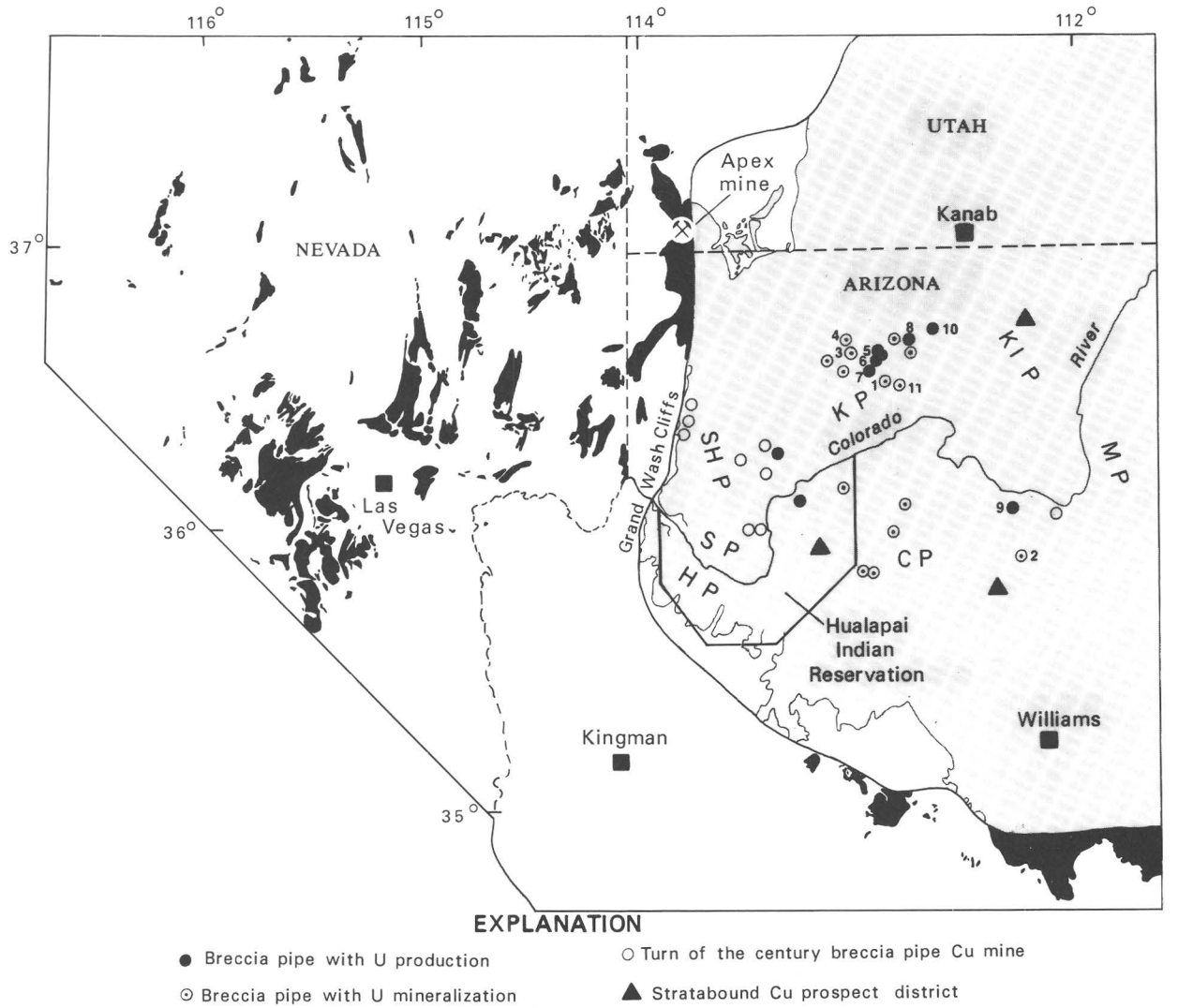

Figure 1 (Wenrich). Map showing the location of U-rich breccia pipes, copper prospects, and the Apex mine (a Ga-Ge-rich breccia pipe). The lightly shaded area on the Colorado Plateau indicates terrane capped by the Mississippian Redwall Limestone or younger strata—rock necessary for the formation of solution-collapse breccia pipes containing uranium orebodies. The dark shading indicates the same terrane in the Basin and Range—areas that have potential for breccia pipes, but have not been explored for them. Breccia pipes discussed in the text are shown with the following numbers on the map: (1) Arizona 1, (2) Canyon, (3) EZ-1, (4) EZ-2, (5) Hack 1, (6) Hack 2, (7) Hack 3, (8) Kanab N, (9) Orphan, (10) Pigeon, and (11) Pinenut. Plateaus mentioned in the text are shown with the following letters on the map: (CP) Coconino Plateau, (HP) Hualapai Plateau, (KIP) Kaibab Plateau, (KP) Kanab Plateau, (MP) Marble Plateau, (SP) Sanup Plateau, and (SHP) Shivwits Plateau.

Mississippian, extensive karst had formed in the Redwall—extensive enough to promote the formation of thousands of breccia pipes, typically 100–500 ft in diameter. The breccia pipes later propagated upward by stoping and collapse of as much as 3,000 ft of overlying Pennsylvanian and Permian sandstone, shale, and limestone. The karst provided channelways for removal of disaggregated material by circulating waters that dissolved the carbonate cement of the overlying strata and reactivated the Redwall karst. Breccia pipes were actively stoping upward during the Leonardian (about 260–270 Ma), as shown by the thickening of the Harrisburg Member of the Lower Permian Kaibab Limestone over the Canyon breccia pipe (W.P. Casadevall, oral presentation, AAPG Albuquerque meeting, 1989). Pipes either continued to stope or were

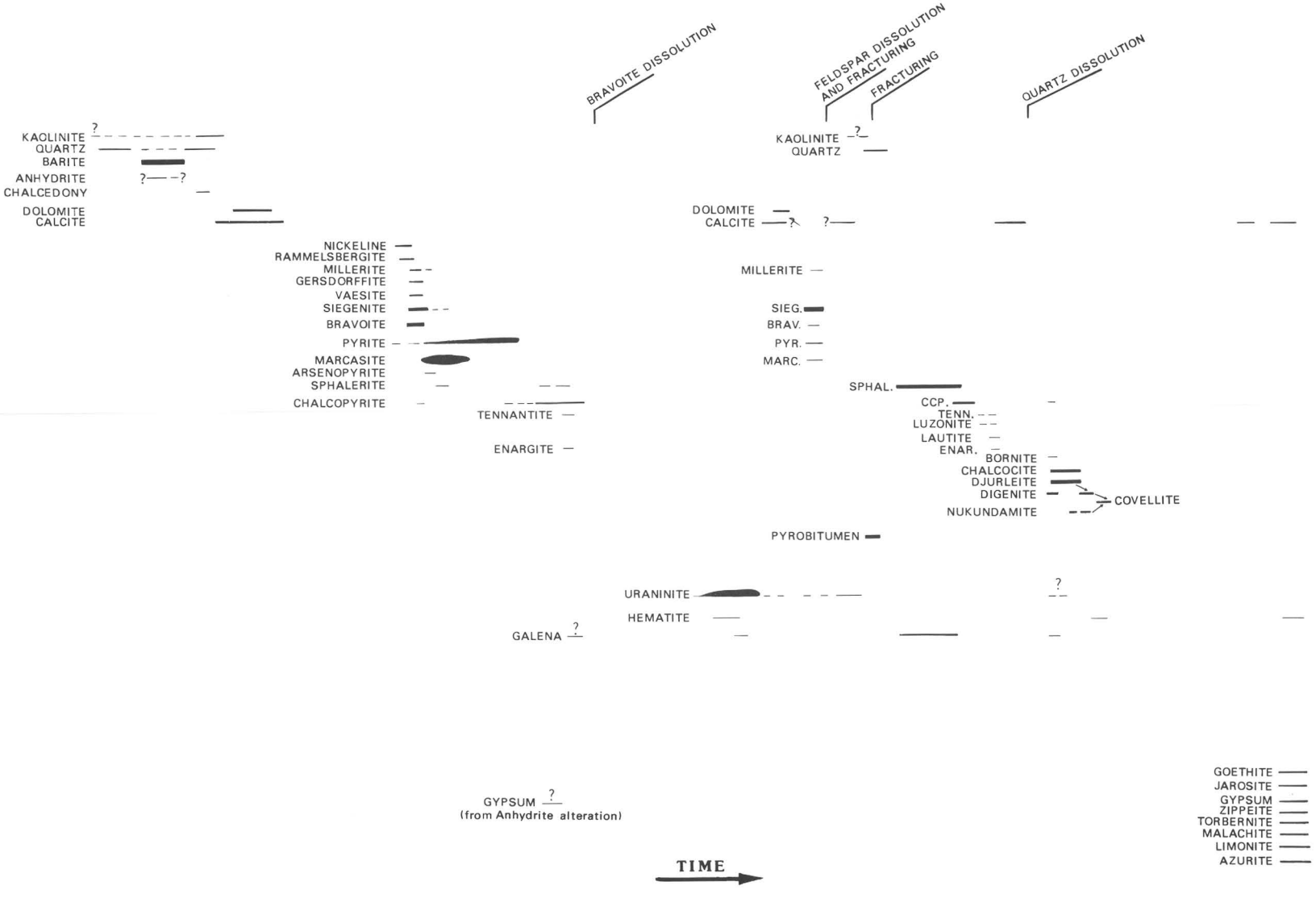

Figure 2 (Wenrich). Paragenetic sequence for minerals in solution-collapse breccia pipes of the southwestern Colorado Plateau. Thickness of bar indicates relative mineral abundance. Arrows point to a mineral that is replacing the mineral located at the tail of the arrow.

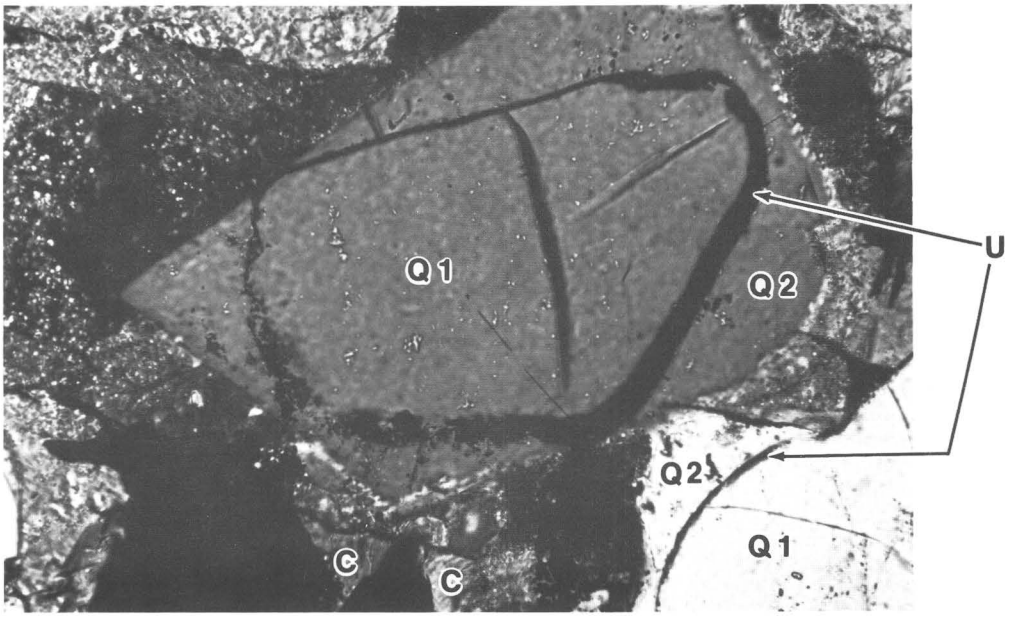

Figure 3 (Wenrich). Detrital quartz grain (Q1) rimmed by uraninite (U). Later silica deposition encased the uraninite with a quartz overgrowth (Q2). The quartz lies within a carbonate matrix (C). Transmitted light photomicrograph with crossed nicols. Long dimension of photo = 0.4 mm.

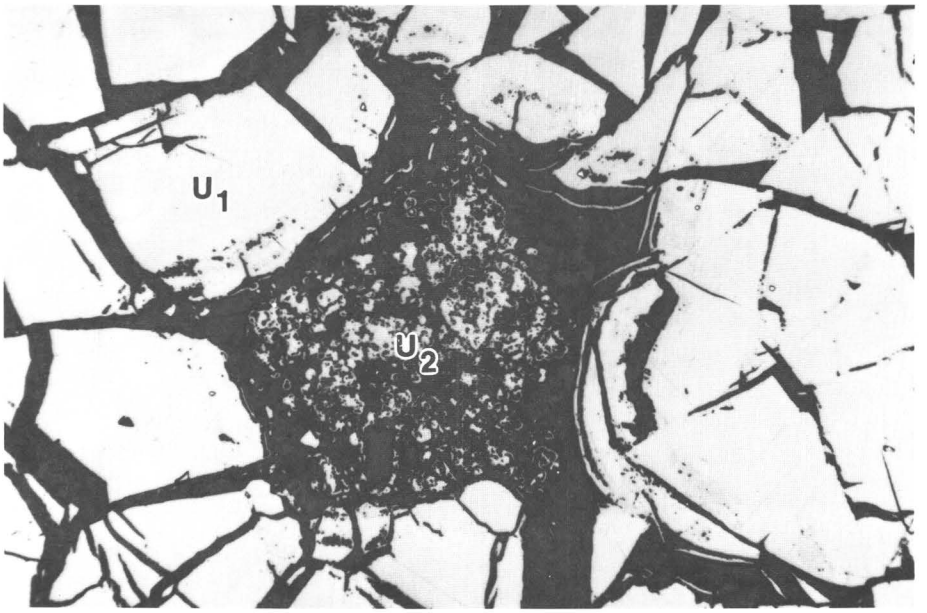

Figure 4 (Wenrich). Two stages of uraninite mineralization. The early uraninite (large grains around the outside, labeled U_1) was fractured and then uraninite was again deposited in a more wormy, less massive habit (unfractured material in center of view, labeled U_2). Reflected light photomicrograph. Long dimension of photo = 1.34 mm.

reactivated during the Triassic, as beds of the Upper Triassic Chinle can be observed dipping concentrically into pipes on the Marble Plateau just east of the Grand Canyon.

The Redwall Limestone is an excellent aquifer, as are many of the overlying sandstone units. When the breccia pipes formed, they connected several of these aquifers whose waters probably used the breccia pipes as

conduits, thus permitting waters from different aquifers to mix. This unique scenario included: (1) highly permeable well-developed passageways for large-scale fluid movement, (2) access to the breccia pipes by several aquifers that undoubtedly contained diverse water compositions, and (3) the development of this linking of the aquifers during a relatively short period of time following a long period of total confinement. These unique conditions were amenable to deposition of a large suite of elements (including U, Ag, As, Co, Cu, Mo, Ni, Pb, V, and Zn); as a result rich deposits of uraninite formed that contain an unusual and large assemblage of minerals (104 species—some of which are listed in fig. 2).

Mining of breccia pipes began during the late 1870's, at which time essentially all mining was for copper with minor production of Ag, Pb, and Zn. In 1951 uranium was discovered at the existing copper prospect in the Orphan breccia pipe (fig. 1). Until 1975 the Orphan was the only known breccia pipe uranium deposit in northwestern Arizona. During the period 1956–1969, the Orphan mine yielded 4.26 million pounds of U_3O_8 from ore with an average grade of 0.42 percent U_3O_8 (figures from 1986 study by W.L. Chenoweth). In addition to uranium, 6.68 million pounds of copper, 107,000 ounces of silver, and 3,400 pounds of V_2O_5 were recovered from the ore (figures from 1986 study by W.L. Chenoweth). Between 1975 and the close of the 1980's, exploration was intensive, and 19 deposits containing over 50 million pounds of U_3O_8 were recognized; 10 million pounds were mined between 1980 and 1987 from ore with an average grade of 0.65 percent U_3O_8 (figures from 1987 report by I.W. Mathisen, Jr.) from the 5 (Hack 1, Hack 2, Hack 3, Pigeon, and Kanab N) of these deposits that were put into production since 1980. Another 46 pipes have been identified that contain >1 ft of 0.01 percent U_3O_8 (data from 1989 study by Sutphin and Wenrich). Most of the breccia pipes presently known to contain uranium resources lie on the Kanab and Coconino Plateaus—the two areas where exploration has been most intensive. Many additional pipes are buried with no expression on the overlying plateau surface, and many parts of northwestern Arizona need equally intensive exploration and drilling; thus, the potential for discovery of additional uranium reserves is enormous. Unfortunately, with the 1980's slide of uranium prices, which by 1989 had reached the low prices of the late 1960's, no new mines are expected to go into production in the near future.

The 104 minerals that have been identified within the breccia pipes can be roughly divided into six depositional stages with some overlap during the 3–5th stages (fig. 2). Abundant sulfides of Fe, Cu, Co, Ni and As from stages 2–3 provided enough reductant to permit precipitation of high-grade uranium. Uraninite (UO_2)—the only primary uranium-bearing phase identified—was precipitated (1) in minor vugs, (2) as rims around detrital quartz grains (fig. 3), and (3) within the coarsely crystalline calcite matrix of stage 1. The morphology of uraninite is variable, ranging from distinct spheres and clusters of spheres to botryoidal crusts, thin "wisps," and irregular patches that replace previous matrix material. Uranium-bearing material of lower reflectivity has been observed associated with uraninite; microprobe analyses indicate that this Ca-P-U-bearing material is not a discrete phase, but perhaps a fine-grained mixture of uraninite and apatite. Two periods of uraninite mineralization have been observed (fig. 4)—all late stage, that is, after deposition of most sulfides: (1) massive uraninite, which may have been deposited in two separate events prior to a major fracturing event within the pipes, and (2) a post-fracturing, wormy, finer grained uraninite. A large set of U-Pb isotopic analyses from the Hack 2, Hack 3, Pigeon, Kanab North, EZ-1, EZ-2, Arizona 1, Pinenut, and Canyon pipe orebodies shows that the main uranium-mineralizing event occurred roughly 200 Ma, that is, Early Jurassic; data from the Canyon and Pinenut pipes, however, indicate at least one earlier period of mineralization roughly at 260 Ma, Early Permian (data from 1988 study by K.R. Ludwig and K.R. Simmons). Whether or not these two isotopic ages correspond to the two stages of uraninite mineralization has not been determined.

Although most of the primary ore minerals in the breccia pipes were deposited prior to the uraninite, some pyrite, sphalerite, and galena formed contemporaneous with, or after, the uraninite. In addition, pyrobitumen was deposited after the uraninite; in the more southern breccia pipes so was a sequence of the copper sulfides: bornite, chalcocite, djurleite, digenite, and covellite. Fluid inclusions within sphalerite, calcite, and dolomite indicate that ore-forming fluids had temperatures in the range of 80°C to 173°C, with salinities consistently >9 wt. percent NaCl equivalent and most commonly >18 wt. percent NaCl equivalent. Little quartz precipitation accompanied breccia pipe mineralization, except for late-stage silica deposition as quartz overgrowths on detrital quartz grains; this quartz clearly follows uraninite deposition because the quartz overgrowths surround uraninite rims that enclose detrital quartz grains (fig. 4). Apparently, an earlier period of quartz instability occurred, presumably associated with deposition of the early uraninite—detrital quartz grains associated with some uraninite deposition are corroded. In addition, strong evidence exists that within breccia pipes the silica cement of the Coconino Sandstone was totally removed, causing the Coconino to settle downward into the pipe as loose sand (Vivian Gornitz, written commun., 1987; N.A. Brown, oral presentation, AAPG Albuquerque meeting, 1989).

Understanding the genesis of such high-grade sedimentary uranium deposits lies in recognizing the significance of the aquifer systems and the high permeability of the breccia pipes themselves, rather than in debating the age-old question of "source rock." Whether the ground water transporting the uranium carried 0.1 ppb or 10 ppb uranium is insignificant compared to the importance of the volume of water that was apparently flushed through the Paleozoic aquifers and breccia pipe conduits, and its interaction with the large mass of sulfides already residing in the pipes. This interaction would have reduced and precipitated the uranium from the ground water.

The stability of the Colorado Plateau, perhaps aided by the reducing pyrite cap over most of the orebodies, preserved the high-grade uranium since its deposition 200 Ma. Canyon dissection, which probably occurred throughout the past 5 m.y., has subjected many breccia pipes on the well-dissected Shivwits, Sanup, and Hualapai Plateaus to extensive erosion that permitted oxidation of their orebodies and formation of colorful supergene minerals (stage 6—fig. 2). The relatively undissected Kaibab, Kanab, Coconino, and Marble Plateaus undoubtedly contain most of the remaining breccia pipe uranium resources.

The Point Lookout Sandstone—Changing Formation Architecture from Strandplain to Delta

Robert S. Zech and Robyn Wright-Dunbar

Throughout most of the San Juan Basin, New Mexico and Colorado, the Upper Cretaceous Point Lookout Sandstone generally fits a cyclic shoreface model in which the dominant architectural element is a prograding linear strandplain lithosome. This is best shown in the Cortez, Colorado area (the Cortez strandplain), where repetitive lithologic units that accumulated in beach to inner-shelf environments record multiple transgressive-regressive cycles. (See fig. 1, p. 92.) Deposits from about five of these cycles are locally grouped into bundles that extend at least 20 km along depositional strike and change basinward over 17–20 km from foreshore sandstone to offshore mudrock of the time-equivalent Mancos Shale. Where the bundles of well-sorted shoreface sandstone are stacked, the formation thickens and forms excellent hydrocarbon reservoirs.

The depositional setting changed in the vicinity of Durango, Colorado. There, deposits of a fluvial-dominated delta-front and associated large distributary channels make up the Point Lookout Sandstone and overlying Menefee Formation (the Durango delta). Lenticular sandstone units, pervasive mudrock interbeds, and local slump features are common in the deltaic strata. Abundant current ripples in the distal delta-front deposits indicate northeast-flowing (offshore) and southeast-flowing (longshore) paleocurrents. Proposed subsurface models for the Durango area must include the alignment of local distributary axes, delta-mouth bars (strike-aligned reservoir discontinuity), and possible sandy clastic shelf plumes originating from the delta. Continuing research will focus on the transitional area between the strandplain and the delta, on delta-sandstone geometry, and on reservoir compartmentalization, which will be directly applicable to the Ignacio-Blanco field.

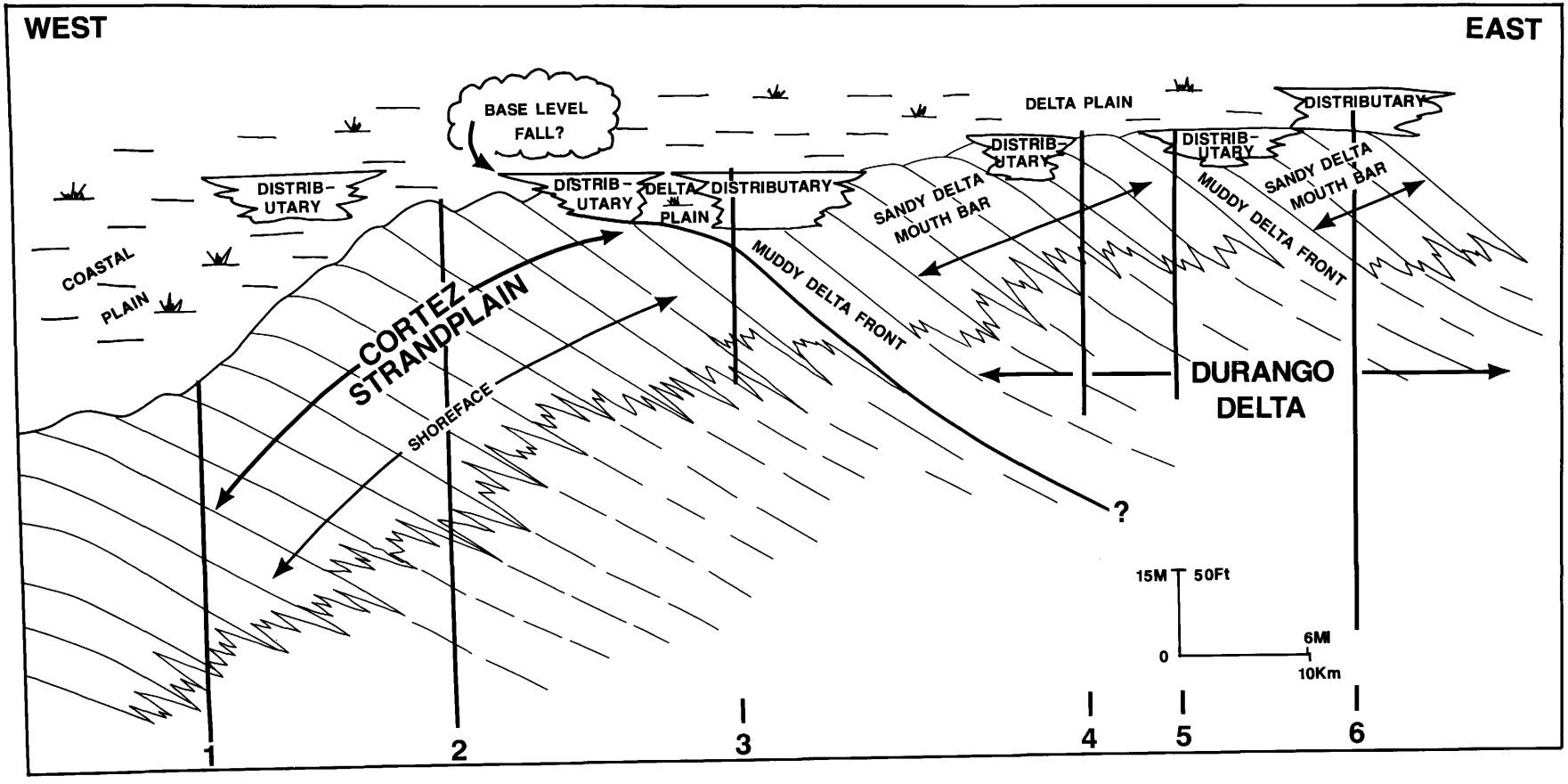

Figure 1 (Zech). Cross section from the Cortez area (west) to the Durango area (east) showing depositional environments of Point Lookout Sandstone. Vertical lines and numbers indicate locations of measured (outcrop) sections.

ORGANIZATION OF THE U.S. GEOLOGICAL SURVEY

Office	Name	Telephone	City
Office of the Director			
Director	Dallas L. Peck	703/648–7411	Reston
Associate Director	Doyle G. Frederick	703/648–7412	Reston
Assistant Director for Research	Bruce R. Doe	703/648–4450	Reston
Assistant Director for Engineering Geology	Eugene H. Roseboom, Jr.	703/648–4423	Reston
Assistant Director for Administration	Jack J. Stassi	703/648–7200	Reston
Assistant Director for Programs	Peter F. Bermel	703/648–4430	Reston
Assistant Director for Intergovernmental Affairs	John J. Dragonetti	703/648–4427	Reston
Chief, Public Affairs Office	Donovan B. Kelly	703/648–4459	Reston
Assistant Director for Information Systems	James E. Biesecker	703/648–7108	Reston
National Mapping Division			
Chief	Lowell E. Starr	703/648–5748	Reston
Geologic Division			
Chief Geologist	Benjamin A. Morgan	703/648–6600	Reston
Water Resources Division			
Chief Hydrologist	Philip Cohen	703/648–5215	Reston

ORGANIZATION OF THE GEOLOGIC DIVISION

Office of the Chief Geologist			
Chief Geologist	Benjamin A. Morgan	703/648–6600	Reston
Associate Chief Geologist	William R. Greenwood	703/648–6601	Reston
Assistant Chief Geologist for Program	David P. Russ	703/648–6640	Reston
Assistant Chief Geologist, Eastern Region	Jack H. Medlin	703/648–6660	Reston
Assistant Chief Geologist, Central Region	Harry A. Tourtelot	303/236–5438	Denver
Assistant Chief Geologist, Western Region	William R. Normark	415/329–5101	Menlo Park
Office of Mineral Resources			
Chief	Glenn H. Allcott	703/648–6100	Reston
Chief, Branch of Alaskan Geology	Donald J. Grybeck	907/786–7403	Anchorage
Chief, Branch of Eastern Mineral Resources	Klaus J. Schulz	703/648–6327	Reston
Chief, Branch of Central Mineral Resources	David A. Lindsey	303/236–5568	Denver
Chief, Branch of Western Mineral Resources	William C. Bagby	415/329–5477	Menlo Park
Chief, Branch of Geochemistry	Lorraine Filipek	303/236–1800	Denver
Chief, Branch of Resource Analysis	William D. Menzie	703/648–6125	Reston
Chief, Branch of Geophysics	Thomas G. Hildenbrand	303/236–1212	Denver

Office of Energy and Marine Geology

Chief	Gary W. Hill	703/648–6472	Reston
Chief, Branch of Petroleum Geology	Donald L. Gautier	303/236–5711	Denver
Chief, Branch of Coal Geology	Hal Gluskoter	703/648–6401	Reston
Chief, Branch of Sedimentary Processes	Walter E. Dean, Jr.	303/236–1644	Denver
Chief, Branch of Pacific Marine Geology	David A. Cacchione	415/329–3184	Menlo Park
Chief, Branch of Atlantic Marine Geology	Bradford Butman	617/837–4211	Woods Hole

Office of Regional Geology

Chief	Mitchell W. Reynolds	703/648–6960	Reston
Act. Chief, Branch of Eastern Regional Geology	Wayne L. Newell	703/648–6900	Reston
Chief, Branch of Central Regional Geology	David L. Schleicher	303/236–1258	Denver
Chief, Branch of Western Regional Geology	Rowland W. Tabor	415/329–4909	Menlo Park
Chief, Branch of Isotope Geology	Carl E. Hedge	303/236–7880	Denver
Chief, Branch of Astrogeology	Hugh H. Kieffer	602/765–7015	Flagstaff
Chief, Branch of Paleontology and Stratigraphy	John Pojeta, Jr.	703/648–5288	Reston

Office of Earthquakes, Volcanoes, and Engineering

Chief	Robert L. Wesson	703/648–6714	Reston
Chief, Branch of Engineering Seismology and Geology	Thomas L. Holzer	415/329–5613	Menlo Park
Chief, Branch of Global Seismology and Geomagnetism	Robert P. Masse	303/236–1510	Denver
Chief, Branch of Seismology	William H. Bakun	415/329–4793	Menlo Park
Chief, Branch of Geologic Risk Assessment	Kaye M. Shedlock	303/236–1585	Denver
Chief, Branch of Tectonophysics	William H. Prescott	415/329–4810	Menlo Park
Chief, Branch of Igneous and Geothermal Processes	Robert L. Christiansen	415/329–5228	Menlo Park

Office of Scientific Publications

Chief	John M. Aaron	703/648–6077	Reston
Chief, Branch of Eastern Technical Reports	Simon M. Cargill	703/648–4313	Reston
Chief, Branch of Central Technical Reports	Lawrence F. Rooney	303/236–5457	Denver
Chief, Branch of Western Technical Reports	James E. Pinkerton	415/329–5049	Menlo Park
Chief, Library and Information Services	Barbara A. Chappell	703/648–4305	Reston
Chief, Branch of Visual Services	John R. Keith	703/648–4357	Reston

Office of International Geology

Chief	A. Thomas Ovenshine	703/648–6047	Reston

Addresses

U.S. Geological Survey
Reston, VA 22092

U.S. Geological Survey
Box 25046
Denver Federal Center
Denver, CO 80225

U.S. Geological Survey
345 Middlefield Road
Menlo Park, CA 94025

U.S. Geological Survey
Branch of Alaskan Geology
4200 University Drive
Anchorage, AK 99508–4667

U.S. Geological Survey
2255 North Gemini Drive
Flagstaff, AZ 86001

U.S. Geological Survey
Quissett Campus, Building B
Woods Hole, MA 02543

U.S. Geological Survey
Hawaiian Volcano Observatory
Hawaii National Park
HI 96718

U.S. Geological Survey
David A. Johnston Cascades Volcano Observatory
5400 MacArthur Boulevard
Vancouver, WA 98661

AUTHOR INDEX

A

B

C

D

E

F

G

H

I

J

K

L

M

N

O

P

R

S

T

V

W

Y

Z

☆ U.S. GOVERNMENT PRINTING OFFICE: 1989—773-047/06,029 REGION NO. 8